TITLE Single To Three phase conversion for motor Drives

AUTHOR Latif, M.

NAME + PERMANENT ADDRESS	SIGN	DATE
M. Tuncay Canakkale Universitesi/Turkey		18/3/93

SINGLE TO THREE PHASE CONVERSION

FOR MOTOR DRIVES

MOHAMMED LATIF

Thesis submitted to the Council for National Academic Awards
for partial fulfilment of the degree
MASTER OF PHILOSOPHY

Collaboration with CUEL LTD,
12 TULIP TREE AVENUE,
KENILWORTH, ENGLAND.

DEPARTMENT OF ELECTRICAL AND ELECTRONIC ENGINEERING

NOTTINGHAM POLYTECHNIC, NOTTINGHAM.

OCTOBER 1991

ACKNOWLEDGEMENTS

I would like to express my deep thanks to PROFESSOR P. G. HOLMES, my Supervisor, for his patient help, advice and unwavering support throughout the project. I would like to thank MR. I. TAYLOR, my second Supervisor, for his help, especially during the earlier stages of the project.

I would like to thank D. ANTCLIFF for his help and advice in compiling the computer program.

Thanks are also due to MR. P. ROWBOTTOM and his technical staff for their endeavours on my behalf.

Thanks to CUEL LTD, KENILWORTH, for their provision of materials and interest in this project.

Finally, I would like to thank the academic staff of the Electrical and Electronic Engineering Department, and especially DR. L. HAYDOCK for his help and assistance.

ABSTRACT

The object of this research is to investigate the operation of a 3-phase induction motor, on as near a balanced 3-phase supply as possible, obtained from a single-phase source. This was achieved by studying previous research on a phase conversion by static and rotary converters. Fundamental theory of phase conversion was investigated and applied to a single and double element phase converter.

The precise phase balance component parameters were used over the full motor slip range and justified experimentally by laboratory tests. A computer programme, valid for any induction motor for which the running light and locked-rotor test results are known, was developed. The motor can be either Delta or Star connected. The programme was further developed into a user friendly software package. The package works out the values of the equivalent circuit parameters, from the results of the stator resistance test, no-load test and locked rotor test. The computer program goes on to draw the equivalent circuit showing parameter values and plots a graph of capacitance against slip.

A switched capacitor static phase converter with single or double element phase balance components with both capacitance and inductance was designed. A comparison of the various converter combinations was made and the control of these converters by manual and electronic means was investigated.

Using the balance criteria, a power-electronic transient phase converter was designed and constructed to balance at all working slips, for any motor, within a specified range.

A critical survey of the results achieved was projected into future work proposals using gate turn-off (GTO) thyristors (Appendix E). Computer aided design of application specific integrated circuits (ASICS) for the power device switching can greatly simplify the gate circuitry of the transient phase converter (Appendix D).

CONTENTS

LIST OF SYMBOLS

Rs	=	Stator Resistance per phase (ohm)
Rr	=	Rotor resistance per phase (ohm)
Xs	=	Stator leakage reactance per phase (ohm)
Xr	=	Rotor leakage reactance per phase (ohm)
Rm	=	Magnetizing resistance per phase (ohm)
Xm	=	Magnetizing reactance per phase (ohm)
R'r	=	Referred rotor resistance per phase (ohm)
X'r	=	Referred rotor reactance per phase (ohm)
I_1	=	Stator current per phase (A)
I_L	=	Line Current (A)
Im	=	Magnetizing current per phase (A)
I_2	=	Rotor current (A)
I'_2	=	Referred rotor current (A)
Vs	=	Stator terminal voltage per phase (V)
E_{br}, E_{BR}	=	Blocked rotor voltage (V)
sEbr	=	Induced rotor frequency per phase
V_T	=	Terminal voltage (V)
Pd	=	Power developed
T	=	Torque (Nm)
Td	=	Torque developed
N	=	Number of Turns
n_r	=	Rotor speed
ωr	=	Angular velocity of the rotor (radians per sec)
η	=	Efficiency
Pin	=	Input Power (Watt)
Pout	=	Output Power (Watt)
s	=	Slip
X_α, X_β	=	Phase converter reactance (α and β) (ohm)
I_α, I_β	=	Phase converter current (α and β) (A)

C	=	Capacitance (μF)
L	=	Inductance (H)
Vp, Vn, Vo	=	Positive, Negative & Zero sequence voltage (V)
Yp, Yn, Yo	=	Positive, Negative & Zero sequence admittance per phase (ohm $^{-1}$)
Rp, Rn, Ro	=	Positive, Negative & Zero sequence resistance per phase (ohm)
V_{ABC} I_{ABC}	=	Phase A, B, C Voltage and current respectively
TH	=	Thyristor
ϕ	=	Phase angle
x	=	Extinction angle (degrees)
θ	=	Firing angle (°)
γ	=	Mark-space (or duty cycle)
f_{chop}	=	Chopping frequency (Hz)
Tr	=	Transistor
P.U.T.	=	Programmable unijunction transistor
D	=	Diode
ζ	=	Conduction Angle

LIST OF FIGURES

CHAPTER 1

INTRODUCTION

Most pumping systems above 2kW, food processing, woodworking, textile machines and machines for the home industry use 3-phase induction motors as prime movers.

Commercially available equipment is designed to operate on a balanced 3-phase supply. Hence any supply imbalance will impede the performance due to an overheating effect.

Many 3-phase systems operate with direct on-line starting, drawing transient inrush currents of up to six times the steady state full load current. This makes the cost of a single phase input D.C. link inverter, operating at constant output frequency prohibitive. However, a variable frequency inverter using pulse width modulation (PWM), can produce a near sinusoidal 3-phase output, capable of soft-starting induction motors. Such an inverter can provide the supply for a cage machine. If however, several machines are to be supplied from the same inverter, they must be accelerated, simultaneously. Also, the logic required for the variable frequency inverter is expensive, if the running condition only requires a single frequency.

In remote areas of the U.K. and in the developing countries (especially the FAR EAST) rural electrification is commonly based on a single-phase earth return distribution system.

3-phase cage induction motors provide the consumer with a low maintenance high frequency alternative to the gasoline or diesel engines. The transmission distances in sparsely populated areas related to consumer demand, make the cost of a 3-phase distribution system prohibitive. As a result of these limitations the interest in single to 3-phase converters developed, since they enable 3-phase motors to operate from a single phase line. The phase converter has played a key role in rural electrification. Traditionally, there are two methods of phase conversion: Rotary and Static.

Rotary conversion, as the name suggests, has moving parts, which are incorporated in the design. A popular earlier example is the Ferraris-Arno type of rotary converter (squirrel cage motor, floating on a single phase supply). Such rotary systems can become prohibitively expensive, if they are rated to supply frequent direct on-line starting or pole changing motor inrush currents. Rotary converters are best applied to applications when, several motors connected in parallel operate independently. The motors may be pole-changing, instant-reverse or continuous duty.

The criticism of the rotary method is that, it is not suitable for high starting torque applications, due to the inability to handle the large starting power surge of the induction motor. It is not appropriate for single motor applications, where the converter and motor have similar ratings. An example of a leading rotary converter is the ROTOVERTER by RONK Industries Inc. [Appendix D].

Static conversion has no moving parts and is of a greater relevance to this work. Over the years, work on static converters has progressed, from having a single element static converter [1, 2, 4, 6, 7], which cannot give a perfect balance over the complete slip range. Then after further work, the two element static converter [3, 5] was introduced and shown to be able to give perfect balance over the complete slip range. This was achieved in ref [3] by a reactive phase shifting network, instead of the simple passive LC network. Static converters are found to be more reliable, robust and cheaper than rotary converters. They can also be used for collective starting of several motors, connected in parallel.

An example of a leading static converter, again by RONK, is the ADD-A-PHASE static converter. Technically, it is an autotransformer capacitor type converter, which distinguishes it from the many other static converters today. It provides the benefits of high power factor, high efficiency, high starting torque, low idle losses and minimum maintenance. Its special design allows the converter to be used with any type of winding (STAR or DELTA) without motor modifications.

The purpose of the present work is to investigate the operation of 3-phase induction motors, from a single phase supply, with a range of phase converters, to devise a computer program to predict the Impedance requirement of the converter

network, over the whole slip range (0 - 1.0) and hence to obtain optimum performance and efficiency of the motor.

Manual and electronic phase converters are compared and contrasted. The study discusses future improvements that can be made with new power electronic devices.

CHAPTER 2

NETWORK PHASE CONVERSION USING INDUCTIVE AND CAPACITIVE ELEMENTS

The purpose of the static phase converter is to enable the operation of a 3-phase induction motor, connected to a single phase supply system [1].

3-phase voltages required for starting purposes, not necessarily perfectly balanced are derived from the single phase supply, by the action of a static phase converter. The phase converter consists of an external impedance connected between the open-circuited phase of the induction motor and one of the supply lines, as shown in Fig. 2.1.

For the single static element [2, 8], it is found that perfect balanced operation cannot be achieved if the motor power factor angle is less than 60°. If at standstill, the power factor happens to be 60°, then perfect balance can be achieved, by the use of a pure capacitance (of a value, depending on the standstill impedance). If it is greater than 60°, a resistance must be added, in addition to the capacitance (which increases losses). However, it is possible to produce perfect balanced conditions, at any speed or any motor power factor by using two static elements with slip-dependent values [3, 5]. See Figs. 2.2, 2.3 and 2.16.

2.1 Symmetrical Component Analysis of Single Element Phase Converter

The phase converter of Fig. 2.1 can be analysed by the use of symmetrical component analysis using the star configuration, although the Delta configuration is just as easy.

The component operator $a = \exp(j2\pi/3)$ or $-1/2 + j\sqrt{3}/2$

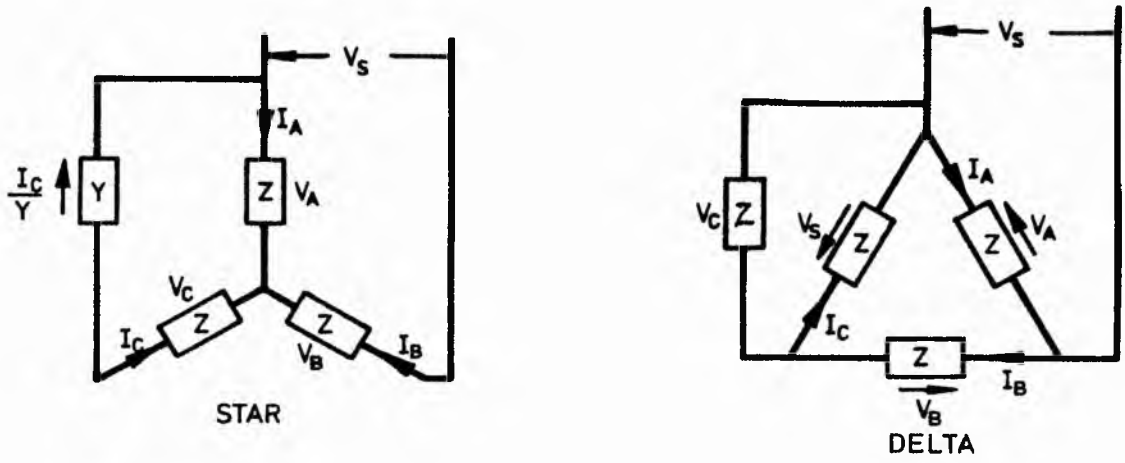

Fig. 2.1 Single element phase converter with star and delta configuration

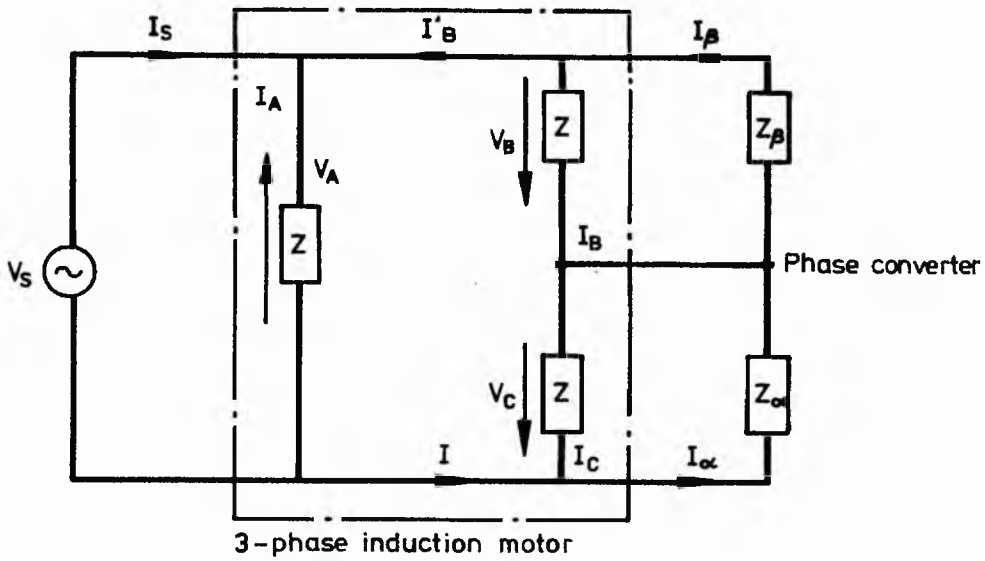

Fig. 2.2 Two element phase converter configuration

Using Kirchoffs laws:

The inspection equations are:-

$$I_A + I_B + I_C = 0 \tag{2.1}$$

$$V - V_A + V_B = 0 \tag{2.2}$$

$$V_A - V_C - I_C/Y = 0 \tag{2.3}$$

Phase and symmetrical components are:-

$$\left.\begin{aligned} V_A &= V_p + V_n + V_o \\ V_B &= a^2V_p + aV_n + V_o \\ V_c &= aV_p + a^2V_n + V_o \end{aligned}\right\} \tag{2.4}$$

and

$$\left.\begin{aligned} I_A &= V_PY_P + V_nY_n + V_oY_o \\ I_B &= a^2V_pY_p + aV_nY_n + V_oY_o \\ I_C &= aV_pY_p + a^2V_nY_n + V_oY_o \end{aligned}\right\} \tag{2.5}$$

Where V_n, V_p, V_o and Y_n, Y_p, Y_o are the negative, positive and zero sequence component and per phase admittances respectively.

It follows directly from equation (2.1) and (2.5) that the zero sequence system is zero for a star connection. Substituting symmetrical components into Eqn. 2.2 and 2.3.

$$V - V_p - V_n + a^2V_p + aV_n = 0$$

$$V = V_p(1 - a^2) + V_n(1 - a) \tag{2.6}$$

and

$$\begin{aligned} V_p + V_n - aV_p - a^2V_n - \frac{aV_pY_p}{Y} - \frac{a^2V_pY_n}{Y} &= 0 \\ V_p\left(1 - a - \frac{aY_p}{Y}\right) + V_n\left(1 - a^2 - \frac{a^2Y_n}{Y}\right) &= 0 \end{aligned} \tag{2.7}$$

Collecting terms and making V_n the subject of the formula.

$$V_n = \frac{V_p(Y + Ya - aY_p)}{(Ya^2 + a^2Y_n - Y)} \tag{2.8}$$

Substituting equation (2.8) into equation (2.6)

$$V = V_p(1 - a^2) + \frac{V_p\,(Y - Ya - aY_p)}{(Ya^2 + a^2Y_n - Y)}\,(1 - a)$$

Multiplying throughout by the denominator and collecting terms

$$V_p = \left(\frac{V}{1 - a^2}\right)\frac{Y\,(1 - a) + Y_n}{3Y + Y_p + Y_n} \qquad (2.9)$$

Similarly if equation (2.8) is transformed in terms of V_p and substituting into equation (2.6)

$$V_n = \left(\frac{V}{1 - a}\right)\frac{Y\,(1 - a) + Y_n}{3Y + Y_p + Y_n} \qquad (2.10)$$

If the particular case of standstill is considered, where $Y_p = Y_n = Y_s$ then:-

$$V_p = \left(\frac{V}{1 - a^2}\right)\frac{Y\,(1 - a) + Y_s}{3Y + 2Y_s} \qquad (2.11)$$

$$V_n = \left(\frac{V}{1 - a}\right)\frac{Y\,(1 - a) + Y_s}{3Y + 2Y_s} \qquad (2.12)$$

It can be seen from equations (2.11) and (2.12) that the values of V_p and V_n at standstill are different, so that the machine will produce a starting torque. Whereas a single phase induction motor produces no starting torque, of its own without the use of a second stator winding. Hence during the starting period, the motor operates as an asymmetrical 2-phase motor, connected to a single phase supply.

2.2 Symmetrical component Analysis of Two Element Phase Converter

The phase converter of Fig. 2.2. can be analysed by the use of symmetrical component analysis. Here the use of the Delta configuration is made, although the star configuration is just as easy to formulate. The symmetrical component operator $a = \exp(j2\pi/3)$

Using Kirchoffs laws:-

Inspection equations are:-

$$V = V_A \tag{2.13}$$

$$0 = V_A + V_B + V_C \tag{2.14}$$

$$V_C = I_\alpha Z_\alpha \tag{2.15}$$

$$V_B = I_\beta Z_\beta \tag{2.16}$$

$$I_\alpha = I_B + I_\beta - I_C \tag{2.17}$$

Phase and symmetrical components are:-

$$\left.\begin{aligned} V_A &= 1/\sqrt{3}\ (V_p + V_n + V_o) \\ V_B &= 1/\sqrt{3}\ (a^2V_p + aV_n + V_o) \\ V_C &= 1/\sqrt{3}\ (aV_p + a^2V_n + V_o) \end{aligned}\right\} \tag{2.18}$$

$$\left.\begin{aligned} I_A &= \frac{1}{\sqrt{3}}\left(\frac{V_p}{Z_p} + \frac{V_n}{Z_n} + \frac{V_o}{Z_o}\right) \\ I_B &= \frac{1}{\sqrt{3}}\left(\frac{a^2V_p}{Z_p} + \frac{aV_n}{Z_n} + \frac{V_o}{Z_o}\right) \\ I_C &= \frac{1}{\sqrt{3}}\left(\frac{aV_p}{Z_p} + \frac{a^2V_n}{Z_n} + \frac{V_o}{Z_o}\right) \end{aligned}\right\} \tag{2.19}$$

Where V_n, V_p, V_o and Z_n, Z_p, Z_o are the negative, positive and zero sequence voltage components and per phase impedance respectively.

Using equations (2.17) and (2.18) to eliminate I_α

$$V_C = Z_\alpha (I_B + I_\beta - I_C)$$

From equation (2.16) we have $I_\beta = V_B/Z_\beta$

Therefore, $V_C = Z_\alpha (I_B + V_B/Z_B - I_C)$

Substituting symmetrical components,

$$(aV_p + a^2V_n) = Z_\alpha \left(a^2 I_p + aI_n + \frac{a^2V_p + aV_n}{Z_\beta} - aI_p - a^2I_n\right)$$

$$0 = V_p \left[a - a^2\frac{Z_\alpha}{Z_\beta} - (a^2 - a)\frac{Z_\alpha}{Z_p}\right] + V_n \left[a^2 - a\frac{Z_\alpha}{Z_\beta} - (a - a^2)\frac{Z_\alpha}{Z_n}\right]$$

From equation (2.13)

$$V_p = \sqrt{3}\, V - V_n$$

$$V_n = \sqrt{3}\, V - V_p \qquad (2.20)$$

Thus, substituting for V_p equation (2.20) becomes:-

$$V_n = \frac{\sqrt{3}V \left\{a - a^2\frac{Z_\alpha}{Z_\beta} + (a - a^2)\frac{Z_\alpha}{Z_p}\right\}}{(a - a^2)\left\{1 + \frac{Z_\alpha}{Z_\beta} + \frac{Z_\alpha}{Z_p} + \frac{Z_\alpha}{Z_n}\right\}} \qquad (2.21)$$

Similarly,

$$V_p = \frac{\sqrt{3}V \left\{a - a^2\frac{Z_\alpha}{Z_\beta} + (a - a^2)\frac{Z_\alpha}{Z_p}\right\}}{(a - a^2)\left\{1 + \frac{Z_\alpha}{Z_\beta} + \frac{Z_\alpha}{Z_p} + \frac{Z_\alpha}{Z_n}\right\}} \qquad (2.22)$$

The negative sequence voltage is equated to zero, to determine the balance conditions.

$V_n = 0 = a - a^2 (Z_\alpha/Z_\beta) + (a - a^2) Z_\alpha/Z_p$, and hence

$$Z_p = \frac{(a - a^2)\frac{Z_\alpha}{Z_\beta}}{a^2 Z_\alpha - a Z_\beta} \qquad (2.23)$$

This is the impedance presented per phase to a balanced set of positive sequence voltages and if we assume:-

$$Z_p = R_p + jX_p$$

where R_p and X_p are resistive and reactive components of Z_p.

To minimise losses, it is desirable that Z_α and Z_β should be capacitive.

$Z_\alpha = -jX_\alpha$ and $Z_\beta = -jX_\beta$

$$R_p + jX_p = \frac{jX_\alpha\, jX_\beta\, (a - a^2)}{a^2 (jX_\alpha) - a (jX_\beta)}$$

$$= \frac{\sqrt{3}\, X_\alpha\, X_\beta}{a^2 X_\alpha - a X_\beta}$$

$$= \frac{\sqrt{3}\, X_\alpha\, X_\beta \left[1/2(X_\alpha - X_\beta) - j\sqrt{3}/2\, (X_\alpha + X_\beta)\right]}{X^2_\alpha + X^2_\beta + X_\alpha X_\beta}$$

Equating real and imaginary parts:-

$$R_p = \frac{\sqrt{3} X_\alpha X_\beta (X_\alpha - X_\beta)}{2\left(X^2_\alpha + X^2_\beta + X_\alpha X_\beta\right)}$$

$$X_p = \frac{-3X_\alpha X_\beta (X_\alpha + X_\beta)}{2\left(X^2_\alpha + X^2_\beta + X_\alpha X_\beta\right)} \qquad (2.24)$$

$$\text{but } \frac{X_p}{R_p} = -\frac{\sqrt{3}\,(X_\alpha X_\beta)}{X_\alpha - X_\beta}$$

OR

$$X_\beta = \frac{(X_p + \sqrt{3}R_p)X_\alpha}{X_p - \sqrt{3}R_p} \tag{2.25}$$

Substituting for X_β in equation (2.24)

$$X_\alpha = \frac{-j(X_p^2 + R_p^2)}{X_p + \sqrt{3}R_p} \tag{2.26}$$

and from equation (2.24)

$$X_\beta = \frac{-j(X_p^2 + R_p^2)}{X_p - \sqrt{3}R_p} \tag{2.27}$$

When X_α and X_β are plotted against slip, it can be seen that there is a balance point throughout the slip range. X_α is capacitive throughout the slip range and X_β must change from capacitive to inductive reactance at a slip of 0.22, when the motor is accelerating for the given motor parameters, as shown in Fig. 2.3. Hence the principle of the static phase converter is explained by the fact that X_α and X_β are effectively energy storage elements of variable reactance. Changes in reactance, give corresponding changes in I_α and I_β. The passive elements vary with the speed of the machine because the power factor and slip are different at starting, run up (acceleration) and full load. In simple terms the values have to change in order to compensate for any imbalance caused so that the motor has a balanced supply. In most of the earlier investigations, the researchers have carried out tests by choosing two optimum capacitor sizes, one for starting and another for running at normal speed [2, 3, 5]. However, recent research has been able to introduce systems that have automatic current demand sensors (electronic system) [3]. The phasor diagram for a two element phase converter is shown in Fig. 2.4.

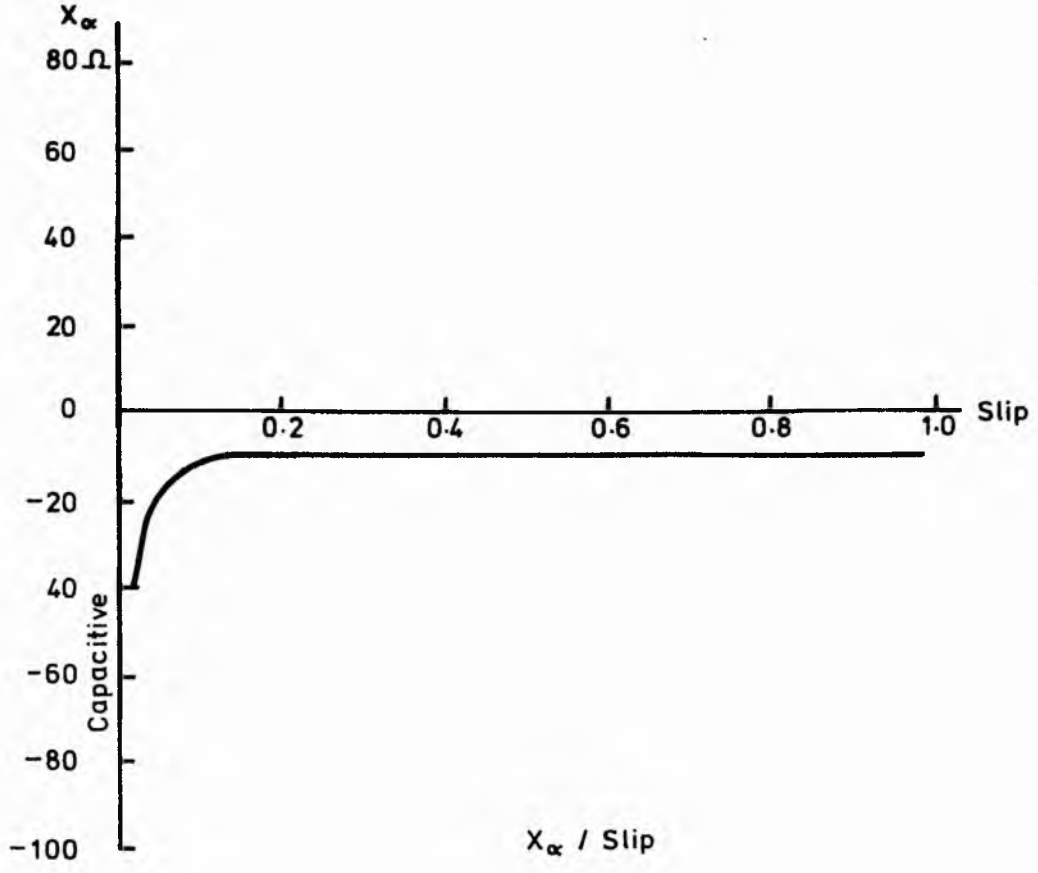

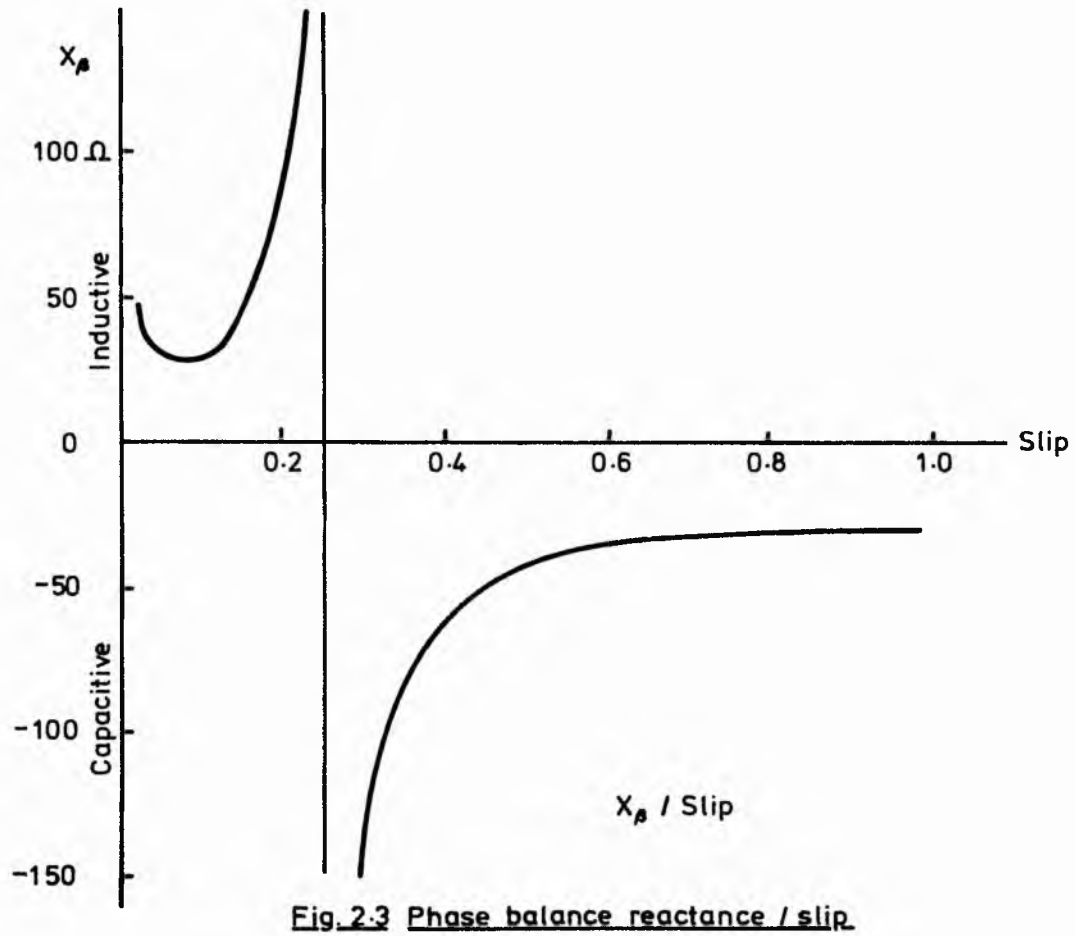

Fig. 2·3 Phase balance reactance / slip

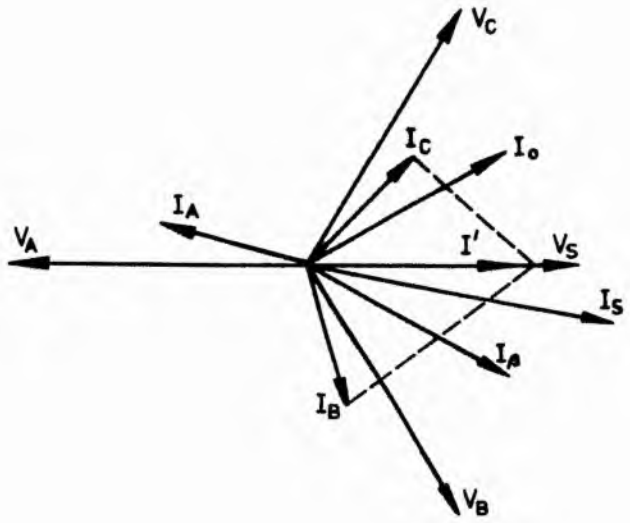

Fig. 2.4 Phasor diagram at balance for a two element phase converter

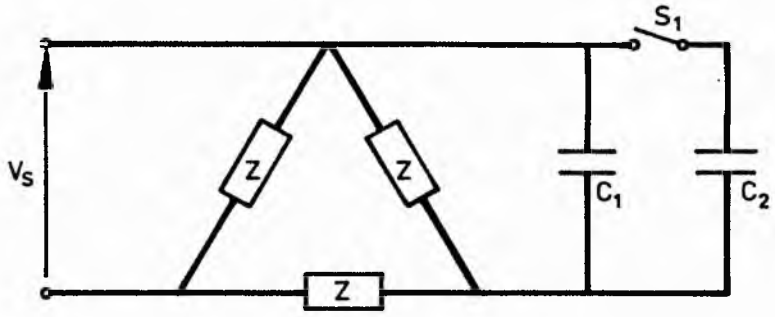

Fig. 2.5 Switched Capacitance (Two values)

2.3 Possibilities of Fulfilling. Induction Motor Requirements Using:

2.3.1. Fixed and Switched Values of Capacitance Alone:-

From the very early research into this field, when investigations found an optimum single capacitor size, it was found that, although the operation was satisfactory at the start, it would result in heavy currents and high torque pulsations as the motor accelerates [1, 2, 4, 5]. Therefore, it was concluded that a two capacitor network as shown in Fig. 2.5., be used with one capacitor value for starting and the other for running. The transition being enabled by a sensitive relay, that switches from one to the other when the motor comes up to speed. An autotransformer may be used to obtain a more suitable capacitor voltage or to adjust it to a particular operating speed (idea used by Ronk Industries). It was found that the motor operating, from a phase converter should be rated at 2/3 of the 3-phase motor rating.

The 3-phase motor must be derated when operated in this way otherwise a motor operated in this manner will have a shorter life and not provide the satisfactory margin for overloads and line voltage variation [1].

Further research has shown that ideally the impedance should vary continuously with the speed [2] and that in general, the best performance is obtained when the starting conditions approach those of balanced 3-phase operation. The ideal combination consists of a machine having a standstill phase angle of 60° together with a pure capacitor impedance of $\sqrt{3}$ times the standstill impedance per phase of the machine. Although relatively satisfactory performance can be realised with the fixed and switched capacitance alone, it does have its limitations especially when the phase angle is below 60°. (It will be shown later, that the introduction of inductance can solve this problem.)

As an example, a 3.7 kW, 3-phase, 4-pole, 50Hz, 415V 7.6A delta connected motor was analysed. Fig. 2.6., which was formulated by finding p.u. values of X_c to give minimum unbalance at different speeds. From this, suitable values of starting and running capacitors, were determined, e.g. for this motor;

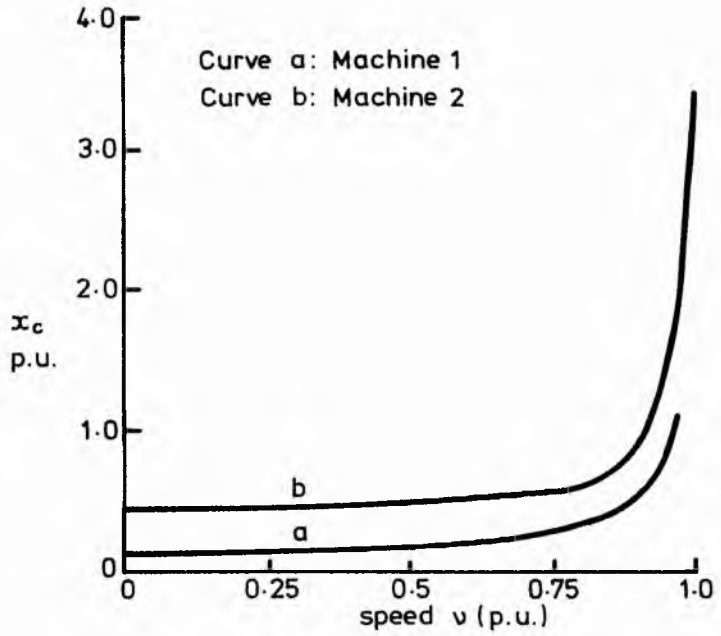

Fig. 2·6 x_c (p.u.) for minimum unbalance at different speeds

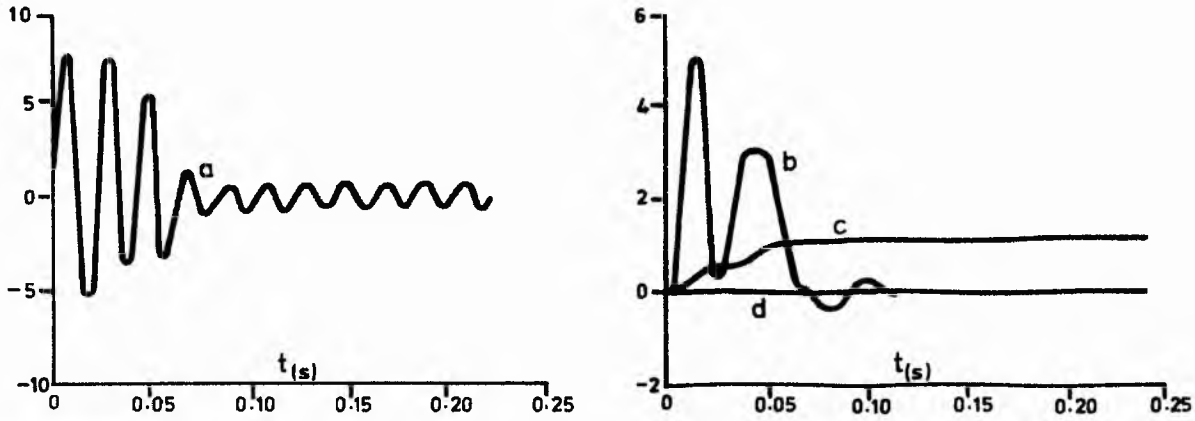

Fig. 2·7 Run-up Transients in P.U. with balanced supply on No Load. (Machine 1)
a) Stator current b) developed torque c) speed d) load torque.

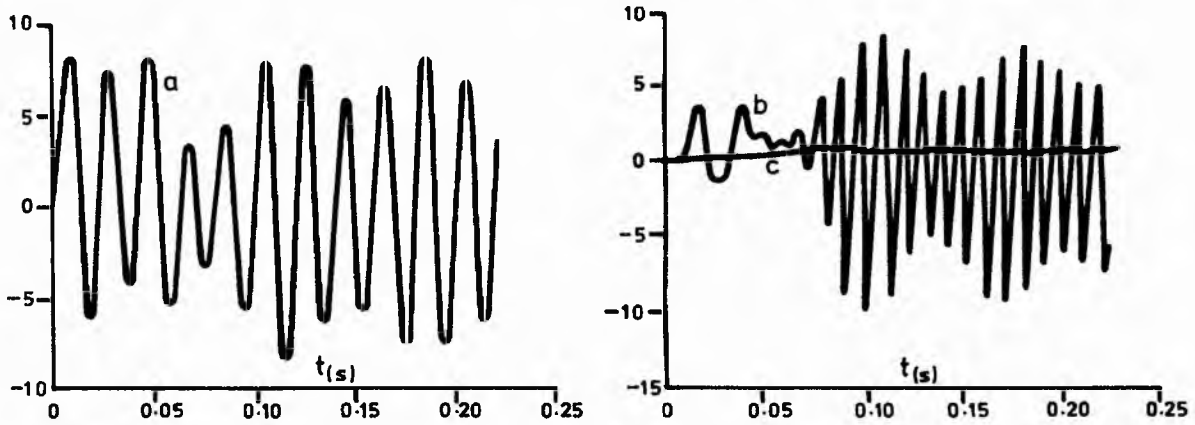

Fig. 2·8 Run-up Transients in P.U. with single-phase supply on No Load. (Machine 1)
$x = 0{\cdot}118$ P.U. throughout run-up a) Stator current b) torque c) speed

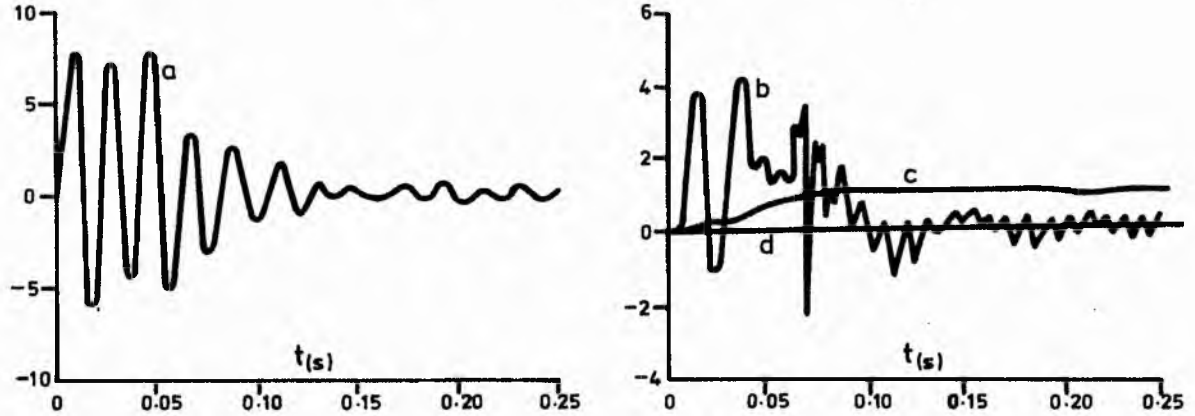

Fig. 2·9 Starting Transients in P.U. with single-phase supply on No Load
x_c(start) = 0·118 P.U. x_c(run) = 119 RU.
a) current b) developed torque c) speed d) load torque

Transient Pattern for Single Element Phase Converter on No Load.

X_c (start) = 0.118 p.u., X_c (run) = 1.19 p.u.

Fig. 2.7. shows the transient run-up patterns at no-load (with only friction torque) on a balanced supply, while Fig. 2.7. indicates the pattern with a single-phase supply and the starting capacitor (X_c = 0.118) used throughout. Fig. 2.9. shows similar results to Fig. 2.7. with two capacitors chosen using Fig. 2.6.

Comparing Fig. 2.8. and Fig. 2.9. it is easy to conclude that single capacitor operation, though satisfactory at starting, results in heavy currents and high torque pulsations as the motor gathers speed. These undesirable features are greatly reduced with two capacitors, as is evident from Fig. 2.9. Comparing Fig. 2.7. and Fig. 2.9. very similar current patterns can be seen in the two cases while small torque pulsations are observed with a single phase supply in steady state operation. The starting torque patterns do not differ significantly but there is a slightly lower-rate of speed build-up under single phase operation.

Fig. 2.10. and Fig. 2.11. show transient patterns with balanced output from a single-phase supply (two capacitors) and on load. No appreciable difference in the starting current pattern is observed. However, there is a 30% increase in steady state current. An oscillatory torque component of 0.3 p.u. prevails under single phase operation, as the motor reaches steady speed, but this is not evident under the balanced supply. The oscillatory torque components are due to the interactions of forward and backward airgap fields.

Fig. 2.11.c. shows the transient voltage build up across the terminal capacitor. A steady state r.m.s. voltage of 0.95 p.u. is indicated. The sudden rise in curves (b) and (c) of Fig. 2.11., at the instant of about 0.07 sec is due to the change of capacitor, from start to run values.

The capacitors have been chosen to minimise unbalance (i.e. the ratio of negative to positive sequence voltage) at the appropriate speeds. However, even with the best choice of starting and running capacitors, the amplitude of steady-state torque pulsations can only be limited to about 0.3 p.u. An improvement can be made, by having a two element static phase converter as shown in Fig. 2.2. and Fig. 2.17.

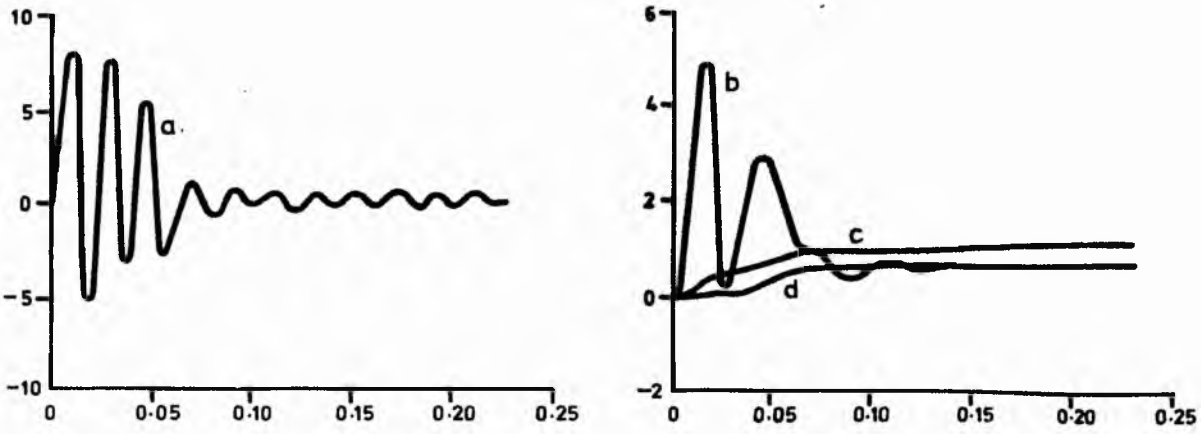

Fig. 2·10 Transients with balanced supply on load (Machine 1) a) Stator current b) developed torque c) speed d) load torque

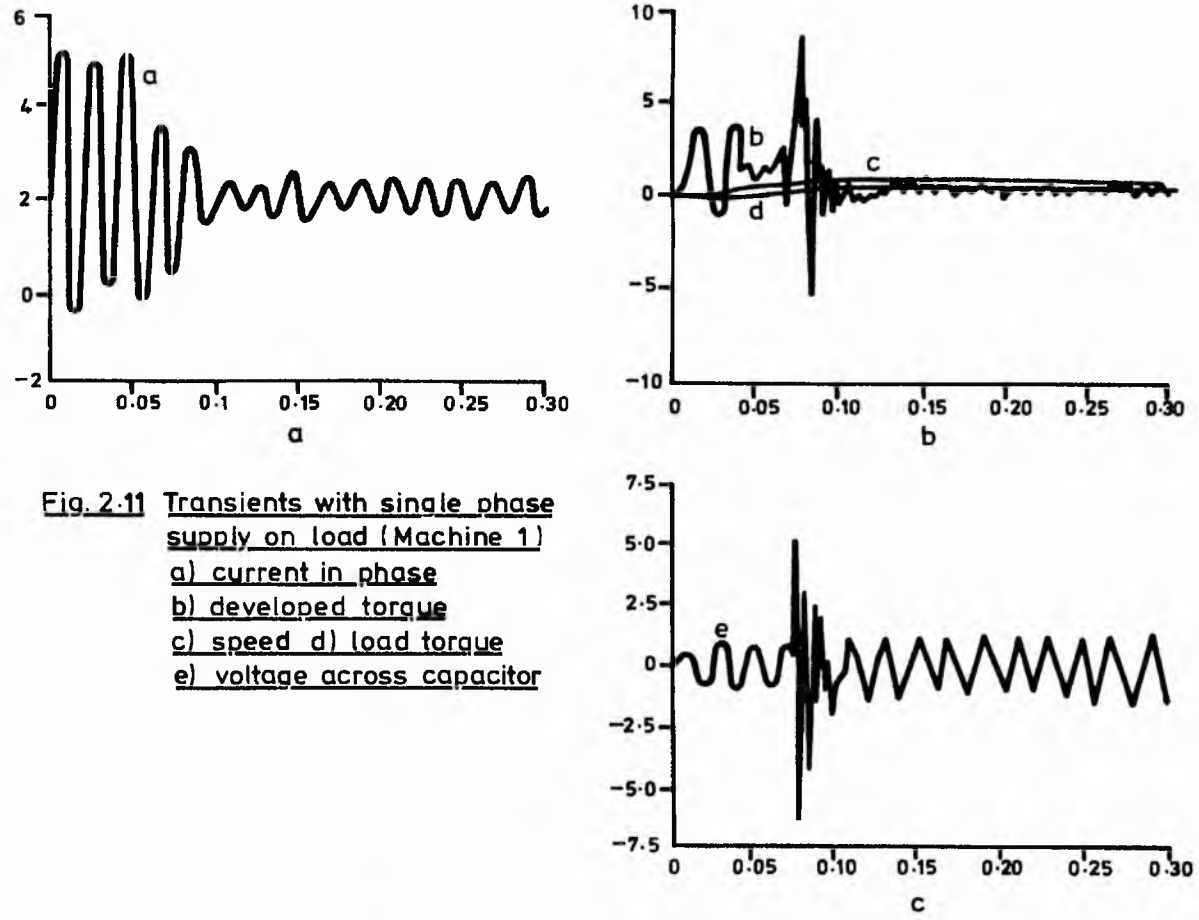

Fig. 2·11 Transients with single phase supply on load (Machine 1)
a) current in phase
b) developed torque
c) speed d) load torque
e) voltage across capacitor

Transient Pattern for Single Element Phase Converter on Load

Most of the earlier researchers have chosen the size of a capacitor for the speed range on the basis of:-

(a) Minimum unbalance (ratio of positive/negative voltage) U.

(b) Minimum or zero negative sequence voltage.

A later paper [6] has shown that criteria to be considered in determining the size and rating of the phase balancer capacitors, further to the above are:-

(c) Maximum torque.

(d) Maximum power factor.

A study was carried out on two motors whose parameters are as follows:-

	MOTOR A	MOTOR B [½ HP, 60 Hz]
V (line to line)	110	380
R_1 (Ω)	0.074	22.5
R_2 (Ω)	0.144	20.17
X_1 (Ω, line frequency)	0.232	25.8
X_2 (Ω, line frequency)	0.232	25.8
X_m (Ω, line frequency)	6.00	150.7
Mechanical & Iron losses	-	48.7W

From Fig. 2.12., it can be seen that the ratio of V_p/V_n, attains a maximum value at $X_c = 1.0\Omega$ and at the point of maximum ratio the phase voltages are nearly equal in magnitude.

The output torque has a maximum value at $X_c = 0.8\Omega$ and motor efficiency has a maximum value at $X_c = 1.0\Omega$

Now, in order to analyse the motor performance with criteria (c) and (d), a plot of X_c (capacitive impedance) for maximum U, maximum torque and maximum power factor against slip for motor (A) and motor (B) was computed and is shown in Fig. 2.13. The hatched area determines the possible range of

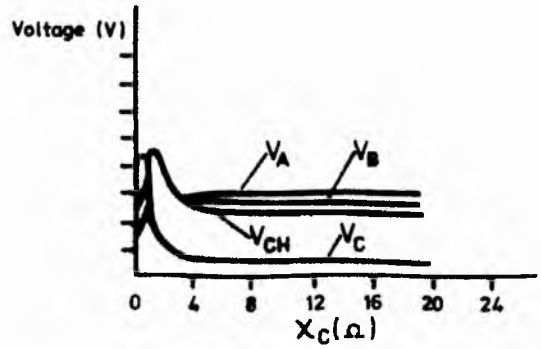

Variation of stator phase voltages versus phase balancer capacitor reactance at slip of 0.5 (Motor A)

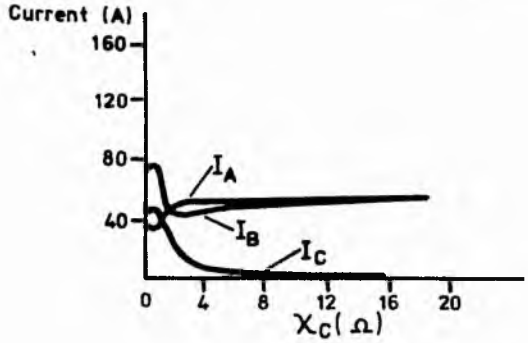

Variation of torque and Unbalance ratio (U) versus phase balancer capacitor reactance at slip of 0.5 (Motor A)

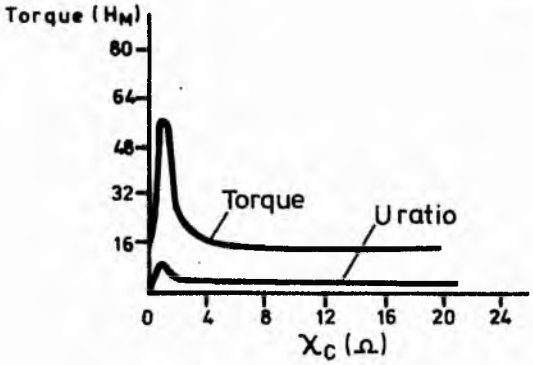

Variation of torque and Unbalance ratio (U) versus phase balancer capacitor reactance at slip of 0.5 (Motor A)

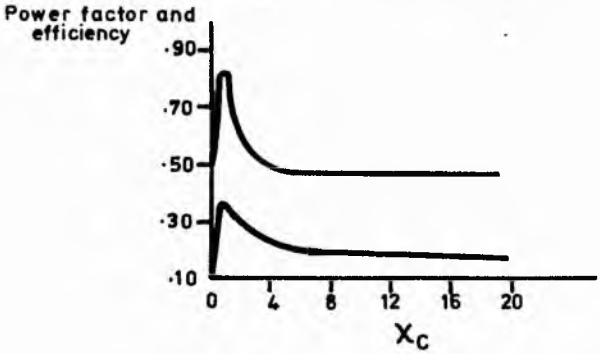

Variation of power factor and efficiency versus phase balancer capacitor reactance at slip of 0.5 (Motor A)

Fig. 2.12 Performance characteristics versus capacitor values

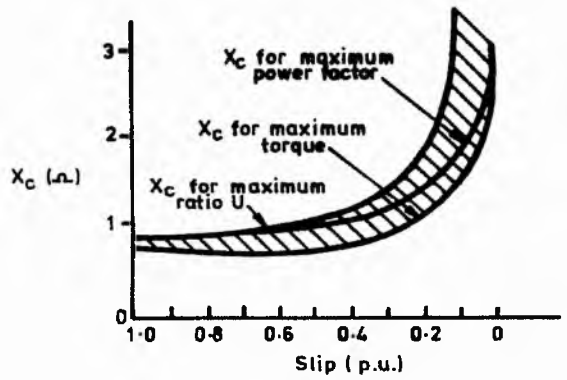

Variation of phase balancer capacitor reactance versus slip for maximum torque, ratio U and power factor (Motor A)

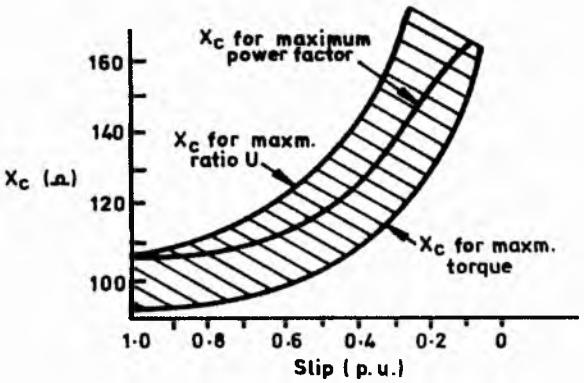

Variation of phase balancer capacitor reactance versus slip for maximum torque, power factor and ratio U (Motor B)

Fig. 2·13

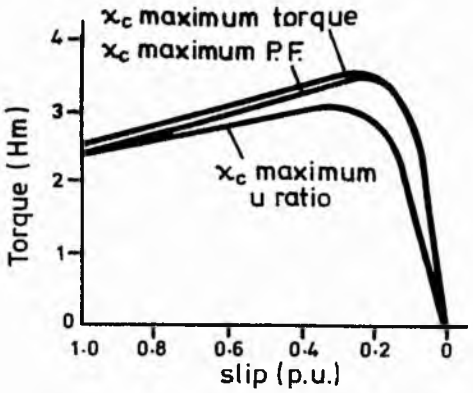

a) Torque / slip variation for motor B, using maximum torque, maximum ratio u and maximum power factor capacitors

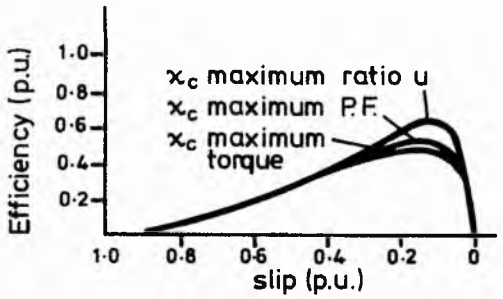

b) Variation of efficiency versus slip for motor B using maximum torque, maximum ratio u and maximum power factor capacitors

Fig. 2·14

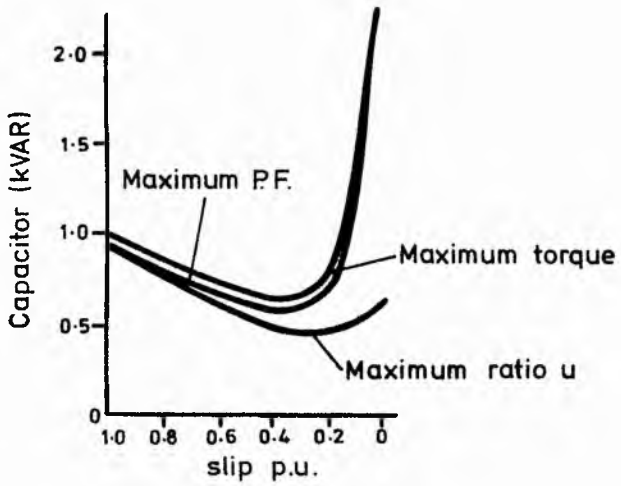

Fig. 2.15 Variation of capacitor kVAR versus slip for motor B. for maximum torque, ratio u and power factor

choice of X_c. Also, it can be observed that the capacitive reactance yielding maximum torque is lower than the corresponding maximum voltage. Capacitive reactance for maximum power factor has intermediate values, being equal to that of maximum U at standstill and approaching that of maximum torque at speeds close to synchronous speeds.

From Fig. 2.14.a., which is a torque/speed relationship with optimum capacitor values, it is evident that torque values obtained by using maximum torque capacitors are higher than those achieved by the use of the maximum power factor ones, but on the other hand maximum U capacitors yielded the lowest torque figures. Hence using maximum torque capacitors achieved an increase in torque of 50% compared with that achieved by maximum U capacitors, at speeds near synchronous and 5% at starting. Fig. 2.14.b. is a plot of motor efficiency against slip and shows that maximum U capacitors yielded the highest values of efficiency followed by maximum power factor and finally maximum torque capacitors achieved the lowest efficiency. The choice of capacitor is mainly controlled by its volt-ampere rating, which is predicted for motor (B) and shown in Fig. 2.15. This shows that the volt ampere rating for the maximum torque capacitor possessed the highest value at standstill. However, it drops to quite a low level, reaching that of maximum U at higher speeds.

Therefore, it can be concluded that phase balancer capacitors may be chosen in a way to achieve either maximum torque or power factor or positive to negative sequence ratio (U).

Using capacitors to yield maximum torque will in turn lead to an increase in torque capabilities for the motor with added running and initial costs, since its volt ampere rating is high combined with lower values of apparent efficiency at low speeds. Hence, maximum torque capacitors are recommended for motors subjected to loads of short duty cycles, where increased phase voltages may result in stator winding damage.

2.3.2. Fixed and Switched Values of Capacitance and Inductance

Research described in references [3.5] has shown that phase balance may be achieved over the whole slip range, whether the load has a leading or lagging power factor. This is only possible with a two element static phase converter (Fig. 2.2.). Fig. 2.16. and Fig. 2.3. show the variation of Z_α and Z_β as functions of the load power factor and slip respectively for the machine parameters given.

Fig. 2.16. is a plot of Z_α and Z_β (divided by the per phase impedance of the machine to positive sequence voltage) against the power factor angle ϕ. This plot clearly shows that phase balance may be achieved, whether the load is of leading or lagging power factor.

The configuration shown in Fig. 2.17. was used where switch S_1 is closed for starting purposes and open under full load conditions. S_2, switching in the capacitor C_2 and inductor L_2 for starting and full load respectively. For purely practical reasons a 4-pole 3kW wound motor machine is selected, in the delta mode.

Fig. 2.18. shows the per-phase impedance and Fig. 2.19. the phase angle plotted against speed. Fig. 2.20. shows the torque/speed curves appropriate to the two different values of rotor resistance and Fig. 2.21. the variation of Z_α and Z_β required for balance. Balance was achieved over the whole speed range (0 - 1500 r/m) for two values of rotor resistance, one being that with no added external resistance, the other being the value which produced peak torque at standstill. The machine will obviously not be balanced at intermediate speeds, S_1 and S_2 being switched at speeds which give an optimum run characteristic but this is likely to be an acceptable compromise for most applications (as the transient waveforms showed earlier).

Such a run-up characteristic is displayed in Fig. 2.22., where the composite wound-rotor torque/speed curve is regarded as the ideal. This notion of an ideal was very much a function of the comparative values of capacitance of Z_α, with and without added rotor resistance, the higher resistance requiring a far more realistic value at starting. The machine was thus started and run at low speeds, with added rotor resistance and with Z_α and Z_β, adjusted for balance at standstill.

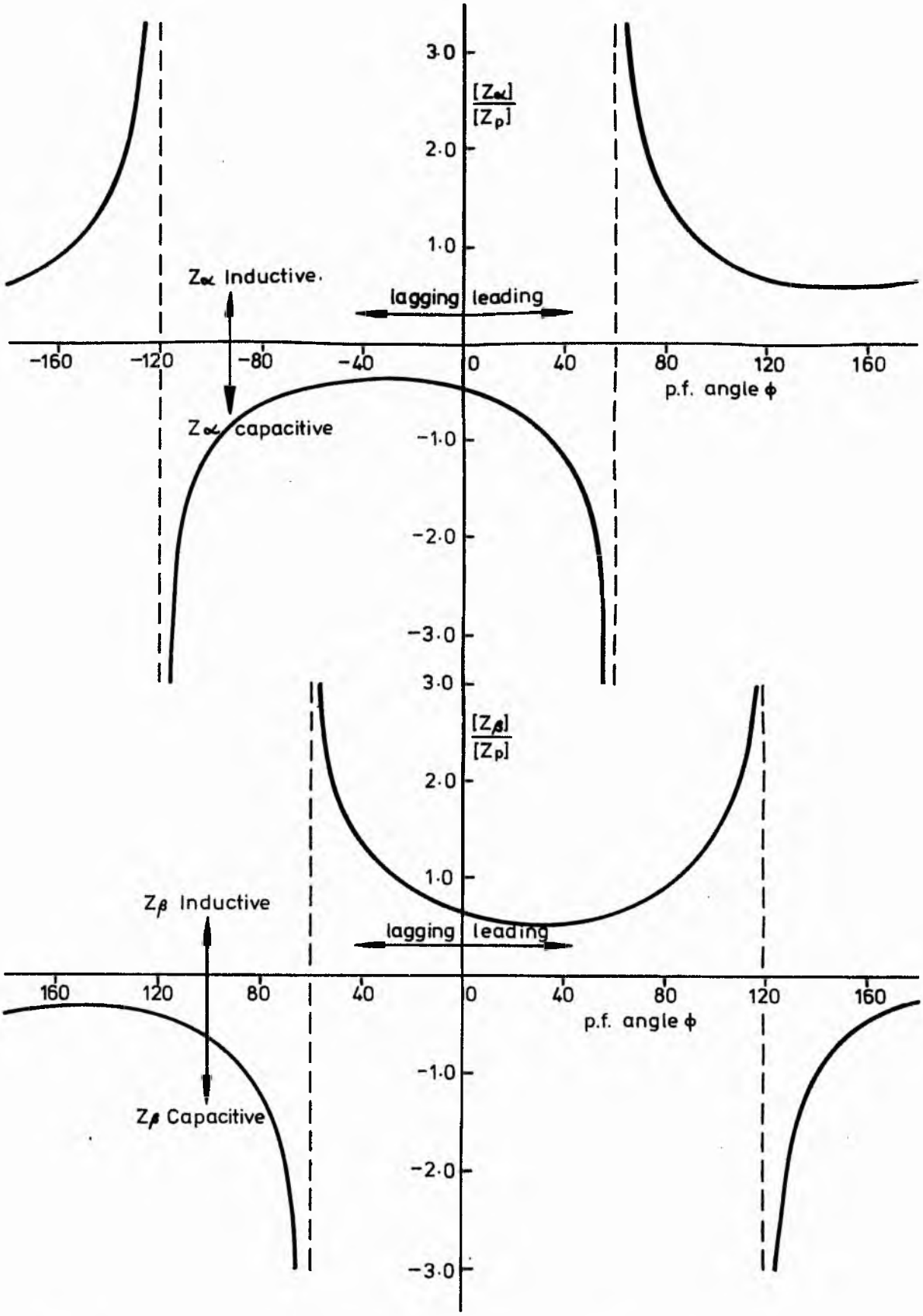

Fig. 2·16 Variation of Z_α and Z_β for balance with varying load power factor

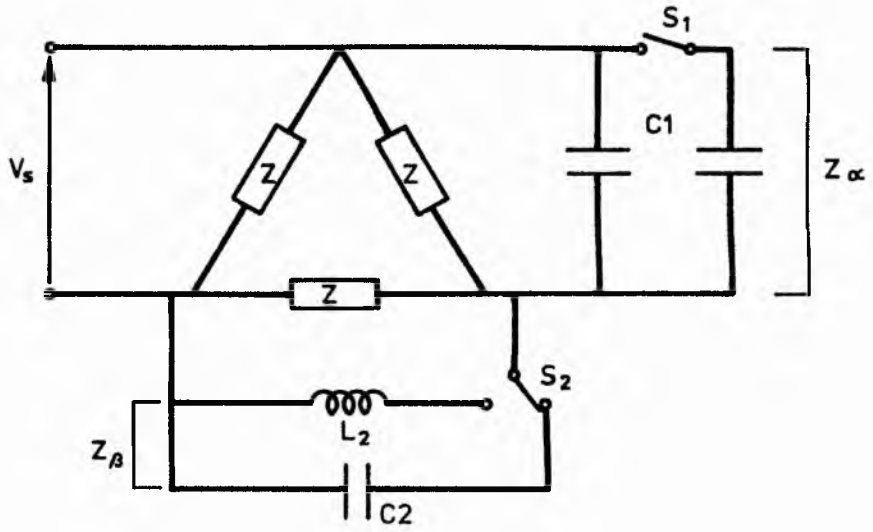

Fig. 2.17 Arrangement for balance at standstill and full load

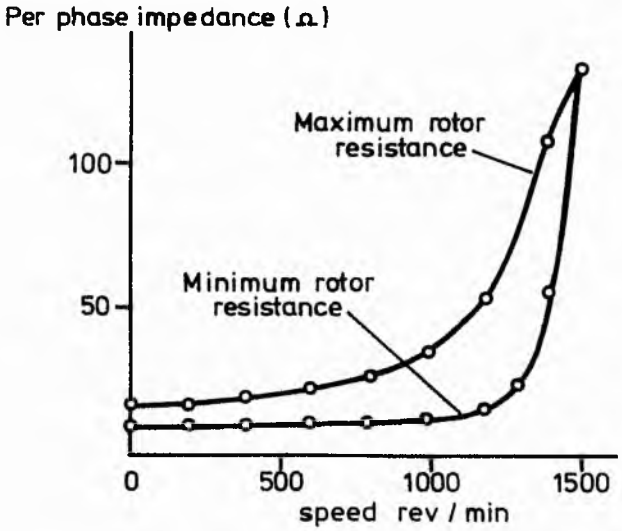

Fig. 2·18 Impedance against speed for minimum and maximum Rotor resistance

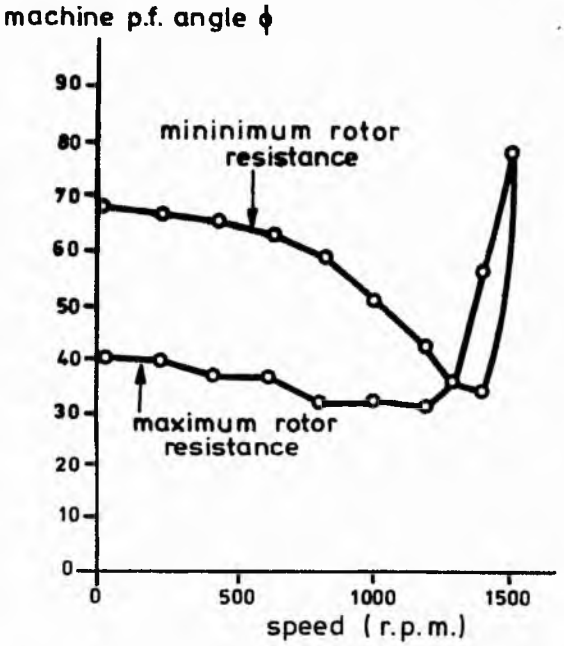

Fig. 2·19 Power factor against speed for minimum and maximum Rotor resistance

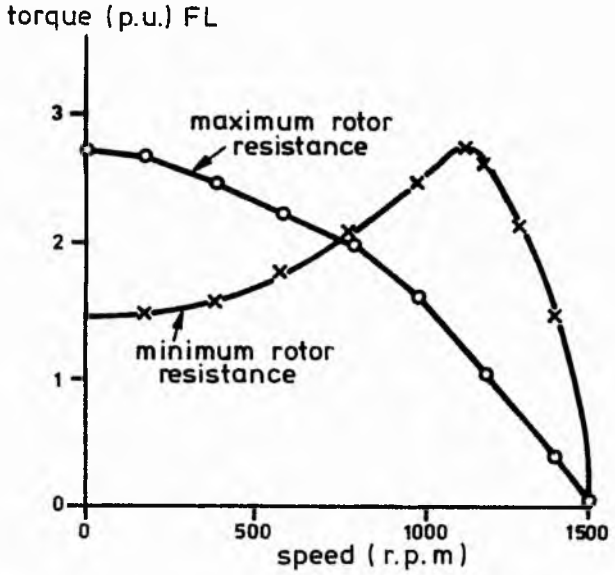

Fig. 2·20 Torque against speed for minimum and maximum Rotor resistance

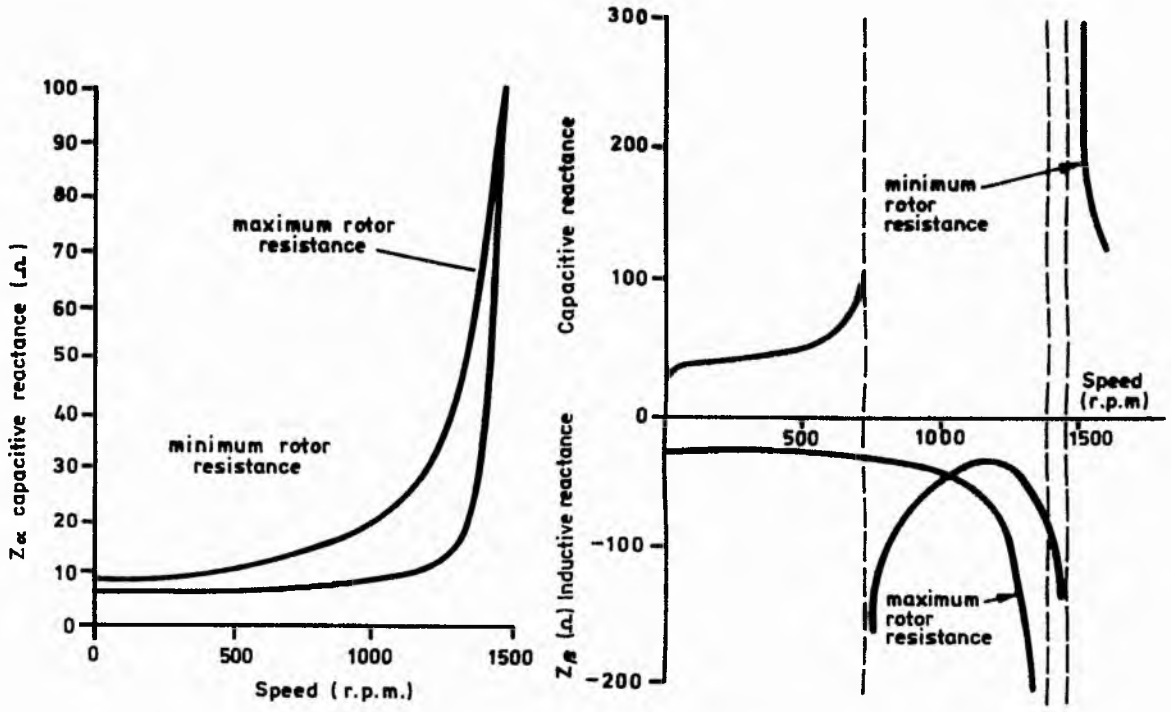

Fig. 2·21 Variation with speed of Z_α and Z_β required for balance

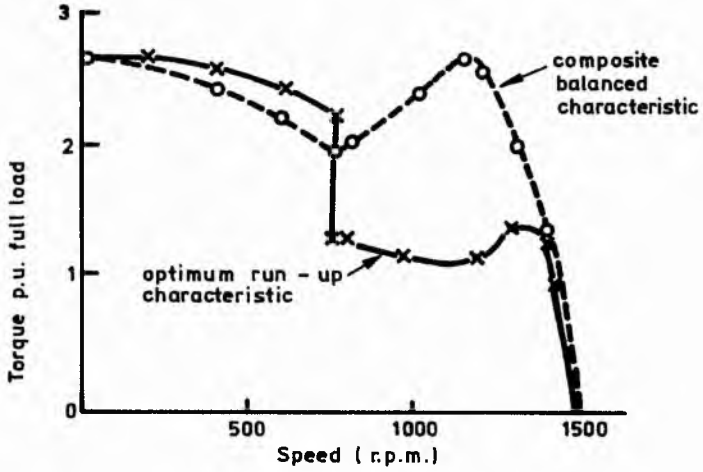

Fig. 2·22 Composite balanced characteristic and optimum run - up characteristic

At the cross-over point (i.e. 760 r/m) the added rotor resistance was removed and Z_α and Z_β were readjusted to the values appropriate for balance at the rated speed, the test then being continued, as shown in Fig. 2.22. On examination of this graph, it would appear that the change from start to run values of Z_α and Z_β might have been made, with some advantage at a higher speed than the crossover point of the torque/speed characteristic. In practice however, this will depend on the particular machine and load characteristic and in the degree of unbalance that can be tolerated during acceleration. For this machine, it is found that appropriate values for C_1, the capacitance of Z_α are 368μF and 462μF with and without added external rotor resistance respectively.

The inductive or capacitive reactances which make up Z_β are of much smaller size. The standstill inductance and capacitance required with and without external rotor resistance being 82mH and 93μF respectively.

A cost analysis example:-

Typical cost of single and 3-phase 240V single-cage machines of 5.5kW rating plus all necessary control equipment.

3-phase machine.

Typical Z_p at starting $2.0 + j4.0\ \Omega$

Typical Z_p at Full Load $2.0 + j15\ \Omega$

So for perfect balance,

at starting	C_1	=	1200μF
	C_2	=	85μF
at full load	C_1	=	250μF
	L_2	=	100mH

Since the starting torque of the single phase machine is rarely, if ever, comparable with that of a balanced three-phase machine of similar rating, it is suggested that the starting value of C_1 may be reduced to a more manageable proportion, with the introduction of a degree of unbalance while still maintaining a superior performance, especially at full load.

A more realistic economic comparison between a 3-phase motor operative with a phase converter and a single phase machine is:-

3-phase machine

C_1 (= 600μF)	£90
C_2 (= 85μF)	£15
L_2 (= 100 mH)	£45
3-phase motor	£240
Starter	£150
Total	£540

Single phase machine

Typical C(= 400μF)	£60
Single phase motor	£495
Starter	£180
Total	£735

For ratings over 0.5kW, 3-phase machines are certainly cheaper and generally easier to obtain. Even if a 3-phase machine has to be downrated to compensate for any unbalance introduced through compromise, with regard to the values of Z_α and Z_β, the economics are still persuasively attractive.

A 2.2kW 3-phase motor, for an example, costs less than a single phase machine of half the rating and this continues to be the case up to the rating limit of single-phase motors, as shown by the example above.

2.4. Switching

Switching in, as appropriate to the motor conditions, discrete values of capacitance, is one way of maintaining balance for a transient load. The test results for Motor 1 of Section 3.2.2. are used as an example.

The ranges of motor conditions over which fixed values of capacitance (C_α and C_β) will give a satisfactory balance. C_α and C_β are determined from Fig. 3.5. and are given in Table 2.1 and Table 2.2.

a) Starting condition : $C_\alpha = 100\ \mu f \quad C_\beta = 0$

b) Running condition :

Slip Range	$C_\alpha \mu F$	$C_\beta \mu F$
0.05 - 0.08	37.2	6.5
0.08 - 0.09	37.2	5.5
0.09 - 0.1	37.2	4.3

TABLE 2.1.

The switching is done by relay. The circuit configuration and the required relay combinations for each slip range are shown in Fig. 2.23. and Table 2.2. respectively.

	Slip Values	Relays			
		RL_1	RL_2	RL_3	RL_4
Running Condition:	0 - 0.08	0	1	1	1
	0.08 - 0.09	0	1	0	1
Starting condition:	0.09 - 0.1	0	1	0	0
	1.0	1	0	d	d

0 = Open Relay

1 = Closed Relay

d = Don't care, since they are latched to previous condition

Table 2.2 Relay Combinations Required for Appropriate Switching of Capacitors.

The decision when to operate a relay is made by sensing the motor slip using a tacho. The tacho gives a linear voltage output proportional to speed and slip s = 1 - speed/synchronous speed. When the slip exceeds or falls below a prescribed level, the relay operates appropriately. The electronics is considered in Section 2.4.1.

Due to the capacitor requirements for balance with the experimental motor the above solution is made simple, requiring 4 capacitors and 4 combinations thereof. For a more realistic motor many more combinations are required. Since 4 capacitors have 16 combinations, the balance requirements can be satisfied with appropriate combinational logic and A to D conversion of the tacho output.

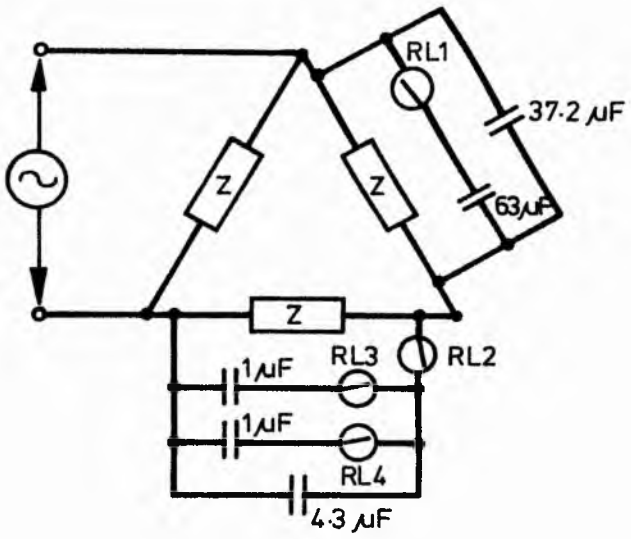

Fig. 2·23 Circuit Configuration for Relay Switching of Capacitors (Four values)

2.4.1. Switching Control Electronics

The tacho voltage V_T is fed into an op-amp comparator and compared to a set reference voltage V_{REF}. The comparator output drives a F.E.T., energising a relay and thus switching in or out a capacitor. The circuit diagram is shown in Fig. 2.24. The comparator is set such that:
if $V_T < V_{REF}$ the FET is OFF and the relay is in its normal state;
if $V_T > V_{REF}$ the FET is ON and the relay is energised.

Some Design Notes

(1) It is necessary for the transition of the comparator output from high to low, (or vice versa), to be smooth and fast thus eliminating relay flicker. This occurs when the applied voltage approaches the relay pull-in voltage. At this voltage the relay makes and breaks contacts successively, causing voltage spikes in the system, harmonics and excessive contact wear.

To eliminate this, the V_T input to the comparator is smoothed by a RC filter (Fig. 2.24.) and the operational amplifier hysteresis is made broad to further remove the effect of any noise on the input. A Schmitt trigger may be used to quicken the transition period.

(2) Once the motor is running in its working range, the large starting capacitance is no longer required. So the output of the appropriate comparator (A) is latched high once the running conditions are met (Fig. 2.24.).

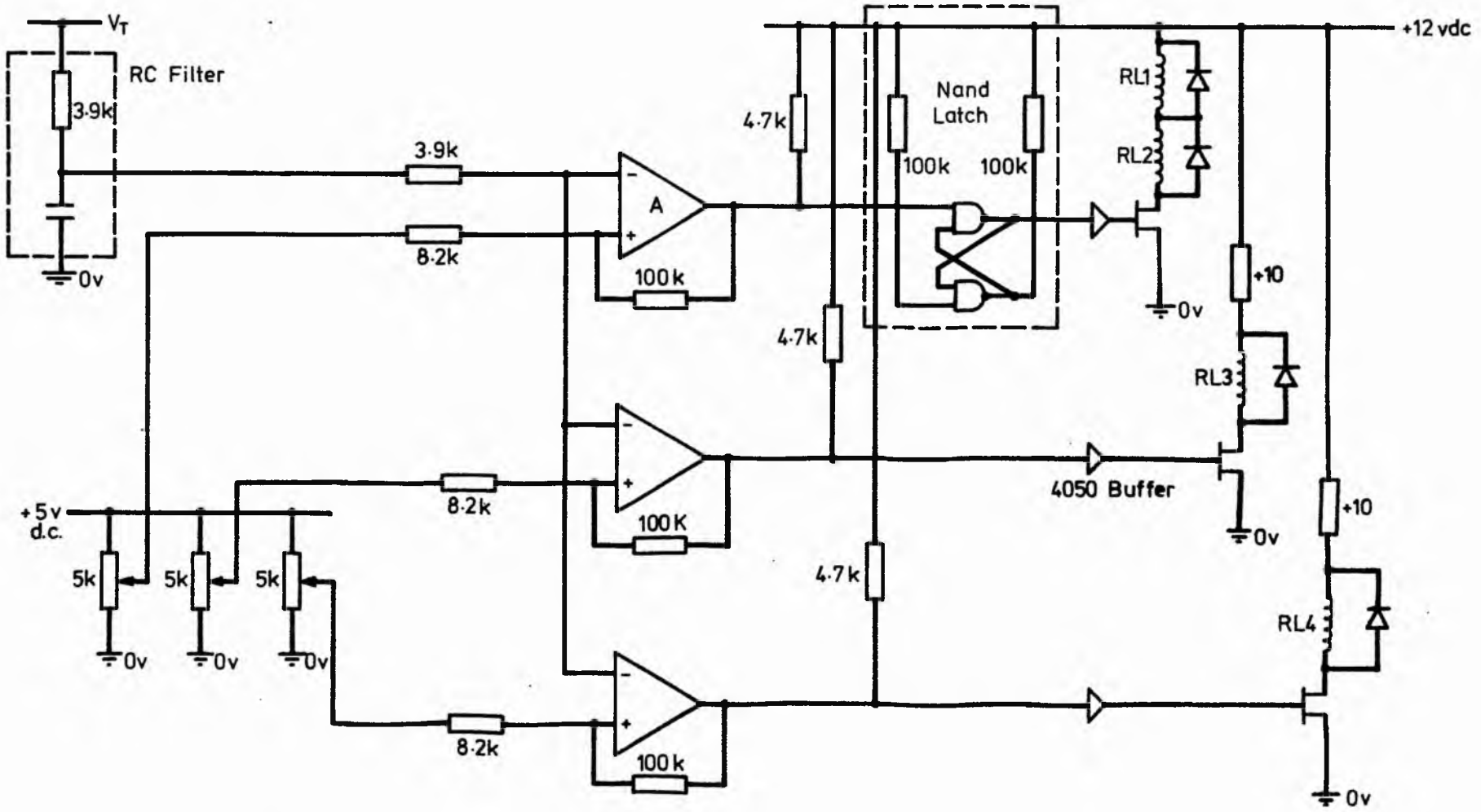

Fig. 2.24 Circuit Diagram for Relay Control Electronics

CHAPTER 3

INDUCTION MOTOR PERFORMANCE ON A STATIC PHASE CONVERTER

Balanced 3-Phase Conversion by Static Phase Converter

The requirement for balance is that the stator voltages V_A, V_B and V_C (Fig. 2.2.) are phase displaced by 120° (Fig. 3.1.) and equal in amplitude. It has been shown in Chapter 2, that it is theoretically possible to balance the stator voltages for any load impedance by using the correct inductance and capacitance values for Z_α and Z_β [3, 5, 9]. In a static phase conversion, the phase displacements are made by the reactive components Z_α and Z_β (Fig. 2.2.). The values of the corresponding reactances X_α and X_β required for balanced operation are obtained by symmetrical component analysis (as shown in Chapter 2).

A summary of the result is given below:-

$$X_\alpha = \frac{-j\left(X_p^2 + R_p^2\right)}{X_p + \sqrt{3}R_p}$$

$$X_\beta = \frac{-j\left(X_p^2 + R_p^2\right)}{X_p - \sqrt{3}R_p}$$

$$\text{Where, } R_p = \frac{R_s X_m}{X_s + X_m} + \frac{R'_r}{S} \qquad (3.1)$$

$$X_p = \frac{X_m^2}{X_s + X_m} + X'_r$$

Where the suffix s refers to the induction machine stator, r the rotor and m the magnetising circuit. A full outline of the induction motor parameters is given in Appendix A.

3.1. Ideal Requirement of Impedances Z_α, Z_β as Functions of Slip

From the exact balance equations for X_α and X_β, it should be noted that

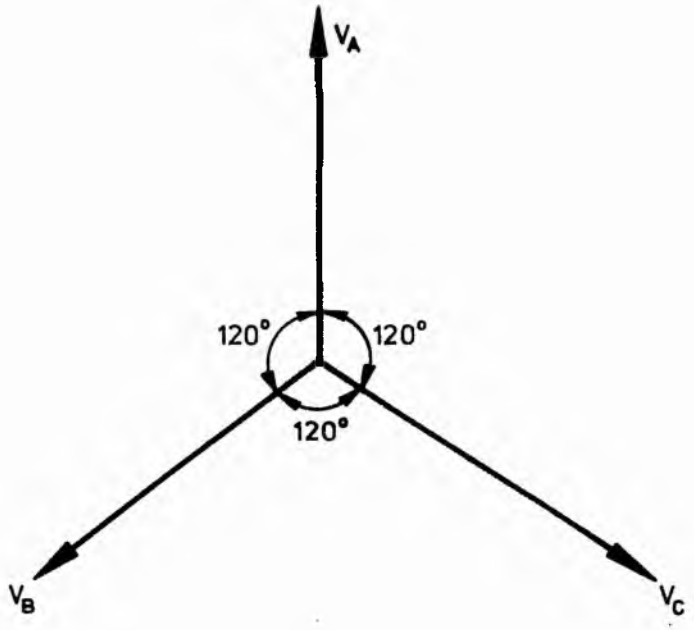

Fig. 3.1 Balanced phase displacement of stator voltages

the equation for X_β, gives a special case in which a single element phase converter achieves balance if $X_\beta \rightarrow \infty$

However, as can be seen from Fig. 2.3., X_α is capacitive throughout the slip range. X_β generally changes from capacitive to inductive reactance. Although for the motor under analysis, the reactance changed from capacitive to inductive reactance at a slip of 0.22 while the motor is accelerating. Thus, the machine parameters determine the phase converter parameters and the induction motor behaviour. According to [3], if a machine with a higher rotor resistance is used, the value of C_α can be reduced by a further 50% and C_β may be omitted.

3.2. An Experimental Converter Using Fixed Values of Capacitance and Inductance

MOTOR 1

A.C. 3-phase, 4 pole, squirrel cage I.M.

Delta connected, 240v supply

Power rating 0.6 h.p.

Jay-Jay Lloyd teaching machine

The parameters of the equivalent circuit, Fig. 3.2. were obtained from the standard tests (see Appendix A). A summary of the test parameters is given below:-

$X_e = X_s + X'_r$ = 49 Ω

R_m = 856.9 Ω

X_m = 143.8 Ω

R_s = 17.86 Ω

R'_r = 17.14 Ω

It is assumed that $X_s = X'_r$ since for an induction motor, they cannot be split experimentally. Hence, $X_s = X'_r = 24.5$ Ω.

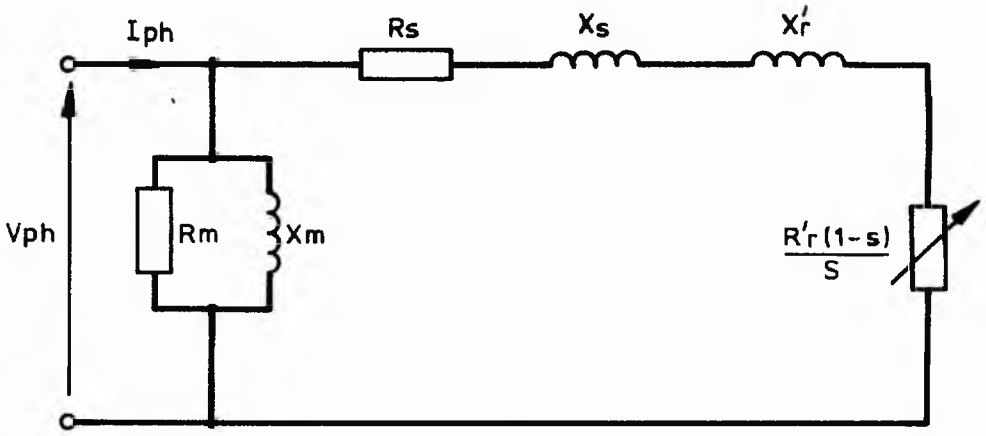

S	:	Slip valve
Rs, Xs	:	Stator resistance and reactance
R'r, X'r		Rotor resistance and reactance referred to the stator winding
Rm, Xm	:	Represents Magnetic and Iron losses
Vph, Iph	:	Per phase voltage and current

Fig. 3.2 Equivalent Circuit of One Stator Winding, for a Cage Induction Motor

FOR MOTOR 1 Experimental Results

Torque in Newton Meters	Slip in RPM	Speed in RPM	W_1 Watts	W_2 Watts	W_1+W_2 Watts In	Line Current in Amps	Watts Out	Eff. %	Power Factor
0.02	20	1480	-18	44	26	0.286	3.1	11.9	0.219
0.1	30	1470	-10	52	42	0.303	15.37	36.6	0.334
0.2	40	1460	0	60	60	0.326	30.4	50.7	0.443
0.3	50	1450	5	71	76	0.346	45.4	59.8	0.528
0.4	60	1440	13	81	94	0.381	60.2	64.0	0.594
0.5	75	1425	22	90	112	0.408	74.3	66.4	0.659
0.6	90	1410	28	100	128	0.450	88.5	69.1	0.684
0.7	105	1395	36	111	147	0.495	100	69.6	0.715
0.8	125	1375	45	122	167	0.536	115	68.9	0.748
0.9	145	1355	54	137	191	0.598	127.3	66.6	0.770
1.0	165	1335	62	152	214	0.658	139.5	65.1	0.782
1.1	190	1310	74	168	242	0.727	151	62.3	0.8
1.2	225	1275	83	185	269	0.805	161	59.8	0.803
1.3	275	1225	92	207	299	0.881	166	55.6	0.806
1.35	310	1190	100	220	320	0.952	168	52.4	0.808
1.40	360	1140	103	235	338	1.04	167	49.4	0.785
1.45	STALL								

TABLE 3.1.

Calculations

$$\% \text{ Efficiency} = \frac{\text{Watts Out}}{\text{Watts In}} = \eta$$

$$\eta = \frac{2\pi \text{ x speed in R.P.M. x Torque in Newton Metres x } 100}{60 \text{ x Watts In}}$$

If speed in radian per second.

$$\eta = \frac{\text{Speed in Rad/Sec x Torque in Newton Metres x } 100}{\text{Watts In}}$$

$$\text{Power Factor} = \frac{\text{Watts In}}{\sqrt{3} \text{ x Voltage between lines x line current}}$$

Locked Rotor Tests (240V between lines)

	Current in Amps	Torque in Newton Metres	Mean Torque
STAR CONNECTED	0.6	0.35 0.36 0.35	0.353
DELTA CONNECTED			
	2.0	1.28 1.30 1.29	1.29

TABLE 3.2.

Conclusion

The power factor of the motor increased to a maximum value of 0.8. The maximum efficiency was 69.6% and occurred at a load of 0.7 Nm and a speed of 1395 R.P.M. The circle diagram and plots of power factor, speed and efficiency against torque are shown in Fig. 3.2.1. and Fig. 3.2.2. respectively.

3.2.1. Prediction of the Reactances X_α and X_β

Using the equivalent circuit parameters of Fig. 3.2., for a supply voltage of 240V, the predicted values of capacitance and inductance are plotted for the slip range 0 to 1.0 (see Fig. 3.3.). The graph enables values of C and L to be determined for various slips and capacitance and inductance values are shown rather than the reactance in ohms. The units of measurement being the microfarad (μF) and Henry (H) respectively. From the onset, it was concluded, firstly that the

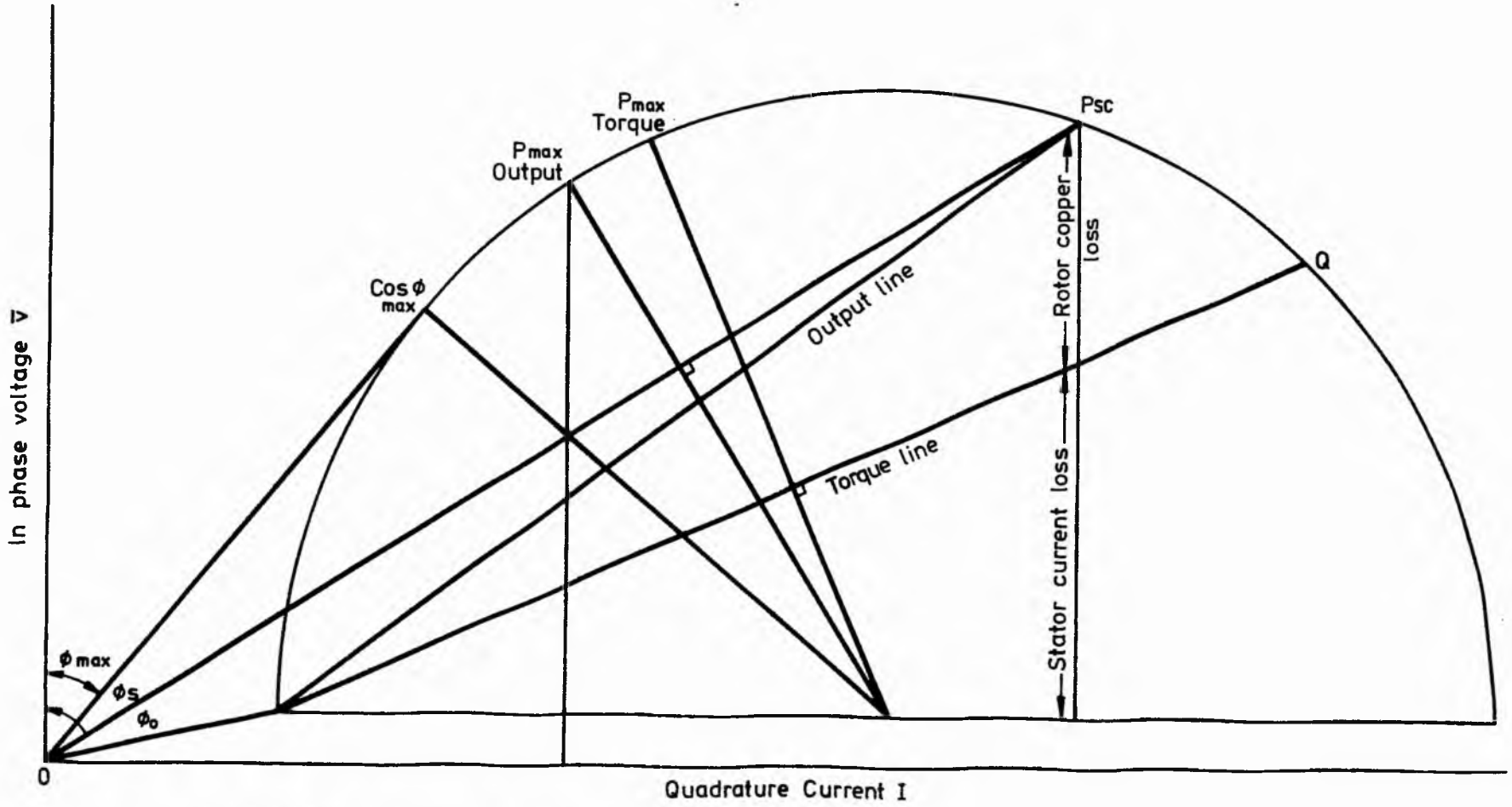

Fig. 3·2·1 Circle diagram for 3 phase squirrel cage motor

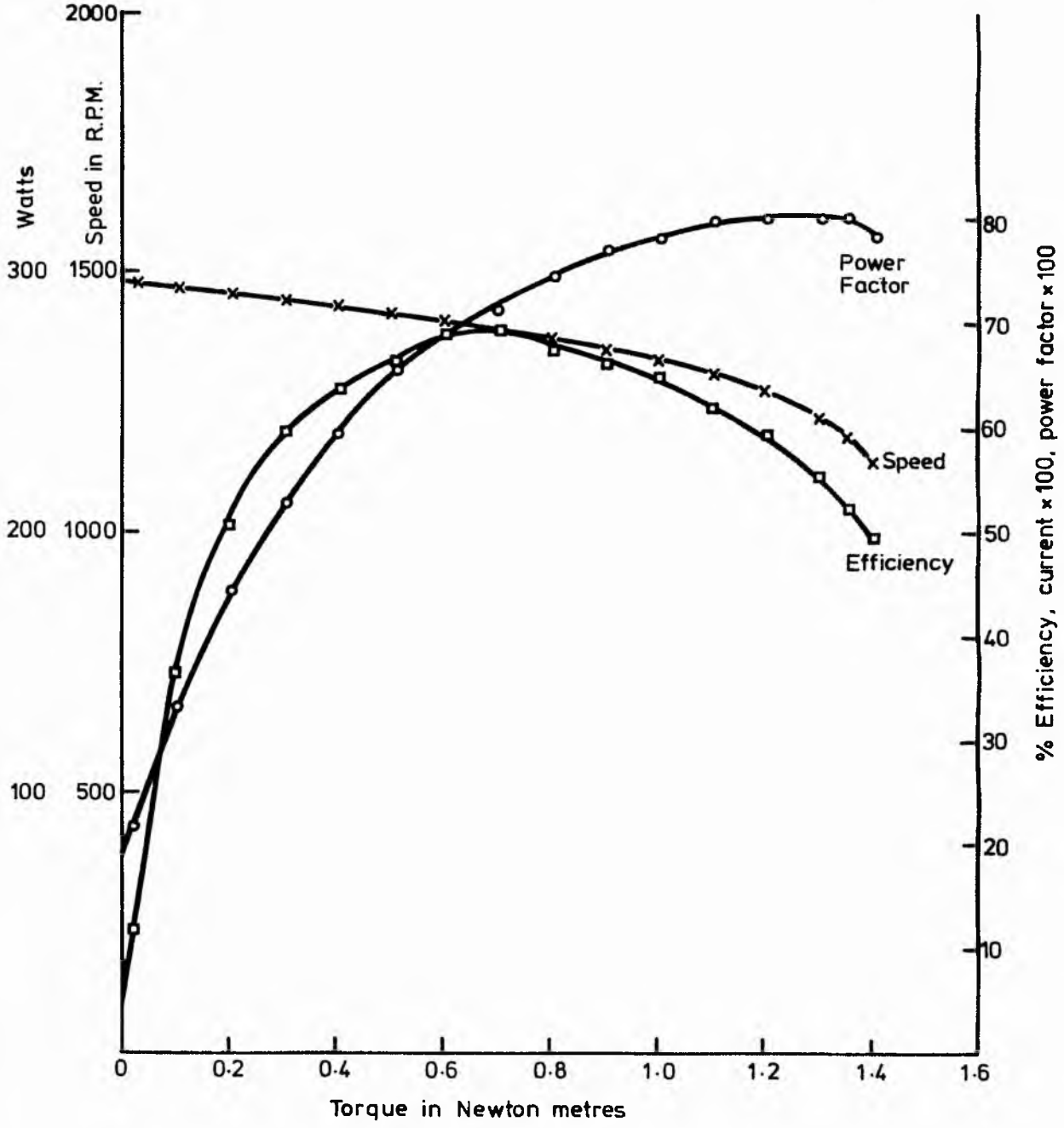

Fig. 3·2·2 Three phase Squirrel cage. J.J. Lloyd motor.

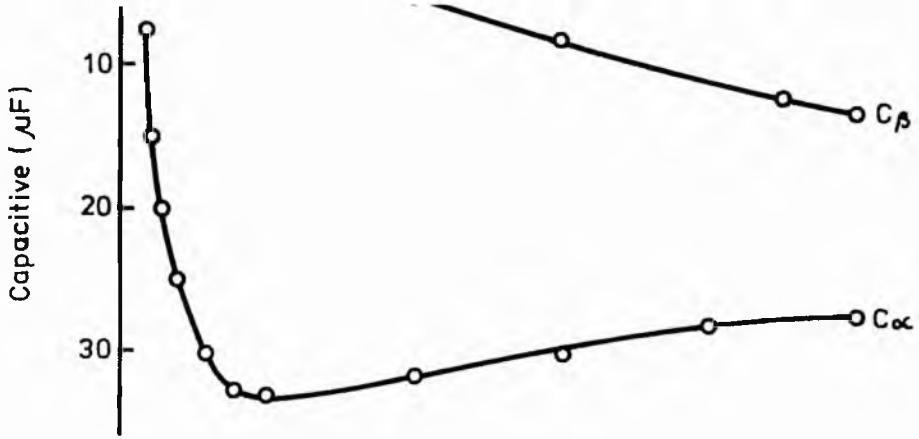

Fig. 3.3 Predicted values of C_α and C_β against Slip

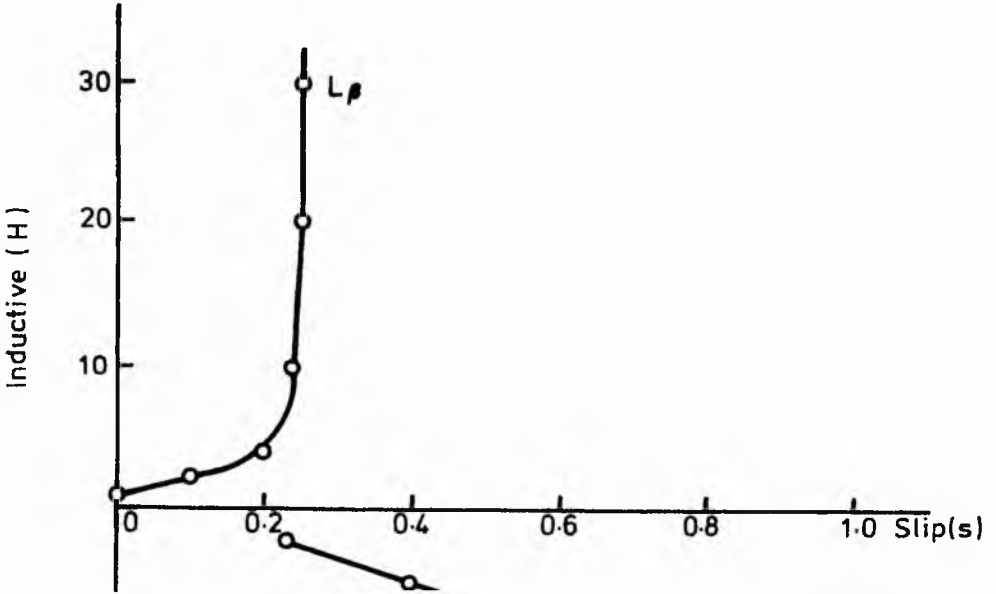
Inductive (H)
30
20
10
L_β
0
0·2
0·4
0·6
0·8
1·0 Slip(s)

starting condition (at standstill s = 1) requires X_α and X_β both to be capacitive. Secondly, over the slip range of 0 to 0.22, X_α and X_β must be capacitive and inductive respectively.

3.2.2. Experimental Investigation of Required X_α and X_β for Minimum Negative Sequence Voltages

(a) Running Condition

A 3-phase induction motor has a limited working range of slip over which it can run at a stable operating point. This range for Motor 1 is approximately 0.05 to 0.1 for the load range 0 to 2.0 Nm. The predicted values of X_α and X_β over this working range are given in Fig. 3.4. When reactances corresponding to the predicted values variation in line voltages from 40 to 60 volts were found, clearly indicating imbalanced operation.

Hence further investigation was undertaken to ascertain the minimum V_n possible for this system and the required values of X_α and X_β. It was observed that to reduce V_n for any given slip, the X_α must exceed the predicted value and X_β be less than the predicted value. Further, for a constant X_α and a variable X_β in the range 0 to 7000 Ω, it is found that for V_n to be a minimum, X_β must be zero. Fig. 3.5. illustrates this.

Then, the balanced values of X_α and X_β were obtained experimentally from two investigations.

(1) For $X_\beta = 0$, the effect of different values of X_α on V_n was observed for slip values in the working range. This observation is shown in Fig. 3.6. and hence it was deduced that the best balance is given by a constant X_α corresponding to a capacitance of 38μF (± 2).

(2) The effect of (capacitance) X_β on V_n was observed with X_α having values obtained in [1]. The result represented in Fig. 3.7. shows that the addition of X_β improves the balance of the motor with only 2.5V of negative sequence at full load (s = 0.1).

(b) Starting Condition

The worst case is the starting condition, when s = 1 (i.e. locked rotor). Investigation of the starting conditions shows that X_α should have a capacitance value of 100μF and $X_\beta = 0$ for min V_n.

3.2.3 Conclusions

The results achieved, correspond to the theory of Chapter 2. The aim of the experiment was to find the two values of capacitance that would produce minimum imbalance. This can only be achieved if the negative sequence voltage V_n is as small as practically possible. Hence, by measuring the value of V_n, for a particular capacitance, a fairly accurate range of values was achieved as shown in Fig. 3.6. and Fig. 3.7.

3.3. Experimental Converter with Fixed Values of Capacitance and Inductance Derived by Computer Program

MOTOR 2

A.C. 3-phase, 4-pole, squirrel cage I.M.

Star connected 415V supply

Power rating 2.5 H.P.

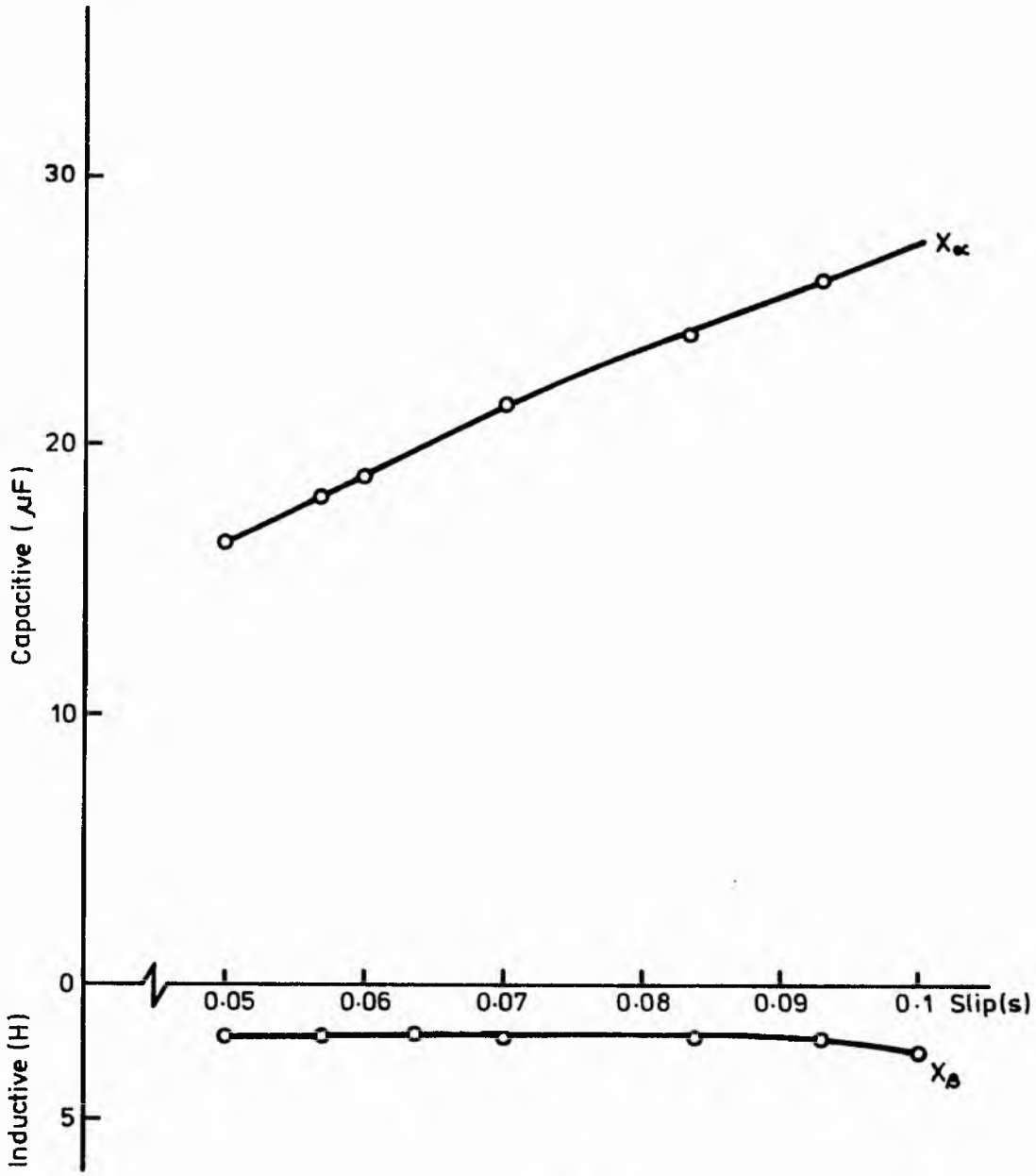

Fig. 3.4 Predicted values of X_α and X_β for Motor working slip range

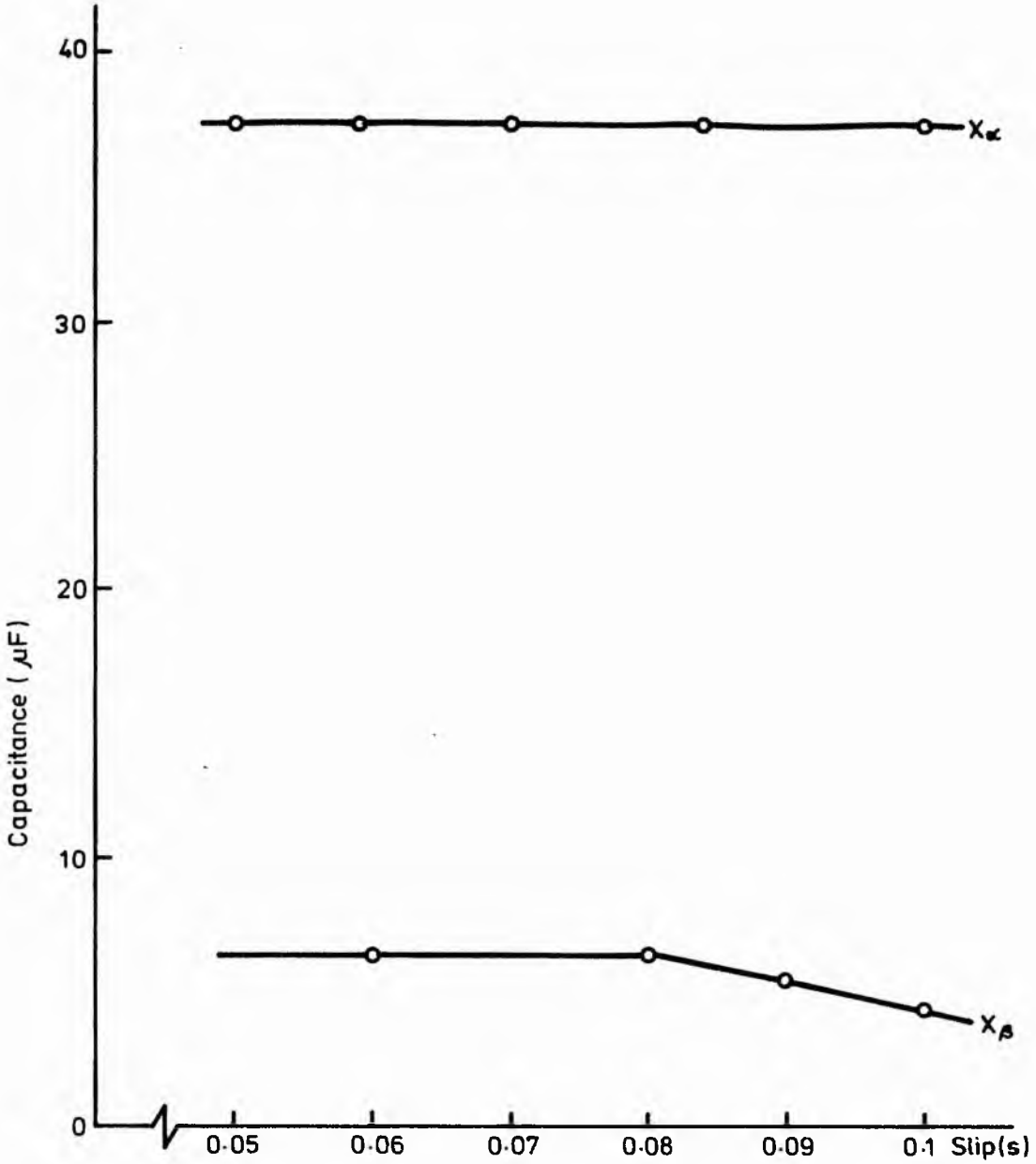

Fig. 3.5 Experimentally obtained values for X_α and X_β in the balanced condition

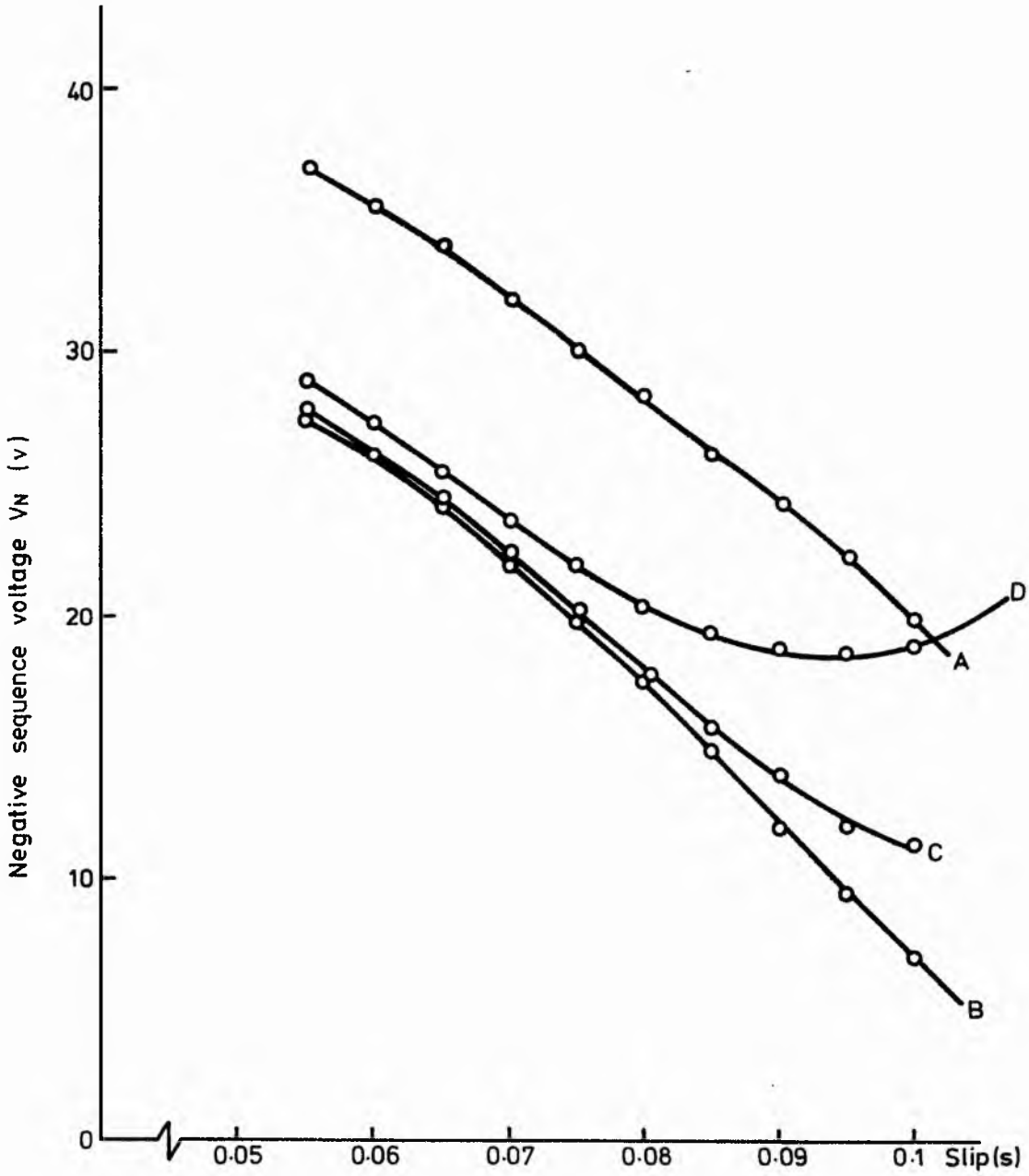

Fig. 3.6 Experimental observations of the variation of Vn with slip for capacitance C

A : C = 44·9 μF

B : C = 38·4 μF

C : C = 36·6 μF

D : C = 32·4 μF

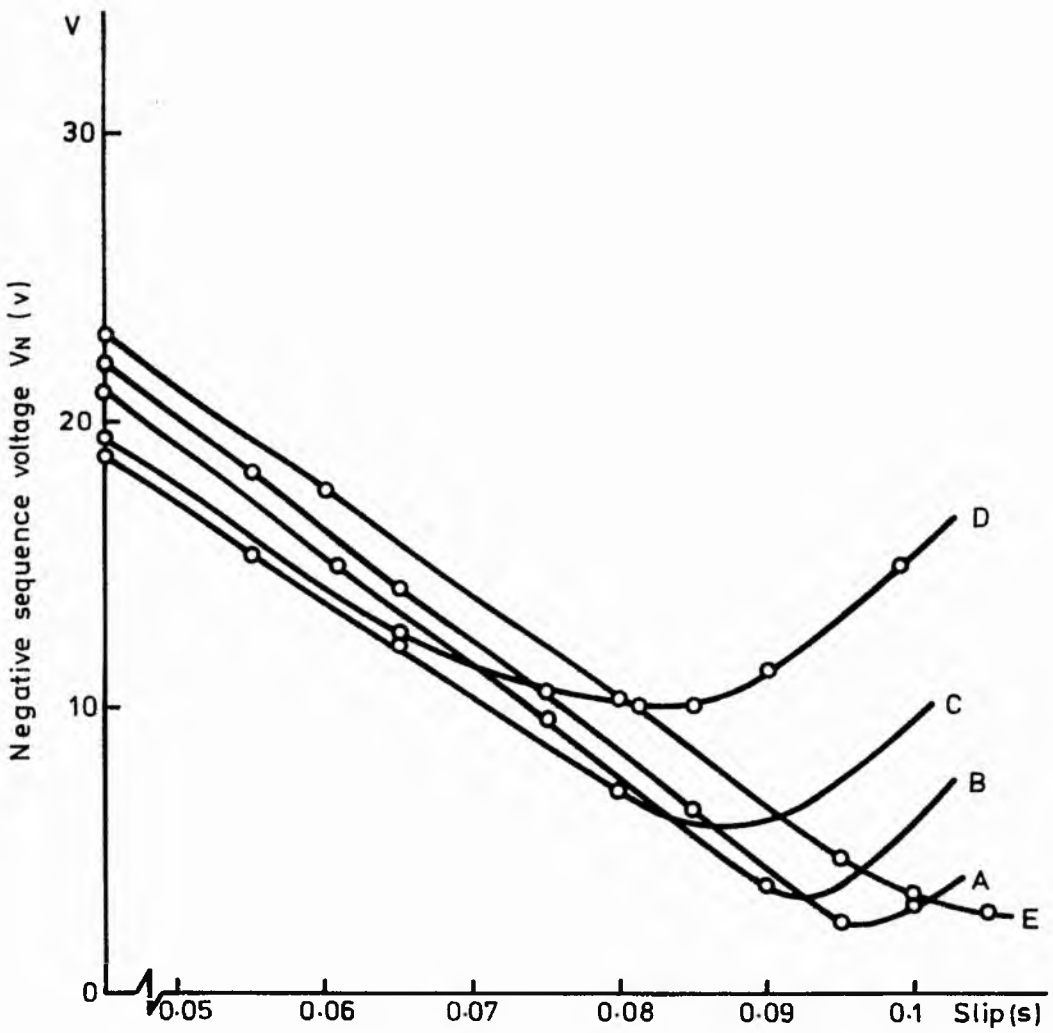

Fig. 3·7 Experimental observation of the variation of negative sequence voltage V_N against slip for capacitive values

A :	C_α = 37·2 μF	C_β = 4·3 μF
B :	C_α = 37·2 μF	C_β = 5·5 μF
C :	C_α = 37·2 μF	C_β = 6·5 μF
D :	C_α = 33·2 μF	C_β = 4·3 μF
E :	C_α = 40·3 μF	C_β = 4·3 μF

In this section, a higher rated machine, star connected was used. To emulate an industrial characteristic, a full set of test results for this motor were obtained. A computer program was developed to calculate the capacitance, as it changes for different values of slip, according to the relationship, $R_r = + sX_r$ (see Appendix B). Since the Rotor resistance R_r, does not change (under balanced conditions), then $X_r = R_r/s$. As s varies from starting (s = 1) to running speed or synchronous speed (s = 0) then X_r and X_T must also vary and a computer program for repetitive calculation.

The computer program was further developed into a user friendly software package. It works out the values of the equivalent circuit parameters (X_m, R_m, R_s, R_r, X_s, X_r) by typing in the results from the stator resistance test, No-load test and locked rotor test. The computer program goes on to draw, the equivalent circuit showing parameter values and plots a graph of capacitance against slip for the slip range 1×10^{-3} to 1.0. A typical graph is shown in Fig. 3.8.

From such a graph it can be determined at which slip value the motor changes from starting current to running current and thus the two values of capacitance can be found.

Also, the computer program was adapted to include the two element phase conversion system, discussed later on in this chapter. It also plots the phase converter capacitance and inductance against slip.

The computer program is written in user friendly mode and self explanatory package. The user types "CAPCALC" and after that the program asks for DATA. A full explanation of the program and the print out of the program is given in Appendix B. The results given by the program for MOTOR 2 follow this section.

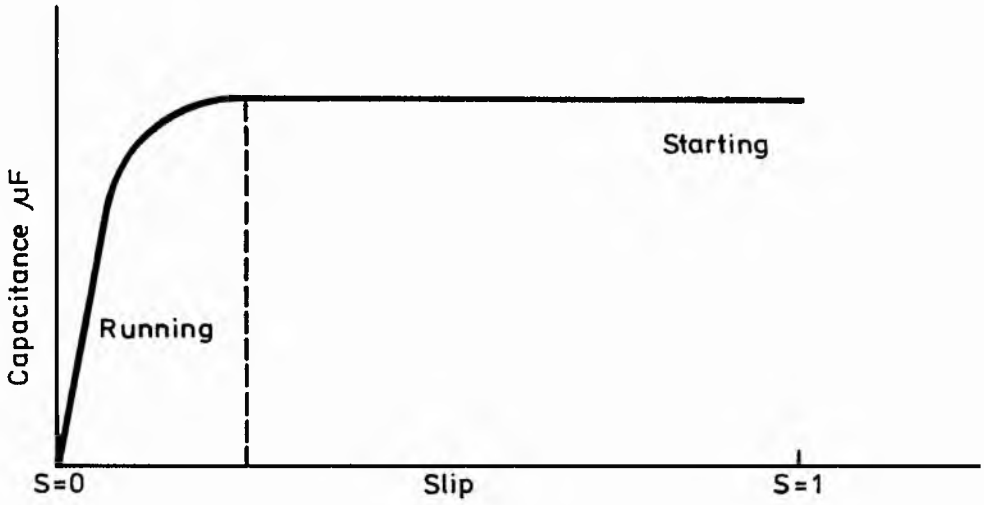

Fig. 3·8 Typical graph of capacitance against slip

C A P C A L C

Written by M.Latif

Department of Electrical and Electronic Engineering

Nottingham Polytechnic 1990

PRESS RETURN TO CONTINUE

Are the Motor conections STAR or DELTA (S/D) s

Enter the No Load Test Data as indicated:-

V1	Stator Volts	415
I1	Stator Amps	1.25
P1 Two Meter Method	Watts	-400
P2 Two Meter Method	Watts	-120
Speed	Rev/min	2990
Torque	Nm	1
Resistance r1	Ohms	2.5

Enter the locked rotor Test Data as indicated:-

Vb Locked Rotor	Volts	73
Ib Locked Rotor	Amps	3.85
P1b Two Meter Method	Watts	-240
P2b Two Meter Method	Watts	-9.5
Frequency of the supply	Hertz	50
No of Poles		2

Is this the correct Data (Y/N)

Slip s	=	0.33 %
X1	=	3.76
X2	=	5.64
Xm	=	152.56
Rm	=	108.43
r2	=	3.11
Stator current I1	=	0.82 amps
output power	=	177.26 watts
Efficiency	=	34.09 %
Power factor	=	0.73

Press the SPACE BAR to continue

Equivalent circuit for one phase

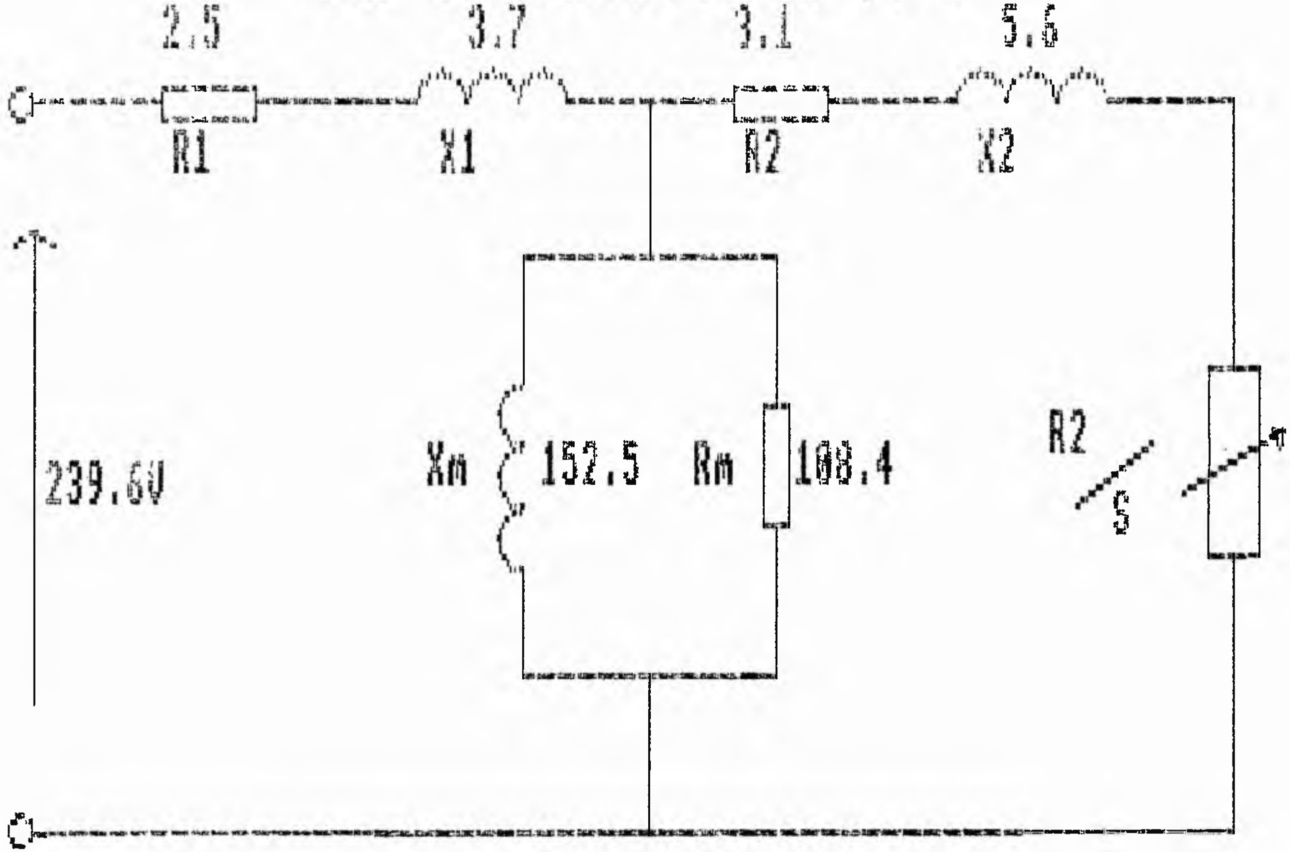

Press the SPACE BAR to Continue

SLIP	CAPACITANCE UF
0.0025	64.3774
0.0050	71.2108
0.0075	78.3762
0.0100	85.8245
0.0125	93.5060
0.0150	101.3715
0.0175	109.3730
0.0200	117.4644
0.0225	125.6021
0.0250	133.7454
0.0275	141.8569
0.0300	149.9025
0.0325	157.8520
0.0350	165.6785
0.0375	173.3588
0.0400	180.8731
0.0425	188.2051
0.0450	195.3413
0.0475	202.2712

Press the SPACE BAR to continue

SLIP	CAPACITANCE UF
0.0500	208.9868
0.0525	215.4826
0.0550	221.7551
0.0575	227.8026
0.0600	233.6252
0.0625	239.2241
0.0650	244.6020
0.0675	249.7625
0.0700	254.7098
0.0725	259.4490
0.0750	263.9858
0.0775	268.3259
0.0800	272.4758
0.0825	276.4420
0.0850	280.2309
0.0875	283.8492
0.0900	287.3037
0.0925	290.6009
0.0950	293.7474
0.0975	296.7496
0.1000	299.6137

Press the SPACE BAR to continue

CAPACITANCE
0
30
60
90
120
150
180
210
240
270
300
SLIP
0.00
0.01
0.02
0.03
0.04
0.05
0.06
0.07
0.08
0.09
0.10

3.3.1. Calculation and Test Results of a 2.5 H.P. IM

No-load, locked rotor and full-load tests were carried out. Torque efficiency and power factor are obtained at each loading.

TEST RESULTS

Load	Speed	F_1	F_2	V_R	I_R	P_R	V_B	I_B	P_B
NO LOAD	2990	0	0	415	1.25	-120	415	1.3	-400
1/4	2950	2.0	0.1	415	0.65	-300	415	1.0	-360
1/2	2910	4.6	0	415	2.0	-390	415	2.2	-880
3/4	2890	8.5	0.1	415	2.76	-660	415	2.95	-1250
4/4	2850	12.5	0.5	415	3.45	-860	415	3.95	-1600
5/4	2800	16.0	1.0	415	4.7	-1250	415	4.9	-2080

TABLE 3.3.

LOCKED ROTOR TEST

V_R	I_R	P_R	V_B	I_B	P_B
73	3.85	-9.5	72.4	3.8	-244

TABLE 3.4.

NOTE The subscript R means the readings taken in the red phase and similarly the subscript B means the blue phase. The yellow phase is used as the reference phase.

From these results, a table can be formed for torque, efficiency and power factor (p.f.) as shown in Table 3.5.

Load	Total P $P_1 + P_2$	bhp $\frac{2\ NT}{33000}$	eff $\frac{\text{Watts Out}}{\text{Watts In}}$	Torque $(f_1 - f_2)$ L 1b/ft	Speed rev/m	pf = $\frac{1}{\sqrt{1+3\frac{(W_1 W_2)}{W_1 + W_2}}}$
No Load	520	0	0	0	2990	0.731
1/4	860	0.445	38.6%	0.792	2950	0.8853
1/2	1270	1.0616	62.22%	1.916	2910	0.831
3/4	1910	1.26	75.22%	3.5	2840	0.8817
4/4	2460	2.7132	82.2%	5.0	2850	0.8868
5/4	3330	3.3319	74.6%	6.25	2800	0.918

TABLE 3.5.

The efficiency is worked by calculating brake horse power (bhp) and multilying by 746 (watts). The product of these two values is the output power of the motor.

Therefore,

$$\text{Efficiency} = \frac{\text{Watts Out}}{\text{Watts In}} = \frac{\text{bhp} \times 746}{P_1 + P_2}$$

3.3.2. Calculating Equivalent Circuit Parameters From Test Results

From Appendix A, an alternative method to find the equivalent circuit parameters.

FOR NO-LOAD TEST:

$$R_m + jX_m = \frac{V}{\sqrt{3}\ I}\left[\frac{\frac{P_{NO}}{3VI}}{\sqrt{3}} + j\sin\cos^{-1}\frac{\frac{P_{NO}}{3VI}}{\sqrt{3}}\right] \qquad (3.2)$$

$$R_m + jX_m = \frac{415}{\sqrt{3} \times 1.25}\left[\frac{\frac{520}{3 \times 415 \times 1.25}}{\sqrt{3}} + j\sin\cos^{-1}\frac{\frac{520}{3 \times 415 \times 1.25}}{\sqrt{3}}\right]$$

$R_m + jX_m = 191.68\,(0.579 + j\,0.8155)$

$R_m + jX_m = 110.98 + j\ 156.32$

Equating real and imaginary parts.

$R_m = 110.98\ \Omega \qquad X_m = 156.32\ \Omega$

LOCKED ROTOR TEST:

$$R_s + R'_r + j(X_s + X_r) = \frac{V}{\sqrt{3}\ I}\left[\frac{\frac{P_L}{3VI}}{\sqrt{3}} + j\sin\cos^{-1}\frac{\frac{P_L}{3VI}}{\sqrt{3}}\right] \qquad (3.3)$$

$$= \frac{73}{\sqrt{3}\ x\ 3.85}\left[\frac{\frac{253.5}{3\ x\ 73\ x\ 3.85}}{\sqrt{3}} + j\sin\cos^{-1}\frac{\frac{253.5}{3\ x\ 73\ x\ 3.85}}{\sqrt{3}}\right]$$

$R_s + R_r + j\,(X_s + X_r) = 5.70 + j\ 9.348\ \Omega$

Equating real and imaginary parts.

$R_s + R_r = 5.70\ \Omega \qquad X_s + X_r = 9.348\ \Omega$

The stator resistance was found to be 2.5 Ω

Therefore, $R_r = 5.70 - 2.5 = 3.20\ \Omega$

$X_s + X_r = 9.348\ \Omega$ Therefore, $X_s = X_r = 9.348/2 = 4.67\ \Omega$

The equivalent circuit is therefore shown in Fig. 3.9.

s at no load is 0.33%

Pole pairs P = 2 Frequency = 50Hz

$$ns = \frac{f(Hz)\ x\ 2}{P} = \frac{50\ x\ 2}{2} = 50$$

$$s = \frac{ns - N/60}{ns} = \frac{50 - 2990/60}{50} \qquad (3.4)$$

$s = 0.0033 \quad$ or $\quad 0.33\%$

These results compare favourably with standard method used in Section 3.2.

Using the computer program mentioned earlier, the next stage is to find the two values of capacitance. Therefore, by inputting the no-load test and locked rotor test, the program will plot the graph of capacitance against slip and an equivalent circuit for one phase as shown in section 3.3.

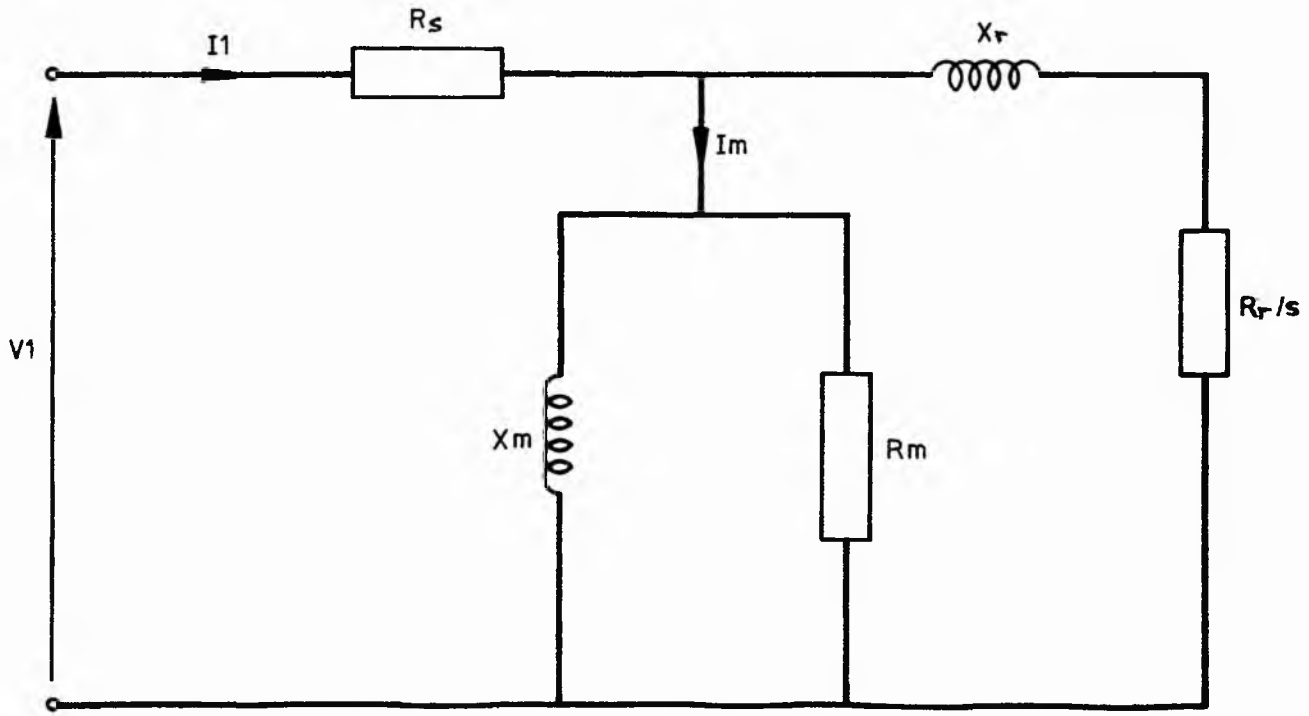

Fig.3-9 Induction motor equivalent circuit

3.4. Using the Electronic System for Verification of Results

The Electronic system developed at the Nottingham Polytechnic works on the simple principle of using two values of capacitance. One for starting and the other for running conditions of the induction motor.

The Electronic System uses a current sensor (see Fig. 3.10) which is set at a level above running current but below the starting current level. The starting current can be up to five or six times full load running current. The starting current switches in the appropriate values of capacitors. It must not, however, detect a lower value of inrush current, as the running value of capacitance will already be in and no optimisation can be achieved.

It also has a time setting switch which is set so that it is just sufficient to retain the starting capacitance in circuit, whilst the motor accelerates from standstill to full speed. A correct setting of both these switches maintains the input current approximately constant, while the motor accelerates until full speed is reached. After the set time, the input current will fall to the running value of current.

If however, the time sequence is too long the input current will increase at the end of the acceleration time before the contactors are released. The heart of the Electronic system lies in the control box, which activates the necessary electronics to operate the contacters for switching in or out the two values of capacitance. In order to obtain maximum efficiency it is essential that the two values of capacitance are correctly chosen for the required induction motor.

3.4.1. Testing the Electronic System with Calculated Values of Capacitance

The values of capacitance found in section 3.3. were wired into the Electronic system and the no-load tests were redone.

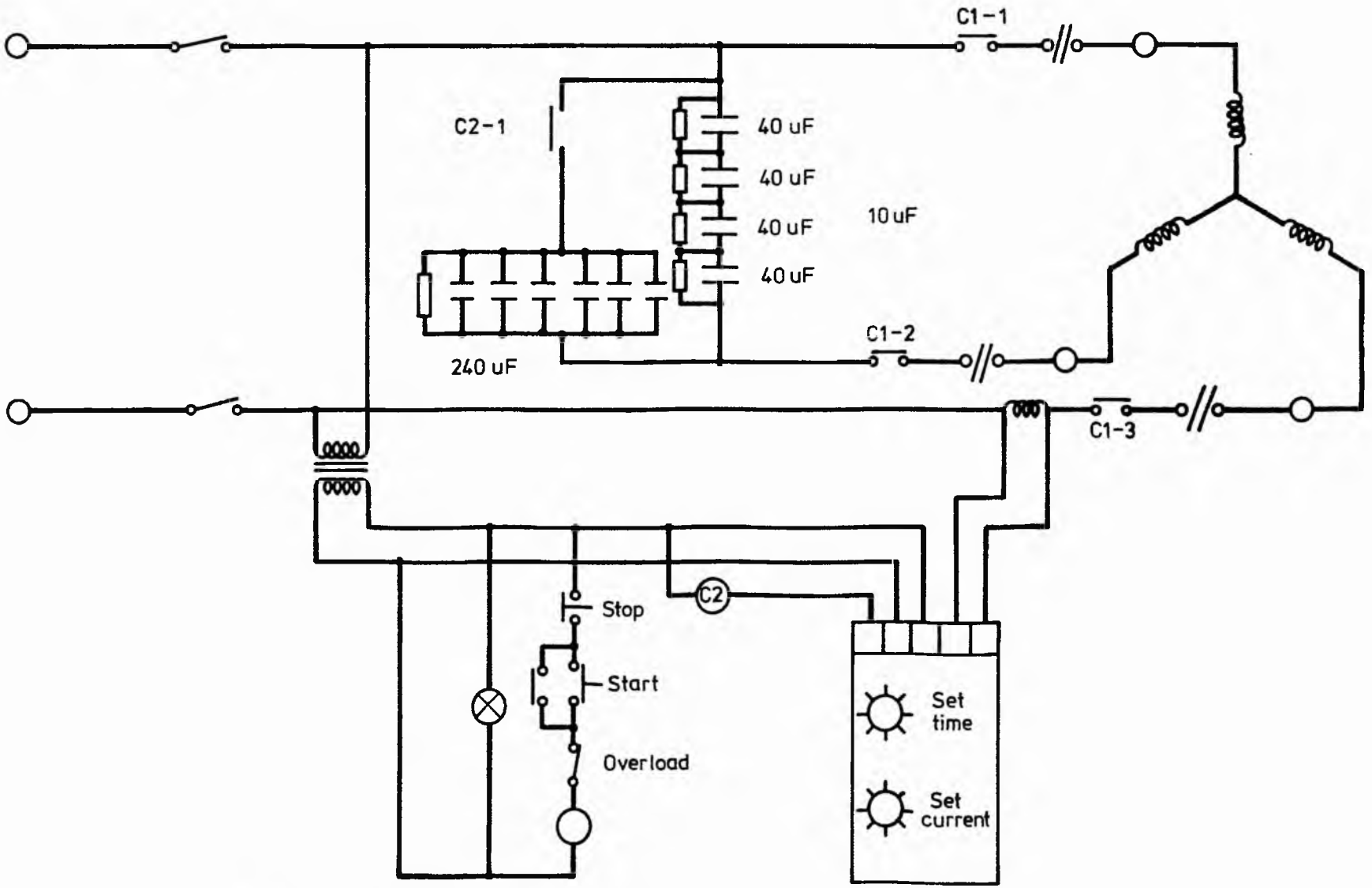

Fig. 3.10 Wiring of the Phase Converter

Speed	V_R	I_R	P_R	V_B	I_B	P_B	TOTAL	P.F.
2990	415	1.25	-120	415	1.3	- 400	520	0.731
ELECTRONIC SYSTEM								
2900	415	0.66	150	415	0.57	450	600	0.8

TABLE 3.6

By comparing the results in table 3.6, it can be seen that the motor is running at a current much smaller than before. Also the p.f. has increased by a small amount. It is better to have a high p.f. rather than a lower p.f. because a given load takes more current at lower p.f. than it does at high p.f. Also for this reason, larger cables, switch gear and transformers are required within an installation and in the supply mains feeding it. Since the majority of low power factors are lagging due to the inductive loads, such as transformers or induction motors, improvements may be implemented by the use of capacitors in parallel with the load.

3.5. Analytic Approach to Phase Conversion

As mentioned earlier, in a three phase system, each phase is separated by 120°. Also the magnitude of each phase must be equal (see Fig. 3.11.).

If the diagram is now modifed so that V_{ab} remains the reference voltage but V_{ac} and V_{bc} are shifted by 180°. Therefore, by reversing polarity of the supply, instead of requiring 120° phase shift, a phase shift of 60° can be used (see Fig. 3.12.). Analysing a three phase induction motor connected to a single phase supply (see Fig. 3.12.) it can be seen that $V_{ab} = V_s$ but $V_c = V_b = V_s/2$.

Also they are all in phase as I_1 and I_2 are in phase (see Fig. 3.13.). To show this more clearly, the approximate values of impedance found by the equivalent circuit diagram are used. If we let s = 1.

$$Z_T = R_S + \frac{R_r}{s} + jX_T$$

From the computer program and Fig. 3.14,

$R_1 = 2.5\ \Omega \quad R_2 = 3.11\ \Omega \quad X_T = 9.4\ \Omega$

Therefore, $R_T + jX_r = 5.61 + j\ 9.4 = 10.95 \angle 59.17°$

$I_1 \neq I_2$

$$I_1 = \frac{415}{10.95 \angle 59.17°} = 37.90 \angle -59.17° \text{ A} \qquad (3.5)$$

$$I_2 = \frac{415}{Z_a + Z_b}$$

$$Z_a + Z_b = 5.61 + j9.4 + 5.61 + j9.4$$

$$= 11.22 + j18.8$$

$$Z_a + Z_b = 21.89 \angle 59.17° \ \Omega$$

$$\text{Therefore, } I_2 = \frac{415}{21.89 \angle 59.17°} = 18.95 \angle -59.17° \text{ A} \qquad (3.6)$$

Therefore, $\phi I_1 = \phi I_2$ hence voltages and current are in phase (see Fig. 3.15.).

Therefore, to create the situation shown in Fig. 3.15., a correct value of capacitance placed in parallel with Z_b will give a phase shift of 60°. This will cause the current I_2 to change and Z_c will also be affected. This capacitor will magnify the voltage across the two phases Z_b and Z_c.

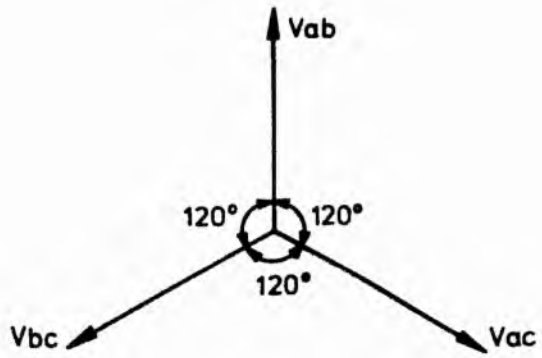

Fig. 3.11 Phasor diagram of balanced voltages

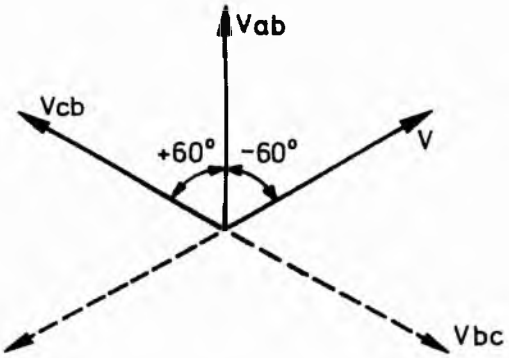

Fig. 3.12 Phasor diagram of 180° shifted voltages

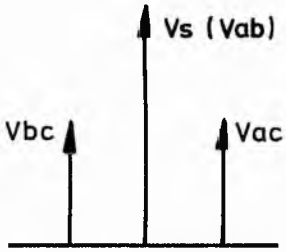

Fig. 3.13 Phasor magnitude diagram

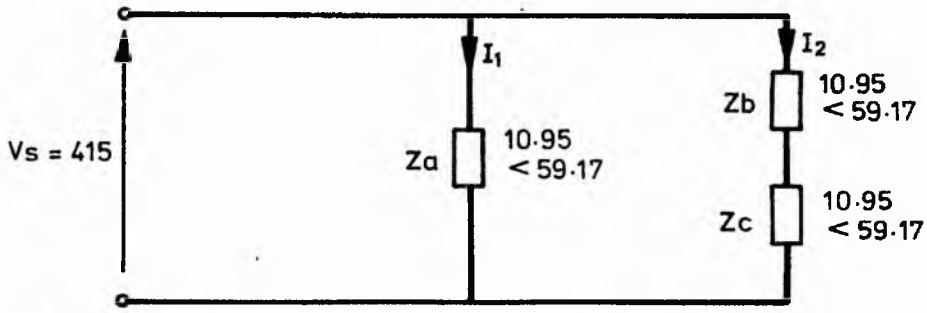

Fig. 3.14 Induction motor impedance diagram

3.5.1. Calculation of Capacitor Value

From Fig. 3.16 representing the two impedances in the admittance form.

$$\frac{1}{Z_b} \angle \theta = Y_b \angle \theta \qquad \frac{1}{Z_\alpha} = Y_\alpha \angle 90$$

For V to have angles of 60°

$$Y_T = 60° \qquad Y_\alpha = \omega C \angle 90°$$

Taking $Y_T \angle \theta = G - jB + j\omega C$

Where G - jB is the conductance and susceptance of one phase of the motor.

$Y_T \angle \theta° = G + j(\omega C - B)$

and

$$\text{Tan}\theta = \frac{\omega C - B}{G}$$

θ must equal 60° or $\text{Tan}^{-1}\theta = 1.732$

$$\text{Since } Z_b = \left(R_s + \frac{R_r}{s}\right) + jX_T$$

$$\text{Then, } Y_b = \frac{1}{R_s + \frac{R_r}{s} + jX_T} \qquad (3.7)$$

$$= \frac{R_s + \frac{R_r}{s} - jX_T}{\left[\left(R_s + \frac{R_r}{s}\right)^2 + X_T^2\right]}$$

$$\text{Now, } \text{Tan}\theta = 1.732 = \frac{\frac{100\pi C}{10^6} - \frac{X_T}{\left[\left(R_s + \frac{R_r}{s}\right)^2 + X_T^2\right]}}{\frac{R_s + \frac{R_r}{s}}{\left[\left(\frac{R_x}{R_r} + \frac{R_r}{s}\right)^2 + X_T^2\right]}}$$

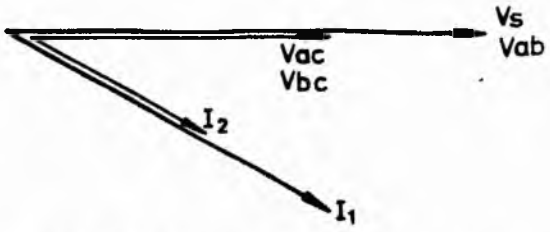

Fig. 3.15 Current phasor diagram

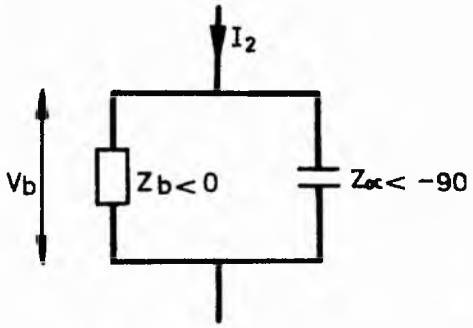

Fig. 3.16 Single element analysis

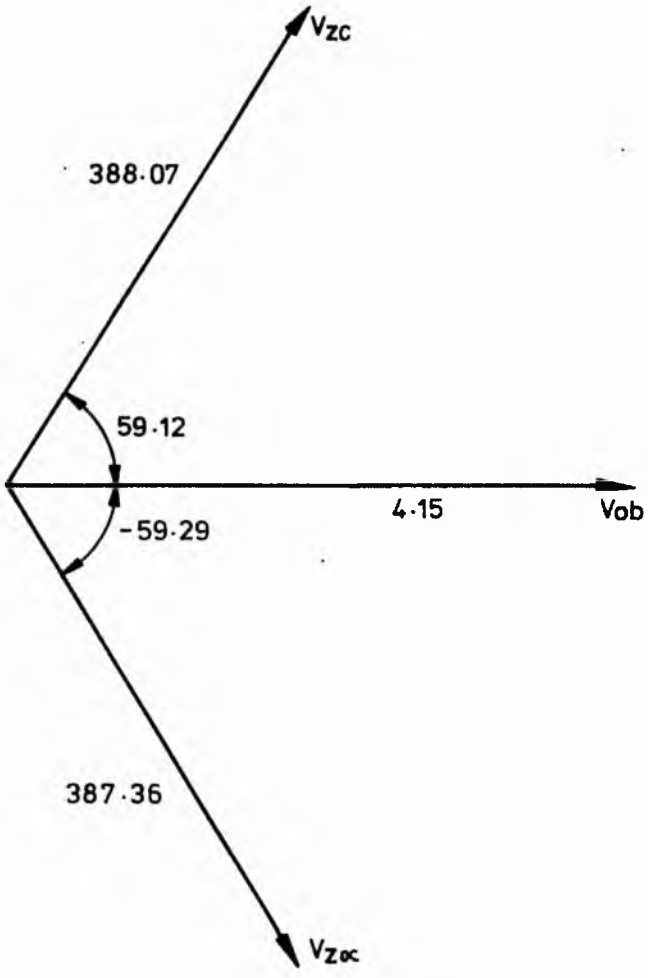

Fig. 3.17 Phasor diagram for single element converter

$$1.732 = \frac{\frac{100\pi\, C}{10^6}\left[\left(R_s + \frac{R_r}{s}\right)^2 + X_T^2\right] - X_T}{R_s + \frac{R_r}{s}}$$

$$\text{Therefore,}\quad C = \frac{1.732\left(R_s + \frac{R_r}{s}\right)^2 + X_I}{\left(R_s + \frac{R_r}{s}\right)^2 + X_T^2} \times \frac{10^6}{100\pi} \qquad (3.8)$$

Using this formula, the computer program was developed so that values of capacitance can be calculated for varying slip.

Assuming s = 1

$$\frac{1.732\,(R_T + X_T)}{R_T^2 + X_T^2} \times \frac{10^6}{100\pi} = C$$

$$\frac{1.732\,(5.61 + 9.4)}{(5.61)^2 + (9.4)^2} \times \frac{10^6}{100\pi} \approx 500\mu F$$

$X_c = 6.366 = -jX_c = 6.366 \angle -90\ \Omega$

Putting this value back into the circuit as shown in Fig. 3.16.

Now let $Z_{\alpha 1} = Z_b$ in parallel with Z_α

$$Z_{\alpha 1} = \frac{10.95 \angle 59.17^\circ \times 6.366 \angle -90^\circ}{5.61 + j9.4 - j6.366} \qquad (3.9)$$

$$= \frac{69.71 \angle -30.83^\circ}{6.378 \angle 28.41^\circ}$$

$Z_{\alpha 1} = 10.93 \angle -59.24^\circ = 5.56 - j9.39\ \Omega$

$Z_{\alpha 1} + Z_c = 5.56 - j9.39 + 5.61 + j9.4$

$= 11.17 + j0.01$

$= 11.17 \angle 0.05^\circ\ \Omega$

$$\text{Therefore,}\quad I_2 = \frac{415}{11.17 \angle 0.05^\circ} = 35.44 \angle -0.05\ A \qquad (3.10)$$

$Vz_{\alpha 1} = 10.93 \angle -59.24^\circ \times 35.44 \angle -0.05^\circ$

$= 387.36 \angle -59.29^\circ\ V$

$Vz_c = 10.95 \angle 59.17^\circ \times 35.44 \angle -0.05^\circ$

$= 388.07 \angle 59.12^\circ\ V$

If V_{ab} is taken as the reference and a phasor diagram can be drawn, for the single element converter as shown in Fig. 3.17.

The computer program plots out the capacitance versus slip graph, as shown earlier. From this graph the starting and running value of capacitance is determined.

3.5.2. Test Results of Single Element Phase Converter

The values of capacitance were found using the computer program mentioned in the previous section. These values were connected to the electronic system as shown in Fig. 3.10.

The tests were carried out using the same method as before except the locked rotor is not done.

Load	Speed	F_1F_2	V_R	I_R	P_R	V_B	I_B	P_B
-	2990	0-0	420	1.34	-500	419	1.34	+108
1/4	2850	2	427	1.35	-500	426	1.3	-190
1/2	2650	4	427	1.3	-500	426	1.85	-590
3/4	2550	6	425	1.25	-440	425	2.75	-850
4/4	2400	8	422	1.2	-480	425	3.32	-1290
5/4	2350	10	419	1.15	-440	425	4.8	-1890

TABLE 3.7.

From these results the efficiency and power factor is calculated.

Load	Torque	Total Power	bhp $\frac{2\pi nT}{33000}$	Efficiency $\frac{\text{Watts Out}}{\text{Watts In}}$	Speed rev/min	p.f.
-	-	608	-	-	2900	0.667
1/4	0.833	690	0.452	48%	2850	0.69
1/2	1.666	10906	0.841	57%	2650	0.98
3/4	2.5	1340	1.213	67%	2550	0.91
4/4	3.333	1770	1.523	64.8%	2400	0.78
5/4	4.16	2330	1.861	59%	2350	0.68

TABLE 3.8.

The phase converter was also tested for balance by measuring the line to line voltages.

	No load	1/4 Load	Load	3/4 Load	4/4 Load	5/4 Load
$V_R - V_Y$	405	404	403	401	400	399
$V_B - V_Y$	405	405	403	406	401	401
$V_R - V_B$	411	405	391	380	352	535

TABLE 3.9.

Looking at the results, shows that the motor, when supplied through the phase converter, operated just as well as when used direct on line.

At no-load the converter operated under totally balanced conditions. However, as the load increased, the system tended to become unbalanced. The unbalance is due to negative sequence components, which will be explained in detail later on in this chapter.

3.6. Two Element Phase Converter

In order to minimise the negative sequence components further, an inductor of the correct value is placed in parallel with Z_c. This inductor effects the phase angle of Z_c in a similar way to the capacitor in parallel with Z_b, except in the opposite direction.

Using the same method to calculate the value of inductance as the capacitance, except with the angle - 60°.

$$Y_T = Y \angle -\theta° + Y_\beta \angle -90°$$

$$Y_\beta = \frac{1}{\omega L} \angle 90°$$

$$Y\theta = G - jB - j\frac{1}{\omega L} = G - j\left(B + \frac{1}{\omega L}\right)$$

$$\text{Tan}\theta = \frac{-\left(B + \frac{1}{\omega L}\right)}{G} \quad \text{where } \tan\theta \text{ needs to be } -60° = -1.732$$

$$Z_c \text{ of motor} = R_s + \frac{R_r}{s} + jX_T$$

$$Y_c = \frac{1}{R_s + \frac{R_r}{s} + jX_T} = \frac{R_s + \frac{R_r}{s} - jX_T}{\left[\left(R_s + \frac{R_r}{s}\right)^2 + X_T^2\right]} \tag{3.11}$$

Therefore,

$$-1.732 = \frac{\left[-X_T - \left(\left(R_s + \frac{R_r}{s}\right)^2 + X_T^2\right)\right]}{\frac{100\pi L}{R_s + \frac{R_r}{s}}}$$

$$L = \frac{-\left(\left(R_s + \frac{R_r}{s}\right)^2 + X_T^2\right)}{-1.732\left(\left(R_s + \frac{R_r}{s}\right) + X_T\right) 100\pi} \tag{3.12}$$

Again, as slip (s) varies, then so will the value of inductance. Therefore, the computer program was extended to work out the value of L for the changing value of slip. The value of inductance found from the printout at s = 1 is 1.199H.

3.6.1. Verification of the Need of an Inductor in a Two Element Phase Converter

To see how the inductor in the circuit will affect the system, the value of the inductance at Slip = 1, found from the computer results was installed in the circuit shown in Fig. 3.18.

$jX_T = 2\pi fL = 376.7\ \Omega$

Z_C in parallel with $Z_\beta = Z_{c\beta}$

$$Z_{c\beta} = \frac{10.95 \angle 59.17^\circ \times 376.7 \angle 90^\circ}{5.61 + j9.4 + j376.7} = \frac{4124.9 \angle 149.17^\circ}{386.1 \angle 89.92^\circ} \qquad (3.13)$$

$$= 10.68 \angle 59.25^\circ = 5.46 + j9.18\ \Omega$$

Therefore, Total impedance $Z_{\beta\alpha}$ and $Z_{c\beta} = Z_\alpha$

Therefore, $Z_\alpha = 5.59 - j9.39 + 5.46 + j9.18$

$= 11.05 - j0.21\ \Omega$

Therefore, current through network $I'_Z = \frac{415}{11.05 \angle -1.09^\circ}$

$I'_z = 37.56 \angle 1.09^\circ$ A

Therefore, Voltage across $Z_{\beta\alpha}$

$V_{\beta\alpha} = 37.56 \angle 1.09^\circ \times 10.93 \angle -59.24^\circ$

$V_{\beta\alpha} = 410.5 \angle -58.15^\circ$ V

Voltage across $Z_{c\beta}$

$V_{c\beta} = 37.56 \angle 1.09^\circ \times 10.68 \angle 59.25^\circ$

$= 401.1 \angle 60.34^\circ$ V

It can be seen that the voltages across Z_A, Z_B and Z_C are now closer in magnitude than they were, just using the capacitor (See Fig. 3.19).

This in turn, will bring the negative sequence component down to a lower value and lead to a better balanced system.

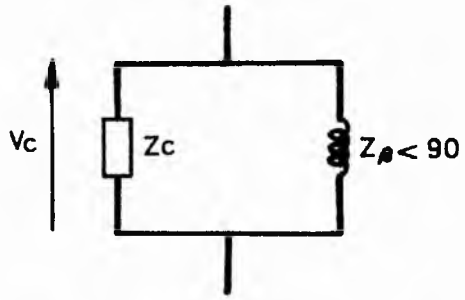

Fig. 3.18 Single element analysis

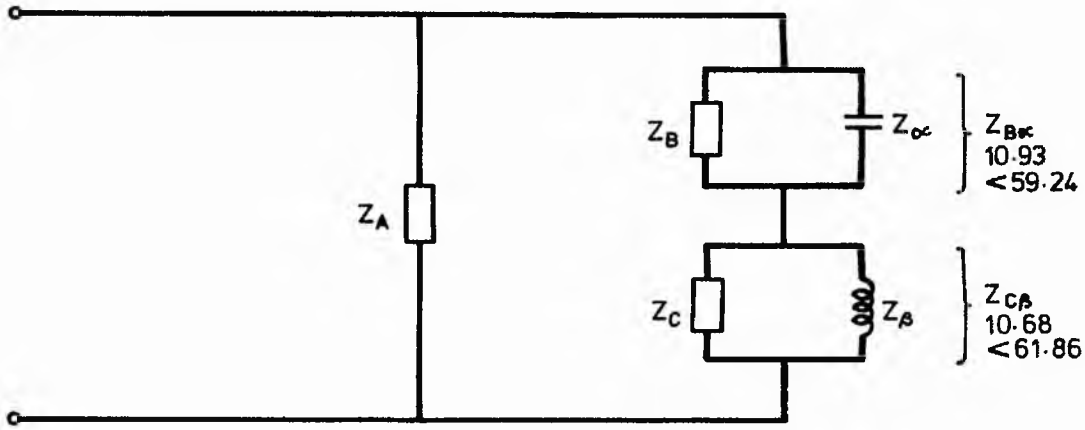

Fig. 3.19 Double element analysis

3.7. Effect of Imbalance on Induction Motor

When imbalanced voltages are applied to a polyphase induction motor, the effect is equivalent to the superposition of a negative sequence voltage onto the normal positive sequence voltage. This leads to an imbalance of currents in each of the windings. Excessive heating of induction motor will take place, due to the following factors:-

(1) Negative sequence currents produce a reduction in net output torque and increases losses in the machine.

(2) These currents produce heating effect, which is not uniform throughout the machine.

Negative sequence currents produce more heat per amp, than do positive sequence currents, due to the fact that the resistance to positive sequence is less than that to negative sequence.

Also the ratio of stator and rotor current are greater for negative sequence, due to the increase of slip, when considering negative sequence.

3.8. The Effect of Unbalanced Voltages on an Induction Motor

A system of unbalanced line voltages can be broken down into a series of three separate systems:-

i) Positive sequence components (V_p, I_p).

ii) Negative sequence components (V_n, I_n).

iii) Zero sequence components (V_o, I_o).

In the Delta configuration, there will be no zero sequence currents in line voltages. From Chapter 2, the symmetrical components follow the relationship shown:

$V_p = 1/3\ (Va + aVb + a^2Vc)$

$V_n = 1/3\ (Va + a^2Vb + aVc)$

$V_o = 1/3\ (Va + Vb + Vc)$

We will first consider the application of the positive sequence system. With positive sequence voltage applied to the stator, the rotor will rotate in the same direction as the magnetic field.

Fig. 3.20. shows the induction motor equivalent circuit, for one phase. Normally the equivalent circuit is referred to the primary or stator side because the number of turns of the STATOR : ROTOR are not the same, and hence the referred values are used (similar manner to transformer). e.g. $R'_r = N^2R_r$ (rotor resistance referred value).

Where N = Number of Turns

R_r = Rotor Resistance.

If a voltage V_1 is applied to the circuit, by Kirchoffs law we get:-

$V_1 = V_2 + I_1 (R_s + jX_s)$

Now, V_2 can be written as

$$V_2 = \left(\frac{R'_r}{s} + jX'_r\right)I'_2$$

So that,

$$V_1 = \left(\frac{R'_r}{s} + jX'_r\right)I'_2 + I_1(R_s + jX_s) \qquad (3.14)$$

The shunt elements may be moved across the supply terminal. However, this approximation introduces a larger error than for a transformer, since the series impedance/shunt impedance is not as large.

Power developed in the rotor circuit is:-

$$P_p = |I'_2|^2 \frac{R'_r}{s} \text{ (per phase)}$$

$$P_p = |I'_2|^2 R'_r + |I'_2|^2 R'_r \frac{(1 - s)}{s} \qquad (3.15)$$

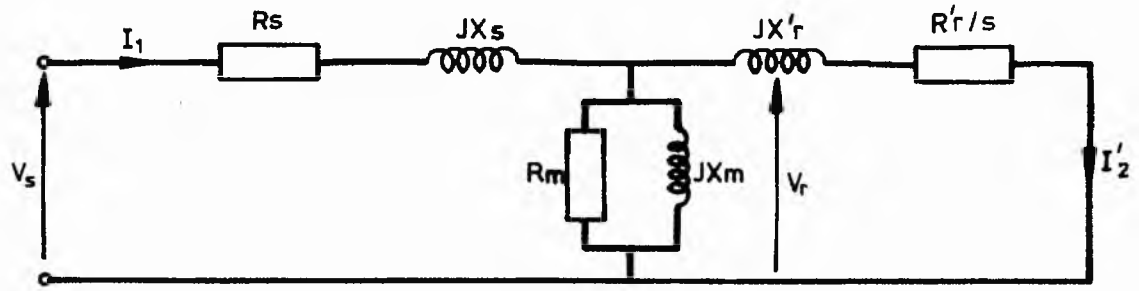

Equivalent Circuit of Induction Motor

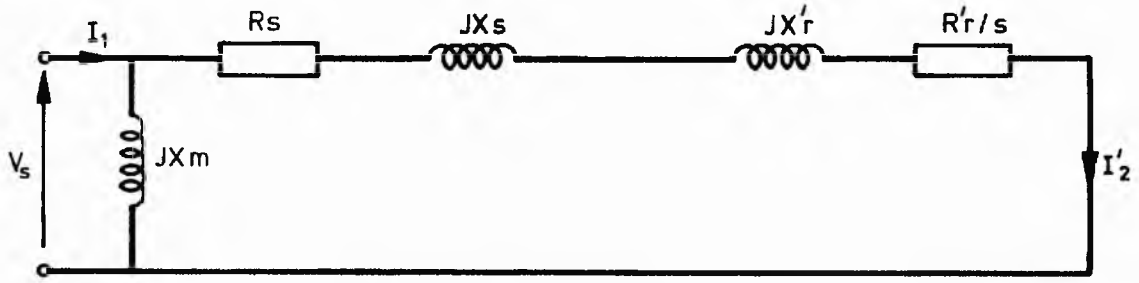

Referred Primary Side Equivalent Circuit

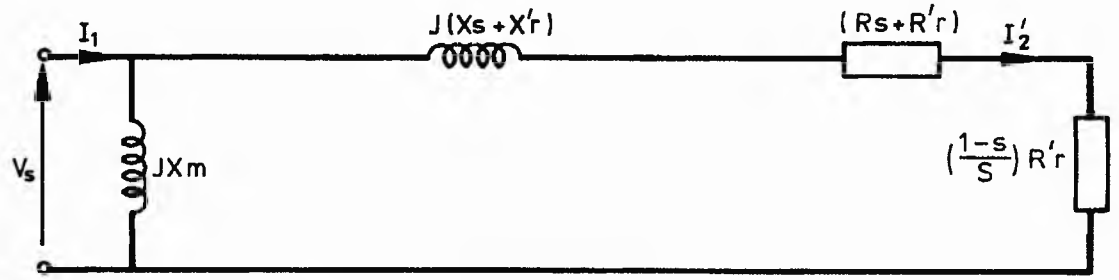

Positive Sequence Circuit

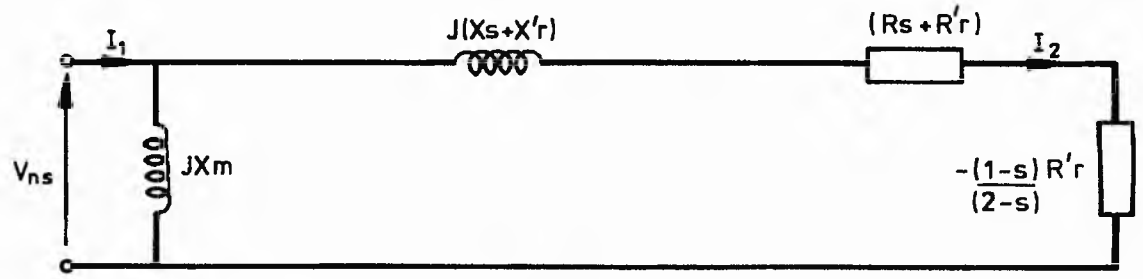

Negative Sequence Circuit

Fig. 3.20

Current Loss Power to mechanical work

The resistance R'_r/s is split up so that the element represents a component for rotor copper losses and total output power.

$$\text{Torque (Nm)} = T_P = \frac{|I'_2|^2 R'_r \frac{(1 - s)}{s}}{\text{Mechanical sync speed (Mech rad/s)}} \tag{3.16}$$

Where ω_r (angular velocity) = pole pairs x ω_m = (1 - s) ω
(mechanical sync speed) ω_m = (1 -s)ω/pole pairs.

The application of negative sequence voltage to the stator is similar to the interchanging of two leads of the positive sequence system.

A field is set up by the negative sequence voltages, which rotates in an opposite direction to the motion of the rotor. The slip for negative is therefore s_2 = 2 - s, where s is the positive sequence slip.

The equivalent circuit is obtained by merely replacing s by 2 - s.

It is noted that the mechanical power in this case is negative, which indicates that the motor absorbs power from the shaft, reducing the positive sequence power to the load.

$$\text{Negative sequence Power } P_n = - |I'_3|^2 R'_r \frac{(1 - s)}{(2 - s)} \tag{3.17}$$

$$\text{Torque (Nm)} = T_n = \frac{- |I'_3|^2 R'_r \frac{(1 - s)}{(2 - s)}}{\omega_m}$$

$$\text{Hence, Total Power } P_t = P_p + P_n$$

$$= \left(\frac{(1 - s)}{s} I'_2 - \frac{(1 - s)}{(2 - s)} I'_3\right) R'_r$$

$$\text{Total torque } T_t = \frac{\left(\frac{(1 - s)}{s} I'_2 - \frac{(1 - s)}{(2 - s)} I'_3\right) R'_r}{\omega_m} \tag{3.18}$$

If the negative sequence component becomes larger in value than the positive sequence, the machine will run in the opposite direction and follow, waveform shown in Fig. 3.21.

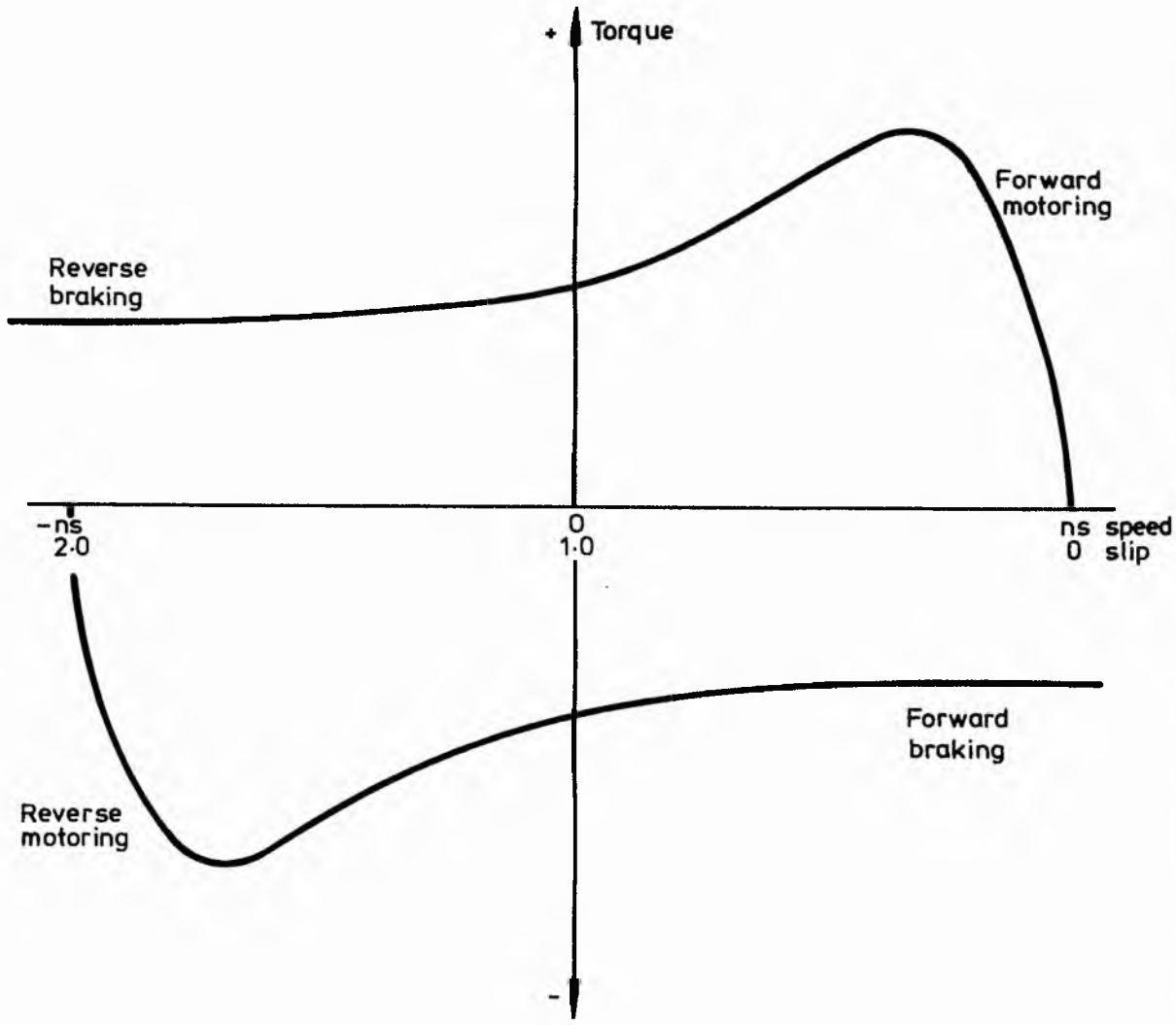

Fig. 3.21 Torque against slip and speed general characteristic for induction motor

3.8.1. Experimental Application of Unbalanced Voltages on Induction Motor

Torque is proportional to the square of the applied voltage. We will consider the case when the positive sequence slip is 0.1 and the negative sequence voltage of 0.1 p.u. is superimposed onto the positive sequence voltage of 1 p.u.

From Fig. 3.22b, we see that the torque produced by the positive sequence voltage of 0.8 p.u. at normal voltage. The negative sequence slip is however 2 - s, which gives a torque of 0.4 p.u., at a slip of 1.9. But the negative sequence voltage is 0.1 p.u., so that the torque is reduced from 0.4 to (0.1^2 x 0.4) 0.004 p.u. Now, as stated in the previous section, the negative sequence torque subtracts from the positive sequence torque. It is obvious that the reduction is small, from the above calculation giving a reduction from 0.8 to 0.796 p.u. Neglecting iron losses, the variation of the losses with slip is shown in Fig. 3.22b. The positive sequence voltage is 1.0 p.u., the losses can be seen to be 0.04 p.u., at a slip of 0.1. However, the losses attributed to the negative sequence voltage are high, being 1.8 p.u. at a negative sequence slip of 1.9. The losses are also proportional to V^2 and so the losses will be reduced to 1.8 x 0.1^2 = 0.018 p.u. The heating is approximately one half of that produced by the positive sequence and therefore the rating of the machine will be reduced as it is the positive sequence heating that originally determined the rating of the machine.

As mentioned earlier, any unbalanced system of voltages or currents may be broken down into three separate systems, i.e. positive, negative and zero.

Consider two sequence sets of currents applied to the induction motor, such that the currents through the red phase are:-

$I_r = Ia_p + Ia_n$

p = positive sequence

n = negative sequence

The currents to produce the losses in the red phase are:-

$|I_r| = |Ia_p| + |Ia_n|$

as they are in phase with each other (Fig. 3.23.). However as the negative

sequence rotates to the position shown dotted, then the current I_r will reduce to:-

$I_r = Ia_p + Ia_n = Ia_p + Ia_n \cos \theta$.

Thus, it can be seen that for any given percentage of negative sequence, the current I_r will be a maximum when Ia_p and Ia_n are in phase (Cos θ = 1) varying through a minimum position when Cos θ = -1 (Ia_p and Ia_n in anti-phase). It is obvious from the vector diagram of Fig. 3.23. that when the red phase current is a maximum, the other two phases are not at maximum.

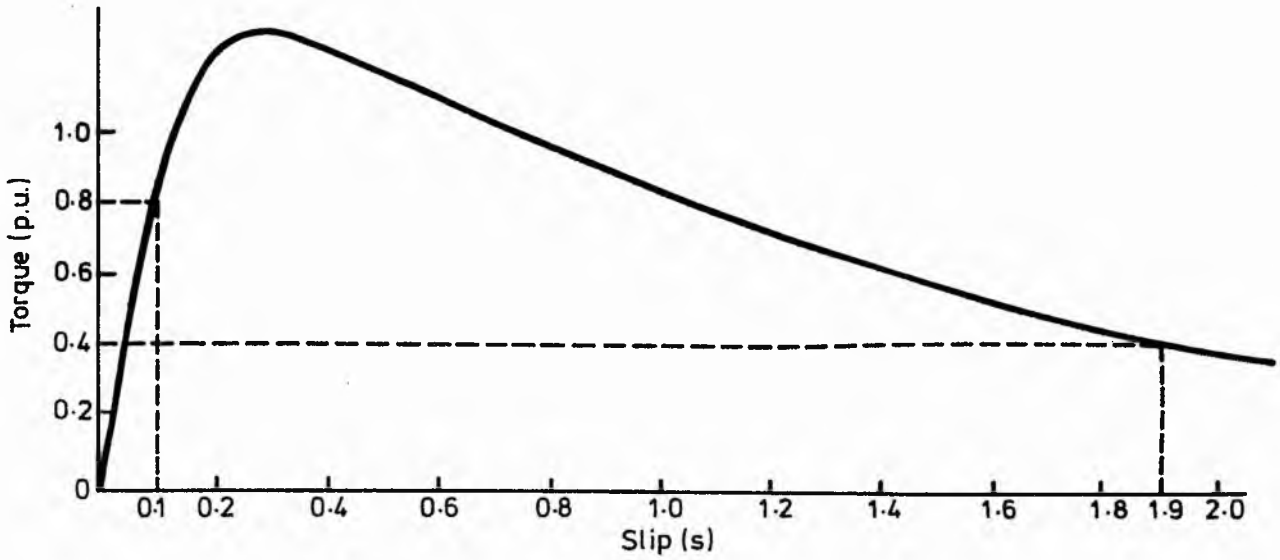

a) Torque / slip characteristic

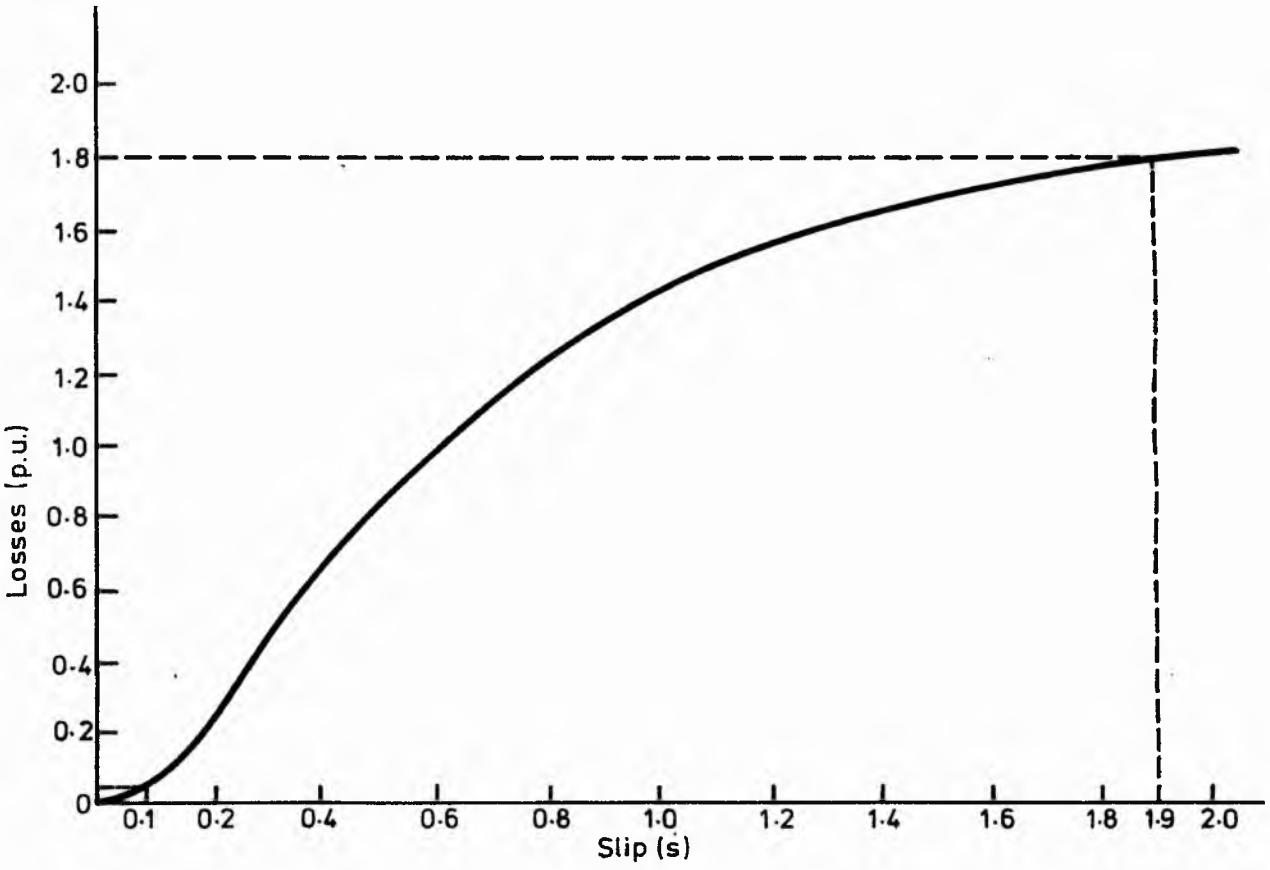

b) Losses / slip characteristic

Fig. 3·22

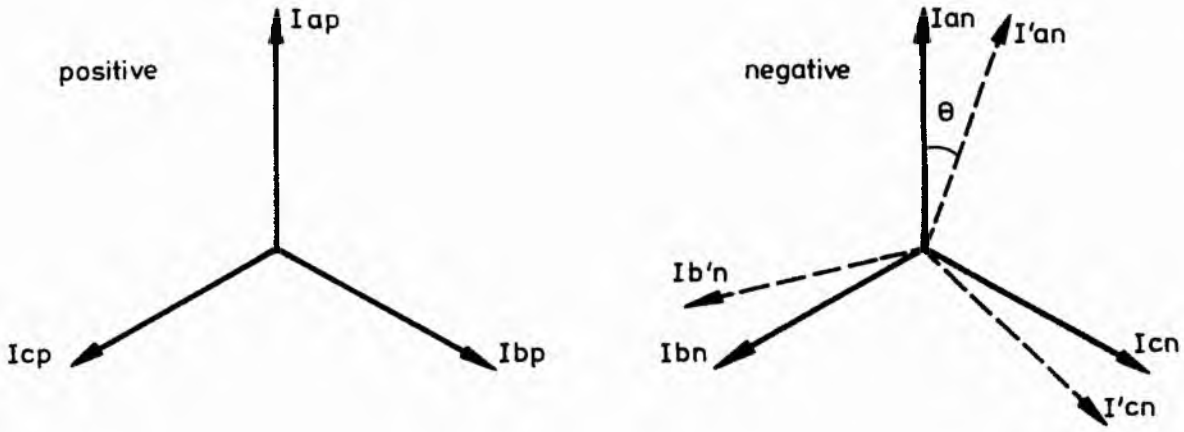

Fig. 3·23 Positive and negative sequence current phasor diagram

CHAPTER 4

ELECTRONICALLY CONTROLLED PHASE-CONVERSION

Chapters 2 and 3 have shown that if slip-dependent values of capacitance and inductance can be selected, phase balance can be achieved for the whole load range of a particular motor. Early static phase converters supplied by the U.S. Ronk Corporation for Illinois farmers rely on manual dexterity to select capacitor switching points. Any system operating in a remote location or on continuous duty-cycle such as an air conditioning plant requires automatic electronic control (Appendix D).

4.1. Electronically Controlled Relay Switching

A drive in which frequent starts are required with full-speed running under load can operate successfully with two capacitor values, one for starting and one for running. Usually, the starting value is between 4 and 6 times the running value. Fig. 4.1. shows the circuit of a 2-capacitor value, electronically switched phase-converter constructed in prototype form at the Polytechnic and marketed by CUEL Ltd. This is a single-capacitor phase converter in which the value is changed by a relay shorting out one of the two capacitors connected in series. Control of capacitance is maintained by an electronic sensing and timing circuit (Fig. 4.2.). The current transformer shown in Fig. 4.1. is connected to terminals 9 and 10 of the "black box". R1 closes the current transformer secondary through a 4-diode bridge. The voltage across R1 is proportional to the motor line current. This voltage is smoothed by C1 and compared with a preset voltage from potentiometer P1. Thus, P1 sets the initiating threshold of current. In the operating system, P1 is set so that the circuit operates at a current above running load current and below starting inrush current. When the circuit operates, the operator, short-circuiting one of the phase converter capacitors to present the large capacitance required to start the motor. Operational amplifier A1 performs this

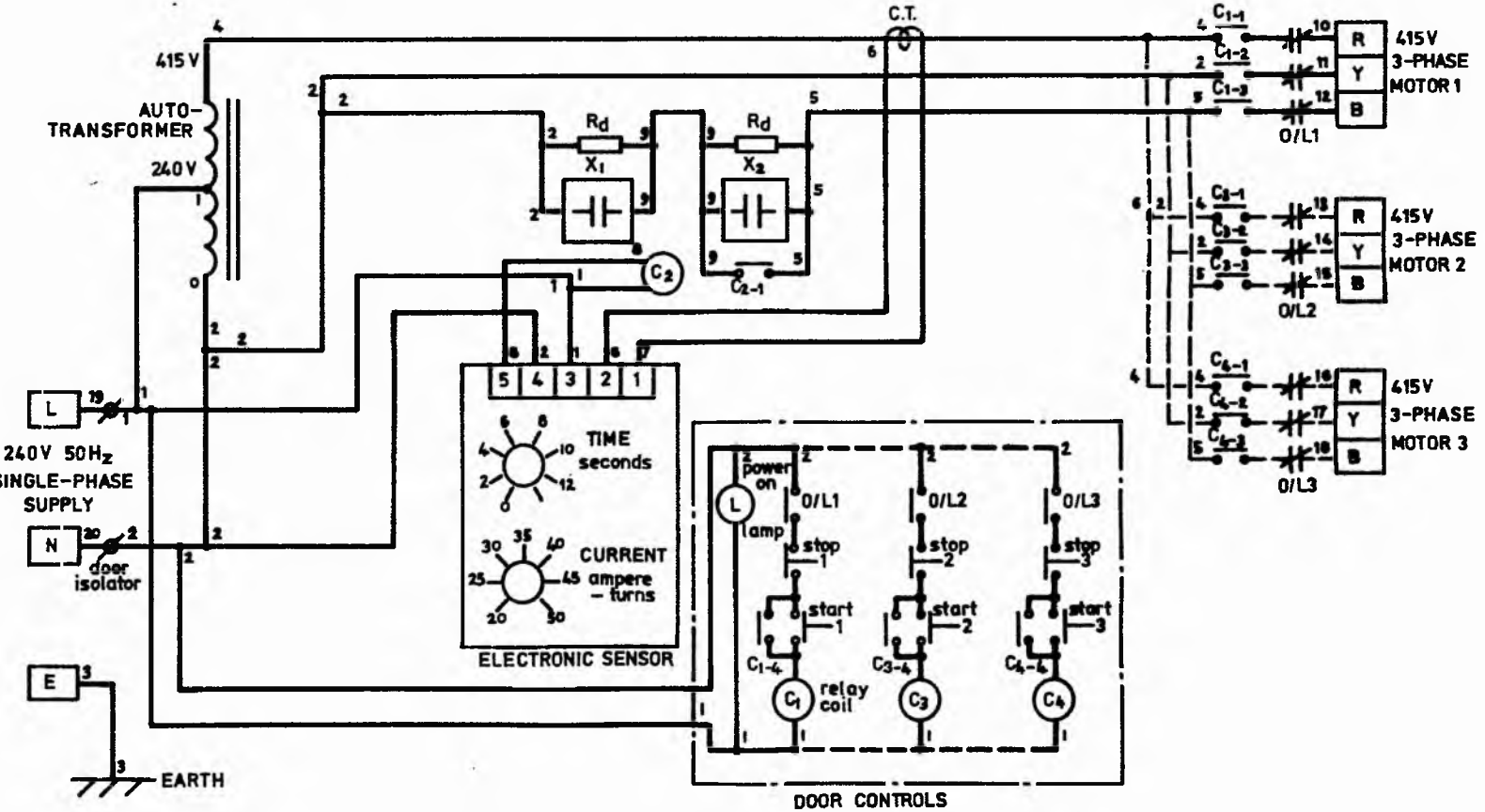

Fig. 4.1 Circuit diagram for multi-output 1 to 3 phase converter
240V, 50 Hz input, 415 V, 3-phase output
(Wire numbering shown)

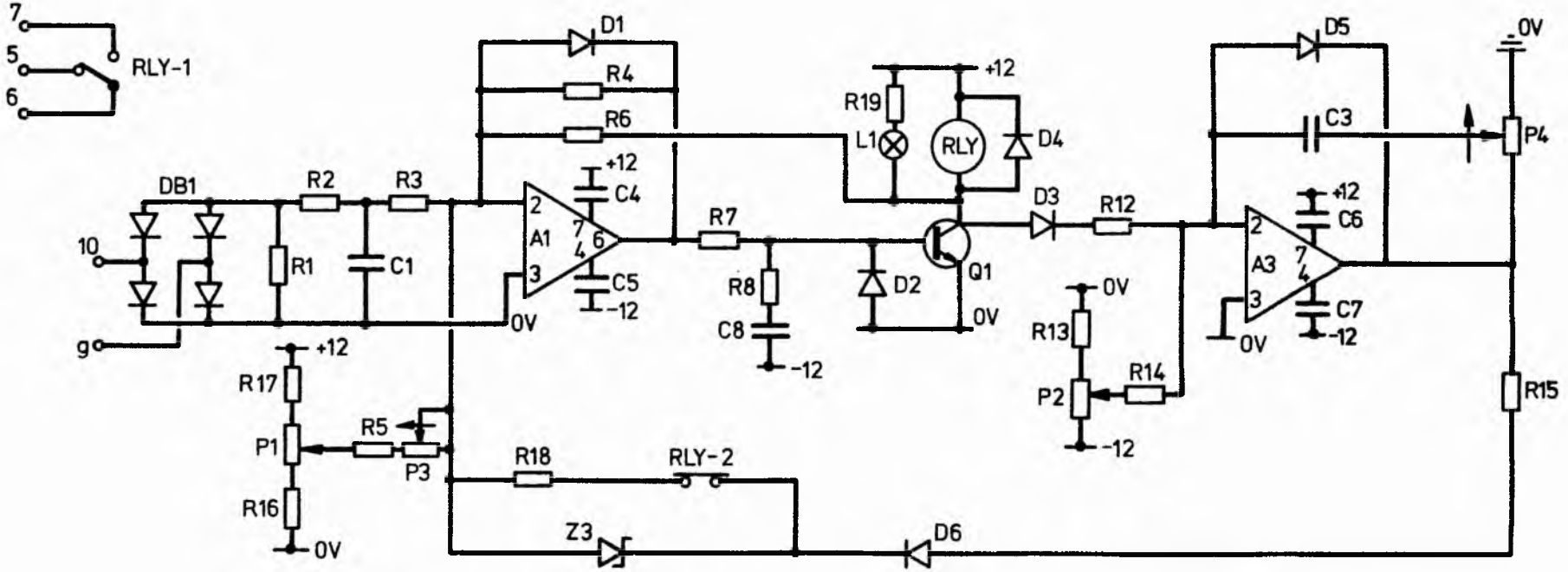

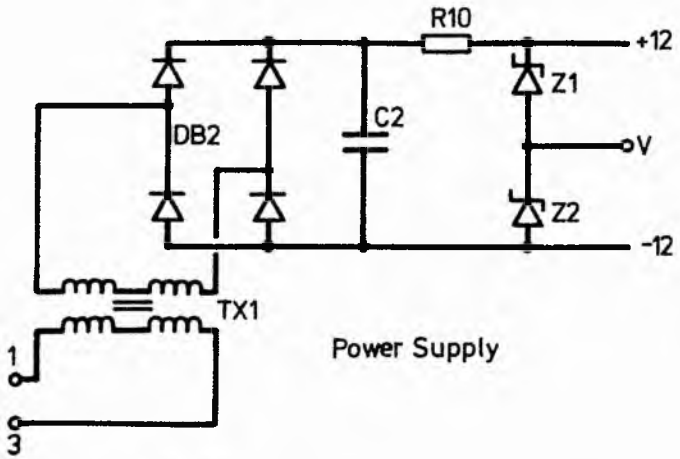

Fig.4.2 Start sensor and timer unit

R2, 8,13	1K		C1	100 uF		RLY		
R9			C2	100 uF		DB1		
R10	120Ω	2ω	C3	10 uF		DB2		
R1	1Ω	4ω	C4,5,6,7	0·1 uF				
R16			C8	4·7 uF				
R7,3	2·2K					Term		
R4	1M							
R6	100K		D1-6			R12		
R5	68K		Z1,2	12V		R14	50K	
R15,16	3K		Z3	1·5V		R17, 19	1·5K	
R12	680K					R18	3·3K	
P4	1K		A1,2	741		R11		
P3	10K		Q1			P1	1K	
			L1			D2	10K	
			TX1					

comparator function, while operational amplifier A2 is a timing circuit. The time constant is C3 R14, which can be adjusted by potentiometer P2. P2 must be so that the relay is energised for the duration of the motor acceleration. The installer must set the current threshold by P1 and the acceleration time by P2. A unique advantage of this electronically controlled converter is that an unlimited number of repeated motor starts can be accommodated. A further significant advantage is that pole-change-switching in a 2-speed Dahlander wound motor is accommodated. This is vital in many food processing plants.

This phase-controller strategy can be used with symmetrical capacitance between lines for starting power factor correction in 3-phase system. Fig. 4.3. shows this adaptation of the converter. Starting inrush currents are reduced by 45%, while full-torque is maintained. This is particularly useful in weak-supply 3-phase systems. Fig. 4.3. operates on the capacitor shorting principle. This can be avoided by the use of the Dahlander type connection shown in Fig. 4.4. A limitation of this system is that the change in capacitance, when the relay operates is 4 times the running capacitance. However, capacitor short-circuiting is avoided.

The capacitors shown in the dotted box of Fig. 4.3. are wired in parallel for starting and in series for motor running. This is further clarified by Fig. 4.4.a).

Fig. 4.4.b) shows how these capacitors are re-configured with the use of contactor C2 into series capacitors, thus reducing the value of capacitance by four times the starting value. This network also has a time switch which is set just so that it is sufficient to retain the starting capacitance circuit, while the motor accelerates from standstill to full speed. As shown in Chapter 3, a software package has been developed, which calculates the equivalent circuit parameters and plots graphs of capacitance, converter capacitance and converter inductance against slip. From the capacitance against slip graph, the value of capacitance required at different slips, can be directly read off and the appropriate value capacitors put in to the capacitor switching network. This technique was used in Chapter 3 and was found to give a better motor performance (due to balanced voltages). Table 4.1. gives the required capacitance for the switched phase converter of Fig. 4.1.

Slip (s)	Capacitance (μF)
1 (standstill)	355.3
0.75	357.2
0.50	359.5
0.25	356.6
0.10	299.6
0.01	60.5

TABLE 4.1.

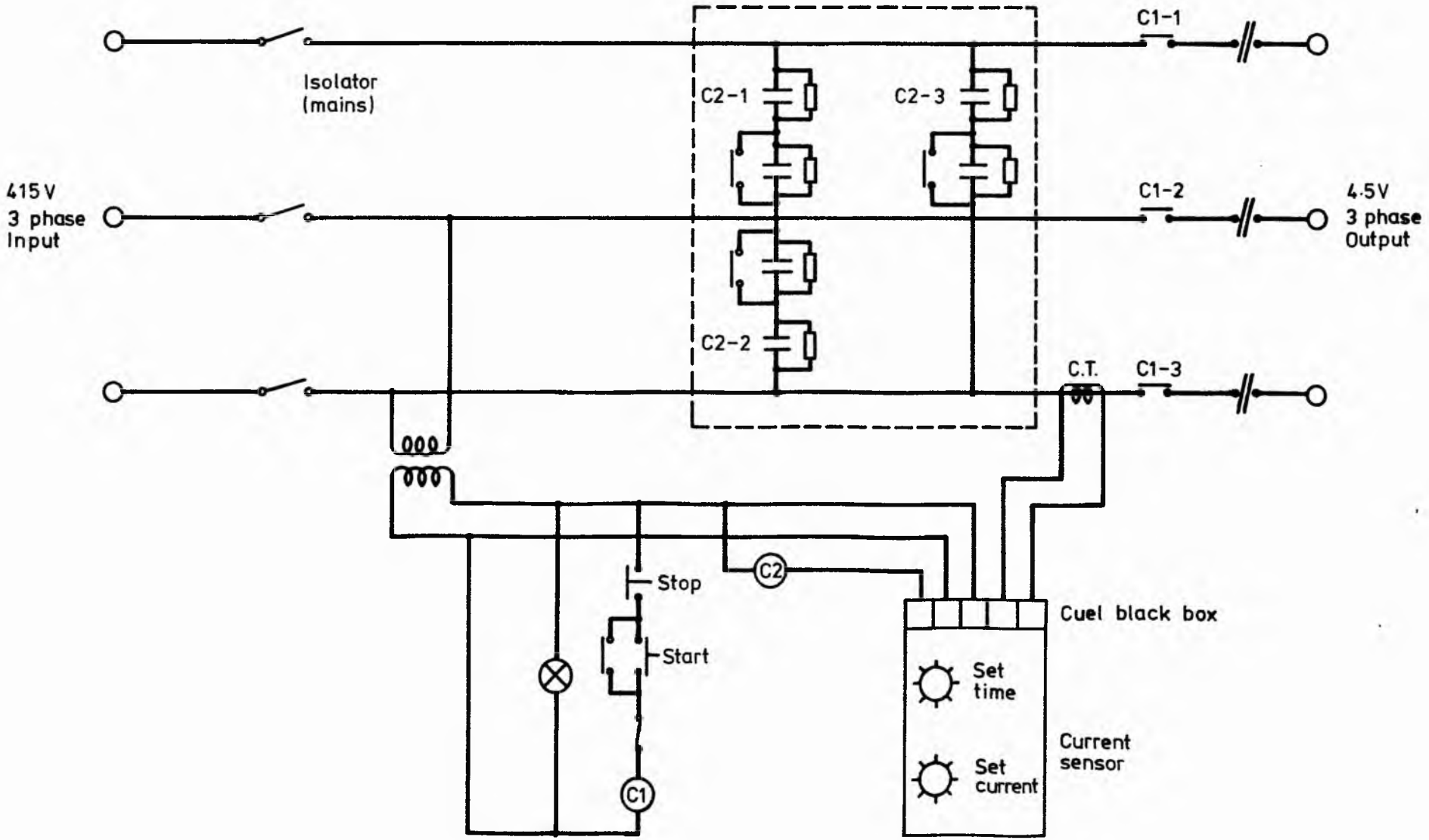

Fig. 4.3 Capacitor Switching Network

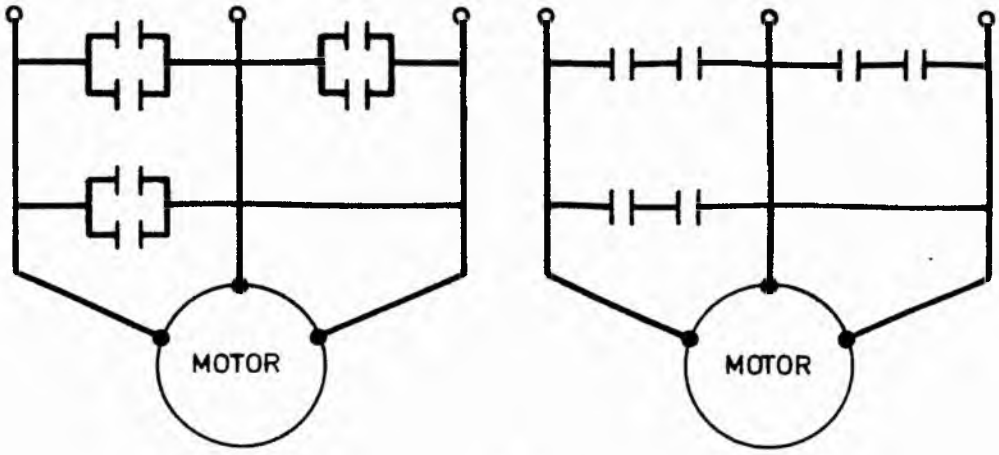

(a)

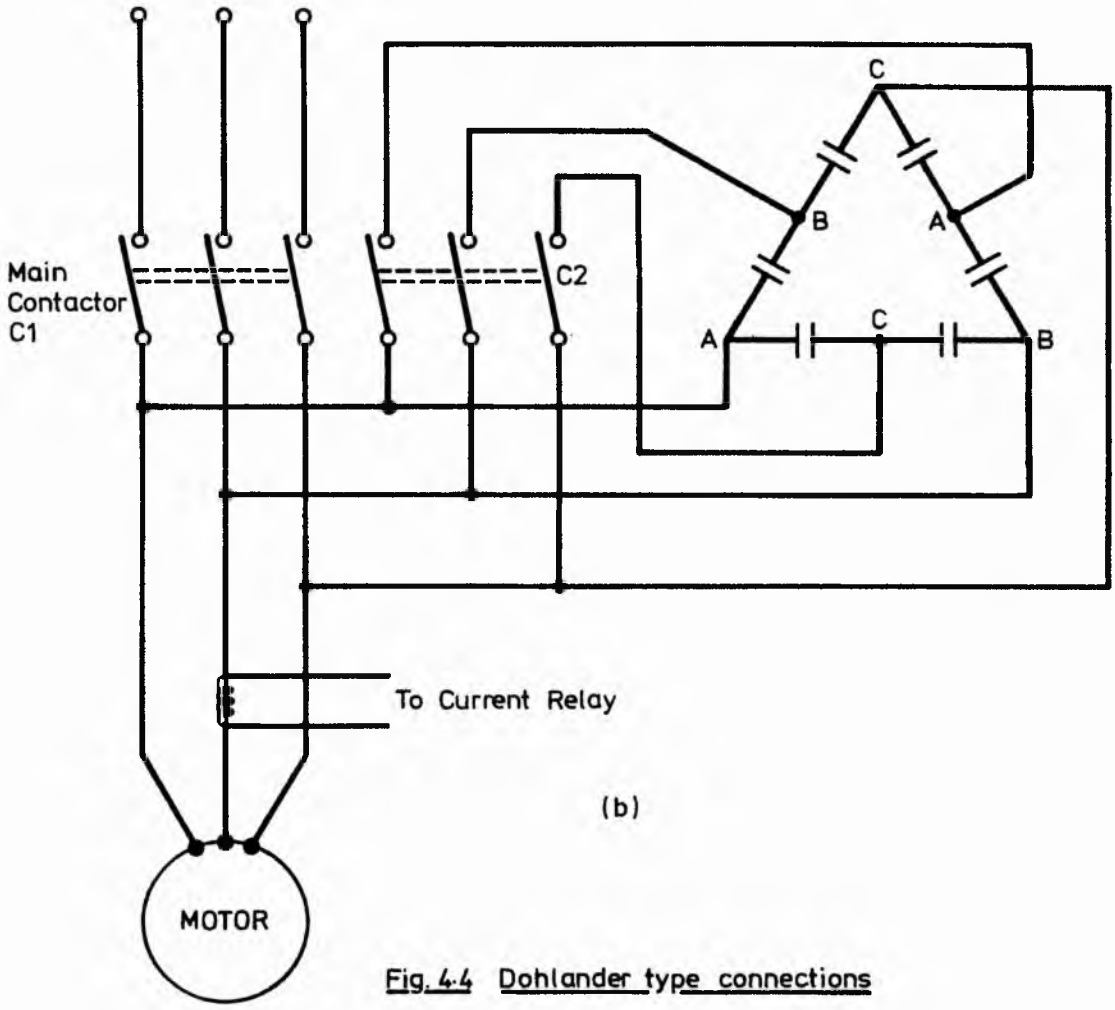

(b)

Fig. 4.4 Dohlander type connections

The most critical range of the induction motor is between 0.2 to 0. Here the capacitance value ranges between 360 μF - 60 μF. It is difficult to maintain maximum control, when the motor is on load and accelerating. This range is commonly referred to as the working range of the motor.

Two values of capacitance 360 μF and 60 μF are used for this phase conversion.

4.2. Electronic Phase Balance

Attempts at near transient phase balance have ben made by switching capacitors in and out of circuits at appropriate speeds [7]. These systems are adequate when speed and load variations are slight. Then the slow response of the contactor system does not matter greatly. However, a system with frequent stops and starts, and a requirement for rapid acceleration on load must respond much more quickly. Clearly a variable capacitor of the values required is impractical and a variable inductor implies a moving iron core which is equally impractical. Transient phase balance requires a velocity controlled variation of the charge and energy storage elements Z_α and Z_β. Electronic interruption of the current I_α and I_β will provide a variation of energy and charge storage capacity corresponding to variations of C and L. Although the net storage capacity of the circuits operating with current interruption will correspond to the capacity of a theoretically equivalent network of variables C and L, the current profile will be altered and harmonics will be introduced into the system. Providing care is taken to balance the positive and negative half cycles of the currents I_α and I_β, no sub-harmonics or d.c. components will be introduced. The frequency of the harmonics generated will depend on the rate of current interruption. Two practical methods of current interruption have been implemented in this work, voltage phase control and current chopping after rectification.

The phase-balancing impedances Z_α and Z_β are essentially stores of energy (½ CV^2) or energy (½ Li^2) dependent on whether capacitive or inductive reactance are required. A capacitor will charge to a voltage expressed as a function

of the current passing through it following the law $V = 1/C \int i\, dt$. In either case, therefore, control of the current passing through the reactive component will effectively be a control of reactance.

Fig. 2.3. shows that Z_α is always capacitive and so an electronic means of controlling the current fed into a capacitive load is required. Z_β from Fig. 2.3. must change from capacitive to inductive reactance. This is achieved by a capacitor in parallel with a controlled inductor.

4.3. Reactive Element Phase Control

The simplest form of voltage control is phase control using a back-to-back (i.e. inverse-parallel) thyristor pair or a triac. A back-to-back pair is chosen for this work to give an increased "di/dt" capability. Gate pulses fire the forward thyristor at angles θ, $\theta+2\pi$ etc. and the reverse thyristor at angles $\theta+\pi$, $\theta+3\pi$ etc. If the firing angle tolerance is good, there will be virtually zero d.c. voltage and the lowest harmonic frequency will be three times the fundamental frequency.

Conduction in the phase controller network ceases when the current naturally falls below the thyristor holding current. Effectively, this means zero current. The range of control will be determined by the nature of the load. A voltage phase controller driving into a capacitive load as shown in Fig. 4.5. may have problems of excessive "di/dt" together with a limited range of control. When the thyristor turns on, the current flows into an initially uncharged capacitor. A small resistor, R_α, is required to limit the current to give safe operation at the expense of power dissipation and slight change of phase angle. However, $|X_\alpha| >> |R_\alpha|$ and the load impedance can be assumed to be purely capacitive.

Fig. 4.6. shows the current and voltage waveforms of a back-to-back controller operating into a capacitive load. When the thyristor conducts, the current rises almost instantaneously to the value V/R_α; then decaying exponentially to zero following the relation $(V/R_\alpha)\, e^{-t/R_\alpha C}$. Say V is the instantaneous value, $V_m \sin \omega t$, at the instant of switch on, i.e. when $\omega t = \theta$. When the capacitor current falls to zero, the voltage across the capacitor remains constant

at a voltage, V_m sin X; where X indicates the extinction angle. The analysis of reactive loads will be explained in the next sections. However, some charge control is possible if the impulsive current can be tolerated.

A preferred form of phase control is that of a back-to-back controller feeding on inductive load as shown in Fig. 4.7. Here, for a firing angle θ, the thyristor will remain in conduction until the current falls below the holding level at the extinction angle X.

A choice of the appropriate design can be made from an analysis of each "back-to-back" control combination.

In the case of an inductive load the extinction angle at which the thyristor ceases to conduct is particularly important in the prediction of the harmonics generated in a reactive load. In the following sections, series R-C and R-L loads controlled by a back-to-back thyristor pair will be considered.

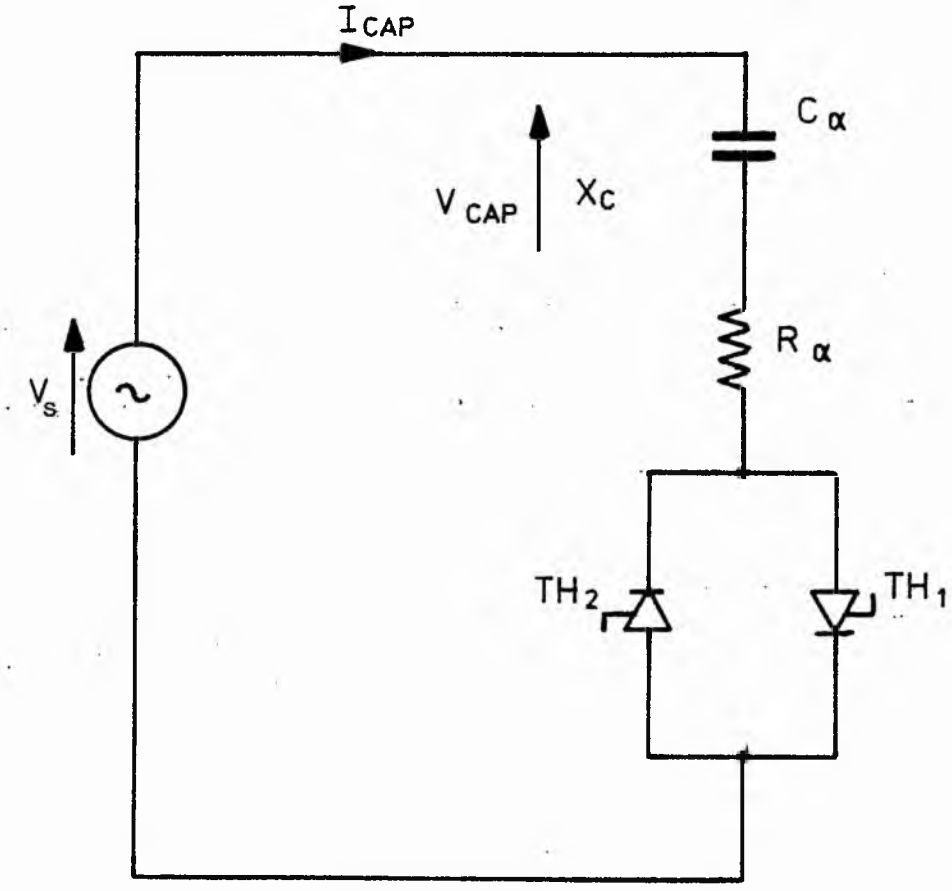

Fig. 4.5 Capacitive load control by a back to back thyristor pair.

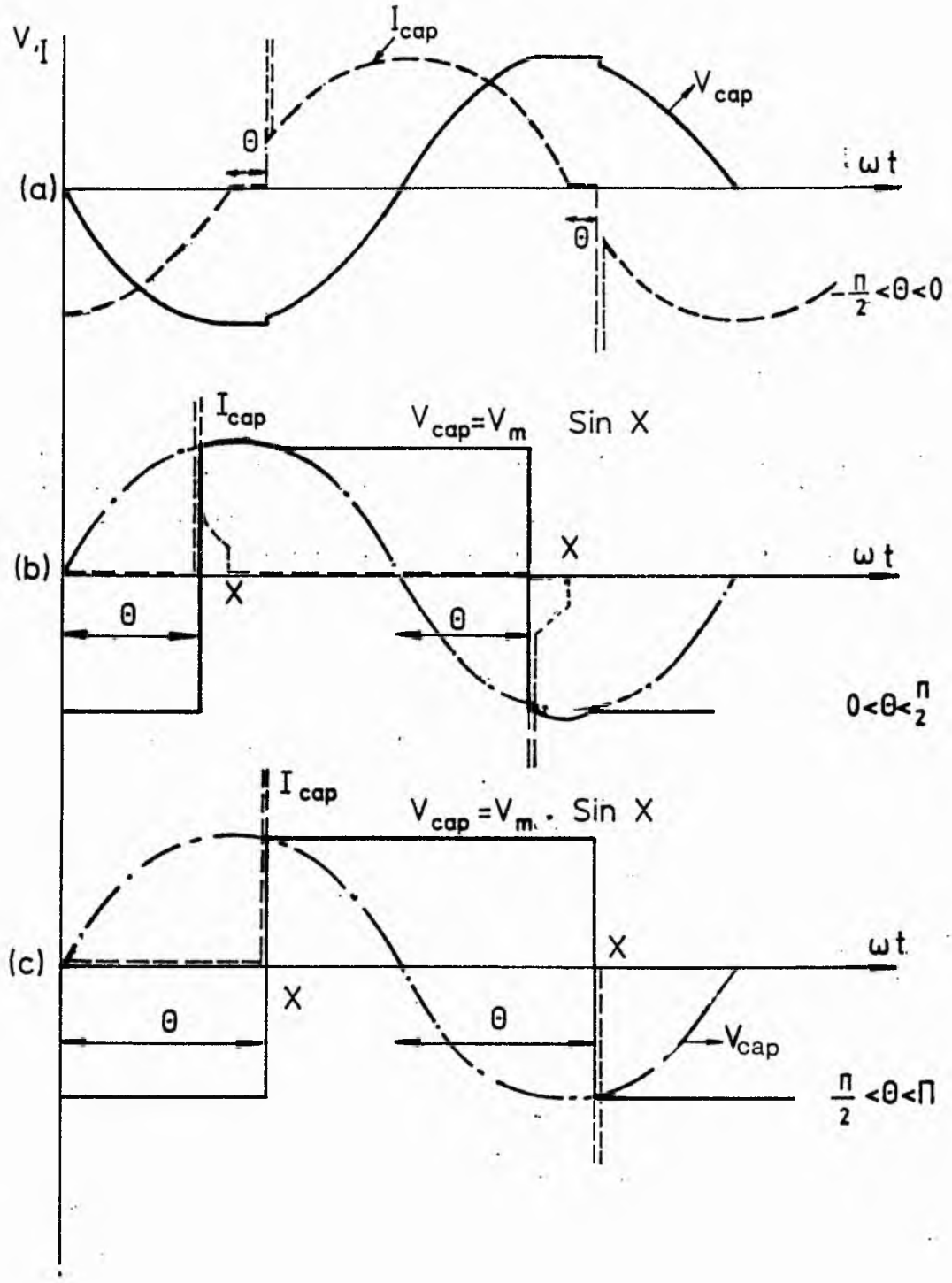

Fig. 4.6 Capacitive load control by a back-to-back thyristor pair as shown in Fig. 4.5

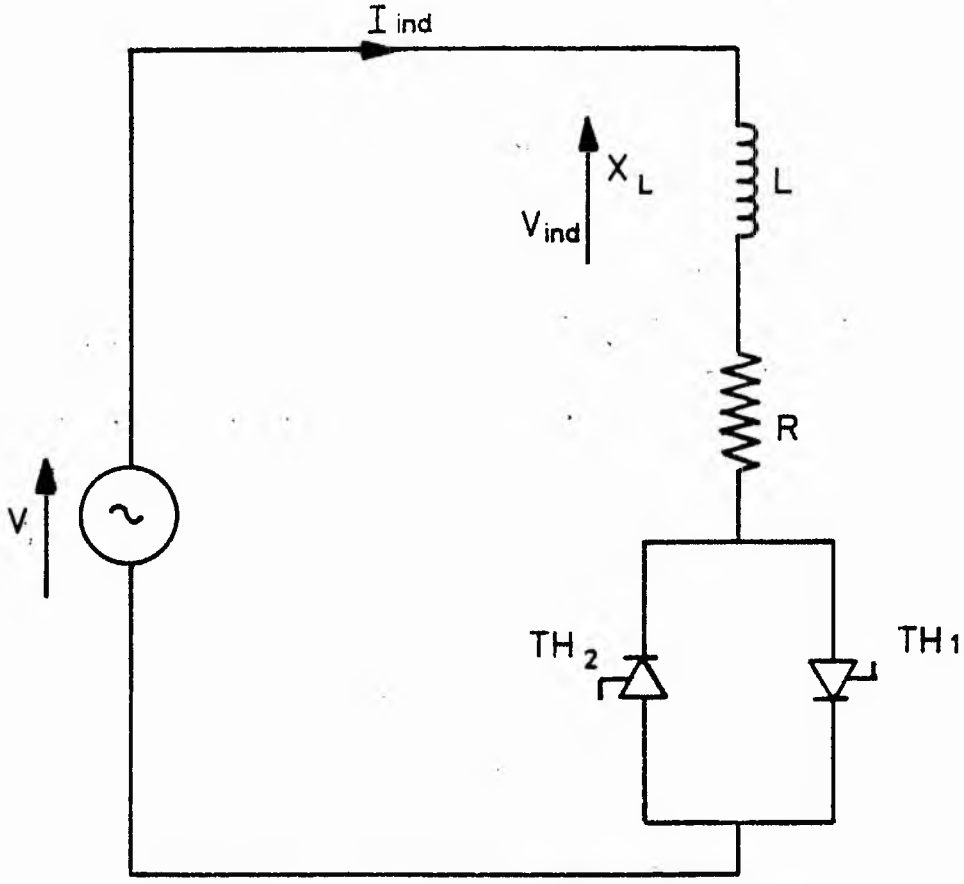

Fig. 4.7 Inductive load control by a back to back thyristor pair.

4.3.1. Voltage Control of a Phase Controlled RC Load

The capacitor load voltages and current waveform are considered to be as shown in Fig. 4.6. In the case of purely capacitive load or series capacitive-resistive load, a pulse duration of a few microseconds will trigger the thyristor, whereas with an inductive load, it is necessary to sustain the pulse during the thyristor conduction interval until the thyristor current reaches the holding level, or to use a repetitive train of pulses.

The load current during the conduction period $\theta < \omega t < X$ is illustrated in Fig. 4.6. where θ is the firing delay angle and X is the extinction angle. The current is given by the sum of a sinusoidal steady state component $I_m \sin(\omega t + \phi)$ plus an exponential component initiated at the instant of triggering and decaying at a rate determined by the time constant $\tau = RC$ of the capacitive load impedance as:-

$$i = \frac{V_m}{|Z|} \sin(\omega t + \phi) + I\sigma\, e^{-\tan\phi.\omega t} \qquad (4.1)$$

Where Z indicates the total capacitive impedance, and ϕ indicates the phase angle which is:

$$\phi = \tan^{-1} \frac{1}{\omega CR} \qquad (4.2)$$

At the instant of switch on, the inrush current is

$$i(\theta) = \frac{V_m (\sin\theta + \sin X)}{R} = \frac{V_m}{|Z|} \left[\frac{\sin\theta + \sin X}{\cos\phi}\right] \qquad (4.3)$$

Thus the transient current will be

$$I_o = i(\theta) - \left[\frac{V_m}{|Z|} \sin(\omega t + \phi)\right]_{\omega t = \theta}$$

$$= \frac{V_m}{|Z|} \left[\frac{\sin\theta + \sin X}{\cos\phi} - \sin(\theta + \phi)\right] \qquad (4.4)$$

and the instantaneous current from Eqn. (4.5) and (4.8) will be

$$i = I_m \left[\sin(\omega t + \phi) + \left\{\frac{\sin\theta + \sin X}{\cos\phi} - \sin(\theta + \phi)\right\} e^{-\tan\phi.\omega t}\right]_{\theta}^{X} \qquad (4.5)$$

The extinction angle X has a particular importance in the control of a capacitive load and in the analysis of harmonics in the capacitor.

The extinction angle depends on both the load angle and firing delay angle θ, and it can be found from the general expression for current given in Eqn. (4.5) equating this equation to zero, when ωt = X gives,

$$\sin(X + \phi) + \left\{\frac{\sin\theta + \sin X}{\cos\phi} - \sin(\theta + \phi)\right\} e^{-x\tan\phi} = 0 \qquad (4.6)$$

The computer solution of this equation is given in Fig. 4.8.

Any form of current interruption in the phase balancing network will produce a non-sinusoidal current through Z_α or Z_β and a non-sinusoidal voltage across it. Current harmonics will be drawn from the supply, affecting the quality of the system input current. Voltage harmonics generated by the reactive elements Z_α and Z_β will be effectively applied to the motor asymetrically giving an impaired performance. The choice of the appropriate electronic controller will therefore be determined by the amount of harmonic generation as well as the range of control. Each control combination is therefore investigated by harmonic analysis.

The Fourier coefficients of the current are as follows.

For the fundamental

$$a_1 = \frac{1}{\pi} \int_0^{2\pi} i.\sin\omega t \, d(\omega t) \qquad (4.7)$$

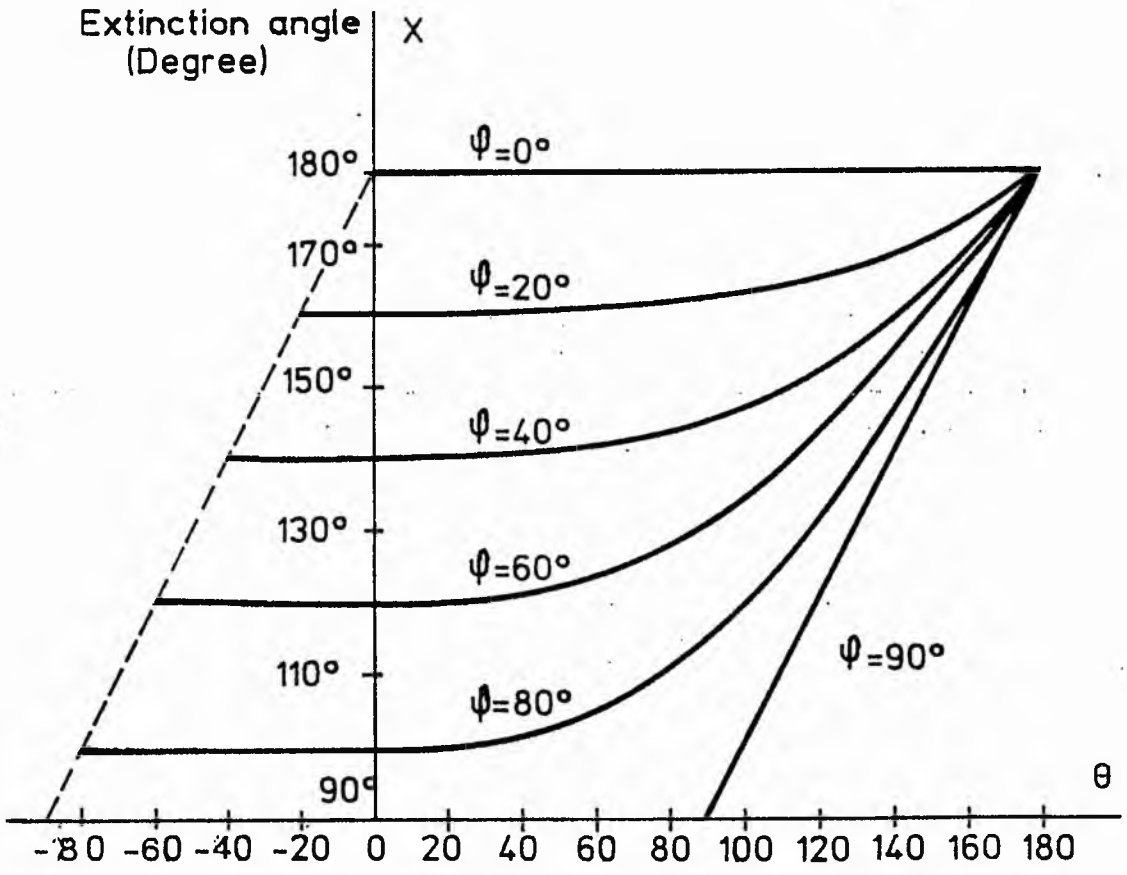

Fig 4.8 Firing delay angle/extinction angle for a series R-C load

and so, from eqns. (4.5) and (4.7)

$$a_1 = \frac{I_m}{\pi} - \left[\cos(\theta + X + \phi)\sin(X - \theta) + (X - \theta)\cos\phi + 2\left\{\frac{\sin X + \sin\theta}{\cos\phi} - \sin(\theta + \phi)\right\}\cos\phi\left\{-\cos(X - \phi)e^{-(x-\phi)\tan\phi} + \cos(\theta - \phi)\right\}\right] \quad (4.8)$$

$$b_1 = \frac{1}{\pi}\int_0^2 i\cos\omega t\, d(\omega t) \quad (4.9)$$

and from eqns. (4.5) and (4.9)

$$b_1 = \frac{I_m}{\pi}\left[\sin(\theta + X + \phi)\sin(X - \theta) + (X - \theta)\sin\phi + 2\left\{\frac{\sin X + \sin\theta}{\cos\phi} - \sin(\theta + \phi)\right\}\cos\phi\left\{\sin(X - \phi)e^{-(x-\theta)\tan\phi} - \sin(\theta - \phi)\right\}\right] \quad (4.10)$$

The other higher-order harmonics will be

$$a_n = -\frac{I_m}{\pi}\left[\frac{\sin\{(1+n)\theta + \phi\} - \sin\{(1+n)X + \phi\}}{1 - n} + \frac{-\sin\{(1-n)\theta + \phi\} + \sin\{(1-n)X + \phi\}}{1 + n} + \frac{2\left(\frac{\sin\theta + \sin X}{\cos\phi} - \sin(\theta + \phi)\right)}{\sqrt{n^2 + \tan^2\phi}}\left\{-\cos(nX - \rho)e^{-(x-\theta)\tan\phi} + \cos(nX - \rho)\right\}\right] \quad (4.11)$$

where $\rho = \tan^{-1}\left(\frac{\tan\phi}{n}\right)$

$$b_n = \frac{I_m}{\pi}\left[\frac{\cos\{(1+n)\theta+\phi\} - \cos\{(1+n)X+\phi\}}{1+n}\right.$$

$$+ \frac{\cos\{(1-n)\theta+\phi\} - \cos\{(1-n)X+\phi\}}{1-n}$$

$$+ \frac{2\left(\frac{\sin\theta + \sin X}{\cos\phi} - \sin(\theta+\phi)\right)}{\sqrt{n^2 + \tan^2\phi}}$$

$$\left.\{\sin(nX-\rho)e^{-(x-\theta)\tan\phi} - \sin(n\theta-\rho)\}\right] \qquad (4.12)$$

The variation of current harmonics is shown in Figs. 4.9A and B for two different load angles. Since the function considered is f (y+π) = - f (y), there are no even harmonics and the negative half cycle is a reflection of positive half cycle.

The load voltage is defined with respect to Fig. 4.6.B as:-

$$V = V_m \sin\omega t \Big|_{\theta,\pi+\theta}^{x,\pi+x} - V_m \sin X \Big|_{0,\pi+x}^{\theta,2\pi}$$

$$+ V_m \sin X \Big|_{x}^{x+\theta} \qquad (4.13)$$

The Fourier coefficient can now be calculated.

For the fundamental components:

$$a_{v1} = \frac{1}{\pi}\int_0^{2\pi} V \sin\omega t \, d(\omega t) \qquad (4.14)$$

and from eqns. (4.13) and (4.14)

$$a_{v1} = \frac{V_m}{\pi}\left[2\sin X(\cos\theta + \cos X) + X - \theta + \frac{1}{2}(\sin 2\theta - \sin 2X)\right] \qquad (4.15)$$

and

$$b_{v1} = \frac{1}{\pi}\int_0^{2\pi} V \cos\omega t \, d(\omega t) \qquad (4.16)$$

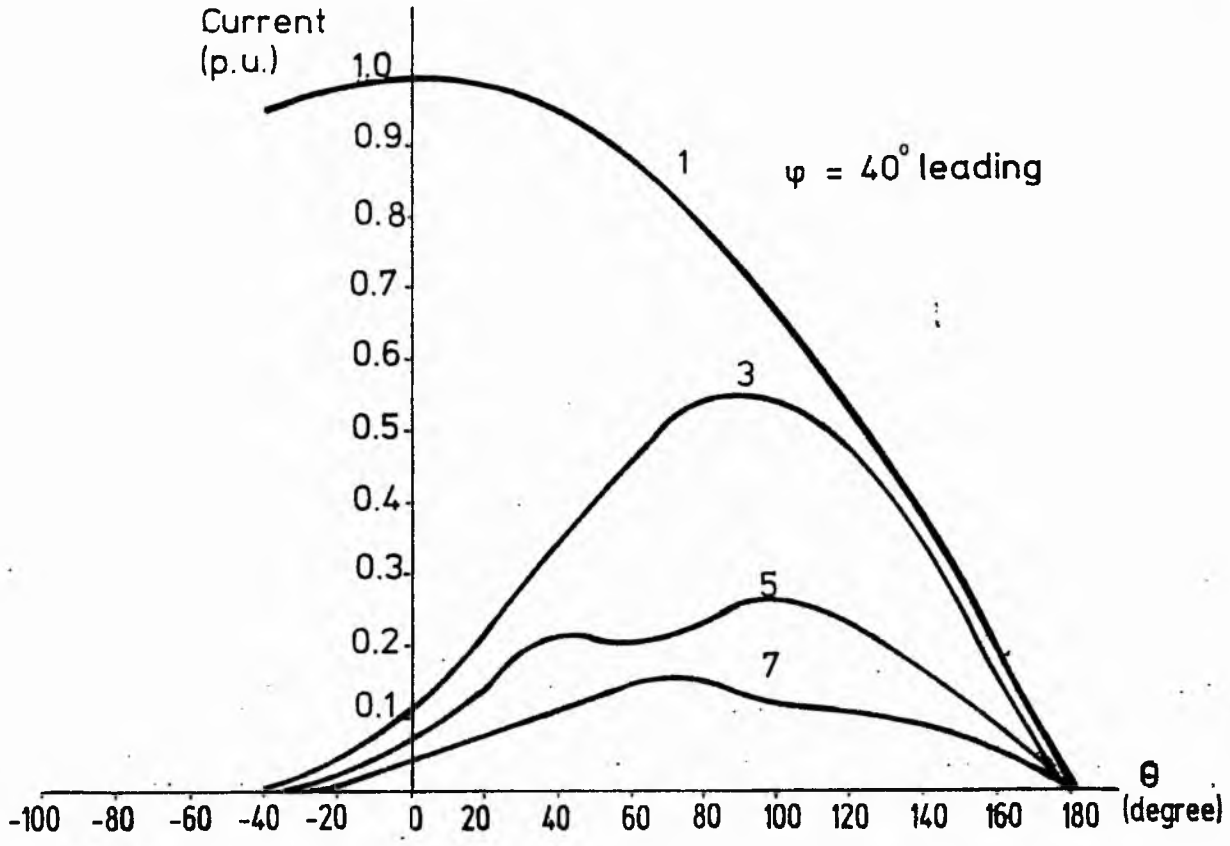

Fig. 4.9A Harmonic components of current/firing delay angle for series R-C load.

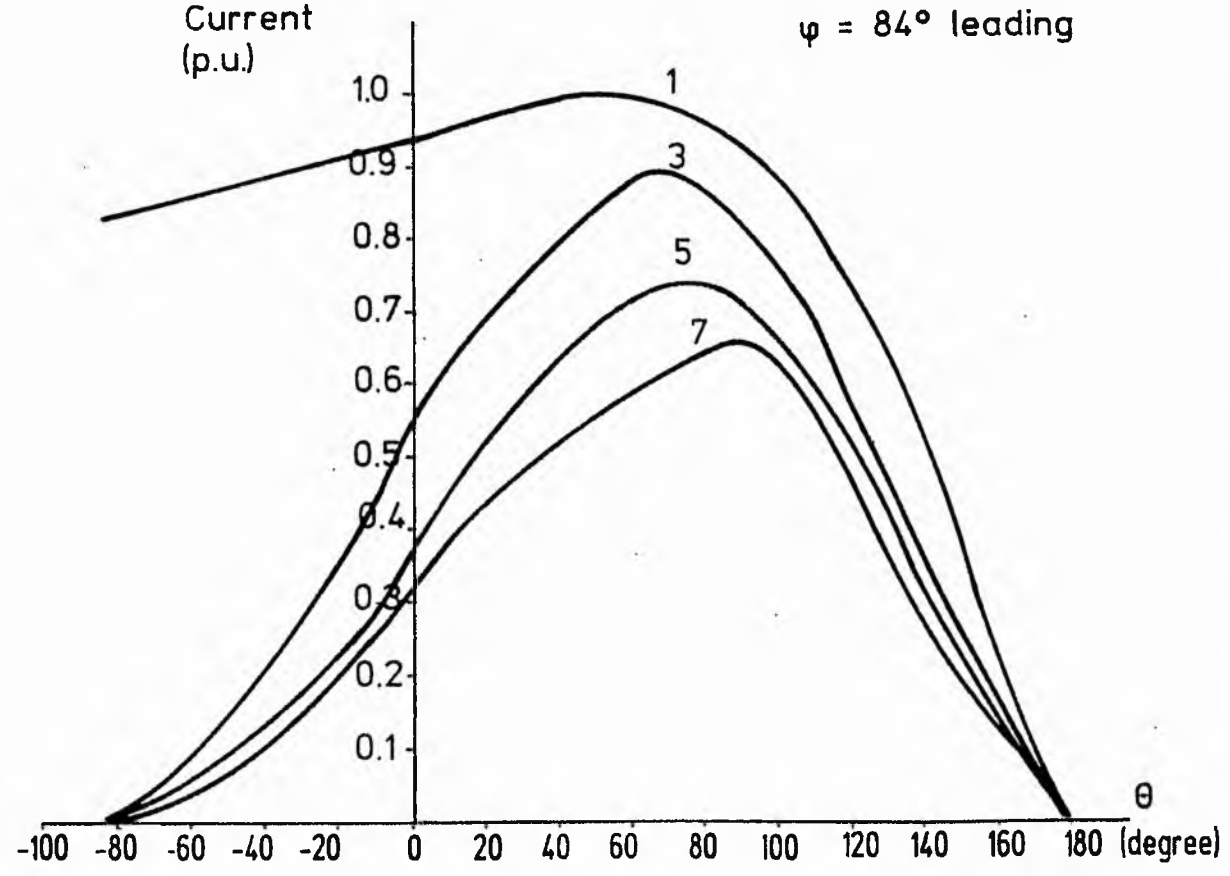

Fig. 4.9.B Harmonic components of current/ firing delay angle for series R-C load

From eqns. (4.13) and (4.16)

$$b_{v1} = \frac{V_m}{\pi}\left[2\sin X\,(-\sin\theta - \sin X) + \frac{1}{2}(\cos 2\theta - \cos 2X)\right] \tag{4.17}$$

For the other higher-order harmonic components

$$a_{vn} = \frac{1}{\pi}\int_0^{2\pi} V \sin n\omega t\, d(\omega t) \tag{4.18}$$

and, from eqns. (4.13.) and (4.18.),

$$a_{vn} = \frac{V_m}{\pi}\left[\frac{2\sin X}{n}(\cos n\theta + \cos nX) + \frac{\sin[(1+n)\theta] - \sin[(1+n)X]}{1+n} + \frac{-\sin[(1-n)\theta] + \sin[(1-n)X]}{1-n}\right] \tag{4.19}$$

and

$$b_{vn} = \frac{1}{\pi}\int_0^{2\pi} V \cos n\omega t\, d(\omega t) \tag{4.20}$$

From eqns. (4.13) and (4.20)

$$b_{vn} = \frac{V_m}{\pi}\left[\frac{2\sin X}{n}(-\sin n\theta - \sin nX) + \frac{\cos[(1+n)\theta] - \cos[(1+n)X]}{1+n} + \frac{\cos[(1-n)\theta] - \cos[(1-n)X]}{1-n}\right] \tag{4.21}$$

The variation of voltage harmonics is illustrated in Figs. 4.10A and B. The negative half cycle is the reflection of positive half cycle.

The current and voltage harmonics resemble each other; but the current harmonic components are greater than the voltage harmonic components. In the case when $\phi = 84°$ leading, the current harmonics are twice the load voltage harmonics. When $\phi = 40°$ leading, the current harmonics are 1.5 times the voltage harmonics. This indicates that, as the capacitive phase angle decreases (i.e. the phase angle increases negatively), the current waveform for a given triggering angle becomes progressively more spiky and the proportion of harmonic increases.

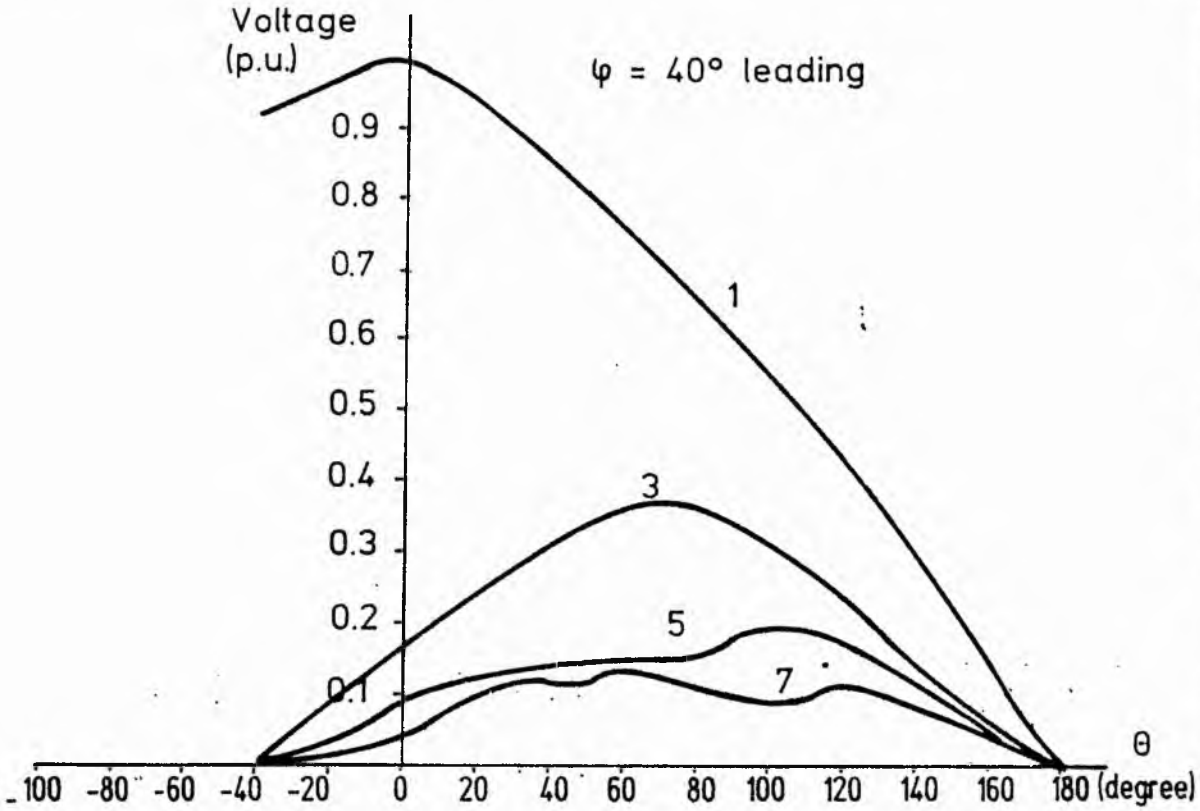

Fig. 4.10.A Voltage harmonics/firing delay angle for capacitive load.

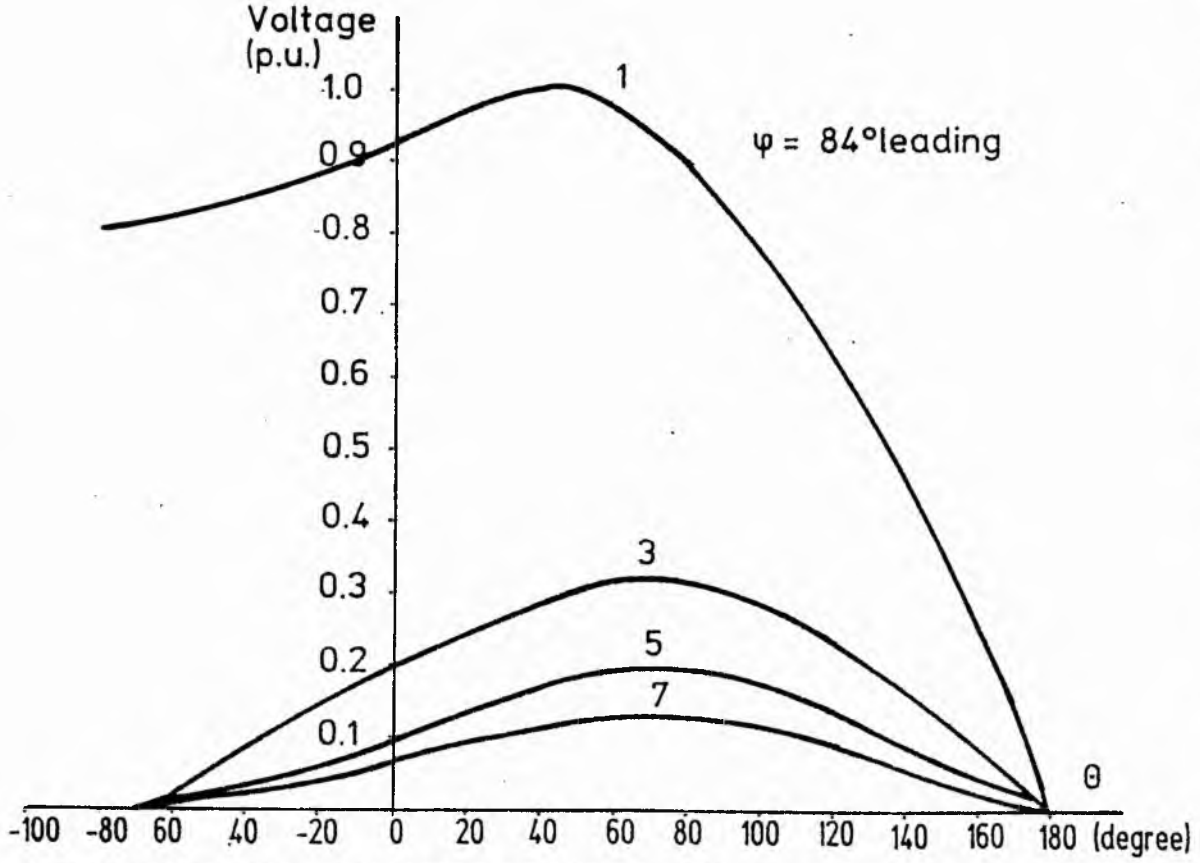

Fig. 4.10.B Voltage harmonics/firing delay angle for capacitive load.

The higher frequency harmonics will cause an induction motor to overheat if they appear across the motor winding. The required load for the induction motor is only the fundamental component. Hence, the harmonic currents cause increased copper loss in the winding without contributing to the useful output. If the harmonic current increases, efficiency decreases and excessive heating may result. Thus, phase angle contol into a capacitive load is inefficient. Apart from the high harmonic components, the operational difficulties are encountered in the limited range of control of a capacitive load. This can be seen in Fig. 4.6. When the current passes zero (i.e. it reaches its extinction angle) the capacitor is left charged and the succeeding switch-on of the thyristor causes high inrush current. On the other hand, in the case of a phase converter application, the controlled load is highly capacitive (i.e. load angle approaching to 90° leading). Thus the control range is limited as shown in Fig. 4.8.

4.3.2. Phase Control of Voltage in a Series R-L Load

4.3.2.1 General

If the load current I_L, in a series R-L load controlled by a back-to-back thyristor pair is considered, at the instant θ of thyristor triggering, the load current is zero as shown in Fig. 4.11. The sinusoidal load current for a phase angle ϕ at this instant would have the instantaneous value $I_m \sin(\omega t - \phi)$. The resultant load current is then the sinusoidal current $I_m \sin(\omega t - \phi)$ less a transient current having a value $I_m \sin(\theta - \phi)$ at $\omega t = \theta$. This transient must decay depending on the circuit time constant by an exponential $e^{-R/\omega L (\omega t - \theta)}$; where R and ωL are the resistance and fundamental frequency reactance of the controlled inductive load. It is shown in Fig. 4.11. that in the range of $X < \omega t < \pi + \phi$; the resultant current is mathematically negative. However, the conducting thyristor will not permit the flow of reverse current, consequently the conduction ceases at the point X (i.e. the extinction angle). Thus, the current can be described referring to Fig. 4.11. as;

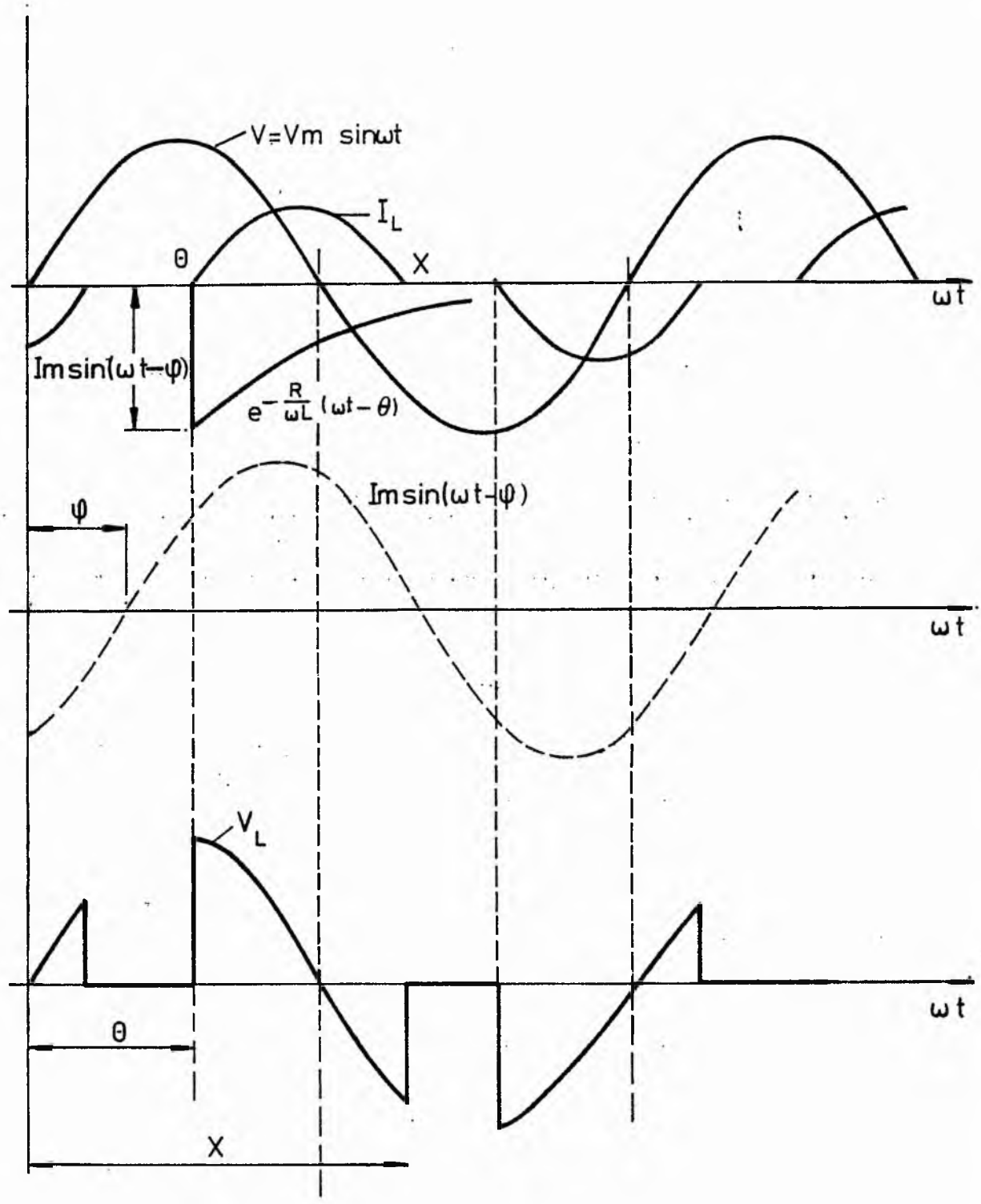

Fig 4.11 Theoretical waveforms of load voltage and current for series R-L load (Fig 3-3)

$$i_L = I_m \left[\sin(\omega t - \phi) \Big|_{0,\theta,\pi+\theta}^{x-\pi,x,2\pi} + \sin(\theta - \phi) e^{-\cot g\phi(\omega t+\pi-\theta)} \Big|_{0}^{x-\pi} \right.$$

$$\left. - \sin(\theta - \phi) e^{-\cot g\phi(\omega t-\theta)} \Big|_{\theta}^{x} + \sin(\theta - \phi) e^{-\cot g\phi(\omega t-\pi-\theta)} \Big|_{\pi+\theta}^{2\pi} \right] \quad (4.22)$$

Putting Eqn. (4.22) equal to zero and making $\omega t = X$; the extinction angle for a given load angle can be found as a function of the firing delay angle, θ. This gives,

$$\sin(x - \phi) - \sin(\theta - \phi) e^{-\cot g\phi(x-\theta)} = 0 \quad (4.23)$$

The computer solution of Eqn. (4.23) is shown in Fig. 4.12. The variation of extinction angle for a given load is plotted as a function of firing delay angle.

It must be noted that if $\theta < \phi$, the current will only flow in one direction. In fact on the switching-on of the positive cycle conducting thyristor, current starts to flow and is interrupted at the angle "$2\pi - \theta$" ; if the current could decay naturally, the extinction angle would occur after the control signal is received by the negative cycle conducting thyristor. This means that no current can start in the opposite direction. Current will thus flow in one direction only, notably in the direction of the thyristor which is switched on first. The current through the inductance will have a positive or negative d.c. component.

Referring to Eqn. (4.23) if $\theta = \phi$ which represents sinusoidal operation, Eqn. (4.23) reduces to

$$\sin(x - \phi) = \theta \quad (4.24)$$

This satisfies the condition

$$x = \pi + \phi \quad (4.25)$$

for sinusoidal operation. Furthermore, a conduction angle, ζ for the controlled current can be defined as

$$\zeta = x - \theta \quad (4.26)$$

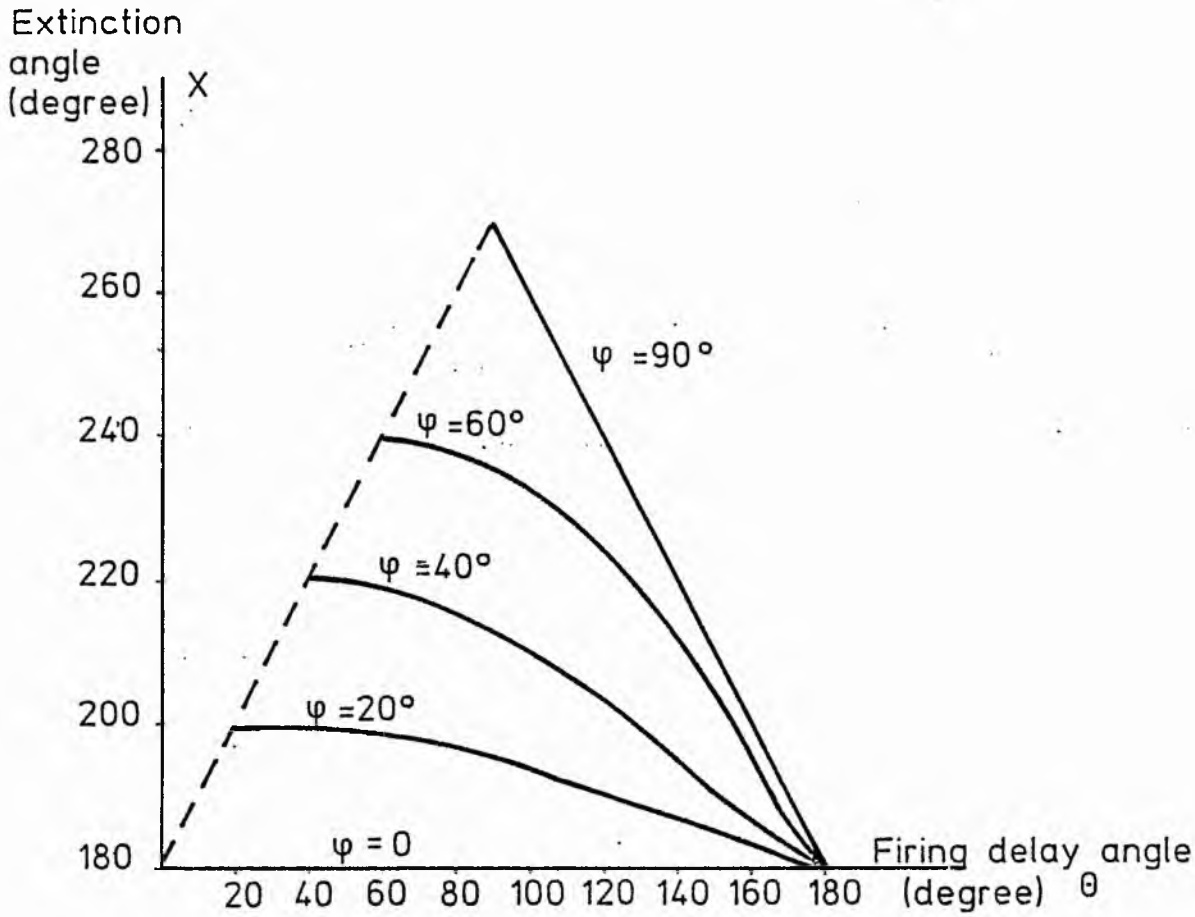

Fig. 4.12 Firing delay angle/extinction angle for a series R-L load.

4.3.2.2. Current Harmonics of a Series R-L Load Controlled by a Back-to-Back Thyristor Pair

The Fourier coefficients of the load current can be found as follows; the d.c. component:

$$a_0 = 2\left[\frac{1}{2\pi}\int_0^{2\pi} i_L(\omega t)\, d(\omega t)\right] = \theta \tag{4.27}$$

The fundamental current component,

$$a_1 = \frac{1}{\pi}\int_0^{2\pi} i_L(\omega t)\, \sin\omega t\, d(\omega t) \tag{4.28}$$

From eqns. (4.22) and (4.27)

$$a_1 = \frac{V_m}{2\pi|Z|}\Big[\sin(2\theta-\phi) - \sin(2X-\phi) + \cos\phi(2X-2\theta) + 4\sin\phi\,\sin(\theta-\phi)\left\{\sin(\phi+X)e^{-\cot g\phi(X-\theta)} - \sin(\theta+\phi)\right\}\Big] \tag{4.29}$$

and

$$b_1 = \frac{1}{\pi}\int_0^{2\pi} i_L(\omega t)\, \cos\omega t\, d(\omega t) \tag{4.30}$$

From eqns. (4.22) and (4.30)

$$b_1 = \frac{V_m}{2\pi|Z|}\Big[\sin(2\theta-\phi) - \sin(2X-\phi) - \sin(2X-2\theta) + 4\sin\phi\,\sin(\theta-\phi)\left\{\cos(\phi+X)e^{-\cot g\phi(X-\theta)} - \cos(\phi+\theta)\right\}\Big] \tag{4.31}$$

As for the other high order harmonic components, the Fourier coefficients will be

$$a_n = \frac{1}{\pi}\int_0^{2\pi} i_L(\omega t)\sin n\omega t\, d(\omega t) \tag{4.32}$$

From eqns. (4.22) and (4.32)

$$a_n = \frac{V_m}{2\pi|Z|}\left[\frac{2}{n+1}\sin[(n+1)\theta-\phi] - \sin[(n+1)X-\phi] - \frac{2}{n-1}\right]$$

$$\{\sin[(n-1)\theta-\phi] - \sin[(n-1)X-\phi]\}$$

$$+\frac{4\sin(\theta-\phi)}{n^2+\cot g^2\phi}\left\{(\cot g\phi \sin nX + n\cos nX)e^{-\cot g\phi(X-\theta)}\right.$$

$$\left.-(\cot g\phi \sin n\theta + n\cos n\theta)\right\}\Big] \tag{4.33}$$

and

$$b_n = \frac{1}{\pi}\int_0^{2\pi} i_L(\omega t)\cos n\omega t\, d(\omega t) \tag{4.34}$$

From eqns. (4.22) and (4.34)

$$b_n = \frac{V_m}{2\pi|Z|}\left[\frac{2}{n+1}\left\{\cos[(n+1)\theta-\phi]\right.\right.$$

$$\left.-\cos[(n+1)X-\phi]\right\} - \frac{2}{n-1}\left\{\cos[(n-1)\theta-\phi]\right.$$

$$-\cos[(n-1)X-\phi] + \frac{4\sin(\theta-\phi)}{n^2+\cot g^2\phi}$$

$$\left\{(\cot g\,\phi\cos nX - n\sin nX)e^{-\cot g\phi(X-\theta)}\right.$$

$$\left.\left.-(\cot g\,\phi\cos n\theta - n\sin n\theta)\right\}\right] \tag{4.35}$$

The computed results of current harmonics are shown in Fig.4.13.A, B and C for third, fifth and seventh harmonics. Since the positive and negative half cycles of the controlled currents are the reflections of each other, only the odd harmonics will be present.

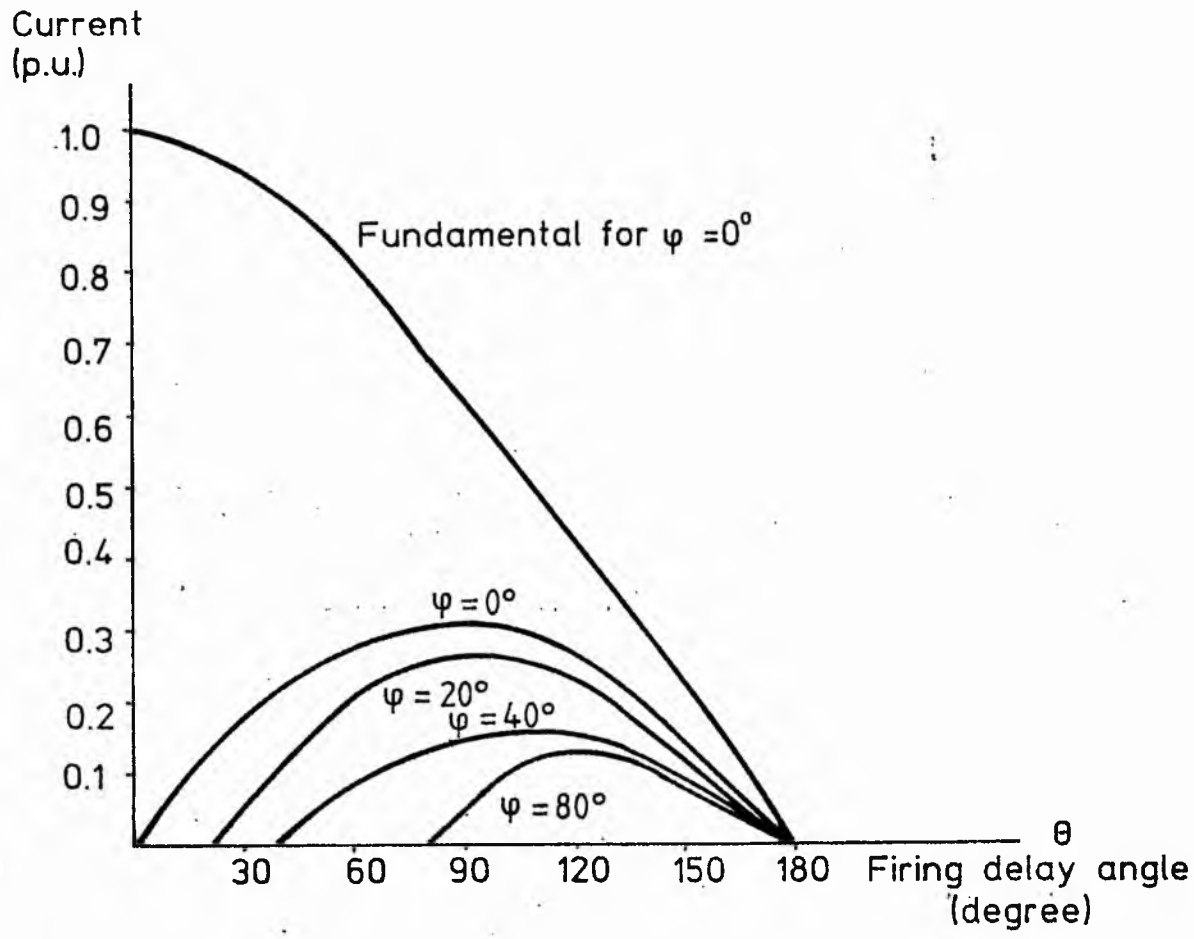

Fig 4.13A Third harmonic/firing delay angle of series R-L load.

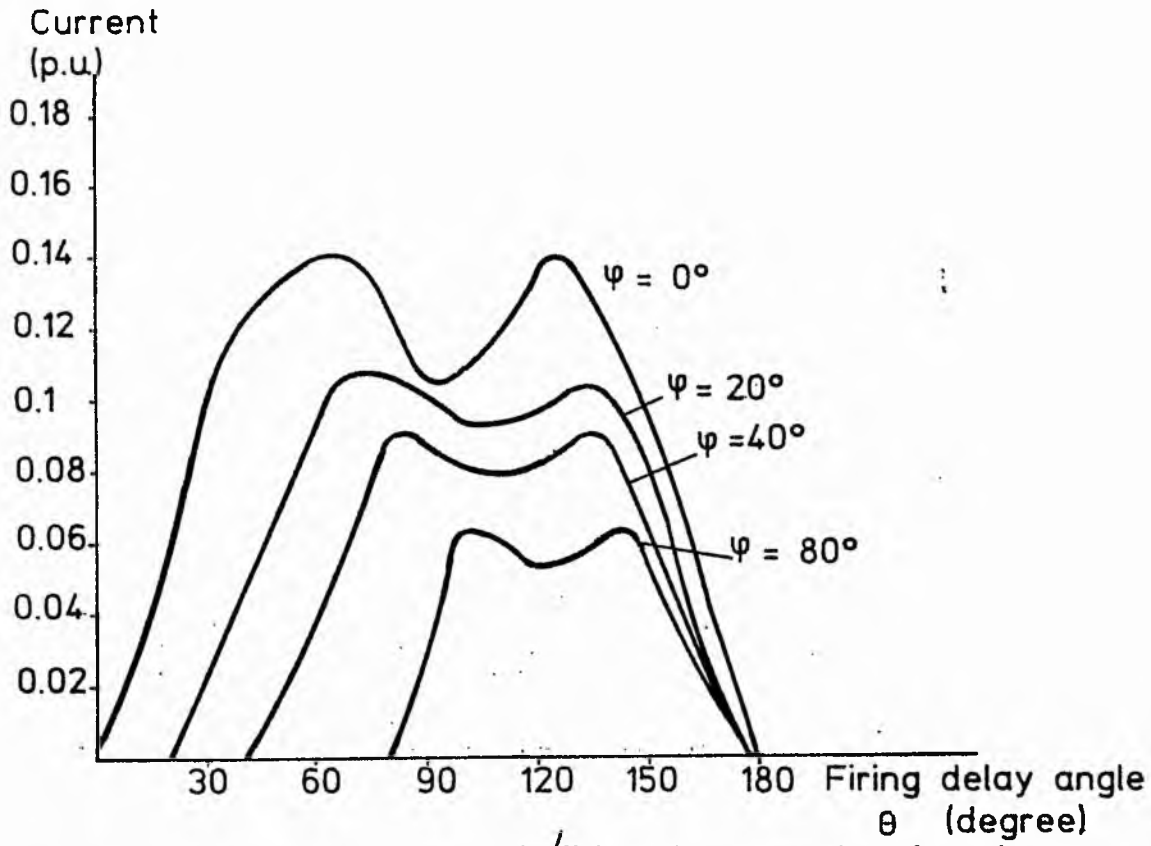

Fig. 4.13B Fifth harmonic/firing delay angle of series R-L load.

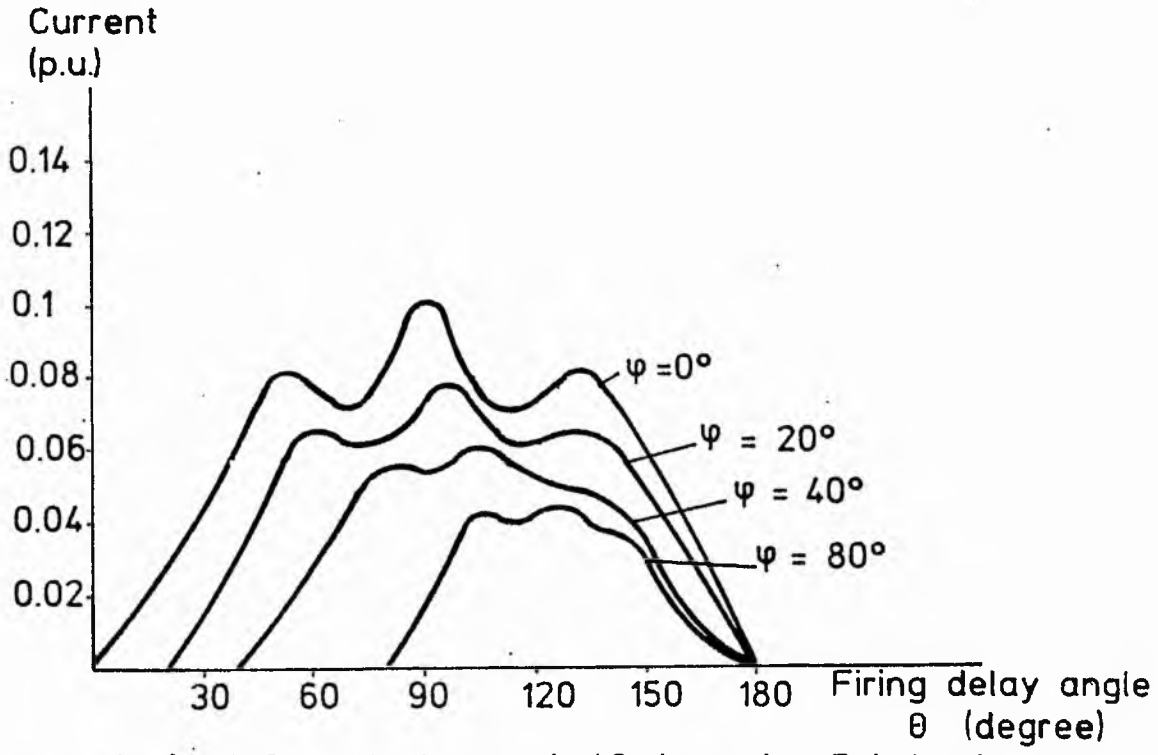

Fig. 4.13C Seventh harmonic/θ in series R-L load

4.3.2.3. Voltage Harmonics of a Series R-L Load Controlled by a Back-to-Back Thyristor Pair

It is shown in Fig.4.11. that, in the case of a series R-L load, the load voltage waveform should ideally have the shape of a sinusoidal wave with a vertical segment chopped out. The missing portion of the load-voltage waveform forms the voltage drop across the thyristor during the extinction periods.

The voltage can be expressed in general, steady-state form as:

$$V_L = V_m \sin\omega t \Big|_{0,\theta,\pi+\theta}^{x-\pi,X,2\pi} \tag{4.36}$$

If the Fourier coefficients are considered, the d.c. component of voltage will be:

$$a_o = 2\left[\frac{1}{2\pi}\int_0^{2\pi} V_L(\omega t)\, d(\omega t)\right] = 0 \tag{4.37}$$

and the fundamental harmonic coefficients will be

$$a_{1v} = \frac{1}{\pi}\int_0^{2\pi} V_L(\omega t) \sin \omega t\, d(\omega t) \tag{4.38}$$

From eqns. (4.36) and (4.38), integrating and rearranging gives

$$a_{1v} = \frac{V_m}{2\pi}[2(X-\theta) - \sin 2X + \sin 2\theta] \tag{4.39}$$

and

$$b_{1v} = \frac{1}{\pi}\int_0^{2\pi} V_L(\omega t) \cos \omega t\, d(\omega t) \tag{4.40}$$

From eqns. (4.36) and (4.40), integrating and rearranging gives

$$b_{1v} = \frac{V_m}{2\pi}(\cos 2\theta - \cos 2X) \tag{4.41}$$

As for the other high-order harmonic components, the Fourier coefficients can be found as

$$a_{nv} = \frac{1}{\pi}\int_0^{2\pi} V_L(\omega t) \sin n\omega t \, d(\omega t) \tag{4.42}$$

Integrating and rearranging eqn. (4.42) and considering eqn. (4.36) gives

$$a_{nv} = \frac{V_m}{2\pi}\left[\frac{2}{n+1}\{\sin[(n+1)\theta] - \sin[(n+1)X]\} - \frac{2}{n-1}\{\sin[(n-1)\theta] - \sin[(n-1)X]\}\right] \tag{4.43}$$

and

$$b_{nv} = \frac{1}{\pi}\int_0^{2\pi} V_L(\omega t) \cos n\omega t \, d(\omega t) \tag{4.44}$$

From Eqns. (4.36) and (4.44), integrating and arranging gives

$$b_{nv} = \frac{V_m}{2\pi}\left[\frac{2}{n+1}\{\cos[(n+1)\theta] - \cos[(n+1)X]\} - \frac{2}{n-1}\{\cos[(n-1)\theta] - \cos[(n-1)X]\}\right] \tag{4.45}$$

when $\phi = 0°$, then $X = \pi$ and it represents a resistive load.

The variation of voltage harmonics in a series R-L load are illustrated in Figs. 4.14.A, B and C.

It can be seen that substantial 3rd and 5th harmonics at the frequencies of 150 Hz and 250 Hz will be injected into the system by a back-to-back thyristor pair controller. Such harmonics can cause serious motor overheating. The higher harmonics will produce much less current in the system; and since the motor impedance depends on frequency, a much higher rate of current interruption is required. In fact, if the motor impedance is considered as a low pass filter to the harmonic currents, the inductive impedance increases with frequency and thus high-frequency harmonics will be blocked.

If the harmonics generated by a back-to-back thyristor pair in a capacitive and an inductive load are considered, it can be seen in Figs. 4.9., 4.10., 4.13. and 4.14. that the current harmonics in the case of a capacitive load are seven times

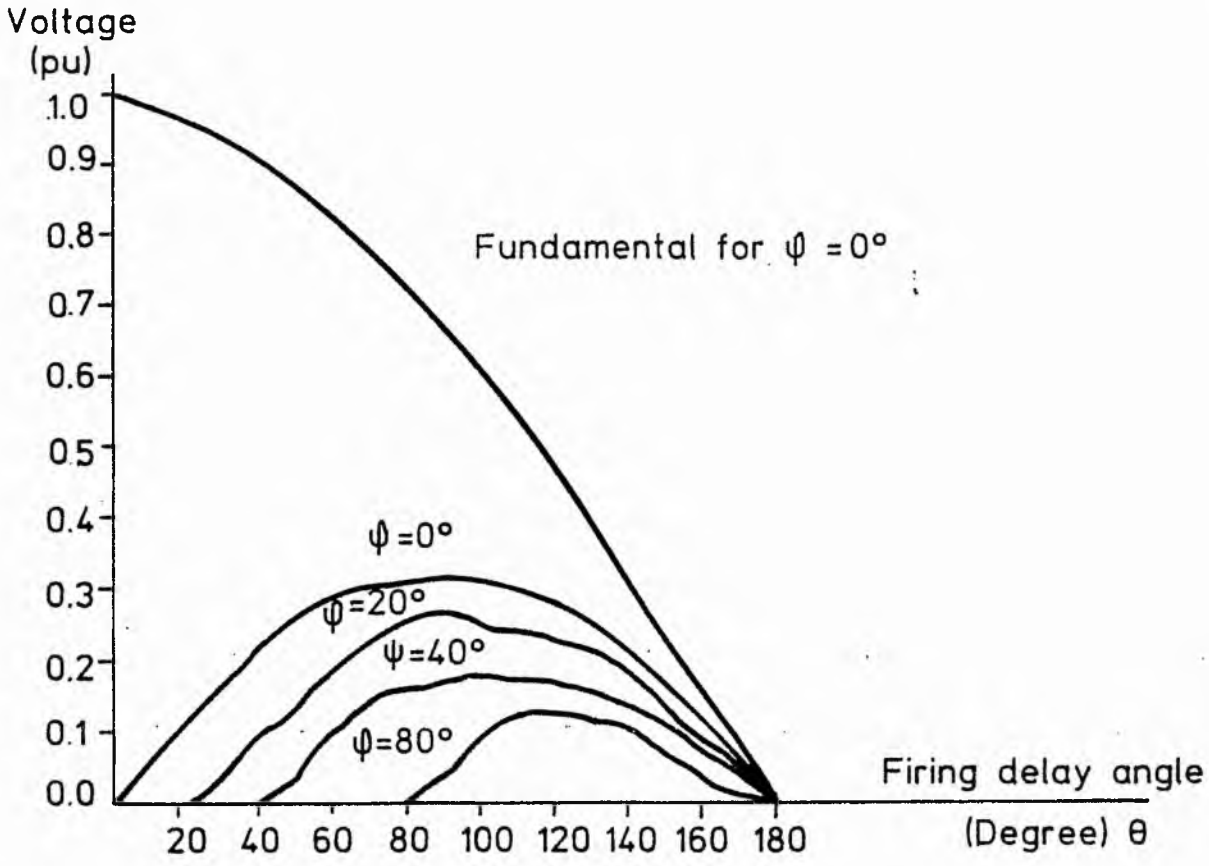

Fig. 4.14A 3rd. harmonic voltage component/θ for R-L load

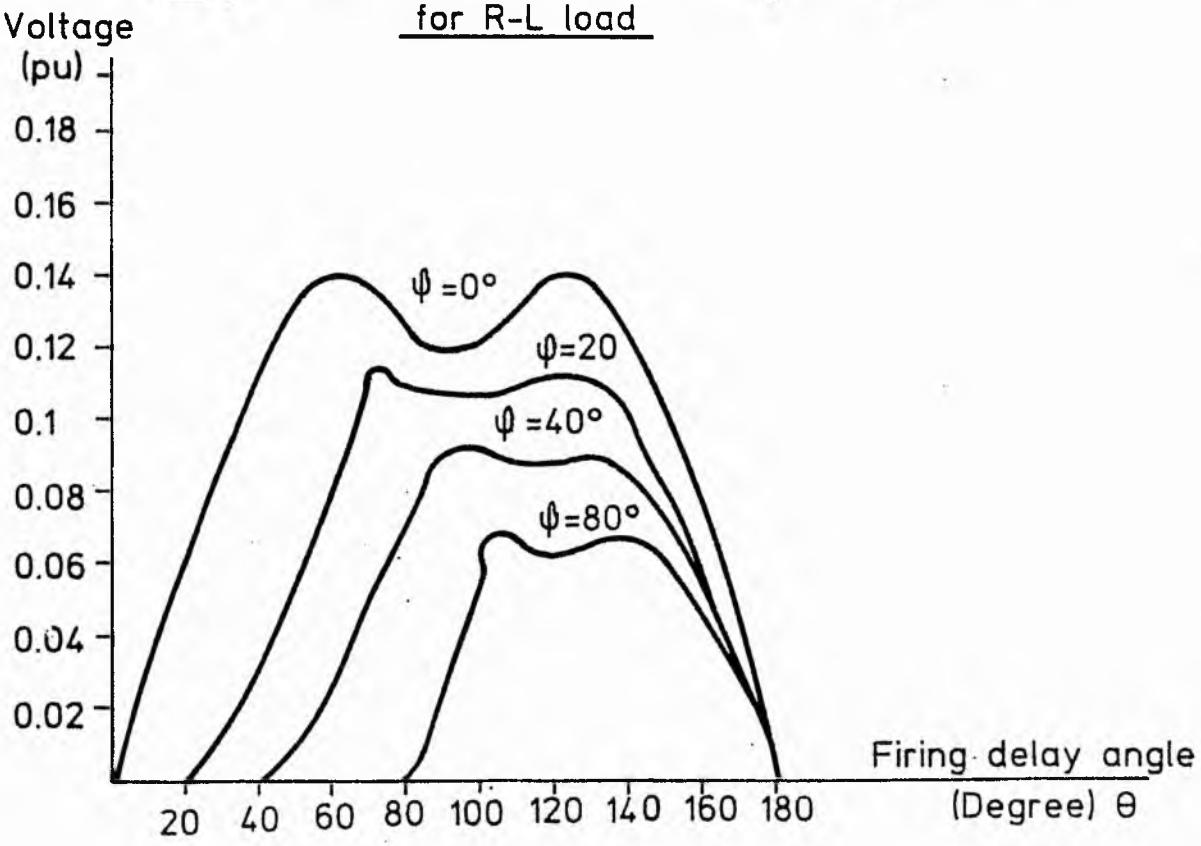

Fig. 4.14B 5th harmonic voltage/θ for R-L load

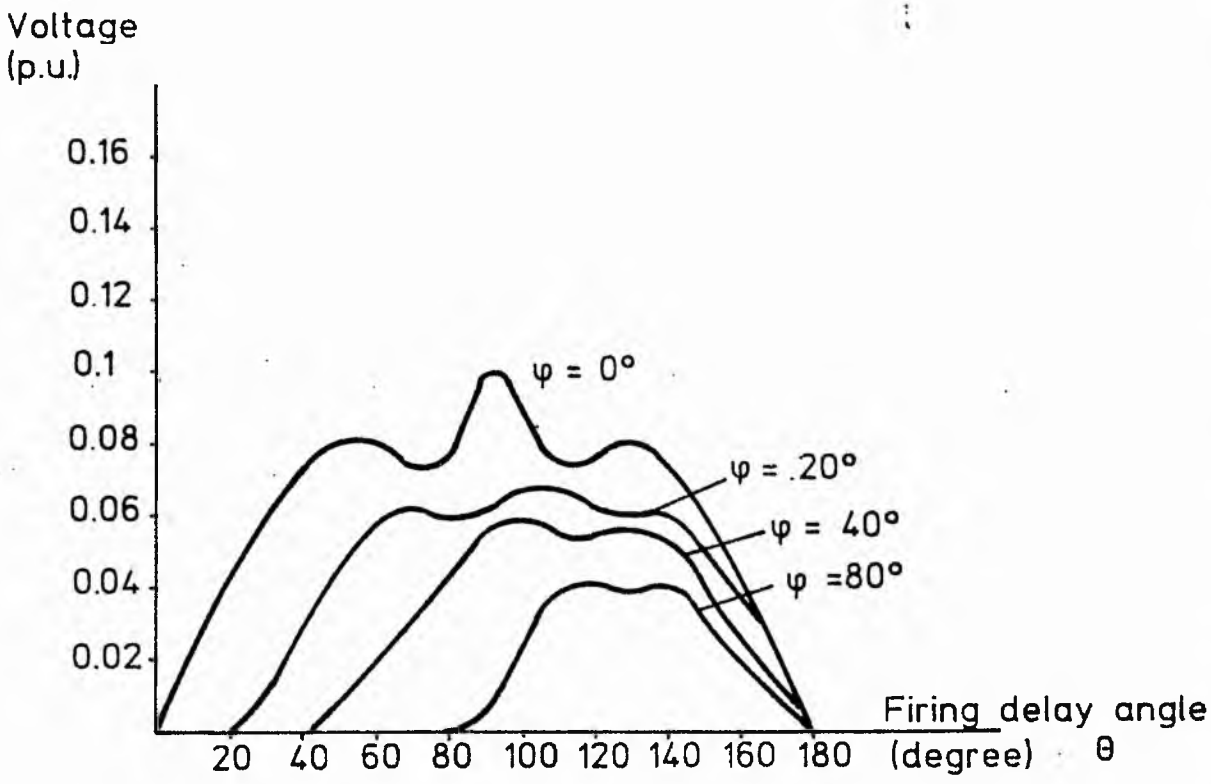

Fig. 4. 14C Seventh harmonic voltage/θ for R-L load.

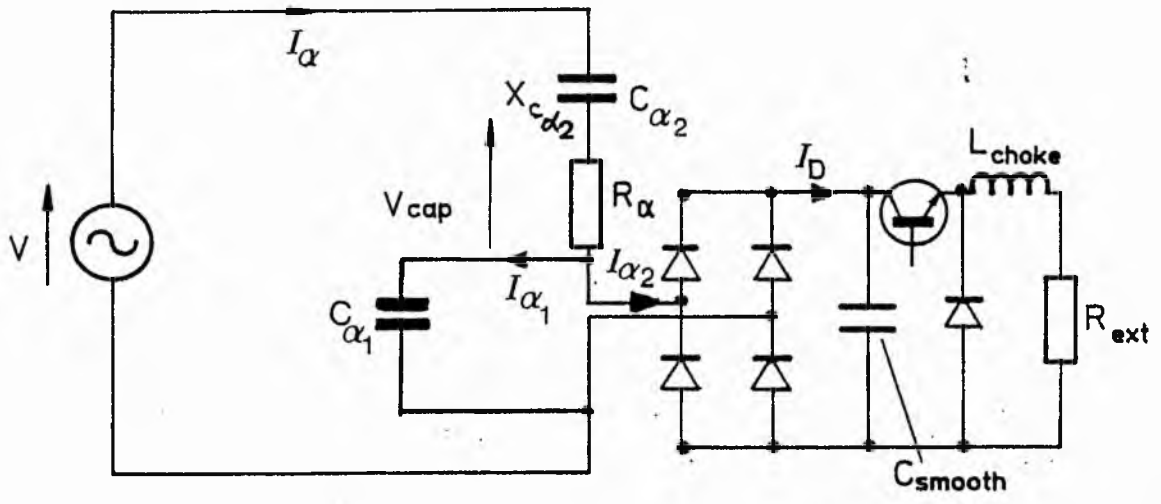

Fig. 4.15 Capacitive load control by transistor chopper

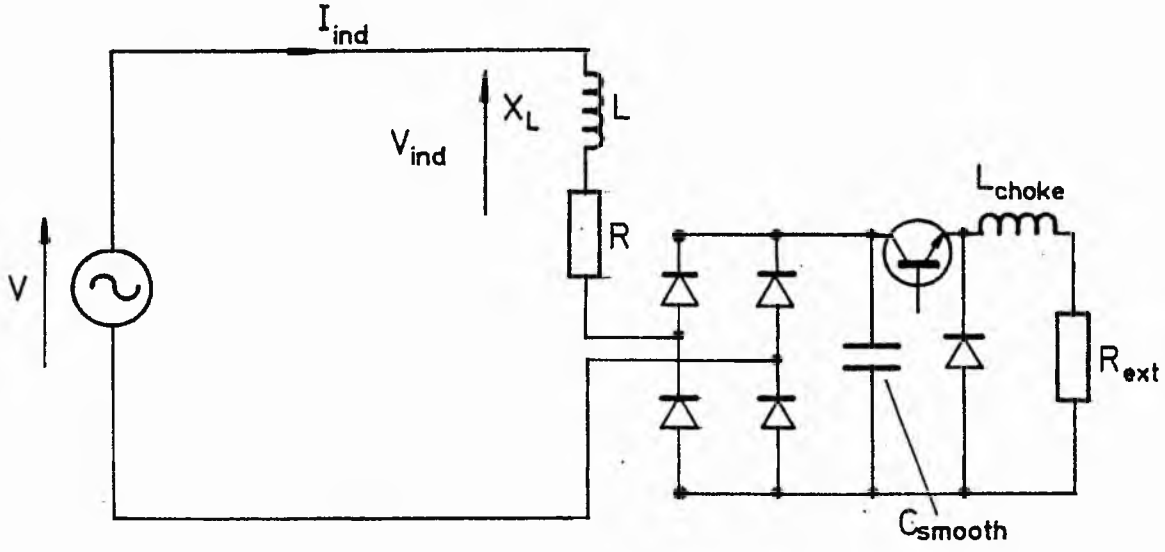

Fig. 4.16 Inductive load control by transistor chopper

higher than the inductive load. The voltage harmonics for the capacitive load are almost three times higher than the inductive load.

4.4. Chopper Controller in the Reactive Load Control

4.4.1. General

The control of reactive energy storage in the network of Figs. 4.15. and 4.16. can be achieved much more effectively by chopping the current at a frequency much greater than the mains frequency. This was achieved by inserting a bridge rectifier into the network with the bridge output connected to a switching Darlington pair power transistor. The transistor chopper operates in the ON-OFF method of power control. The mark-space ratio (or duty cycle) is defined as:

$$\gamma = \frac{\text{ON time}}{\text{ON time} + \text{OFF time}} \tag{4.46}$$

Where "ON time + OFF time" indicates the chopper period, consequently the chopper frequency will be:

$$f_{chop} = \frac{1}{T_{chop}} = \frac{1}{\text{ON time} + \text{OFF time}} \tag{4.47}$$

The chopper frequency was chosen at 400 Hz as a compromise between stable operation and the harmonic frequency. Current control is achieved by means of varying the conduction time of the power transistor. Thus the mark-space will be varied.

4.4.2. Capacitive Load Control by Chopper

Ideally, the chopper will cut the applied voltage and current into a series

of vertical strips as shown in Fig. 4.17. However, due to the storage capacity of the input capacitance, this is effectively a repeated short-circuit of charged capacitor. Although Mazda [12] indicates that this ideal solution can be achieved, power transistors are too sensitive to voltage spikes to achieve this without destroying the device.

In practice, the circuit was operated as shown in Fig. 4.15. with a very large (2000μF) electrolytic capacitor on the bridge output and a 98mH inductive load after the transistor switch. This makes the chopper operate effectively as a constant current sink fed from a constant voltage source.

In this mode of operation the bridge rectifier and smoothing circuit currents are as shown in Fig. 4.18.

The chopper varies the rms value of $I_{\alpha 2}$ which in turn controls the total capacitive current I_{α}. When C_{smooth} is very large, $I_{\alpha 2}$ can be approximated to a triangular wave, whereas $I_{\alpha 1}$ is sinusoidal which gives $I_{\alpha} = I_{\alpha 1} + I_{\alpha 2}$.

The triangular wave current $I_{\alpha 2}$ can then be represented by:

$$I_{\alpha 2} = I_{\alpha 2max} \frac{\Gamma - \Delta}{\Gamma - \Delta_1} \tag{4.48}$$

where Δ_1 and Γ are the beginning and end of the triangular wave. Δ is the time variable parameter of Eqn. 4.48. If the worst case encountered in this system is considered $\Gamma = \pi/2$ and $\Delta = ¼\pi$ making $\Delta = \omega t$ the mean square of the current I_{α} will be:

$$I_{\alpha}^2 = \frac{1}{\pi}\int_0^{\Delta} I_{\alpha 1max}^2 \sin^2\omega t \, d(\omega t) + \int_{\Delta_1}^{\Delta} \left(I_{\alpha 1max}^2 \sin^2\omega t + I_{\alpha 2max}^2\left(\frac{\Gamma - \Delta}{\Gamma - \Delta_1}\right)^2\right) d(\omega t) + \int I_{\alpha 1max} \sin^2\omega t \, d(\omega t) \tag{4.49}$$

Considering:

$$\int \sin^2 u \, du = \frac{u}{2} - \frac{\sin 2u}{4} = \frac{1}{2}(u - \sin u.\cos u)$$
$$\int \sin^2 au \, du = \frac{u}{2} - \frac{\sin 2au}{4a} \tag{4.50}$$

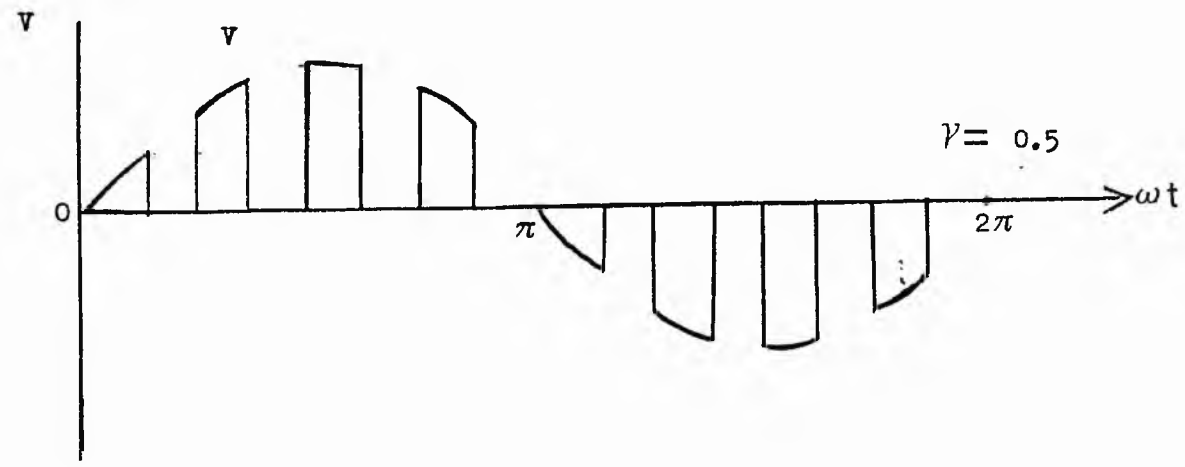

Fig. 4.17 Ideal voltage waveforms of chopper controlled load

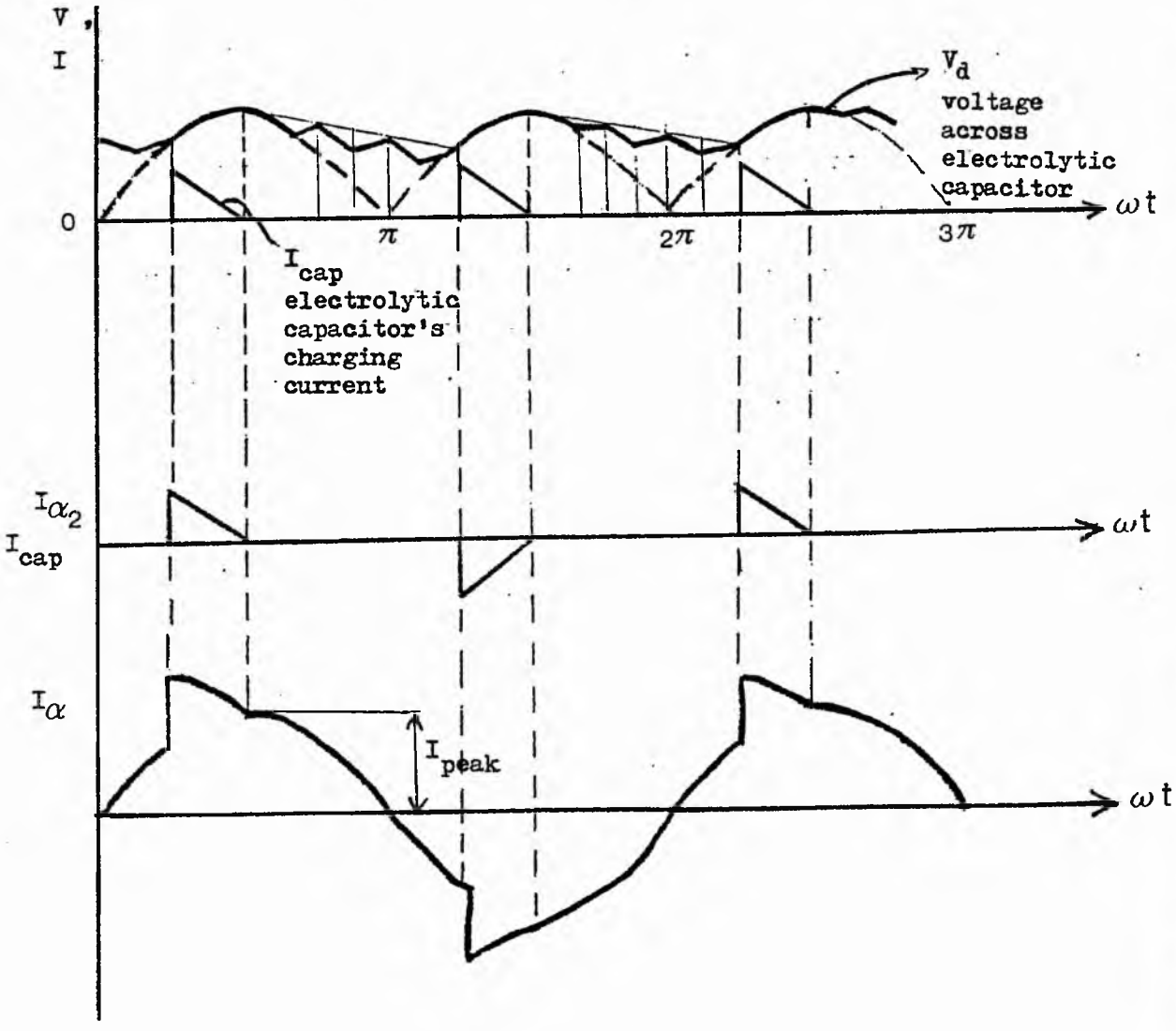

Fig. 4.18 The ideal waveforms of currents shown in Fig. 4.15

and substituting Eqn. 4.50 into Eqn. 4.49 and also making

$\Gamma = \pi/2, \quad \Delta_1 = ¼\pi$

corresponding to the worst experimental case and $\Delta = \omega t$, then integrating and rearranging gives an rms current.

$$I_\alpha = \sqrt{\frac{1}{\pi}\left(I^2_{\alpha 1 max}\,\frac{1}{2}\pi + I^2_{\alpha 2 max}\,\frac{5\pi}{6}\right)} \tag{4.51}$$

$I_{\alpha 2}$ can be represented in terms of $I_{\alpha 1}$. If I_{peak} is the maximum value of the fundamental sinewave of $I_{\alpha 1}$ as shown in Fig.4.18, then

$$I_{\alpha 2max} = k\, I_{peak} \tag{4.52}$$

where k is a constant, hence Eqn. 4.52 can be re-written as

$$I_\alpha = \sqrt{\frac{1}{\pi}\; I^2_{\alpha 1 max}\left(\frac{1}{2}\pi + k^2\left(\frac{5\pi}{6}\right)\right)} \tag{4.53}$$

4.4.3. Current Harmonics Generated by the Chopper Operating with a Capacitive Load

The waveforms shown in Fig. 4.18. are represented as a Fourier series as follows. The positive and negative half cycles are equal and so there is no d.c. component. The sinusoidal rms current I_α shown in Fig. 4.18 therefore becomes

$$I_{\alpha rms} = \sqrt{I^2_{\alpha 1} + I^2_{\alpha 2} + I^2_{\alpha 2n}} \tag{4.54}$$

where $I_{\alpha 2}$ and $I_{\alpha 2n}$ are the fundamental and harmonic components of the controlled current $I_{\alpha 2}$. There will be no cosine term component. Hence the harmonic components of $I_{\alpha 2}$ can be obtained from Eqn. 4.48.

If $I_{\alpha 2} = I_{\alpha 2max}$ and $\Delta_1 = \pi/4$ which gives

$$I_{\alpha 2} = I_{\alpha 2max} \left(2 - \frac{4\Delta}{\pi}\right) \tag{4.55}$$

and the Fourier coefficient will be

$$a_n = \left(2 - \frac{4\Delta}{\pi}\right) \sin n\Delta \, d\Delta \tag{4.56}$$

and considering Eqn. 4.52. the harmonic components of $I_{\alpha 2}$ are shown in TABLE 4.1. in terms of $I_{\alpha 1max}$. When these are seen by motor impedance, they will have very little effect. However, if these values are compared to a capacitive load control by a thyristor pair, it can be seen that when the load current leads the voltage by $\phi = 84°$ the thyristors must be switched on at $\theta \geq \phi$ due to the limited range of conduction. This gives a third harmonic of almost 90% (see Fig. 4.9.B.) of the fundamental value. For the smallest mark-space ratio used experimentally $k = 0.3$ and so the worst case of harmonic generated in the system for the third harmonic is only one tenth (1/10) of the harmonics generated by the thyristor pair in same capacitive load. Hence the chopper controlled system is thus the preferred system.

HARMONIC COMPONENTS OF $I_{\alpha 2}$ IN TERMS OF $I_{\alpha 1}$

($K = 0.3$, $k = I_{\alpha 2}/I_{\alpha 1}$) (Referred to Fig. 4.15.)

Harmonics components	$I_{\alpha 2}$ in terms of $I_{\alpha 1}$
$I_{\alpha 2}$ fundamental	$k \times I_{peak}$
$I_{\alpha 2}$ n = 3	$(1/3) \times k \times I_{peak}$
$I_{\alpha 2}$ n = 5	$(1/5) \times k \times I_{peak}$
$I_{\alpha 2}$ n = 7	$(1/7) \times k \times I_{peak}$
$I_{\alpha 2}$ n = 9	$(1/9) \times k \times I_{peak}$

TABLE 4.1

4.4.4. Effective Capacitance of the Chopper Controlled C_α

In the system shown in Fig.4.15., the charge of $C_{\alpha 2}$ is conducted through a diode bridge to a 2000μF electrolytic capacitor. Because the chopper cannot be used to short-circuit a charged capacitor due to the dangerous dissipation of stored energy. As shown in Fig. 4.18. the electrolytic capacitor is then subjected to a controlled discharge into a choke.

The series capacitors $C_{\alpha 1}$ and $C_{\alpha 2}$ shown in Fig. 4.15. share the voltage between the capacitor. Hence when $\gamma = 0$, the effective capacitance will be

$$C_{eff} = \frac{C_{\alpha 1} C_{\alpha 2}}{C_{\alpha 1} + C_{\alpha 2}}$$

and when $\gamma = 1.0$ $C_{eff} = C_{\alpha 1}$

Assuming a constant current I flowing through the combination, the voltage across the combination will be $I/(\omega C_{\alpha 1}) = V_\alpha$

when $\gamma = 1.0$; also when $\gamma = 0.0$ the voltage will be

$$V_\alpha = I \Big/ \left| \frac{\omega C_{\alpha 1} C_{\alpha 2}}{C_{\alpha 1} + C_{\alpha 2}} \right|$$

At any other mark-space ratio γ, the voltage across the combination will be:

$$V_\alpha = \frac{I}{\omega C_{eff}} = \frac{I}{\omega} \left[\sqrt{\gamma}\ \frac{1}{C_{\alpha 1}} + \sqrt{1-y}\ \frac{C_{\alpha 1} + C_{\alpha 2}}{C_{\alpha 1} C_{\alpha 2}} \right]$$

and so C_{eff} is the effective capacitance given by the expression

$$C_{eff} = \frac{C_{\alpha 1} C_{\alpha 2}}{C_{\alpha 2} + \sqrt{(1-\gamma)}\ C_{\alpha 1}} \qquad (4.57)$$

The variation of effective capacitance with mark-space ratio is shown in Fig. 4.19.

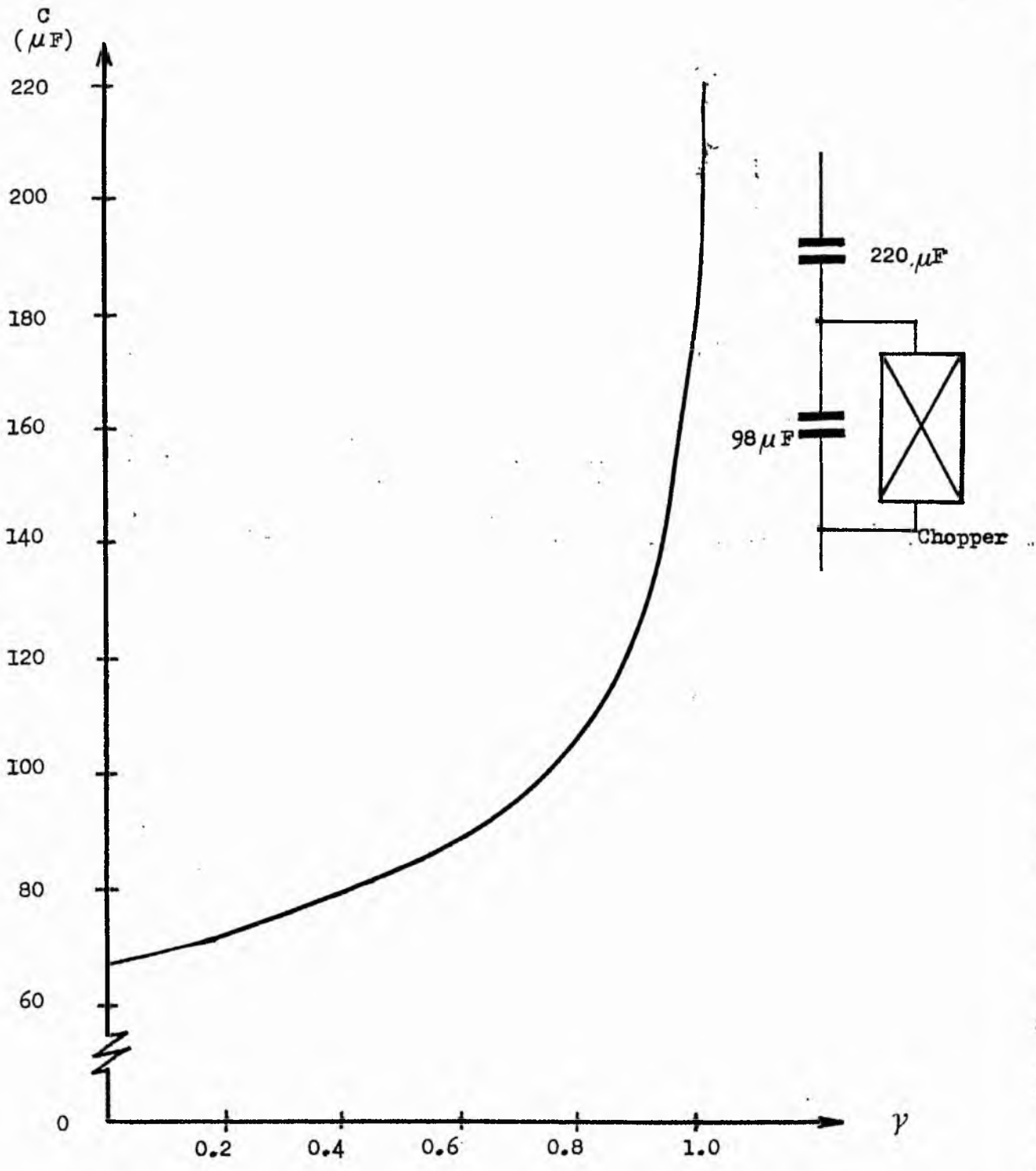

Fig. 4.19 Calculated variation of effective capacitance against mark-space ratio (connected as in Fig. 4.15)

4.4.5. Electronic Reactance Control for X_β:

The connection of the chopper controlled inductive load in parallel with a capacitance is shown in Fig. 4.20.B. If the mark-space ratio is γ, the effective component of the controlled current $I_{L\beta}$ will be $\sqrt{\gamma}\, I_{L\beta}$, where $I_{L\beta}$ is the rms value of the current when $\gamma = 1$.

As mentioned before, the smoothing capacitor of the chopper (Fig. 4.16.) effectively eliminates the harmonics introduced into the motor. In fact when the chopper is off, the voltage is not removed immediately due to the high reservoir of the smoothing capacitance between the input diode bridge and the chopper (which is 2000 μF).

Also the chopping rate is 8 times the supply frequency. The reduced voltage $\sqrt{\gamma}\, V_\beta$ is considered to be sinusoidal. The experimental waveforms verify this as will be illustrated later in this section.

Referring to Fig. 4.20.B the following can be written:

$$I_\beta = I_{c\beta} + \sqrt{\gamma}\, I_{L\beta}$$

or

$$\frac{V_\beta}{Z_\beta} = \frac{V_\beta}{-jX_{c\beta}} + \sqrt{\gamma}\, \frac{V_\beta}{jX_{L\beta}} \tag{4.58}$$

Also,

$$I_\beta = V_\beta \left[\frac{(jX_{L\beta})(-jX_{c\beta})}{(jX_{L\beta}) + \left[\sqrt{\gamma}\, (-jX_{c\beta}) \right]} \right] \tag{4.59}$$

Where,

$$Z_\beta = \frac{X_{L\beta}\, X_{c\beta}}{j\left[X_{L\beta} - \sqrt{\gamma}\, (X_{c\beta})\right]} \tag{4.60}$$

Eqn. 4.60. indicates that $|\sqrt{\gamma}\, X_{C\beta}| > |X_{L\beta}|$ in order to change Z_β from capacitive reactance to inductive reactance as the mark-space ratio increases. If $|\sqrt{\gamma}\, X_{C\beta}| < |X_{L\beta}|$ I_β is leading in the whole control range of mark-space ratio. The variation of Z_β with the values used in the phase converter is shown in Fig. 4.21.

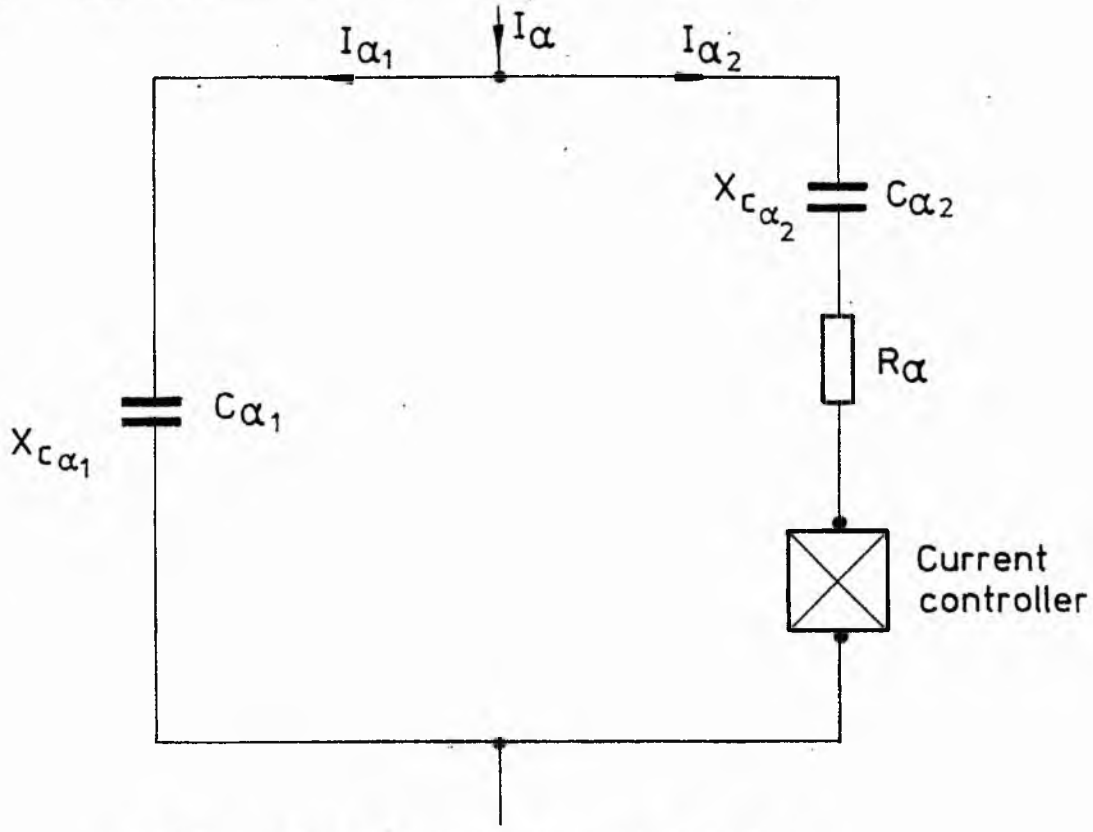

Fig. 4.20A Control element for Z_α

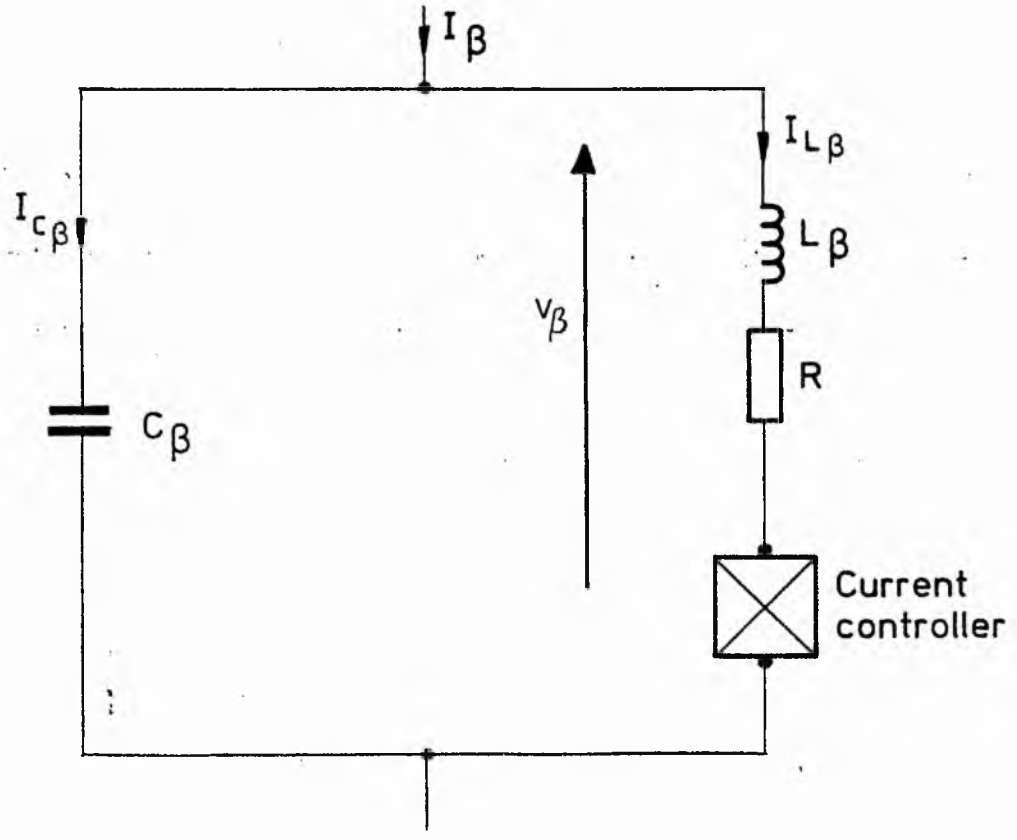

Fig. 4.20B Control element for Z_β

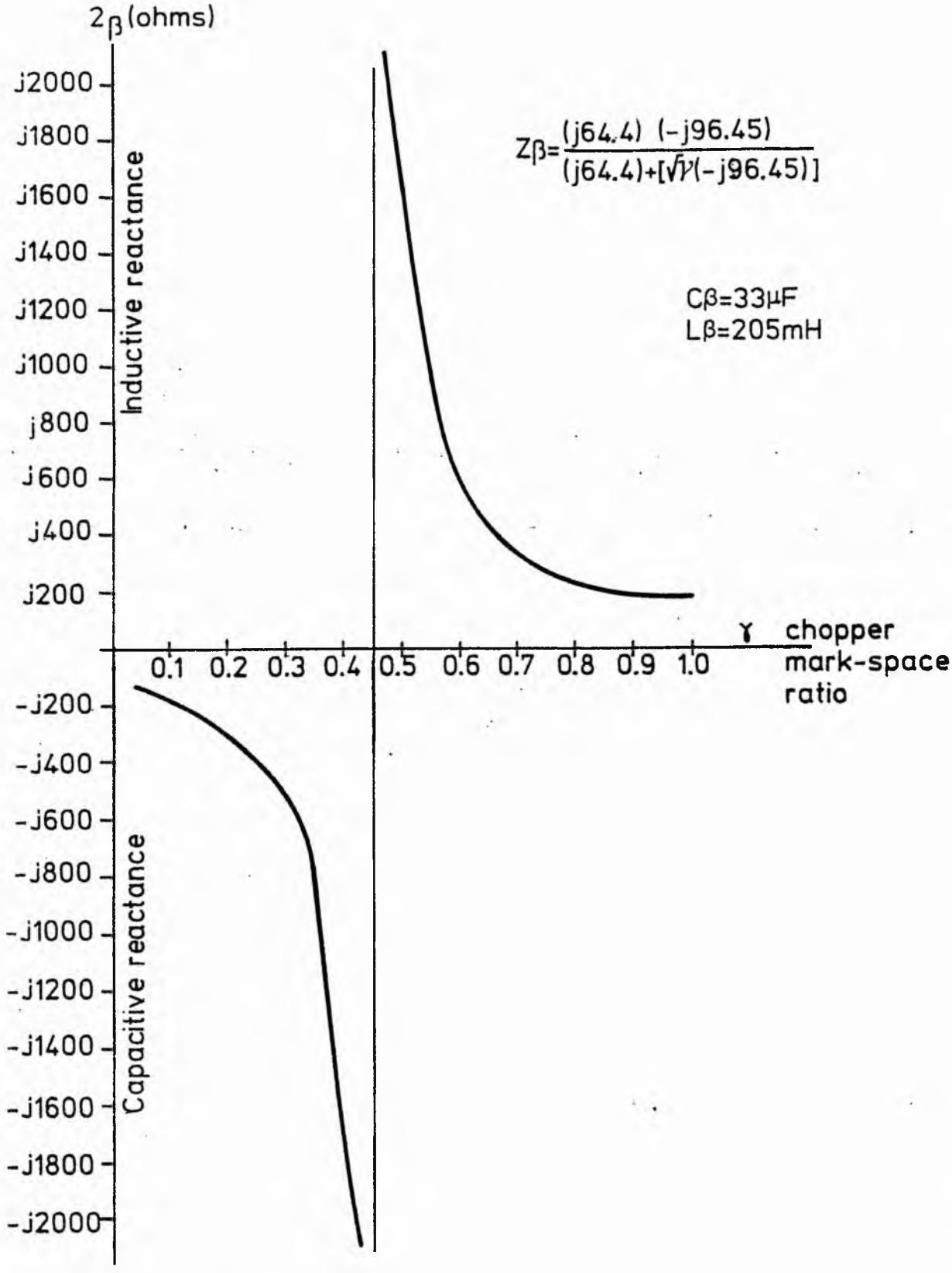

Fig. 4.21 Variation of reactive component Zβ/mark-space ratio connected as shown in Fig. 4.20B

4.5. Design Requirements for a Transient Phase Converter

4.5.1. General

From previous work it has been seen that semiconductor switching of either phase-control or current chopping types will introduce harmonics into the system, the order of which depends on chopping rate.

If a system involving variable-capacitance and variable-inductance can be achieved, the exact balance with the experimental machine will require a current variation as shown in Fig. 4.22. Any electronic phase conversion must constrain I_α and I_β to follow the pattern of Fig. 4.22.

I_α control is effectively a variable capacitance. The parallel element as shown in Fig. 4.20.A will allow $C_{\alpha 1}$ to act as a high-pass filter $C_{\alpha 1}$ across the harmonic generator. Referring back to Fig. 3.3. $C_{\alpha 1}$ will represent the minimum capacitance when the current control switch of Fig. 4.20.A is fully off. In the second arrangement of Fig. 4.15 C_{eff} is a minimum when the chopper has its minimum mark-space ratio.

Similarly, I_β must be controlled by a circuit shown in Fig. 4.20.B where C_β acts as a high-pass filter. The reactance has to change its nature from capacitive to inductive reactance at a slip 0.24 as shown in Fig. 4.22. Values of L_β and C_β must be chosen so that, when the current controller is fully off, $X_\beta = -j / \omega C_\beta$ and when the current controller is fully on, $X_\beta = j (\omega L_\beta - 1/\omega C_\beta)$.

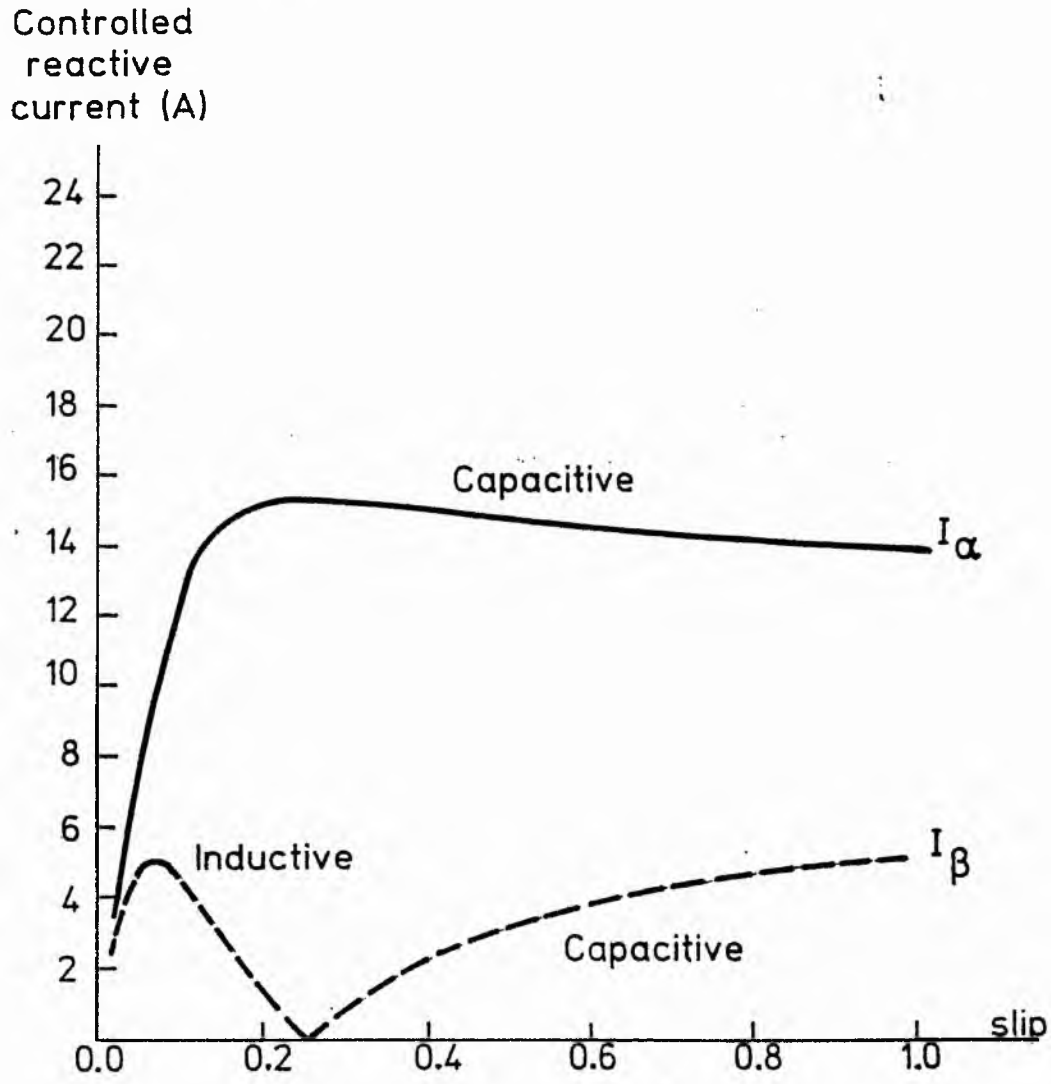

Fig. 4.22 Required variation of control currents for perfect balance (V_{Ref} =240V)

4.5.2. Transient Phase Converters

For a complete investigation of control, most of which was carried out before the preferred approach of the previous section was developed, two alternative designs were investigated; first with inductive currents chopper controlled and capacitive currents controlled by thyristor as shown in Fig. 4.23.; and secondly, the inductive currents controlled by thyristor and a series capacitance controlled by the chopper as shown in Fig. 4.24. In both cases, the change from inductive reactance to capacitive reactance in Z_β limb is achieved by a parallel L-C network, in which the current in the inductor is controlled. When the inductor current is zero, the circuit has maximum capacitive reactance and when the voltage controller is fully conducting, the circuit has maximum inductive reactance.

The required operating characteristic of the phase converter is illustrated in phasor diagrams shown in Fig. 3.4. As shown in Fig. 2.3. and 2.16., the reactive components must vary as the per phase impedance of the machine changes with slip. Consequently, the task of the phase converter is to provide reactive current variation to restore balance with varying load impedance. If the controlled currents I_α and I_β of Fig. 2.1. and 2.2. are considered, the variation of them can be illustrated as a function of slip as shown in Fig. 4.22. where,

$$I_\alpha = \frac{V_\alpha}{-jX_\alpha}$$

$$I_\beta = \frac{V_\beta}{-jX_\beta} \qquad (4.61)$$

In the following analysis each phase is considered individually as a tuned circuit. Two types of control are possible as shown in Figs. 4.23. and 4.24. Since the analysis predicts the ideal condition for I_α and I_β (Fig. 4.22.), each transient phase balance system can be designed to achieve this.

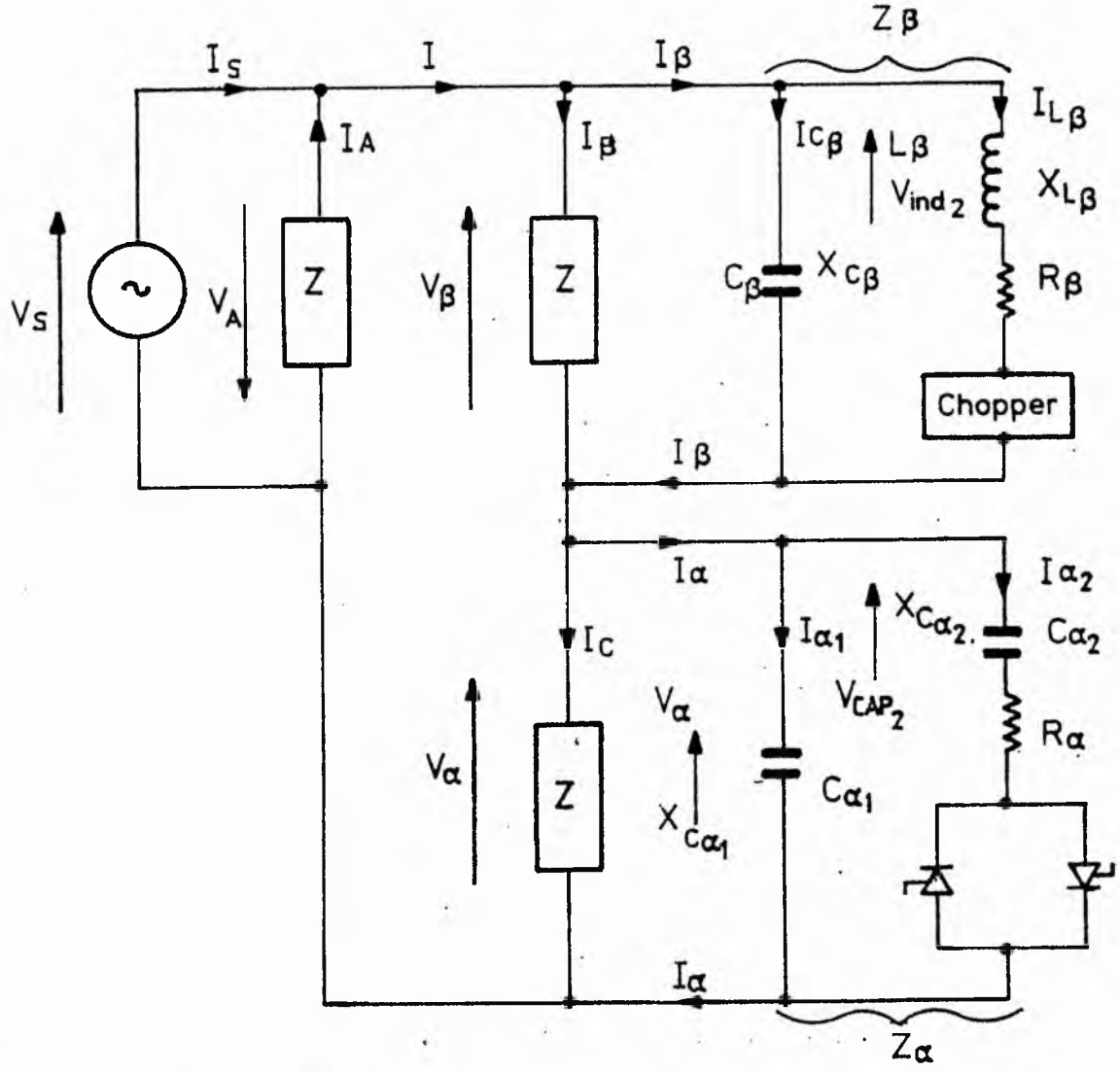

Fig 4.23 First transient phase converter

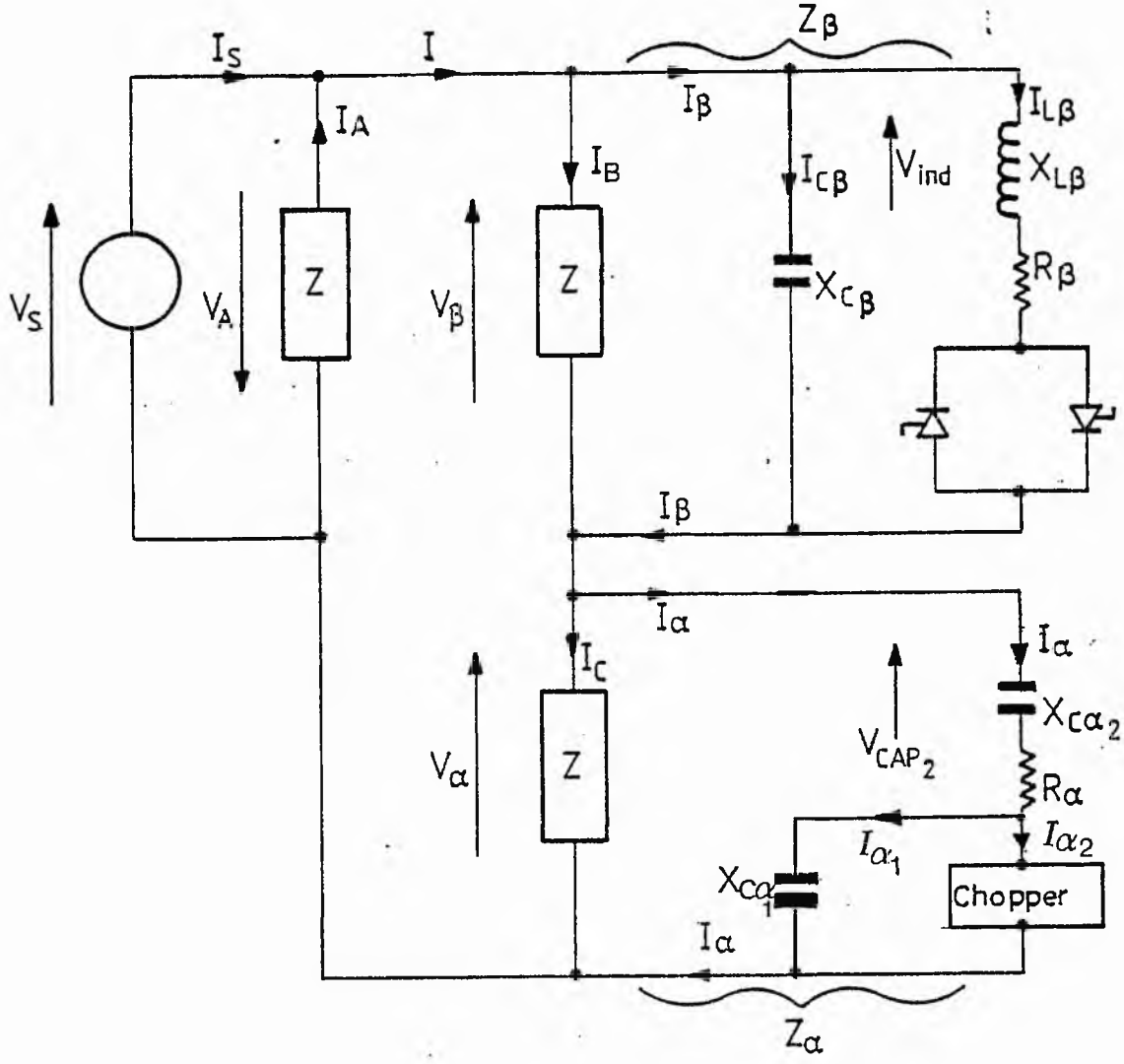

Fig. 4.24 Final transient phase converter.

4.5.3. First Transient Phase Converter

4.5.3.1. General

The first transient phase converter shown in Fig. 4.23. has a reactive impedance Z_β controlled by the transistor chopper and the reactive impedance Z_α controlled by a back-to-back thyristor pair. Fig. 4.22. shows that the required current I_α for Phase C is capacitive for all motoring slips, but the task of the chopper is to change the control impedance Z_β from capacitive to inductive at the slip of 0.24.

4.5.3.2. Controlling of Parallel Capacitance with a Back-to-Back Thyristor Pair

The effect of variable capacitance is achieved by controlling the current in a capacitor in series with a voltage phase controller. The fundamental r.m.s. current is made to correspond to the required r.m.s. value of a sinusoidal current at a particular slip as given in Fig. 4.20.A. The following fundamental r.m.s. current relationships occur,

$$I_\alpha = I_{\alpha 1} + I_{\alpha 2} \tag{4.62.}$$

where $I_{\alpha 1}$ and $I_{\alpha 2}$ are defined in Fig. 4.23. Also, it may be written that,

$$I_\alpha = \frac{V_\alpha}{Z_\alpha} \tag{4.63}$$

$$I_{\alpha 1} = \frac{V_\alpha}{-jX_{c\alpha 1}} \tag{4.64}$$

$$I_{\alpha 2} = \frac{V_\alpha}{-jX_{c\alpha 2}} \tag{4.65}$$

where Z_α indicates the total capacitive reactance required for perfect balance, as shown in Fig. 2.3.

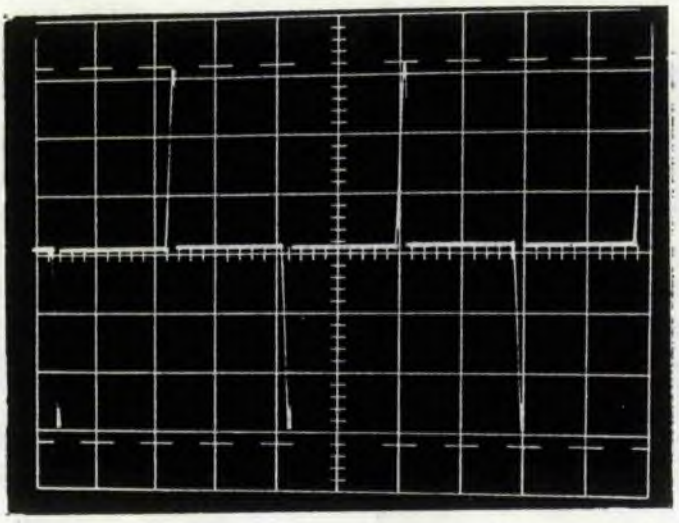

f=50Hz

Current through 50.8 μF capacitor, I_{cap} (Fig. 4.5)

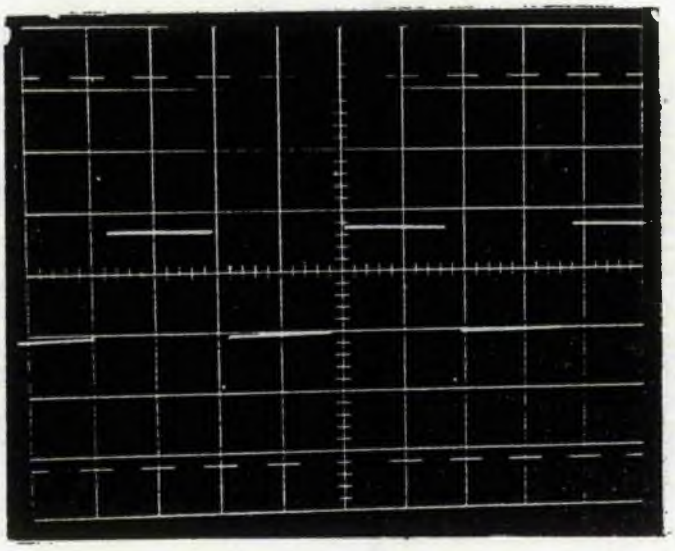

f=50Hz

Voltage across 50.8 μF capacitor, V_{cap} (Fig. 4.5)

Fig. 4.25 Current and voltage waveform of a purely capacitive load controlled by a back-to-back thyristor pair, shown in Fig. 4. (R_α=0, zero resistance)

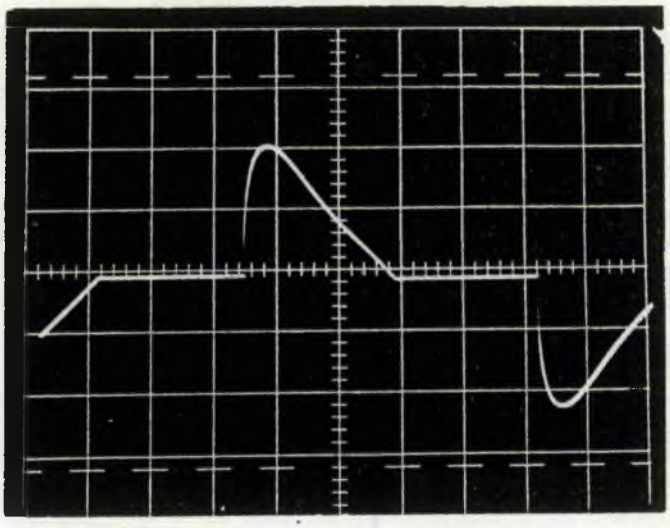

Current through R-C load, I_{cap} (Fig. 4.5)

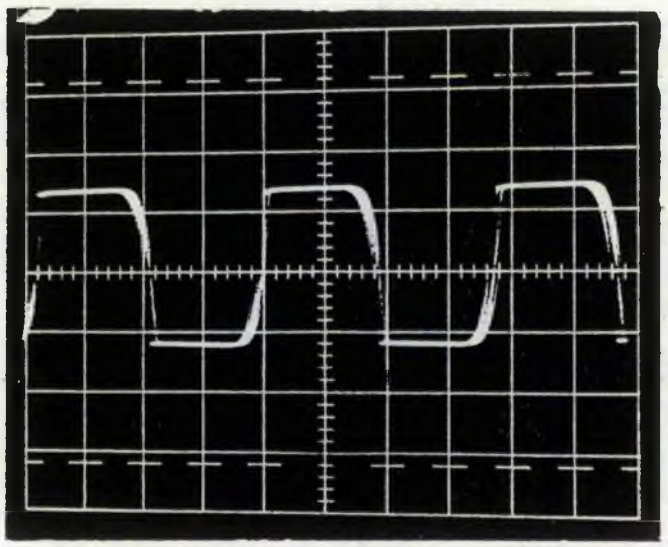

Voltage across R-C load, V_{cap} (Fig. 4.5)

Fig. 4.26A A current and voltage waveforms of an R-C load with ϕ=67.5° at θ=60°

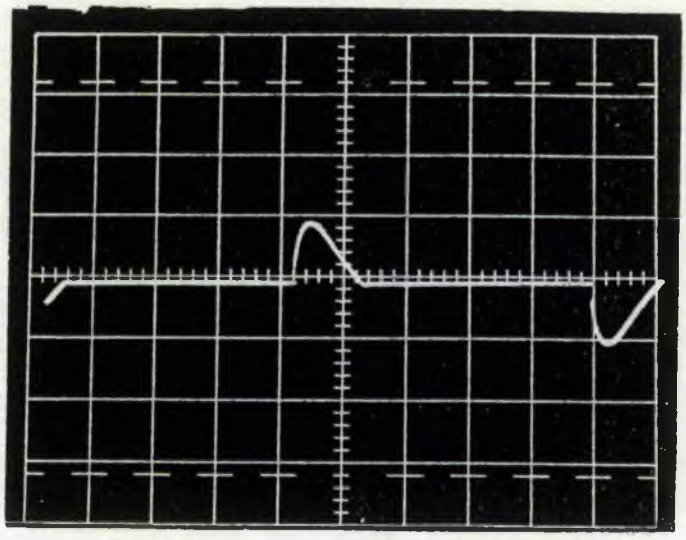

Current through R-C load, I_{cap} (Fig. 4.5)

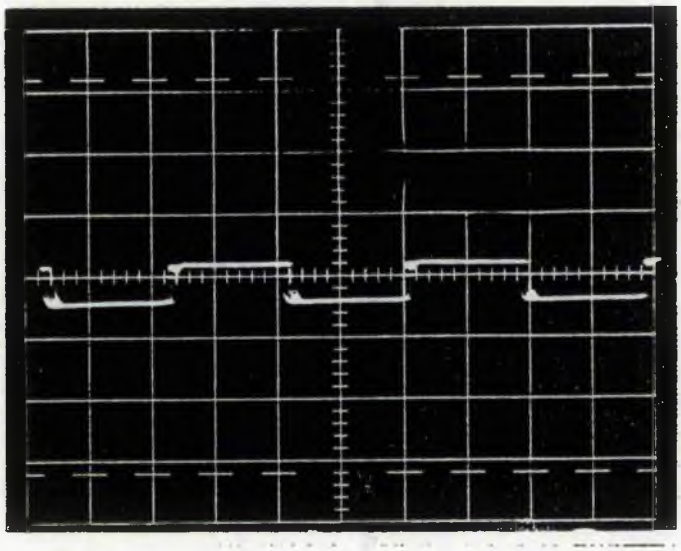

Voltage through R-C load, V_{cap} (Fig. 4.5)

Fig. 4.26B : Current and voltage waveforms of an R-C load of ψ=67.5° at θ=80°

If a purely capacitive load is controlled by a back-to-back thyristor pair, the firing angle and extinction angle are identical; hence no control is possible. This can be seen in Fig. 4.25. The current is an impulse of great height and very small width, cutting off suddenly. This also verifies the capacitive load control characteristics shown in Fig. 4.8. The capacitor charges almost instantaneously, giving the rectangular charge and discharge wave as shown in Fig. 4.25. Immediately after the current is cut off the capacitors remain charged, giving a flat voltage waveform.

However, an increase in the resistive component of the load also increases the control range as shown in Fig. 4.8. This is illustrated in Fig. 4.26. for two different firing delay angles with a capacitive load angle of $\phi = 67.5°$ leading.

Referring back to Figs. 4.20.B and 4.23, the voltage phase controller introduces conduction delay in the $Xc_{\alpha 2}$ limb. Consequently, the current $I_{\alpha 2}$ will be controlled. If the fundamental r.m.s. value of $I_{\alpha 2}$ is considered, considering the firing angle θ and extinction angle X [12].

$$I_{\alpha 2} = \frac{V_{\alpha max}}{R_{\alpha} - jX_{c\alpha 2}} \left[\sin(\omega t + \phi) + \left\{ \frac{\sin\theta + \sin X}{\cos\phi} - \sin(\theta + \phi) \right\} e^{-\tan\phi\omega t} \right] \qquad (4.66)$$

Referring back to Fig. 4.22. it can be seen that the requirement for I_{α} is almost constant in the slip range $1 > S > 0.24$, then it falls rapidly. This means that the thyristors must be fully conducting near to the slip of 0.2, then the firing delay angle must be subsequently increased in order to reduce $I_{\alpha 2}$ as defined in Eqn. (4.62). The thyristor pair will be fully non-conducting at high motoring speeds.

For the purpose of calculation of equivalent capacitance, only the fundamental component of voltage will be considered. This is justified, because the lumped parameter, Z_{α}, consists of the phase control network and a capacitance $X_{c\alpha 1}$ acts as a filter to the higher frequency harmonics. In the connection of Fig. 4.23. the capacitance across the harmonic generator (i.e. the thyristor pair) has a filtering effect in which the reactance falls as the harmonic frequency increases. This diverts the harmonics from the motor. The harmonics are represented in Table 4.2., shown typically for $\phi = 84°$, $\theta = 70°$, for the connection shown in Fig. 4.23.

HARMONICS GENERATED BY THE BACK-TO-BACK THYRISTOR PAIR IN CAPACITIVE LOAD

(Referred to first transient phase converter)

(At S = 0.05 ϕ = 84° leading 0 = 70°

	n (harmonic order)		
	3	5	7
$\lvert I_{\alpha 1} \rvert$	7.319	7.394	6.73
$\lvert I_{\alpha 2} \rvert$	16.43	16.59	15.1
$\lvert V_{\alpha} \rvert$	79.2	48	31.2
$\lvert I_{C\beta} \rvert$	2.46	2.489	2.2644
$\lvert I_{L\beta} \rvert$	0.4099	0.149	0.0692
$\lvert V_{\beta} \rvert$	79.2	48	31.2
$\lvert I_{A} \rvert$	1.5974	0.668	0.325
$\lvert V_{A} \rvert$	79.2	48	31.2
$\lvert I_{B} \rvert$	1.5974	0.668	0.325
$\lvert I_{C} \rvert$	1.5974	0.668	0.325

TABLE 4.2.

(A)

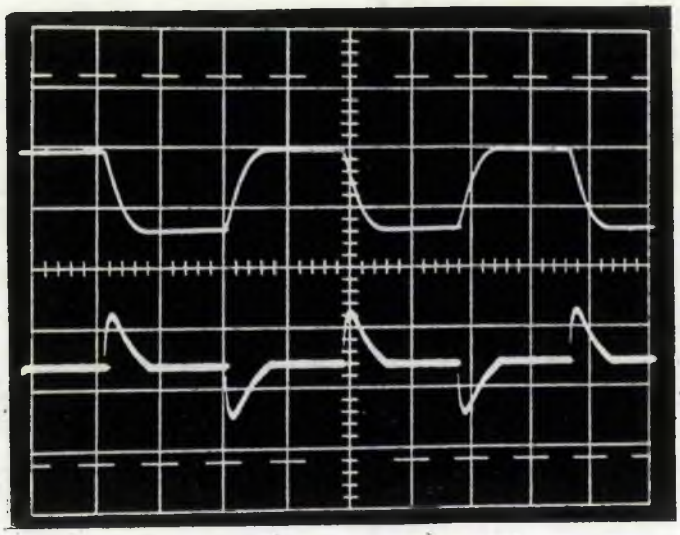

V_{CAP_2}:
(rms 40^V)

$I\alpha_2$
(rms 1.4 A)

θ =40°
X= 95°

(B)

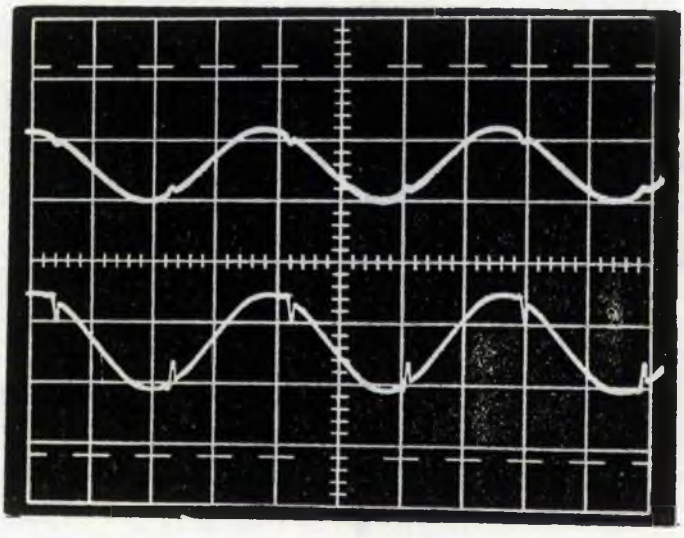

Input voltage
(V_s)
(rms 40^V)
(s=1)
Input current
(I_s)
(rms 2A)
(s=1)

Fig. 4.27 Capacitive load controlled by a back-to- back thyristor pair (Fig. 4.23)

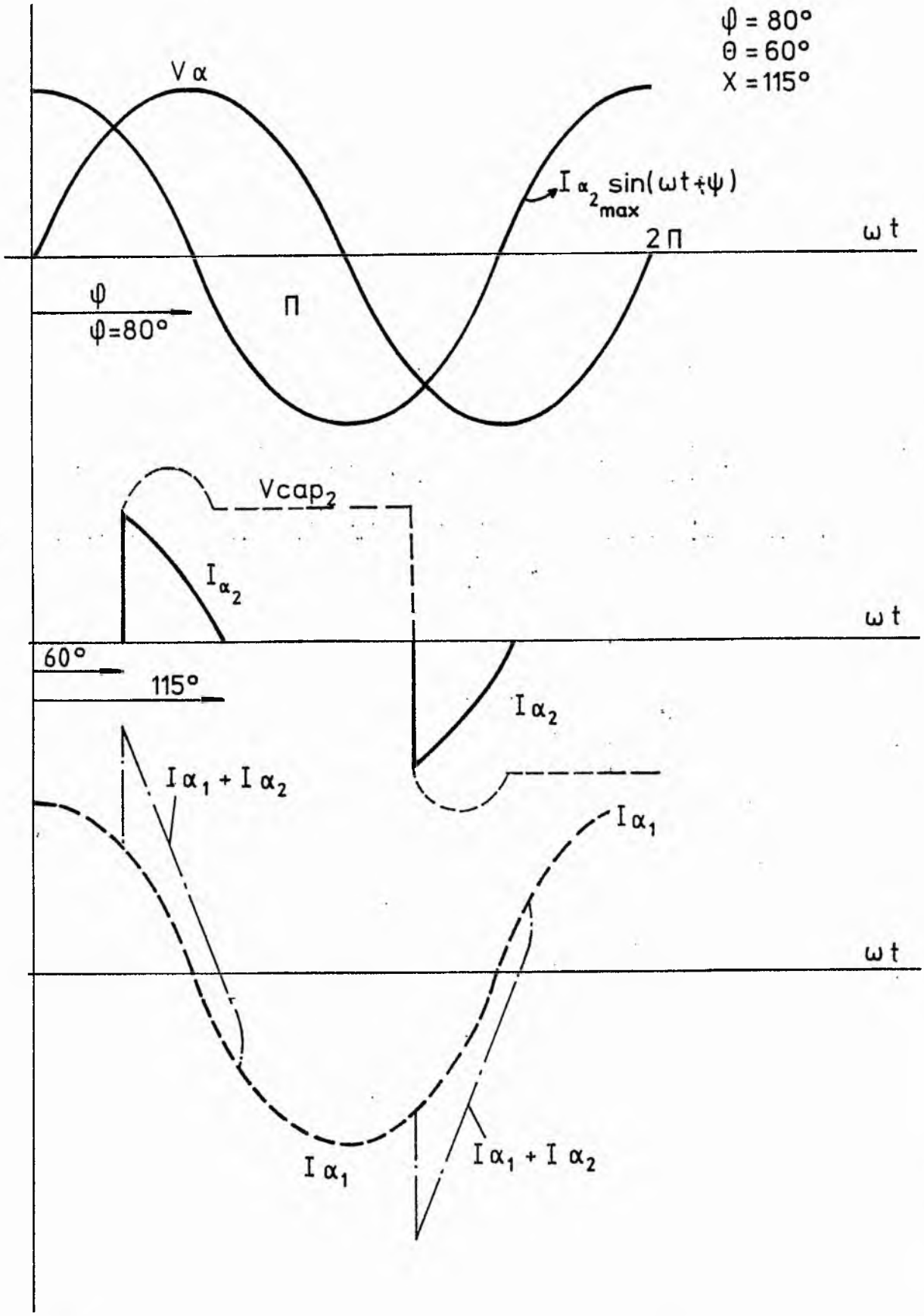

Fig. 4.28 Theoretical waveform of voltages and currents referred to Fig. 4.24

Fig. 4.27. shows the voltage and current waveforms of the phase control system connected as shown in Fig. 4.23. The resistance R_α in series with $C_{\alpha 2} = 98\mu F$ as shown in Fig. 4.23 is $R_\alpha = 2.8$; giving a leading load angle of 85°. The thyristors are fired at 40°, and the current ceases to conduct at 95°. The capacitors are left charged, maintaining a constant voltage until the subsequent firing (i.e. 40° + 180°) of the thyristors. The resistance R_α also limits the current rise "di/dt", avoiding the excessive inrush current.

Fig. 4.27. also shows the system input voltage and phase current at standstill, at the instant of switch on. The input voltage and current contain small "notches". However, the deviation from a sinsusoidal voltage is negligible.

Fig. 4.28. shows the predicted total reactive control element current "$I_{\alpha 1} + I_{\alpha 2}$". In practice the added current "spike" hardly distorts the phase current of the motor as shown in Fig. 4.27.

Capacitive load control by a current controller is limited due to the relation between capacitive load voltage and current. Fig. 4.27. shows that the capacitor current becomes zero when the capacitor voltage reaches a constant level. The following relation relates the current and voltage in a capacitive load,

$$i_{cap} = C \frac{dV_{cap}}{dt} \qquad (4.67.1)$$

when "dV_{cap} / dt" changes, i_{cap} changes simultaneously and when the rate of change "dV_{cap} / dt" is zero, i_{cap} is also zero. When "dV_{cap} / dt" is continuous, the capacitor charges and discharges as long as V_{cap} is a continuous variable of time.

To obtain the voltage-current relationship, Eqn. (4.67.1) can be rewritten as

$$d\, V_{cap} = \frac{1}{C} i_{cap}\, dt \qquad (4.67.2)$$

and integrating both sides from $t = -\infty$ to an arbitrary time t, gives

$$V_{cap}(t) = \frac{1}{C} \int_{-\infty}^{t} i_{cap}\, dt \qquad (4.67.3)$$

or

$$V_{cap}(t) = V_{capo} + \frac{1}{C}\int_{0}^{t} i_{cap}\, dt \qquad (4.67.4)$$

where

$$V_{capo} = \frac{1}{C}\int_{-\infty}^{t} i_{cap}\, dt \qquad (4.67.5)$$

indicating the initial voltage at t = 0. The second term in Eqn. (4.67.4) indicates the subsequent current flow. If a constant current $i_{cap} = I$ is applied at t = 0, then

$$V_{cap}(t) = V_{capo} + \frac{1}{C} I \cdot t \qquad (t > 0) \qquad (4.67.6)$$

Eqn. (4.67.6) means that a constant current yields a linearly increasing voltage or ramp waveform. If the current stops at time t = T, the voltage stops increasing, but stays constant at the value, $V_{cap}(t) = V_{capo} + \frac{I.t}{C}$ for t > T, even though $i_{cap} = 0$ when t > T. Fig. 4.28. verifies this.

4.5.3.3. Controlling an Inductive Load in Parallel with a Capacitor by a Transistor Chopper

As described in Section 4.4.5. an inductive load can be controlled as shown in Fig. 4.20.B. and 4.23.

Referring back to Fig. 4.22. it can be seen that I_β is capacitive at standstill and remains capacitive until the slip value of 0.24 is reached. It can also be seen from Fig. 3.3. that the reactive component Z_β steadily increases as it approaches a slip value of 0.24 and then changes to inductive reactance. This is achieved by further increasing the mark-space ratio. However, it must be noted that $X_{L\beta}$ and $X_{C\beta}$ are in resonance for the mark-space value of 0.44. Hence continuous operation around this mark-space ratio must be avoided. If resonance occurs, V_β may dangerously exceed the rated value.

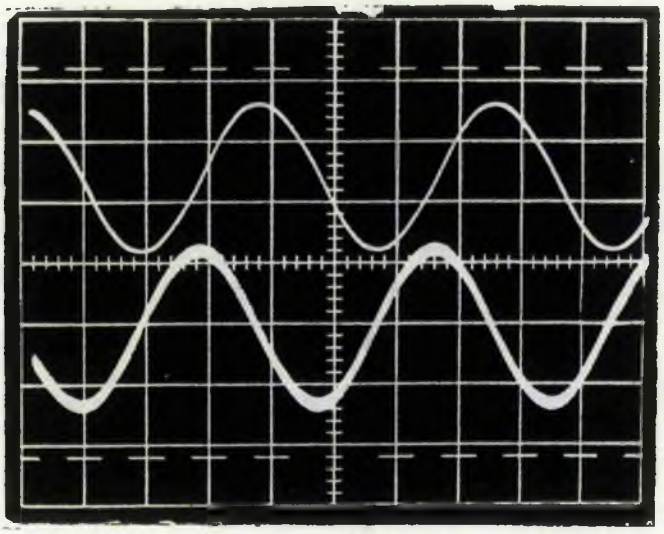

V_{IND_2}
(40v rms)

I_{IND} ($I_{L\beta}$)
(2A rms)

γ =0.6
f=50Hz

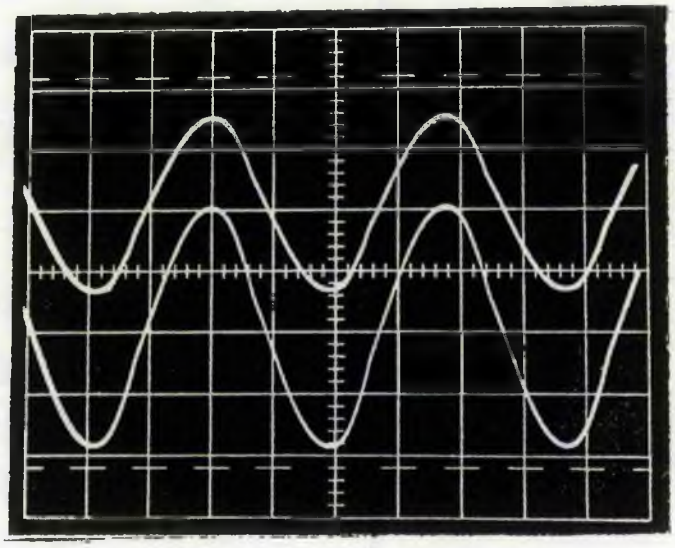

Input voltage V_S
(40v rms)

Input current I_S
(~2.5A rms)

f=50Hz

Fig. 4.29 Chopper controlled inductive load (Fig. 4.24)

Fig. 4.29. shows that, the single-phase input voltage and current are perfectly sinusoidal. This indicates that, the harmonic generated by the chopper in an inductive load is negligible.

The controlled inductive voltage and current in practice do not distort the sinusoidal waveform as predicted in theoretical waveform of Fig. 4.17. This is due to the large filter capacitor and chopper inductance. However, reducing the mark-space ratio reduces the r.m.s. values of V_{ind} and $I_{L\beta}$.

The motor input voltage and current are slightly distorted as shown in Fig. 4.29. The upper voltage and current traces are practically sinusoidal and the small harmonic distortion of the lower trace is probably due to the saturation in the inductor core.

4.5.4. Final Transient Phase Converter

4.5.4.1. General

The serious drawbacks of the first transient phase balancer shown in Fig. 4.27. are mainly due to capacitive load control by a back-to-back thyristor pair, where high harmonic generation is inevitable due to its switching action. This can be seen in Fig. 4.9. In addition, the control range is limited as shown in Fig. 4.8., especially if the load is near to a pure capacitance. Furthermore, due to the early cut-off angle in a highly capacitive load in the operation range of $\pi/2 < \theta < \pi$, the capacitor will be left charged after the thyristor ceases to conduct. Subsequent switch-on may cause a dangerous inrush current and give a "spiky" voltage.

Considering these disadvantages, an improved final transient phase balancer was designed as shown in Fig. 4.24. Here, the series capacitances are controlled by a chopper and the L-C load is controlled by a back-to-back thyristor pair. By voltage delay in the limb $X_{L\beta}$ in Fig. 4.24., the total current I_β will be controlled. The capacitor C_β acts as a high pass harmonic filter. The capacitive reactance $X_{C\beta}$ will be decreased. Thus, a high impedance will be offered to the harmonics.

Referring back to Fig. 4.12. the extinction angle in a purely inductive load is considerably greater than the extinction angle of a purely capacitive load as shown in Fig. 4.8. In the case of a phase converter the controlled currents are assumed to be either purely capacitive or purely inductive. A comparison of current harmonics generated by a back-to-back thyristor pair in the controlling of capacitive or inductive load shows that with 80° leading or lagging load angles the capacitive load current third harmonics are six times greater than the inductive third harmonic lead currents. This can be sen by comparing Figs. 4.9. and 4.13.

4.5.4.2. Inductive Load Control in Parallel with a Capacitive Reactance by a Back-to-Back Thyristor Pair

It has been shown that a "chopper" is necessary for effective capacitive element control. However, a chopper is much more complicated than a phase controller and so the transient phase balancer for the inductive element is the voltage phase controller shown in Fig. 4.24. Referring to Fig. 4.24., the following equations can be written:-

$$I_\beta = \frac{V_\beta}{Z_\beta} \tag{4.72}$$

$$I_{c\beta} = \frac{V_\beta}{-jX_{c\beta}} \tag{4.73}$$

and

$$I_{L\beta} = \frac{V_\beta}{jX_{L\beta}} \tag{4.74}$$

also

$$I_\beta = I_{c\beta} + I_{L\beta} \tag{4.75}$$

A resistance $R_\beta = 1.8$ ohms was connected in series with the inductance in order to aid the latching at the instant of switch on. The r.m.s. value of an inductive current controlled by a back-to-back thyristor pair is given by [12]:

$$I_{L\beta} = \frac{V_{\beta max}}{|R_\beta + jX_{L\beta}|}\left[\frac{1}{2}\left\{\frac{X-\theta}{\pi}\frac{\sin(X-\theta)}{\pi\cos\theta}\cos(\theta+X+\phi)\right\}\right]^{1/2} \tag{4.76}$$

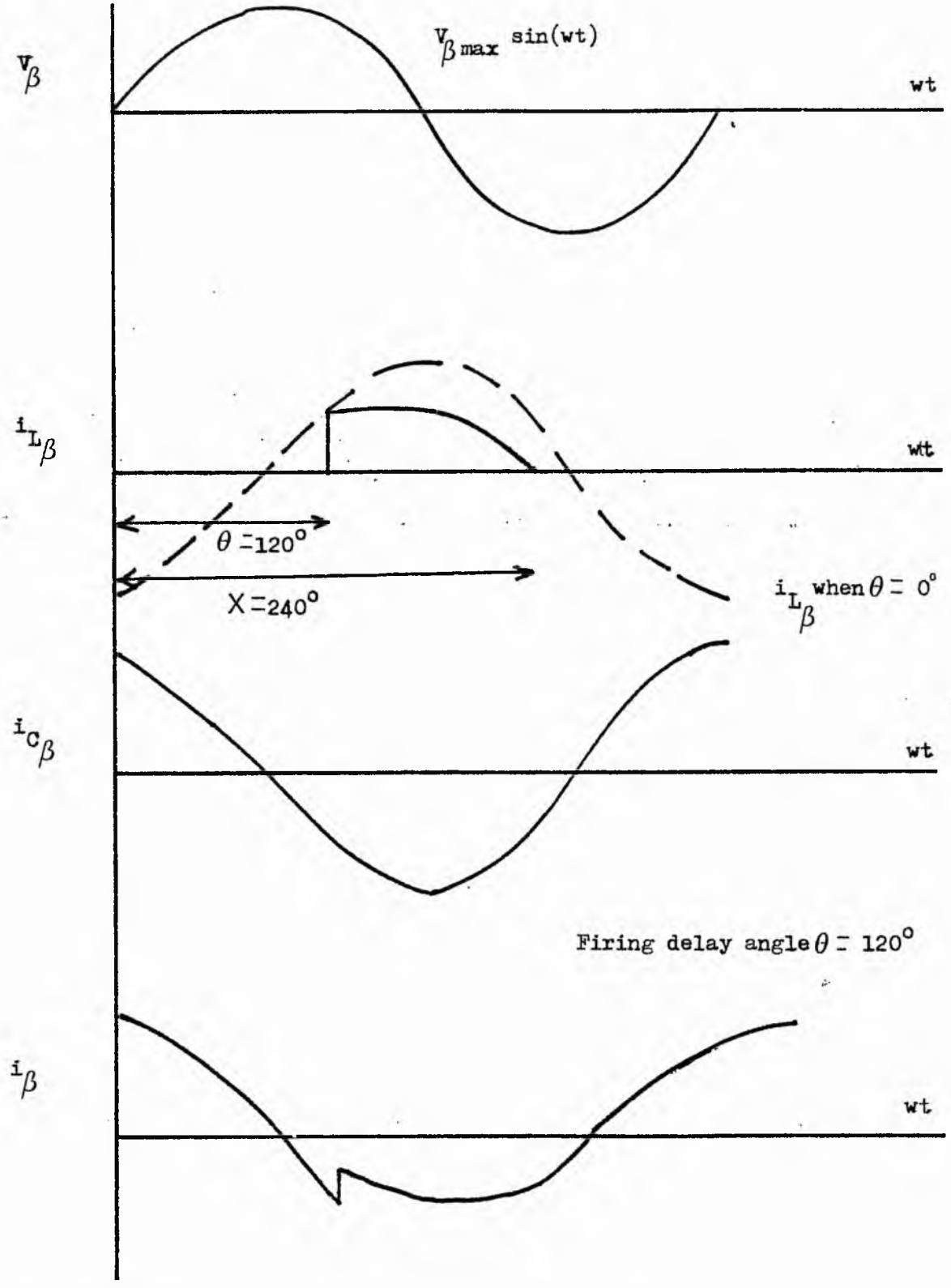

Fig. 4.30 Predicted control current waveforms for phase controlled inductive load in Z_β for $\theta = 120^\circ$

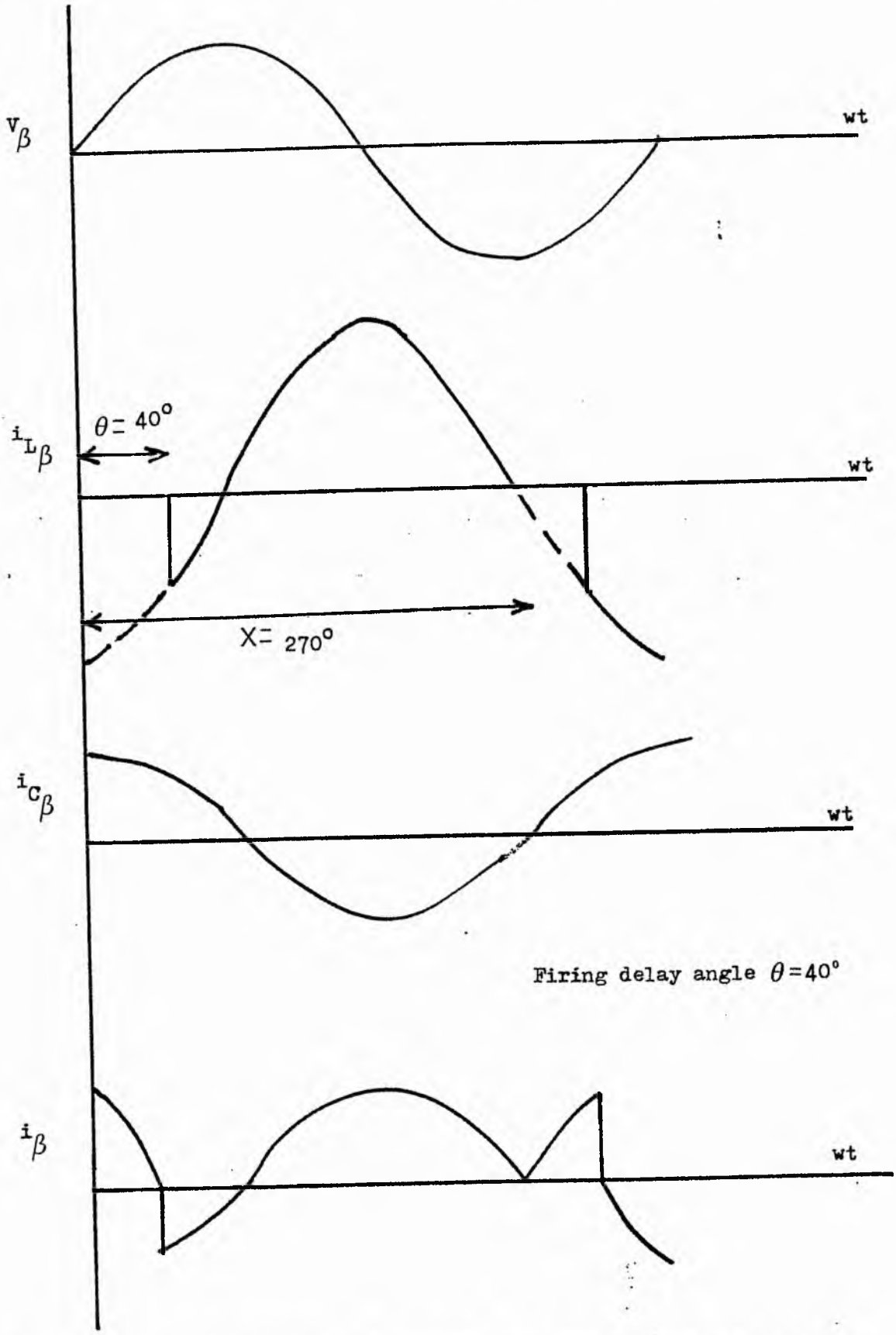

Fig. 4.31 Predicted control current waveforms for phase controlled inductive load in Z_β for $\theta = 40^\circ$

where X indicates the extinction angle as described in section 4.3.2.1. and illustrated in Fig. 4.12.

When the thyristors are fully conducting, the total current I_β will be inductive. If the firing delay angle is increased, the r.m.s. value of $I_{L\beta}$ will be reduced. This in turn varies the total control current, I_β. The theoretical waveforms of the current I_β are illustrated in Figs. 4.30. and 4.31. for two conditions.

At standstill, the requirement for I_β is totally capacitive as shown in Fig. 4.22. However, it steadily reduces as the speed increases. This means that at standstill and throughout the motor acceleration, the thyristor pair must be non-conducting. As the speed increases inductive current will be introduced to the controlled Phase B by reducing the firing delay angle. The capacitive current must be steadily decreased as the speed increases. This is achieved by decreasing the firing delay angle. At a slip of 0.24 the control current I_β must change to inductive current. This is achieved by a further reduction of the firing delay angle. It is particularly important that the values selected for the transient phase converter must enable the control current I_β to change from capacitive to inductive as the speed increases. As shown experimentally (section 4.6.) this is achieved successfully.

The switching action of the thyristor pair inevitably introduces harmonics in the control system. The capacitor C_β in parallel to the harmonic generator acts as a harmonic filter and diverts harmonic current from the motor. The calculated harmonics for Fig. 4.25. are the numerical results shown in Table 4.3.

Fig. 4.32. shows the inductive voltage and the controlled current $I_{L\beta}$. Input phase voltage (Vs) and phase current (Is) are perfectly sinusoidal.

4.5.4.3. Series Capacitance Control by the Transistor Chopper

The operational difficulties (i.e. limited conducting angle and excessive inrush current at switch on) and excessive harmonics introduced in the controlling of the capacitive load by a back-to-back thyristor pair are eliminated by the use of

a transistor chopper. The connection of series capacitance controlled by the transistor chopper is shown in Fig. 4.24.

The chopper control effectively varies the current $I_{\alpha 2}$. If the mark-space ratio of the chopper is γ, the effective component of the control current $I_{\alpha 2}$ will be "$\sqrt{\gamma}\ I_{\alpha 2}$" where $I_{\alpha 2}$ is the r.m.s. value of that controlled current when $\gamma = 1$.

The variation of total capacitive reactance as a function of chopper mark-space ratio is shown in Fig. 4.20. This series branch is employed in the control of Phase C in transient phase converter.

Referring back to Fig. 4.23., it can be seen that the required control current I_{α} is almost constant from standstill to the near slip of 0.24, then it rapidly decreases. This means that the mark-space ratio must remain at maximum and almost constant in the slip range $1.0 > s > 0.24$. This in turn makes the effective control current $I_{\alpha 2}$ constant at the level. When $s < 0.24$, $I_{\alpha 2}$ must be reduced as shown in Fig 4.22. This is achieved by reducing the mark-space ratio.

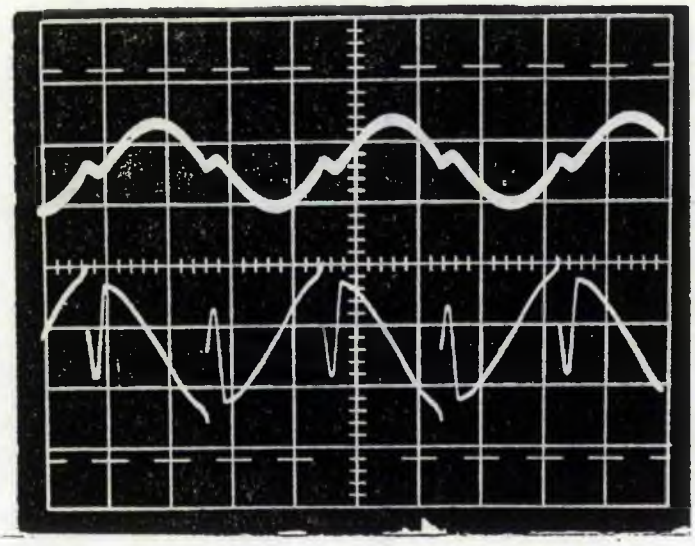

V_{IND_2}
(rms 40^v)

I_{IND} ($I_{L\beta}$)
(rms 2A)
θ=40°
X=270°

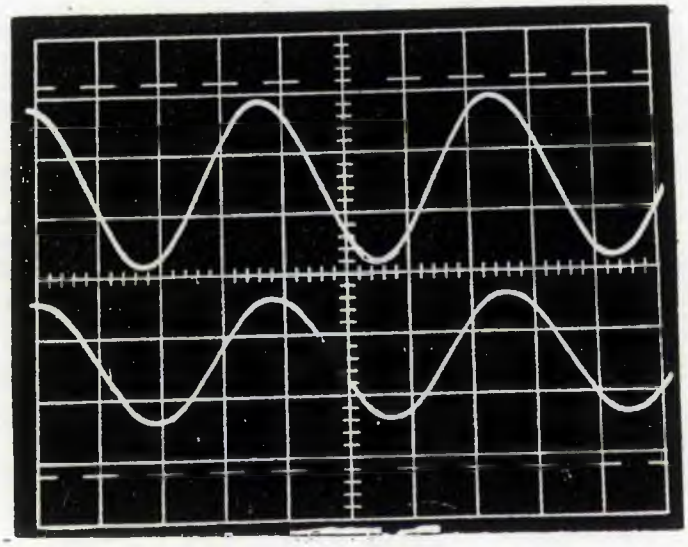

Input voltage
V_S (rms 40^v)

Input current
I_S (rms 2.8A)

f = (50Hz)

Fig. 4.32 Inductive load controlled by a back-to-back thyristor pair. (Circuit of Fig. 4.24

HARMONICS GENERATED BY THE BACK-TO-BACK THYRISTOR PAIR IN INDUCTIVE LOAD

(Referred to first transient phase converter)

(At s = 0.05 ϕ = 84° lagging 0 = 100°

	n (harmonic order)		
	3	5	7
$\lvert I_{\alpha 1} \rvert$	1.38	1.737	0.932
$\lvert I_{\alpha 2} \rvert$	1.38	1.737	0.932
$\lvert V_{\alpha} \rvert$	21.6	16.32	6.24
$\lvert I_{C\beta} \rvert$	0.67185	0.846	0.453
$\lvert I_{L\beta} \rvert$	0.118	0.0506	0.0138
$\lvert V_{\beta} \rvert$	21.6	16.32	6.24
$\lvert I_{A} \rvert$	0.436	0.227	0.065
$\lvert V_{A} \rvert$	21.6	16.32	6.24
$\lvert I_{B} \rvert$	0.436	0.227	0.065
$\lvert I_{C} \rvert$	0.436	0.227	0.065

TABLE 4.3.

As indicated in Eqn. (4.57) a reduction in the mark-space ratio increases the effective impedance Z_α to correspond to the values shown in Fig. 4.19. This means that the effective capacitor value is also reduced. This statement also satisfies the required variation of X_α for perfect balance as shown in Fig. 3.3. The required capacitive reactance must be increased at small slips.

The chopper voltage harmonic analysis given previously in section 4.4.3. To avoid the voltage profile of Fig. 4.17., a 2000 μF smoothing capacitor was added after the diode bridge. Chopping takes place after the smoothing capacitor and the current profile is the smoothed waveform of Fig. 4.32. The chopping frequency is 8 times the supply frequency. Consequently, the undulations of the chopped current cannot be readily detected. The level of current at the zero axis at the beginning and end of the cycles indicate flat voltage level where "dV_{cap} / dt" is zero, hence $i_{cap} = C\, dV_{cap}/dt$ is zero.

The motor input voltage Vs and the corresponding phase current Is are very nearly sinusoidal as shown in Fig. 4.3.

The harmonics generated by the switching action of the chopper are calculated and given in Table 4.4. In this case the harmonic generator is in parallel to $X_{c\alpha 1}$. Hence the harmonic currents in $I_{\alpha 1}$ will be diverted from the motor by the harmonic filter $C_{\alpha 1}$. In practice, the capacitor $C_{\alpha 1}$ may be over stressed by the harmonic current as its losses are frequency dependent. At the higher frequencies, the capacitor presents such a low impedance that it absorbs most of the harmonic current.

HARMONICS GENERATED BY A CHOPPER IN A CAPACITIVE LOAD

(I = 5A, s = 0.005, Vs = 240V)

(Referred to first transient phase converter)

	n (harmonic order)			
	3	5	7	9
$I_{\alpha 1}$	0.76	0.404	0.18	0.16
$I_{\alpha 2}$	1.55	0.88	0.49	0.45
$V_{\alpha 1}$	8.23	2.626	0.81	0.575
$V_{\alpha 2}$	8.61	3.094	1.47	1.02
V_{α}	16.85	5.72	2.3	1.6
$I_{C\beta}$	0.524	0.2965	0.1669	0.149
$I_{L\beta}$	0.087	0.01776	0.005	0.0028
V_{β}	16.85	5.72	2.3	1.6
I_A	0.3415	0.107	0.039	0.0246
V_A	16.85	5.72	2.3	1.6
I_B	0.314	0.107	0.039	1.6
I_C	0.314	0.107	0.039	1.6

TABLE 4.4.

The ideal phase converter must employ two choppers to eliminate the disadvantages of the thyristor pair controlled capacitive load.

4.6. Transient phase Balance in a Motor Drive

Readings of each phase voltage, current, torque and power were taken in a series of steady states over the slip range $0 < s < 1.0$. To obtain stable steady-state operation when $dT/ds < 0$, a Ward-Leonard system was used.

The experimental induction motor, Neco Machine, (parameters given in Appendix A), was mechanically connected to a separately excited d.c. machine. The d.c. load machine's armature was coupled to the armature of a similar machine which was driven at constant speed by another coupled motor. Speed control was achieved by variation of the field current of the second d.c. machine. Fig. 4.33. is a schematic diagram of the test set shown in Fig. 4.34.

Results were obtained for each phase converter, with phase balance constants as follows:-

$X_{L\beta} = j\ 64.4$ ($L_\beta \cong 205$ mH)
$X_{C\beta} = -j\ 96.45$ ($C_\beta \cong 33\ \mu F$)
$R_\beta = 1.8$
$X_{C\alpha 1} = -j\ 32.5$ ($C_{\alpha 1} \cong 98\ \mu F$)
$X_{C\alpha 2} = -j\ 14.46$ ($C_{\alpha 2} \cong 220\ \mu F$)
$R_\alpha = 2.8$

Fig. 4.35. gives the results of the phase controlled capacitor system. The restricted range of operation of the phase-controller made exact balance difficult to achieve at low slips. It can be seen that a resonant condition causes a voltage magnification in phase α (i.e. phase C) of 25%. When running light, phase β (phase B) also experiences a 14% voltage magnification. Light load resonance must be taken into account in rating the phase-balance capacitors. The torque values and efficiencies are comparable with those obtained on the experimental

Neco machine on a balanced three-phase supply. Fig. 4.36. shows the firing angles and mark-space ratios needed to maintain near phase balance.

The semi-resonant condition is predicted in the computed results shown in Fig. 4.37. These results are calculated with the assumption that the listed machine parameters remain constant across the whole slip range. Saturation and stray-load losses will reduce the machine parameters at high slips and this causes the divergence between theory and practice for slips > 0.5.

The predicted firing angles and mark-space ratios shown in Fig. 4.38. vary appreciably from those needed in practice to maintain a near balance. In fact the practical values do not show the "tunnelling" instability and make the system more stable.

Chopper control of the Z_α capacitive circuit of Fig. 4.24. gives a much wider control range, while the phase controller gives adequate control in the inductive circuit, Z_β. Fig 4.39. shows experimental results comparable with those of the first scheme but with a more pronounced resonant magnification of voltage across Z_α. This increases the negative-sequence at low slip. A great advantage is the near-constant firing angle and mark-space ratio over most of the speed range, as shown in Fig. 4.40. Only two levels of control voltage are necessary for effective phase balance. The predicted results of Figs. 4.41. and 4.42 give a favourable verification of the experimental results.

Both control circuits can be determined with their reference controlling voltage. The back-to-back thyristor pair is controlled with a reference control voltage in its firing circuit. This makes it possible to consider firing delay angle as a function of this control reference voltage, as shown in Fig. 4.45. The variation of mark-space ratio can also be determined as a function of the reference voltage of its firing circuit as shown in Fig. 4.46. Once both reference voltages are known as a function of slip, slip-feedback may be used to control the reference voltages to maintain transient phase balance. The feedback and associated logic circuitry are described later in this chapter.

Referring to first transient phase balancer, the requirements of Z_α and Z_β are both capacitive at standstill, as indicated in Figs. 3.3. This is achieved by keeping the mark-space ratio at a maximum as well as making the firing delay

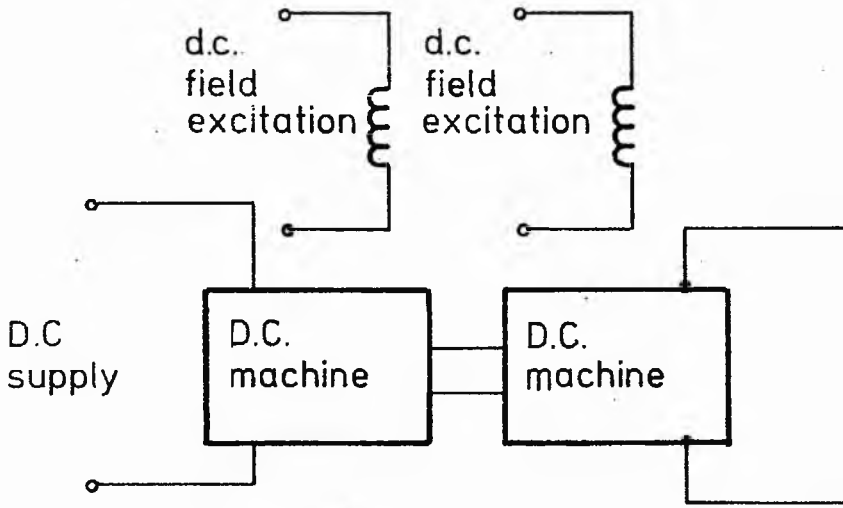

Fig. 4.33 Schematic of test set.

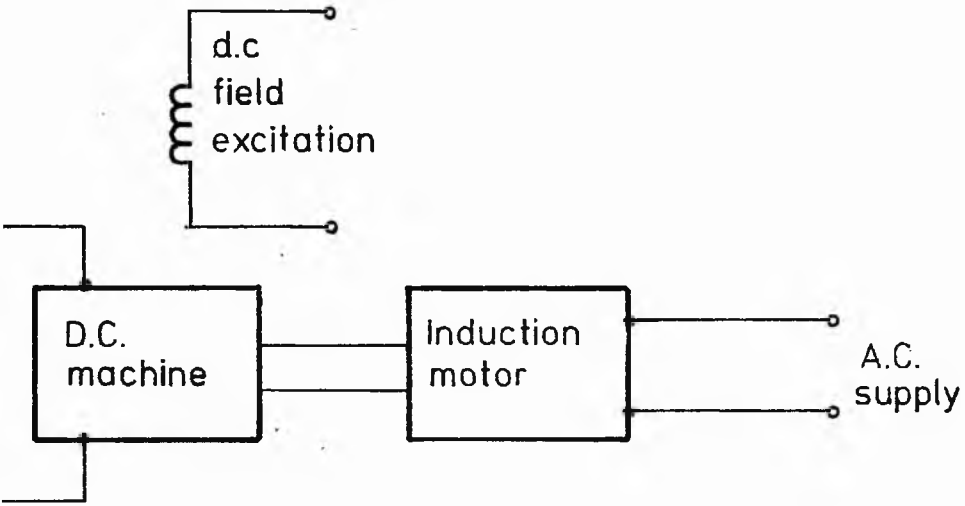
d.c
field
excitation
D.C.
machine
Induction
motor
A.C.
supply

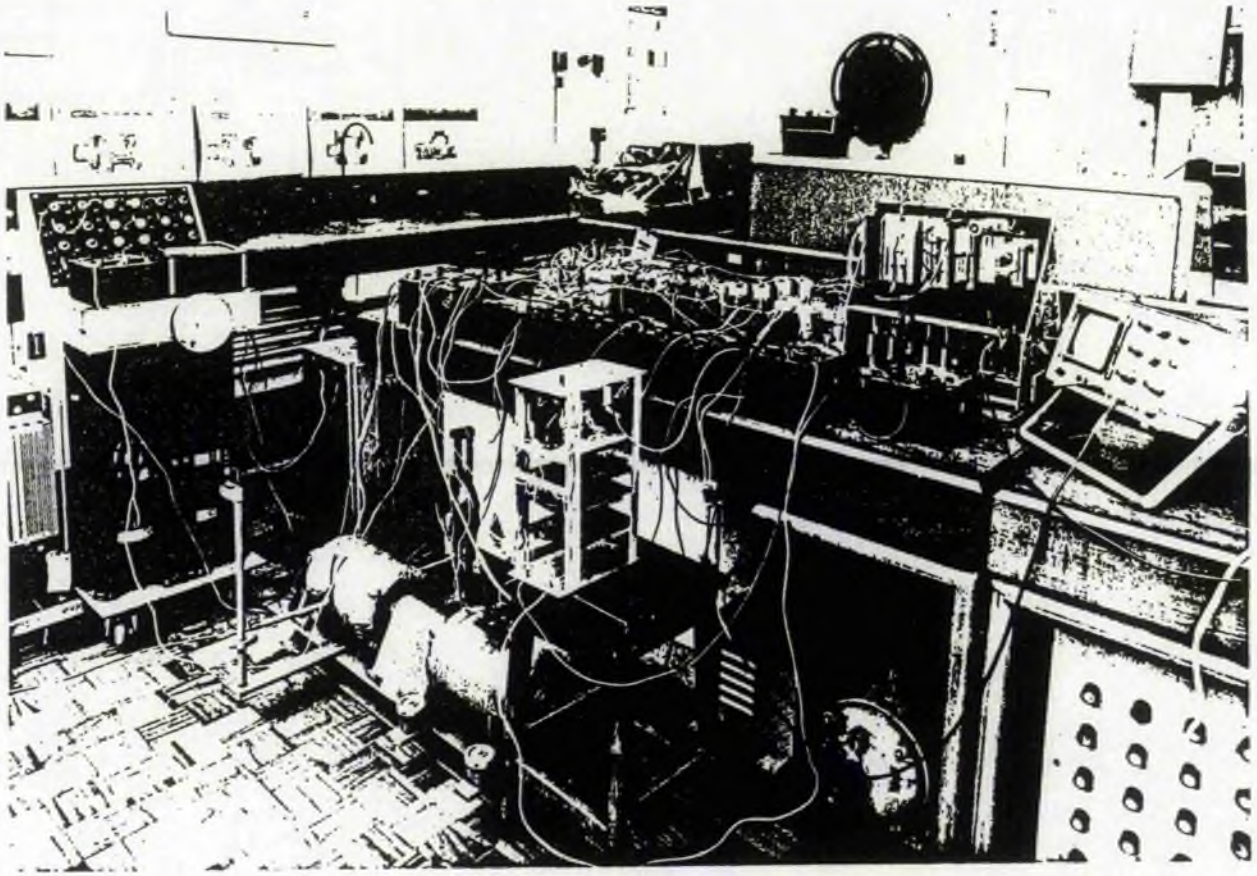

Fig. 4.34 Test set of transient phase balancer.

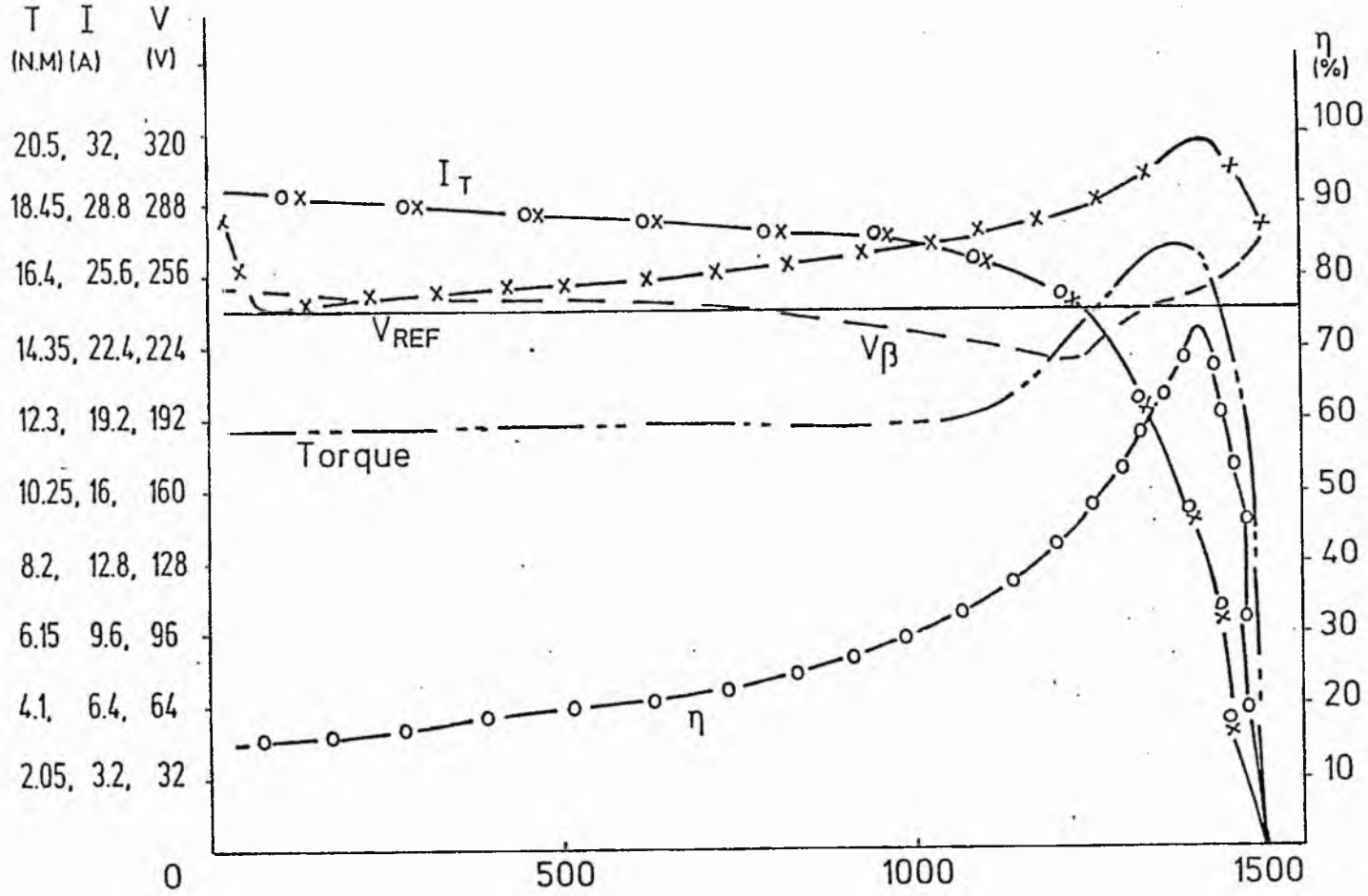

Fig. 4.35 Experimental results of the electronic phase converter shown in Fig. 4.23

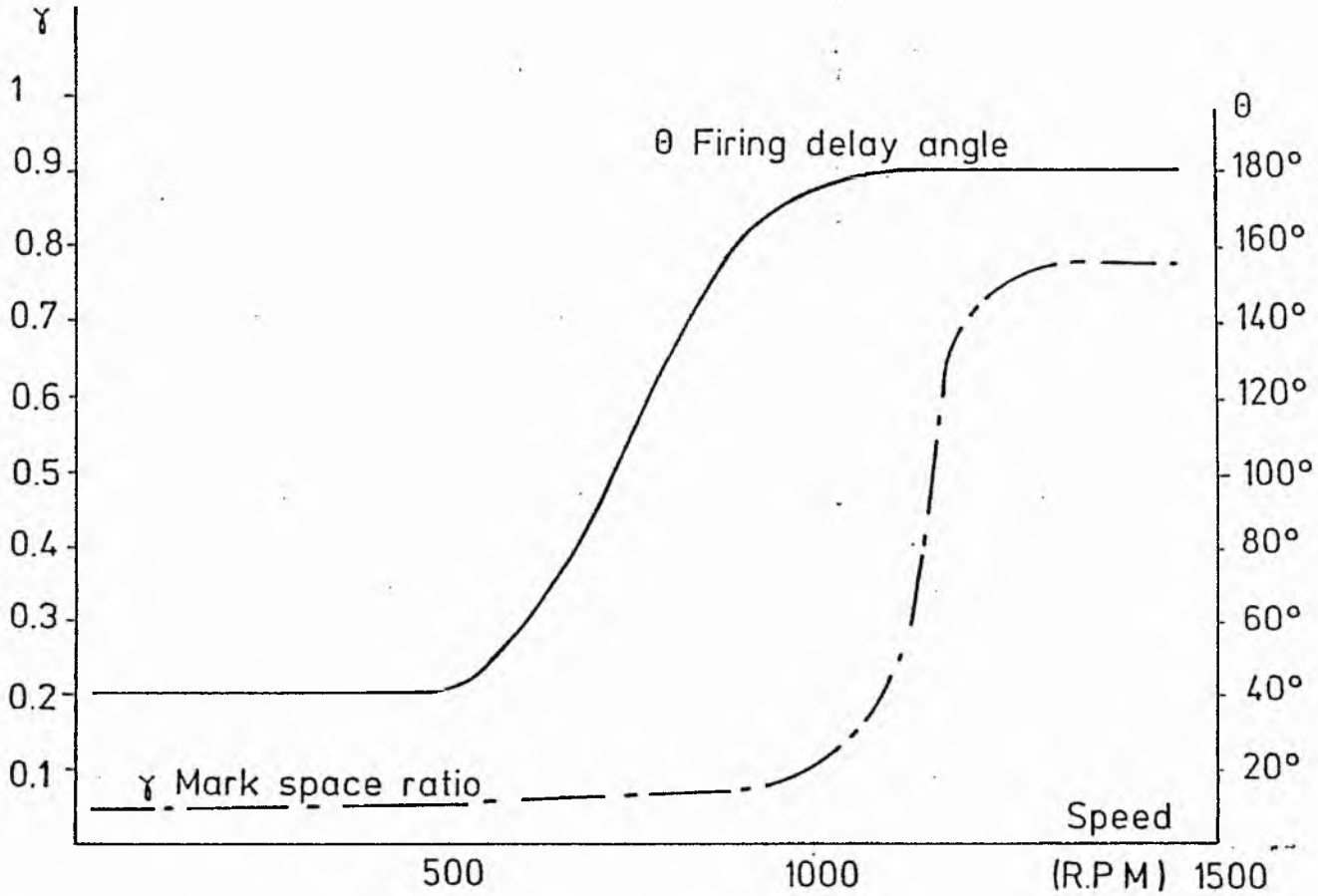

Fig. 4.36 Experimental variations of γ and θ shown in Fig. 4.23

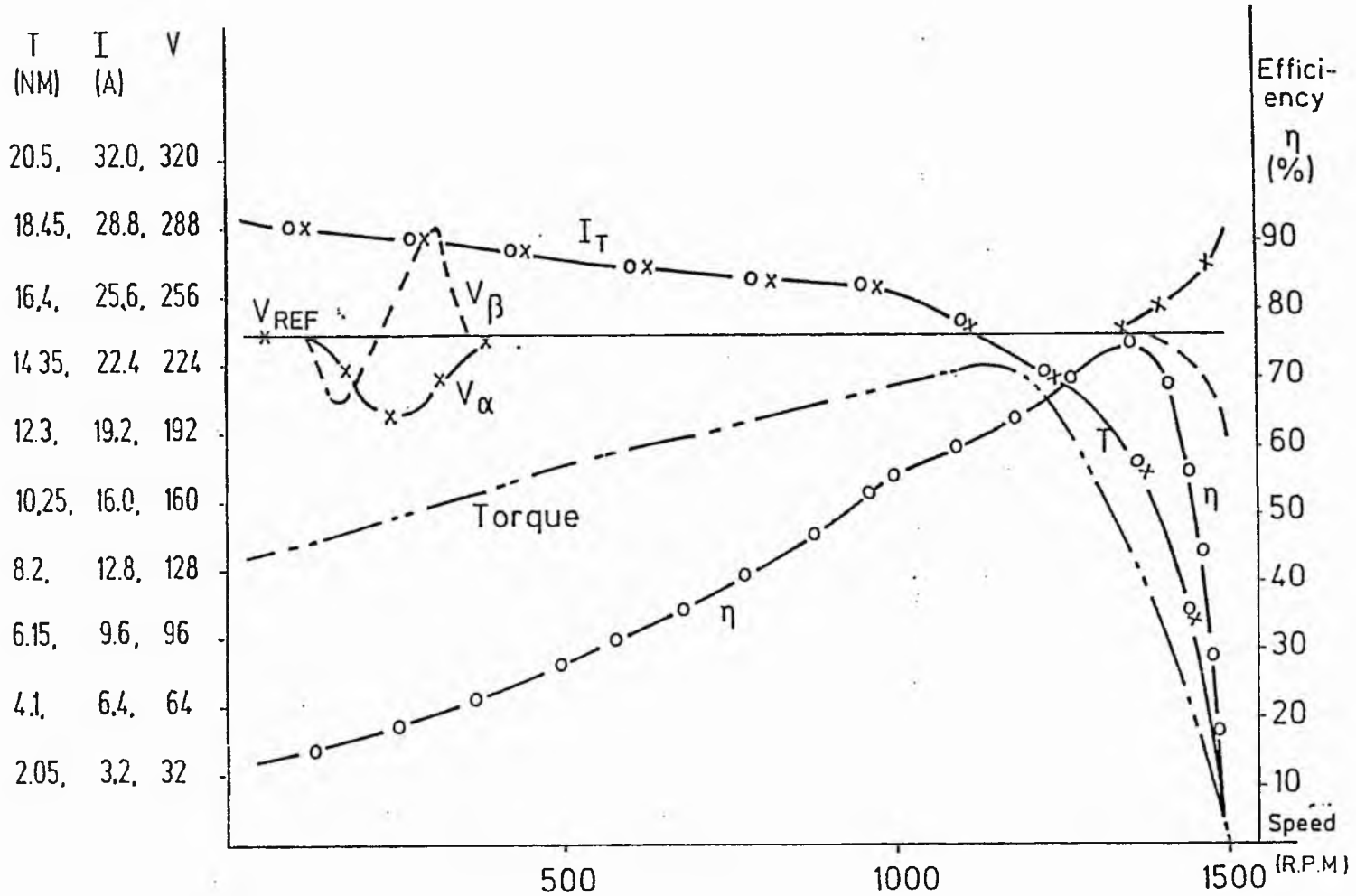

Fig. 4.37 Theoretical results of the phase converter shown in Fig. 4.23

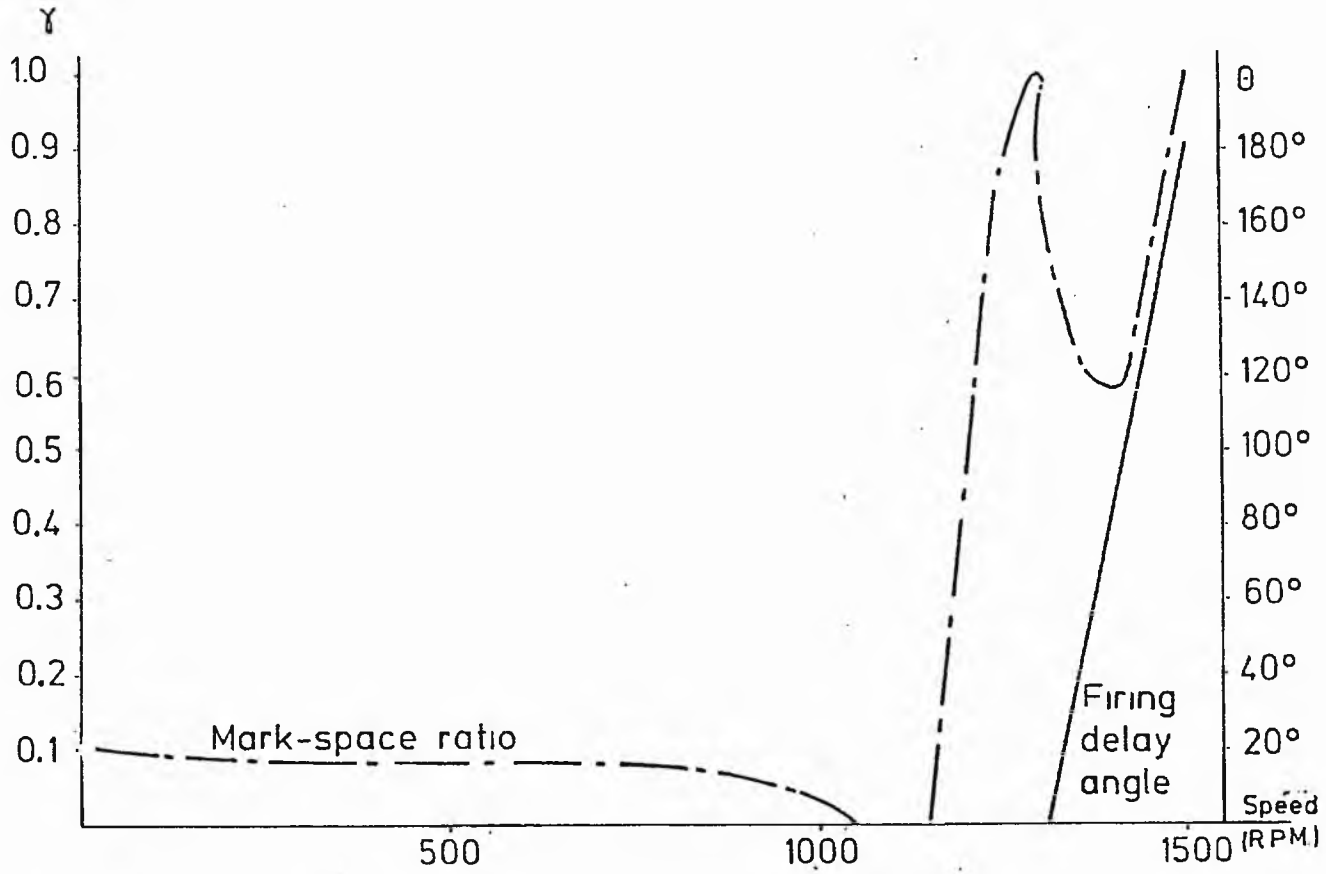

Fig 4.38 Theoretical variation of θ and γ/speed shown in Fig. 4.23

angle a maximum; so that the inductive reactance, $X_{L\beta}$ in Fig. 4.23. is removed, and Z_β is totally capacitive. In this condition, $X_{C\alpha 2}$ will have its maximum value, making Z_α totally capacitive. It can be seen in Fig. 2.3. that Z_α is almost constant in the slip range $1 > s > 0.1$, then the capacitive reactance steadily increases, decreasing the effective capacitor requirement. This is achieved by steadily increasing the firing delay angle at low slips as seen in Fig. 4.36. As for controlling the phase B, the mark-space ratio is steadily increased so $s < 0.24$ (i.e. near speed of 1140 r.p.m.). This, in turn, will increase the effective value of $I_{L\beta}$ in Fig. 4.23. making I_β an inductive current as shown in Fig. 4.22. It must be noted that as $X_{C\beta}$ and $X_{L\beta}$ are in resonance for a mark-space ratio of ≈ 0.445; steady operation at this mark-space ratio must be avoided. Further increases of mark-space ratio make Z_β more inductive.

The variation of V_α and V_β during acceleration until the speed is just below 1000 rev/min are very close to the variation of the reference voltage V_{REF} (i.e. V_A) as shown in Fig. 4.35. This indicates the low degree of unbalance. The experimental results also show that changing Z_β from capacitive reactance to inductive reactance has been achieved successfully. The excessive voltages of V_α and V_β at low slips can be explained due to the near resonance of Z_α and Z_β.
An efficiency of 73.5% at the speed of 1400 r.p.m. has been achieved which is equal to the efficiency of balanced operation.

The predicted performance of the system shown in Fig. 4.23. is illustrated in Fig. 4.37., the variations of mark-space ratio and firing delay of this predicted performance is shown in Fig. 4.38. Predicted torque and phase voltages are very close to the three-phase balanced operation. The variation of mark-space ratio resembles the experimental results from standstill to the changeover point. At the changeover point a mark-space ratio of zero is required, but the minimum mark-space ratio obtainable from the chopper is 0.05, hence the computer program is arranged to match this. Also the near resonance of $X_{C\beta}$ and $X_{L\beta}$ at the mark-space ratio of "0.445" can produce dangerous over-voltage in the chopper.

The predicted performance also suggests that zero firing delay angle from standstill to a near speed of almost 1300 r.p.m. is required. The present inverse-parallel thyristor pair is unable to satisfy this because the minimum firing delay

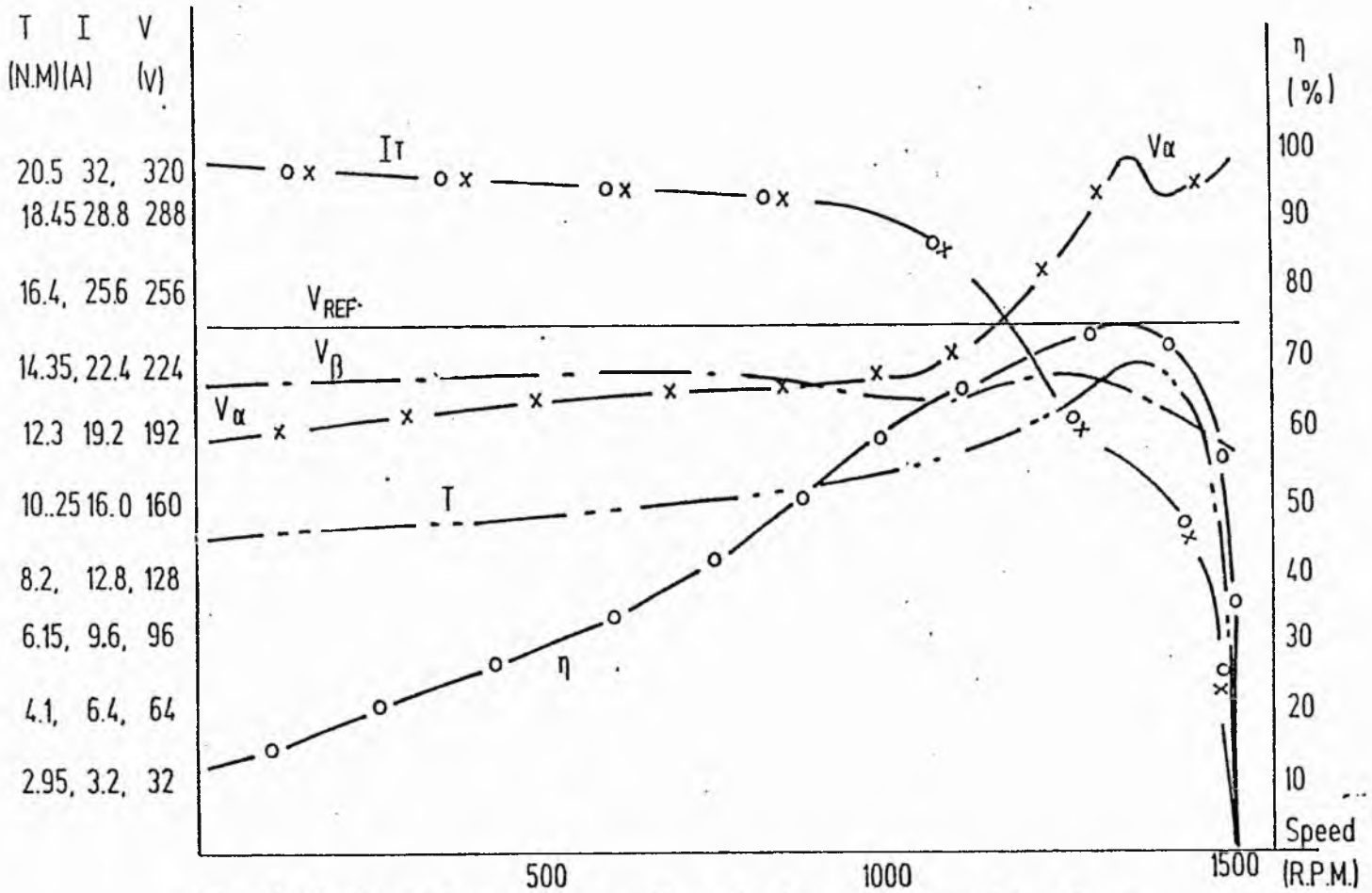

Fig. 4.39 Experimental results of phase converter shown in Fig 4.24

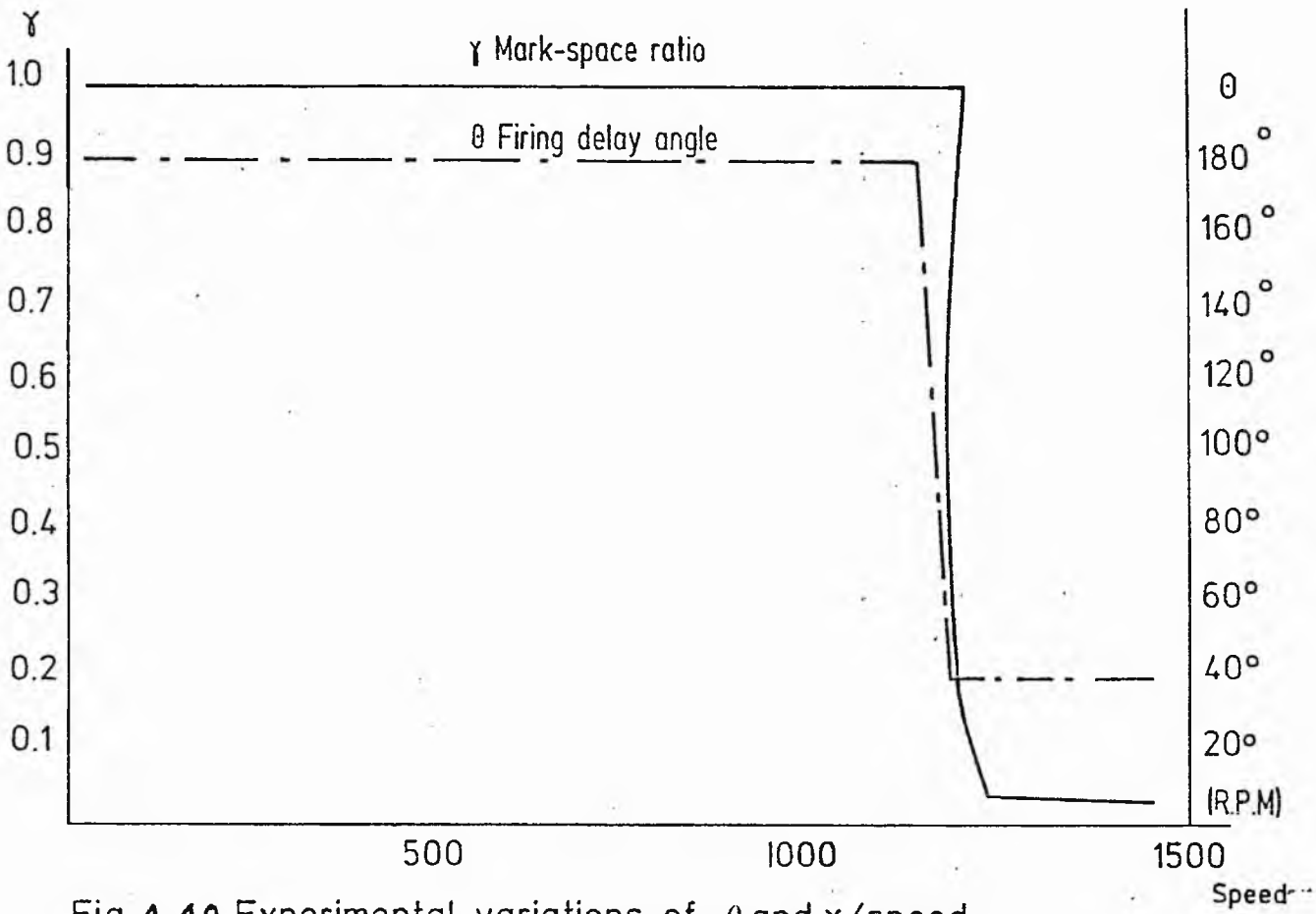

Fig. 4.40 Experimental variations of θ and γ/speed shown in Fig. 4.24

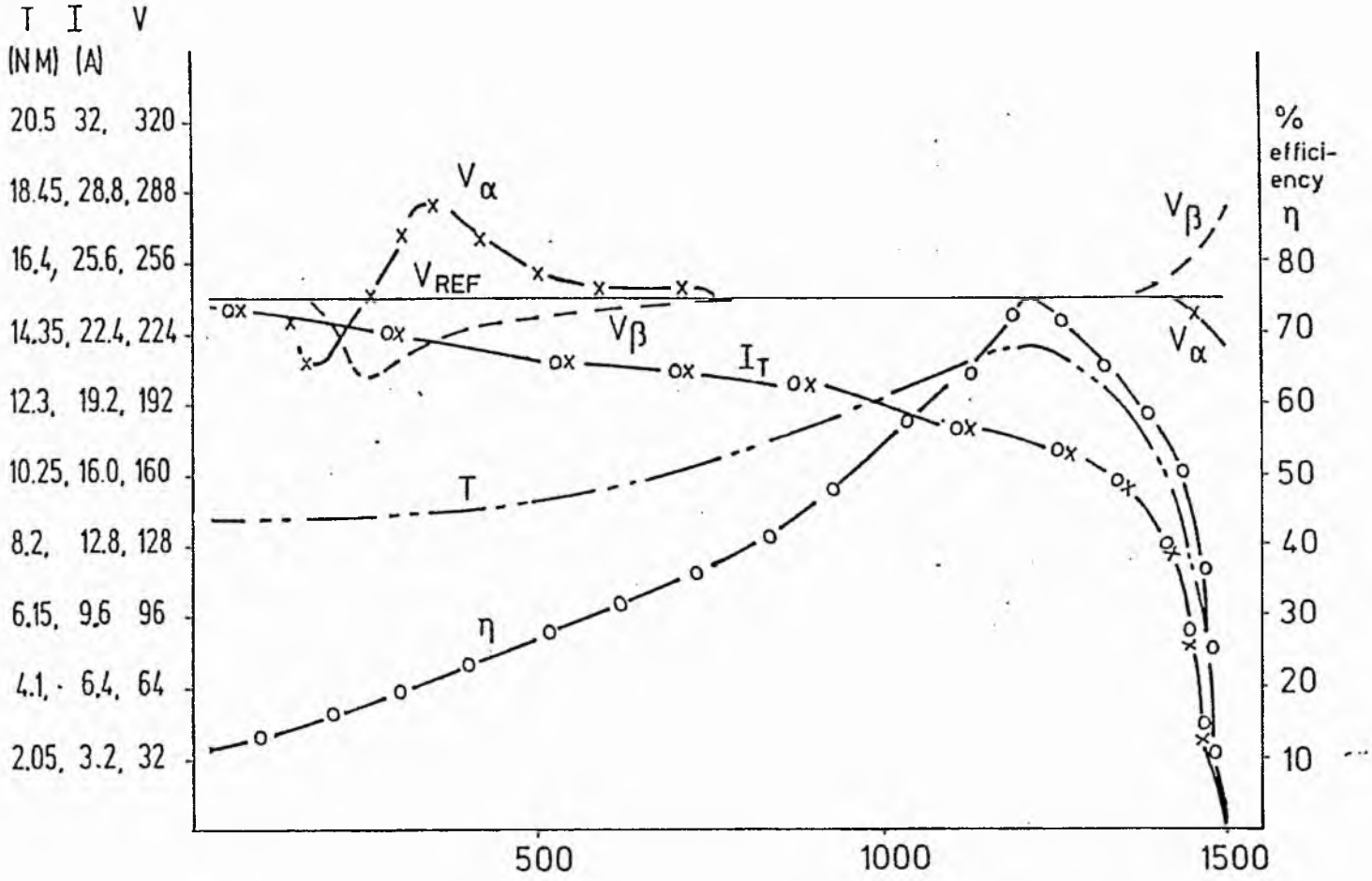

Fig. 4.41 Theoretical results of phase converter shown in Fig. 4.24

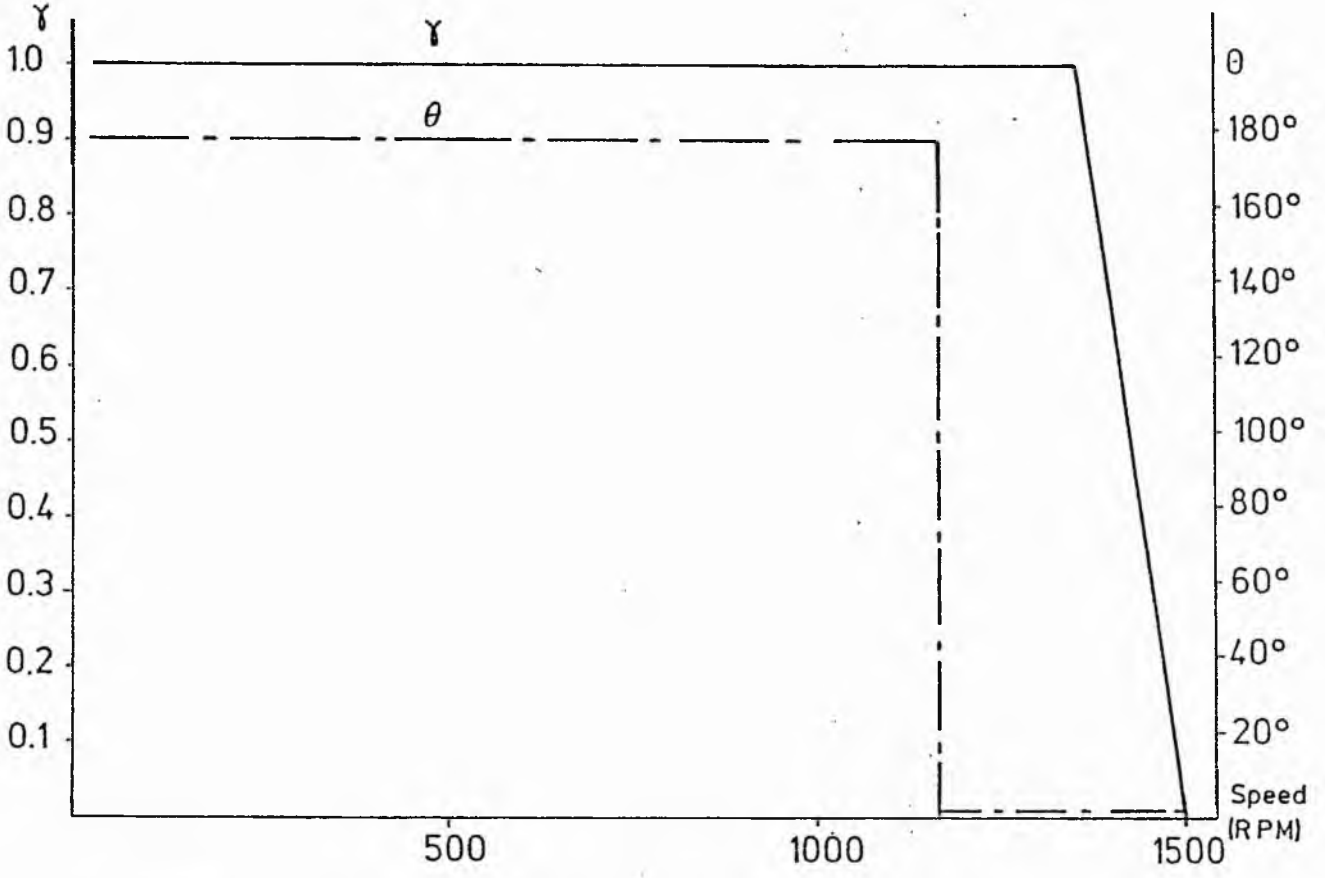

Fig. 4.42 Theoretical variations of θ and γ /speed shown in Fig. 4.24

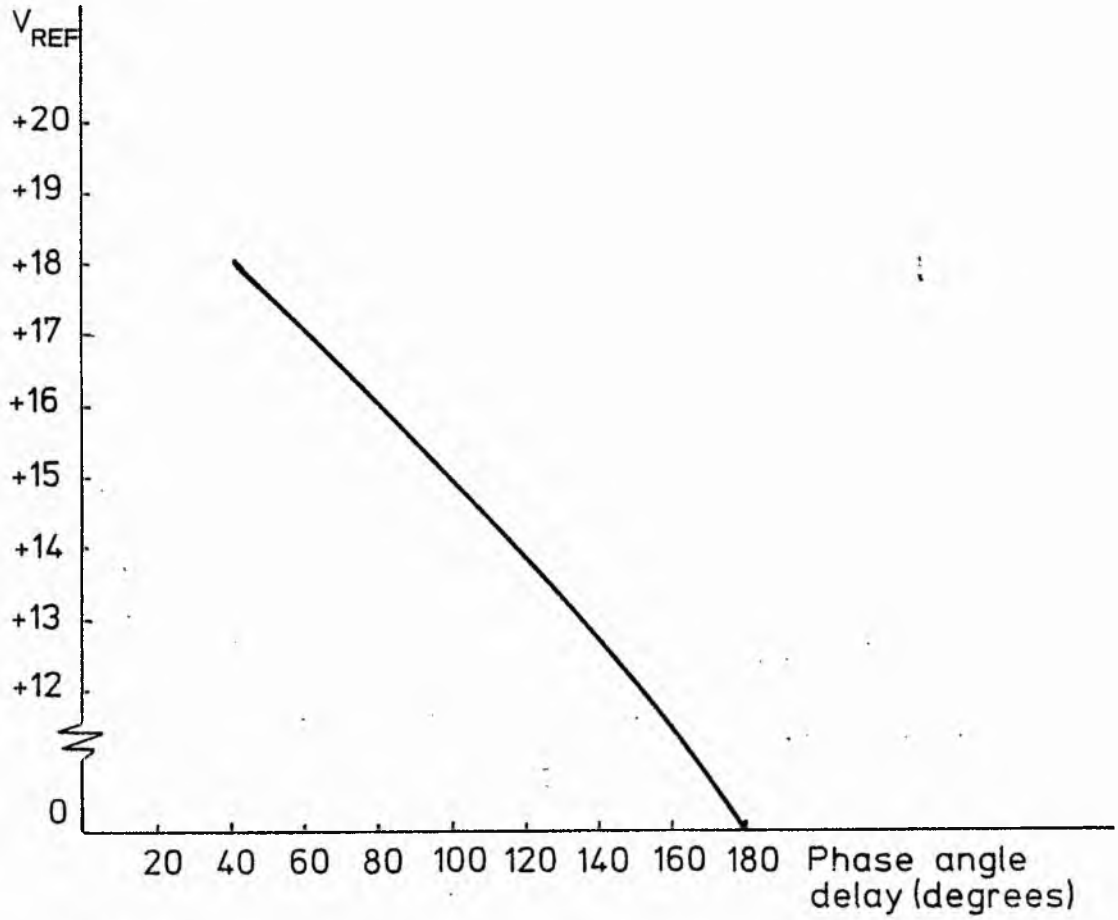

Fig. 4.43 Measured phase angle delay / control voltage

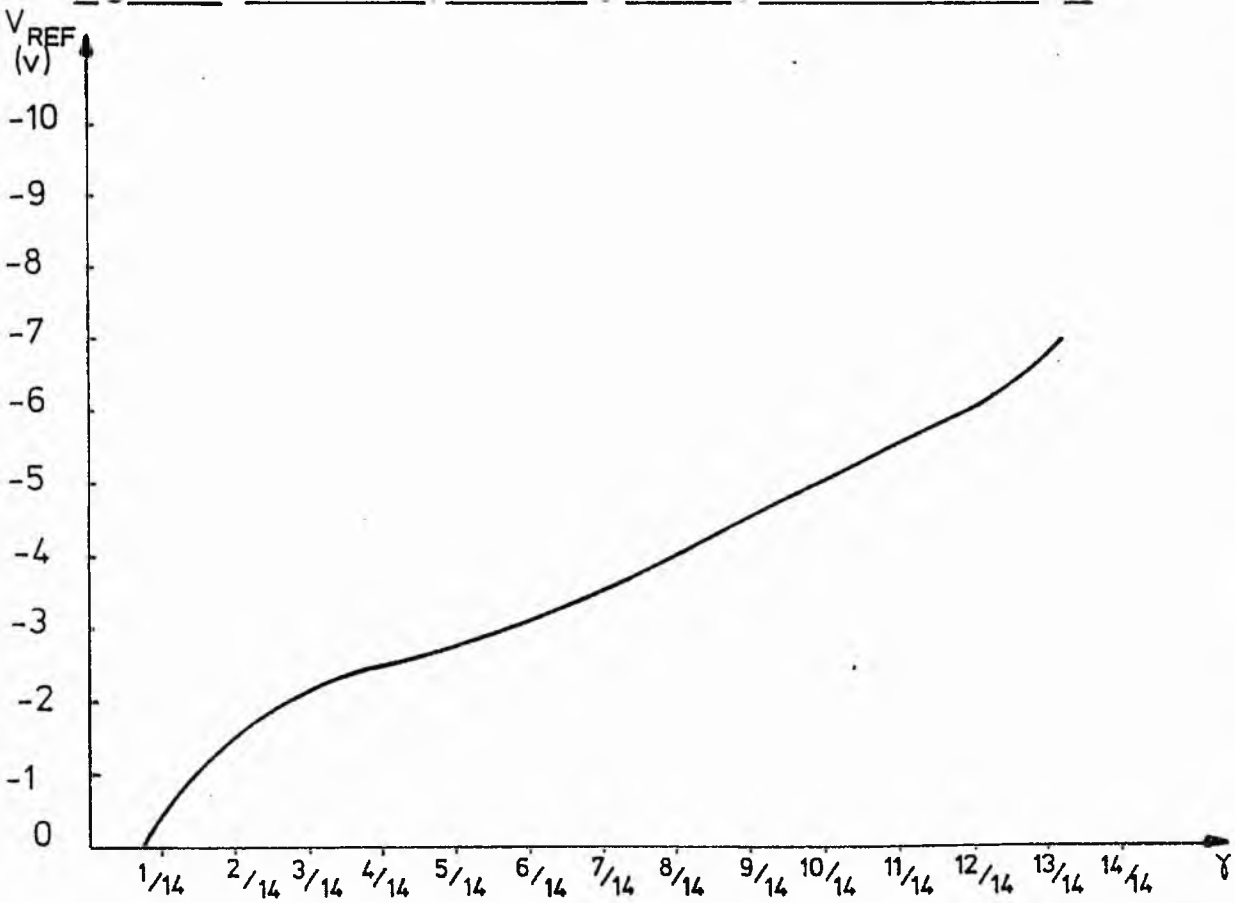

Fig. 4.44 Measured mark-space ratio / control voltage

angle possible experimentally is 40°.

Figs. 4.39 and 4.40 show the experimental results of the electronic phase converter shown in Fig. 4.25. A relatively simple control system is possible with this system. The requirement of capacitive Z_α at standstill is achieved at unity. Z_β is also made capacitive by keeping the firing delay angle at maximum when $X_{L\beta}$ is out of the circuit. The effective value of capacitance is increased by reducing the mark-space as the speed increases. Z_β is also made inductive by making the inverse-parallel thyristor pair conduct at low slips. The variations of voltages V_α and V_β are close to the reference voltage which indicates the low degree of unbalance. A maximum efficiency of 75% is obtained at the speed of 1360 r.p.m.

The predicted performance shown in Fig. 4.41. of this system resembles the experimental results of Fig. 4.39. The predicted variations of mark-space ratio and firing delay angle are shown in Fig. 4.42. which are close to experimental results.

To avoid excessive currents while obtaining the experimental results, the series of steady-state readings were obtained at a constant single-phase input voltage of 100V, then the results obtained were scaled up to 240V reference by multiplying torques by $(2.4)^2$ and voltages by (2.4). The results obtained will be optimistic. In practice, saturation and stray-load losses will be greater.

4.7. Conclusions

Near balanced operation of a single-phase fed three-phase induction motor over a wide speed range has been achieved by an electronic phase conversion.

Slip-dependent variation of the reactive components Z_α and Z_β has been achieved with a voltage phase controller and a transistor chopper. The motor can be accelerated from standstill to full-load speed and the near balance operation can be achieved over the whole speed range. A maximum efficiency of 75% has been achieved which is comparable with the efficiency of the balanced operation.

The detailed examination of the control characteristics of phase-controlled and variable mark-space ratio current interruption led to the rejection of phase control of a back-to-back thyristor pair controlling a capacitive load due to the very

small range of control that can be achieved. An undesirably large voltage harmonic content is also a disadvantage for this system. For these reasons, variable mark-space ratio control of Z_α was adopted.

The phase-controller has a wide range of control when the load is inductive or a combination of resistance and inductance. Moreover, it always operates with a large shunt capacitance which acts as a low-pass filter; therefore phase-control will perform stably adequately for Z_β control.

The selection of an appropriate experimental system is made from the requirement of Z_β changing from capacitive reactance to inductive reactance as the slip decreases leading to a choice of second system. The close relationship of all the phase voltages confirms the near-balanced condition at the changing point of Z_β and at all motoring speeds. It must be noted that the control problems of an experimental machine where Z_β is inductive reactance at all motoring speed, is less complicated than that of the experimental machine used here. Such a system requires a higher rotor resistance (e.g. Mawdsley machine).

The requirement of Z_α and Z_β in practice varies when compared to the predicted values. This may be due to saturation, where tests have been carried out with a low voltage. The low voltage may affect the magnetising and leakage reactance and since the calculation of Z_α and Z_β are merely based on machine parameters, under low voltage conditions the machine parameters may be different at the rated voltage values. This may explain the differences of the predicted and experimental results.

Since the variation of firing delay angle and the mark-space ratio can be set as the function of their reference control voltages of their firing circuits, the system can be automatically monitored. If a programmable logic is employed with the required variation of both the firing delay angle and the mark-space ratio the reference voltages of both firing circuits can be controlled by a feedback from the tachometer. However, this will give coarse control at low slips and a slotted slip-disc may be preferable. As the load varies, the speed will be changed, thus the programmable logic will change the reference control signals of each firing circuit to the values demanded by the slip signal input.

It must be noted that, due to the near-resonance at high motoring speed,

V_α and V_β exceed the rated voltage. Thus both he drive machine and the control circuits must be designed accordingly.

The electronic phase converter described in this chapter is a developed version of a previous phase converter scheme of Holmes and Ozpolar (Ref. 9). In the previous scheme, the stator controlled phase converter used only the transistor chopper control to vary the controller current I_α and I_β with common chopping. In this study two electronic controllers are used, and it is suggested that the electronic converter described may be successfully applied to most of the industrial applications where the supply is restricted to single phase and a single-phase motor can not be used due to its inefficiency and cost [14].

A major limitation of the system is the need for a detailed knowledge of the motor parameters and characteristics over the operating slip range. Given this knowledge a satisfactory transient phase converter may be designed.

If motors of unknown parameters are to be driven by the phase converter, then alternative feedback must be used. Most probably this can be achieved by a system which compares the three line voltages and uses the voltage differences as controlling error signals. The aim of the system must always be to minimise the error signals.

4.8. The Electronic System

Earlier in this chapter a preferred control system for phase conversion consisting of a phase-controlled L/C network and a bridge-chopper controlled capacitor network has been demonstrated in operation in a single-phase fed, three-phase induction motor drive. Near-phase-balance has been achieved from standstill up to a slip of approximately 15%. At small slips, voltage magnification due to resonance occurs.

The results obtained earlier were taken when the system was controlled manually by potentiometer adjustment. Now a discussion on the design of the electronic control circuits and suggested methods of closed-loop-phase-balance as a function of slip using an EPROM and digital logic.

4.9. Back-to-Back Thyristor Pair

4.9.1 Switching Characteristics

To turn on a thyristor it is only necessary to apply a positive gate pulse when a forward voltage is being applied to the thyristor (anode positive). The gate current pulse used has to have sufficient duration to allow the thyristor current to rise above the holding level. In the electronic phase converter the initial current flowing into the thyristors rises rapidly due to the load circuit component, i.e. an initially discharged capacitor, causing a high "di/dt" can be improved by increasing the gate current. If the thyristor is to turn-on successfully (to latch), the gate-pulse width must be sufficient to allow the anode cathode current to rise about the holding level. The thyristor will remain in conduction until the current falls below the holding current level. It will then switch to the OFF state.

The back-to-back thyristor pair is more robust than a triac of a comparable rating. The back-to-back thyristor pair is used as an a.c. switch and it must be capable of being triggered into the ON state with either direction of current flow. The most significant limitation of the triac (the single-package) arises due to the fact that as both directions of current flow are required, when the current stops the triac must immediately accept a high voltage applied at a high "dv/dt". As the silicon has only just been carrying current, its capability to accept this is low. Individual gate "dv/dt" suppression is possible in a thyristor pair as an additional advantage.

The schematic of a back-to-back thyristor pair into a load control application is shown in Fig. 3.5. TH_1 starts conducting after the firing delay angle θ, and TH_2 starts conducting after $\theta+\pi$. During the positive half cycle TH_2 is blocked and TH_1 is blocked during the negative half cycle.

A pulse-circuit to provide the gate pulses specified in the previous paragraph must be synchronised to the input main for one pulse train and to a signal in phase opposition to this voltage to generate the other pulse train.

4.9.2. The Firing Circuit of the Back-to-Back Thyristor Pair

Fig. 4.45. shows the firing circuit. Timing is achieved by varying the charging rate of the timing capacitor, C_o. For better linearity, a double time-constant system is used. C_o must charge to the trigger level of the programmable unijunction transistor (P.U.T.) to initiate a pulse through the transistor Tr_3. The pulse transformer has a third winding (3) coupled to winding (1) in the collector circuit to increase the pulse width by positive feedback.

The firing circuit of the back-to-back thyristor pair generates positive gate pulses which fires each thyristor symmetrically at delay angles θ and $0+\pi$. Consequently, it has the characteristics of a triac.

In Fig. 4.45. the generated pulses are synchronised to the timing voltage by the centre-tapped transformer. When the timing voltage $V_{TIM} > 0$, Tr_1 is switched on, short circuiting C_o and inhibiting all output pulses. If the timing voltage $V_{TIM} < 0$, Tr_1 is switched off and C_o charges until the voltage across it reaches the peak level required to fire the programmable unijunction transistor (P.U.T.). In turn, the P.U.T. drives the switching transistor, Tr_3, giving a sharp rise of current through the primary of the pulse transformer and firing the thyristor. Positive feedback was used by adding a third winding to the pulse transformer in the base load of Tr_3, in order to extend the pulse-width from 40 μs to 70 μs so that latching problems are avoided. Firing times are dictated by the rate of charge of C_o. The timing circuit is effectively the network shown in Fig. 4.46A. The equations of the first loop of Fig. 4.46. are derived as follows:

$$V_{ref} = i_1 R_1 + \frac{1}{C_0}\int_0^t i_1\,dt - \frac{1}{C_0}\int_0^t i_2\,dt \qquad (4.77)$$

$$-V_{DC} = -\frac{1}{C_0}\int_0^t i_1\,dt + i_2R_2 + \frac{1}{C_0}\int_0^t i_2\,dt \qquad (4.78)$$

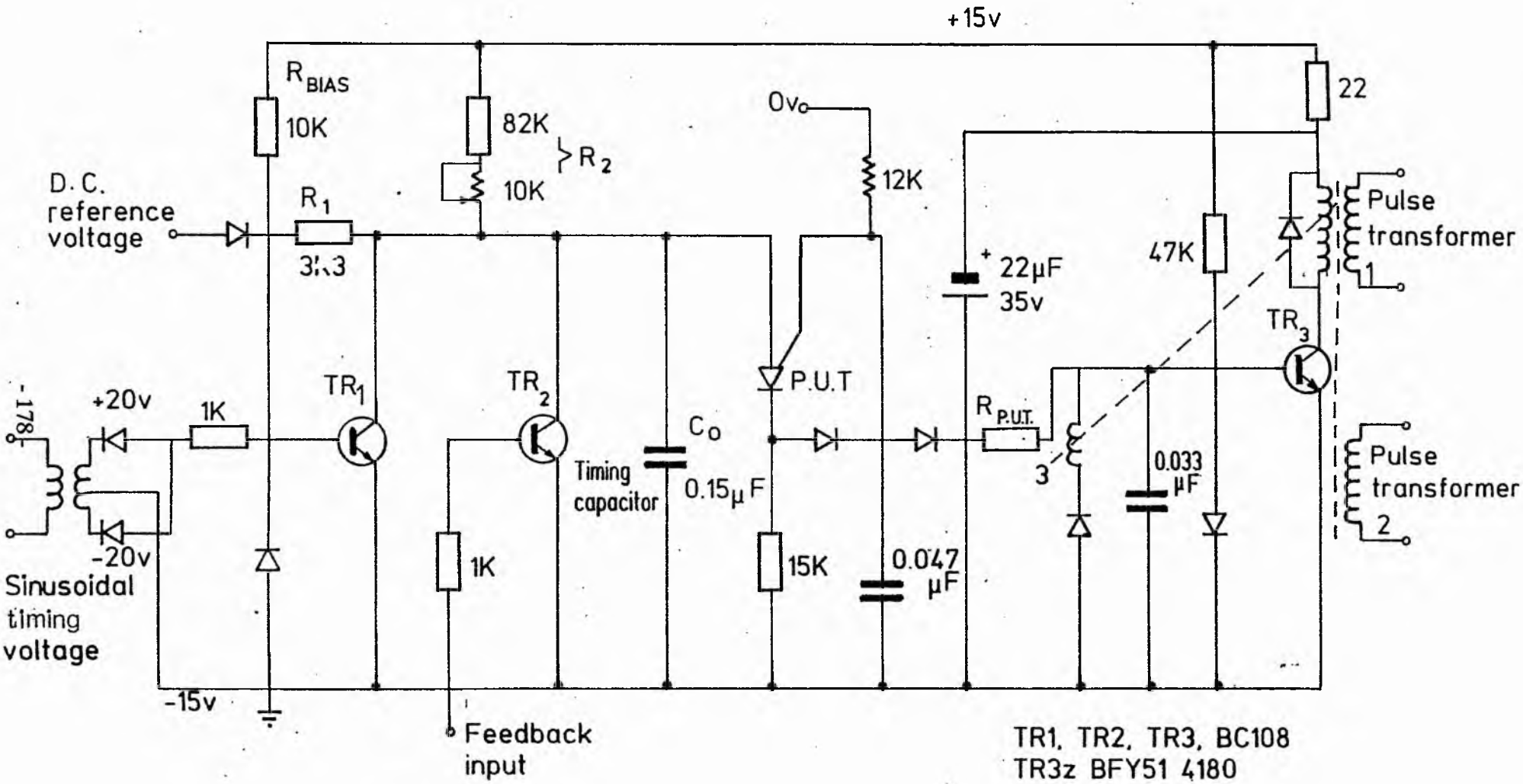

Fig4.45 The firing circuit for the back to back thyristor pair.

also

$$\frac{dV_{C0}}{dt} = \frac{1}{C_0} \quad (i_1 - i_2) \tag{4.79}$$

and

$$V_{C0} = \frac{1}{C_0} \left[\int_0^t (i_1 - i_2)\, dt \right] \tag{4.80}$$

Substituting eqn. 4.80 into eqn. 4.77 and 4.78 gives:

$$V_{ref} = i_1 R_1 + V_{co} \tag{4.81}$$

$$-V_{DC} = i_2 R_2 - V_{co} \tag{4.82}$$

Substituting eqn. 4.81 and 4.82 into eqn. 4.79 and rearranging:-

$$\frac{dV_{C0}}{dt} = \frac{1}{C_0} \left(\frac{V_{ref} - V_{C0}}{R_1} + \frac{V_{DC} - V_{C0}}{R_2} \right) \tag{4.83}$$

Using Laplace transform Eqn. 4.83 can be rewritten as -

$$sV_{C0}(s) - V_{C0}(0^+) = -V_{C0}(s) \frac{R_1 + R_2}{R_1 R_2 C_0} + \frac{1}{s} \frac{V_{ref} R_2 + V_{DC} R_1}{R_1 R_2 C_0} \tag{4.84}$$

where $V_{co}(0^+) = 0$

Assuming

$$\tau = \frac{R_1 + R_2}{R_1 R_2 C_0} \tag{4.85}$$

which makes eqn. 4.84

$$V_{C0}(s) = \frac{V_{ref} R_2 + V_{DC} R_1}{R_1 R_2 C_0} \left[\frac{1}{s} - \frac{1}{s + \tau} \right] \left[\frac{R_1 R_2 C_0}{R_1 + R_2} \right] \tag{4.86}$$

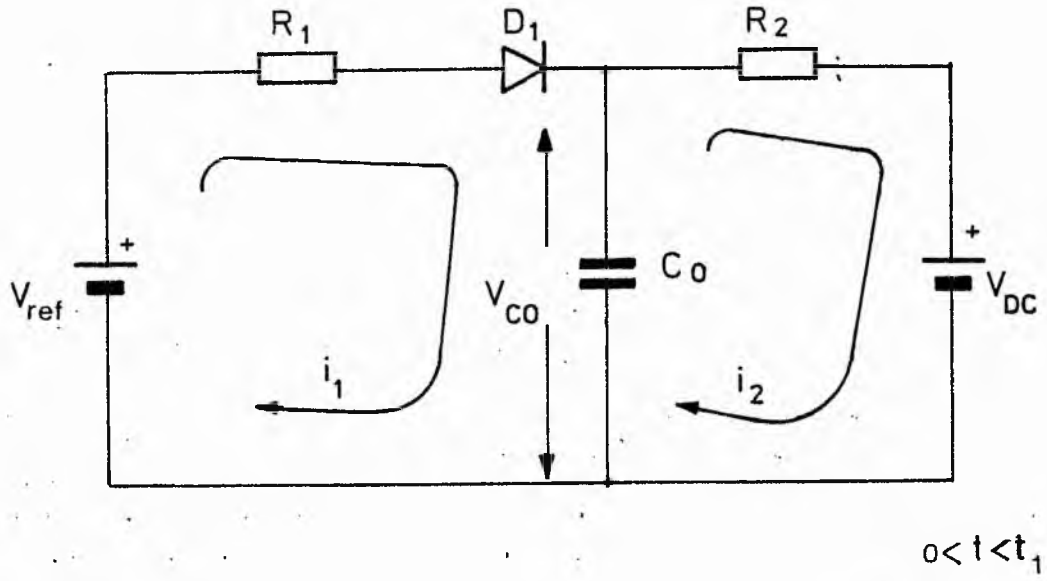

Fig4.4.6A. Equivalent circuit of pulse board timing_

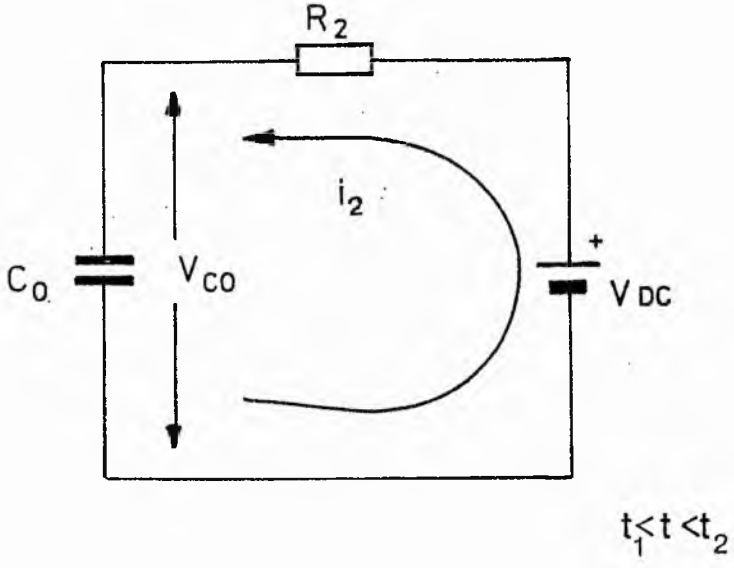

Fig4.4.6B Final timing_

or

$$V_{C0}(t) = \frac{V_{ref}R_2 + V_{DC}R_1}{R_1 + R_2}\left(1 - e^{-\tau t}{}_{0<t<t_1}\right) \tag{4.87}$$

when $V_{ref} = V_{co}$ at $t = t_1$, D_1 becomes reverse-biased. For $t > t_1$ the direction of I_2 is reversed and the timing circuit can now be shown as in Fig. 4.46.B. The following can be written:

$$V_{DC} = I_2 R_2 + V_{C0} \tag{4.88}$$

$$\frac{dV}{dt} = \frac{1}{C_0} I_2 \tag{4.89}$$

Using Laplace transforms eqn. 4.88 and 4.89 can be rewritten as:

$$\frac{V_{DC}}{s} = I_2(s)\, R_2 + V_{C0}(s) \tag{4.90}$$

and

$$sV_{C0}(s) - V_{C00} = \frac{I_2(s)}{C_0} \tag{4.91}$$

which gives

$$I_2(s) = \frac{1}{\left(s + \frac{1}{C_0R_2}\right)}\left(\frac{V_{DC} - V_{C00}}{R_2}\right) \tag{4.92}$$

or

$$I_2(t) = \frac{V_{DC} - V_{C00}}{R_2} e^{-(t - t_1)/C_0R_2} \tag{4.93}$$

Also from eqn. 4.90 and 4.91

$$\frac{V_{DC}}{s} = R_2 \left[C_0 s\, V_{DC}(s) - C_0 V_{C00}\right] + V_{C0}(s) \tag{4.94}$$

and

$$V_{C0}(s)\left|s + \frac{1}{C_0R_2}\right| = \frac{V_{DC}}{sC_0R_2} + V_{C00} \tag{4.95}$$

or

$$V_{C0}(t) = V_{ref}e^{-(t - t_1)/C_0R_2} + V_{DC}\left[1 - e^{-(t - t_1)/C_0R_2}\right] \tag{4.96}$$

here $V_{co}(0^+) = V_{co0} = V_{ref}$ where the diode D_1 reverse biased at $t = t_1$ giving $V_{co} = V_{ref}$

When $t - t_1 = t_2$, $V(t) = V_p$, or

$$V_p = V_{ref} e^{-t_2/CoR_2} + V_{DC}(1-e^{-t_2/CoR_2}) \tag{4.97}$$

where the PUT conducts when V_{CO} reaches this required peak value.

Fig. 4.47 and 4.48. show the predicted and experimental waveforms for the voltage across C_o. Charging starts at the instant when the timing waveform goes negative. The first time constant of Eqn. 4.85 operates until the diode is reverse-biased and switches off. At that instant $t = t_1$ Eqn. 4.87 can be written as :

$$t_1 = \frac{R_1 R_2 C_0}{R_1 + R_2} I_n \left| \frac{V_{ref}R_2 + V_{DC}R_1}{R_1(V_{DC} - V_{ref})} \right| \tag{4.98}$$

Also from eqn. 4.97

$$V_p = e^{-t_2/C_0R_2} (V_{ref} - V_{DC}) + V_{DC} \tag{4.99}$$

which gives

$$t_2 = C_0R_2 I_n \left| \frac{V_{DC} - V_{ref}}{V_{DC} - V_p} \right| \tag{4.100}$$

The firing delay angle θ will be

$$\theta = \omega(t_1 + t_2)$$

or

$$\theta = \frac{R_1 R_2 C_0}{R_1 + R_2} \omega I_n \left| \frac{V_{ref}R_2 + V_{DC}R_1}{R_1(V_{DC} - V_{ref})} \right|$$

$$+ R_2C_0 \omega I_n \left| \frac{V_{DC} - V_{ref}}{V_{DC} - V_p} \right| \tag{4.101}$$

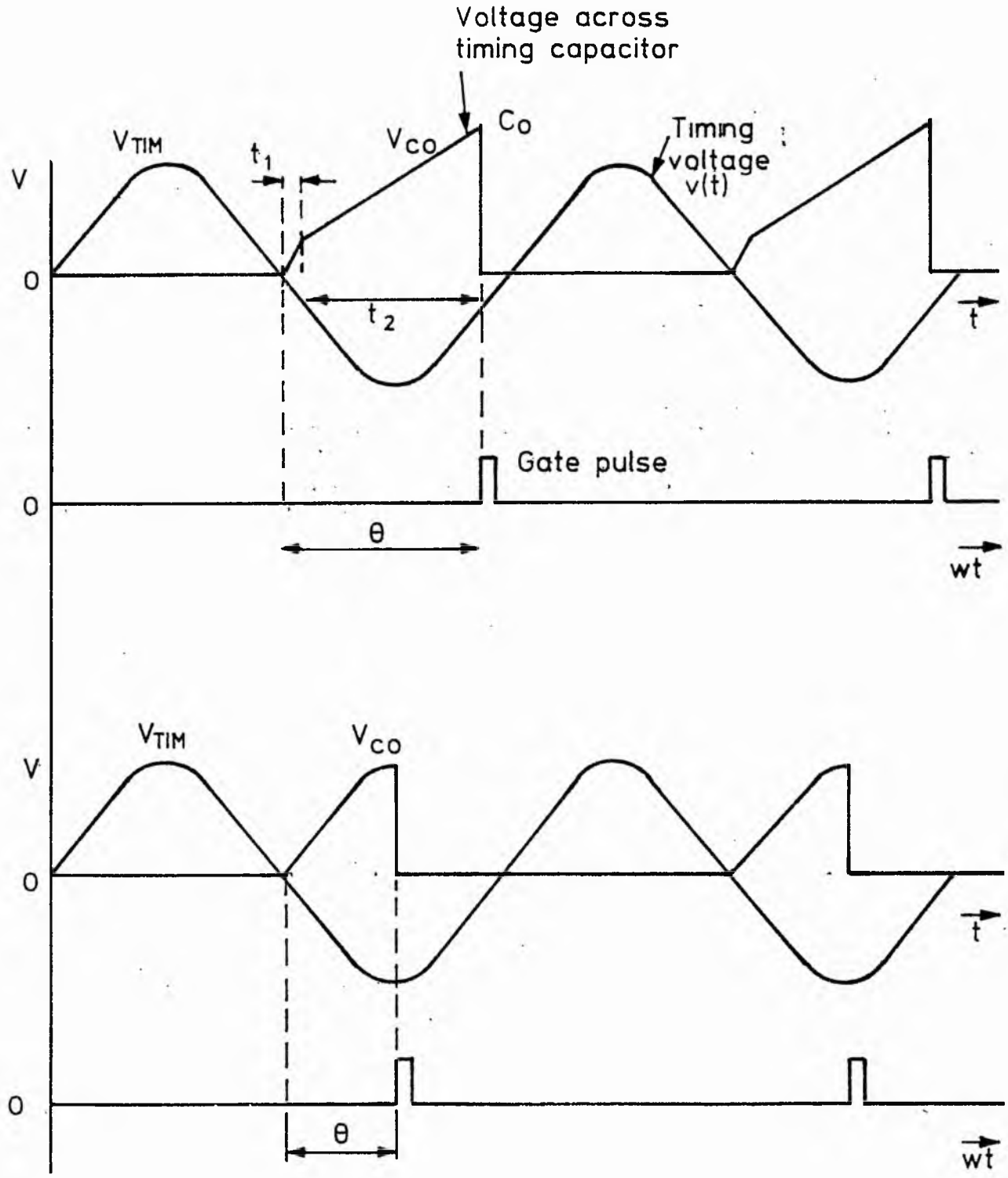

Fig4.47 Timing of firing pulses.

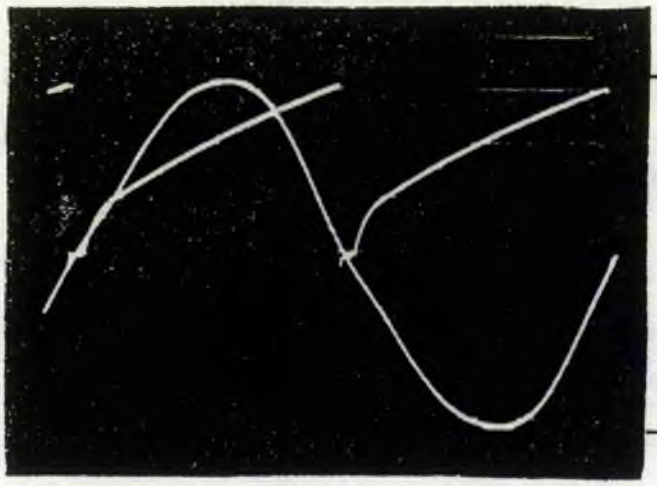

+30V
Timing voltage

Capacitor charging waveform

-30V

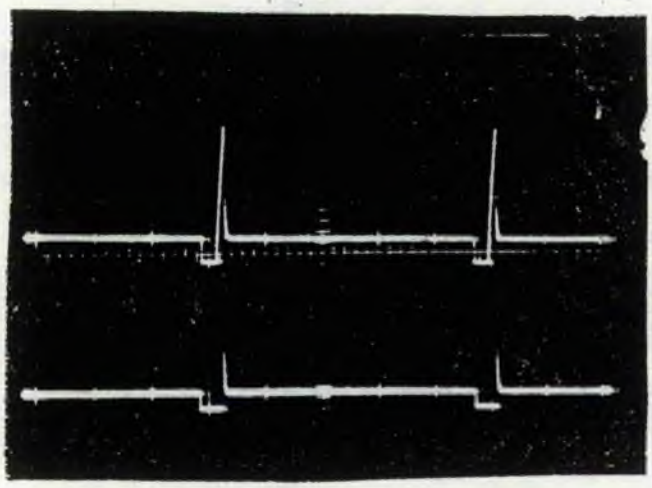

Charging capacitor

P.U.T output pulses

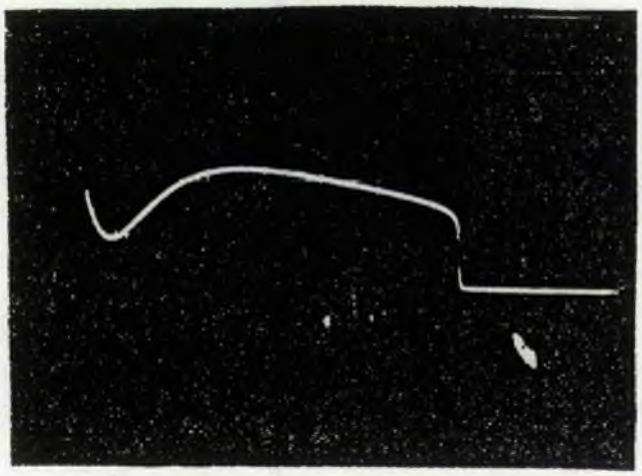

Gate triggering pulse

Fig. 4.48 Pulse circuit waveforms

Any increase in the value of V_{ref} delays the diode turn-off time causing most of the charging to occur at the initial faster rate. V_{CO} reaches the peak value of V_p of P.U.T. sooner and the smaller firing angle shown in the lower diagram of Fig. 4.47. results.

The measured firing delay angle as a function of reference voltage is shown in Fig. 4.43. As explained earlier, the extinction angle has a particular importance in the phase converter operation and it depends upon the nature of the load. The extinction angle as a function of firing delay angle for R-C and R-L loads is shown in Figs. 4.8. and 4.12. respectively.

4.10. The Transistor Chopper

The chopper must accept alternating current, ideally without changing the current waveform, then a controlled and regular current interruption must take place.

A transistor switch is essentially a d.c. current switch and so the a.c. input must be rectified before chopping. The bridge in Fig. 4.49. is used for either a three-phase or a single-phase input.

4.10.1. The Input Bridge

The rectifier peak voltage and r.m.s. current ratings must exceed the load voltage and currency by a substantial amount for safe operation. The assumption is made that the magnitude of the supply voltage is such as to make the diode volt-drop negligible when conducting. The diode will conduct like a closed switch when its anode voltage is positive with respect to its cathode, and ceases to conduct when its currents falls to zero, then it acts like an open switch. The turn-on and turn-off times of the diode are in the range of a few microseconds so that they may be assumed as instantaneous times in relation to the half cycle time for a 50 Hz supply. Input inductance is negligible and so overlap can be ignored.

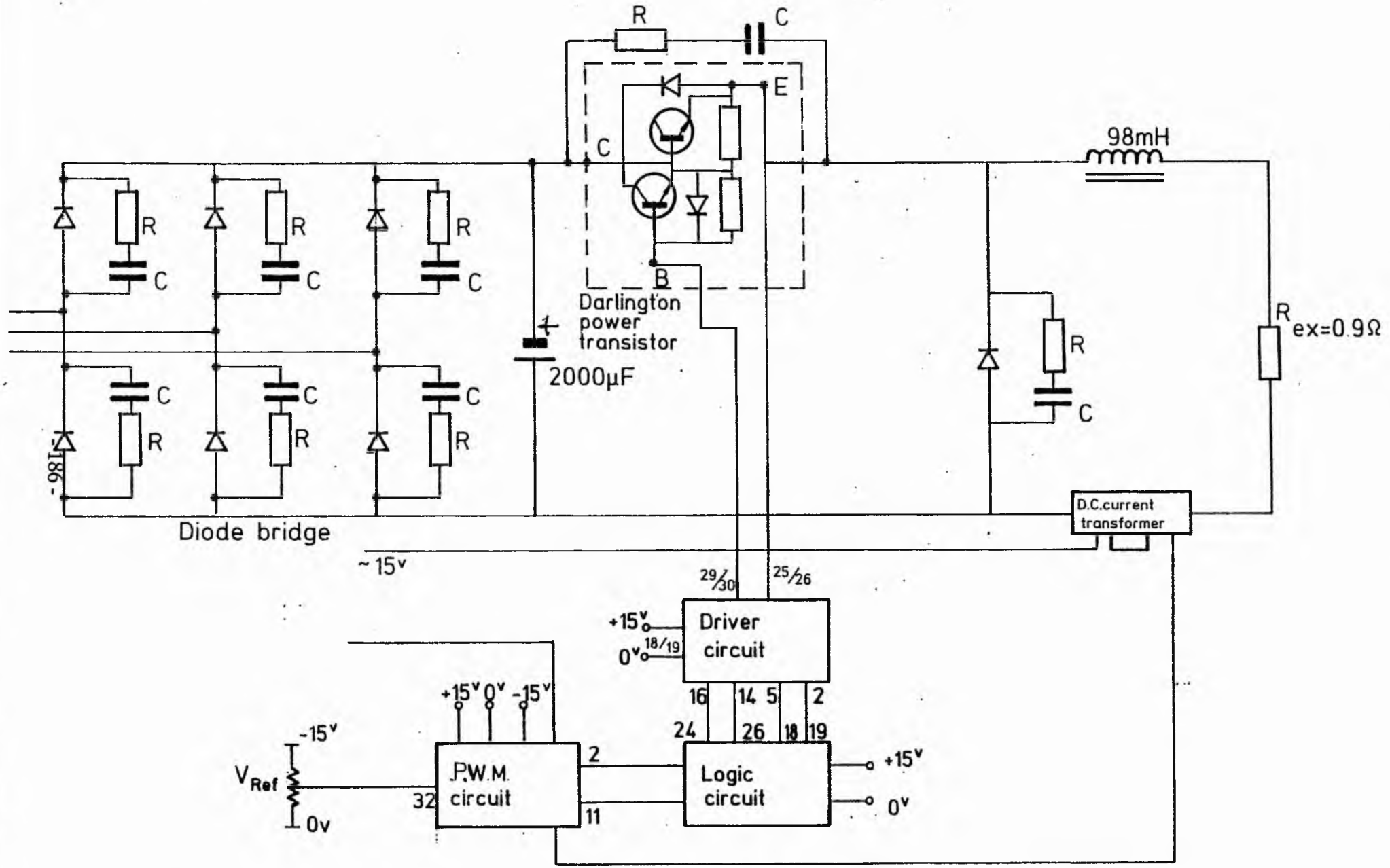

Fig.4.4.9 Transistorized chopper control circuit.

For a given d.c. load current, I_{DC}, the r.m.s. rating per diode is "0.579 I_{DC}" [11] for a three-phase, full-wave bridge and "0.785 I_{DC}" [11] for a single-phase full-wave bridge. Hence, for a load current rating of 20A, the r.m.s. current rating of the diodes for single-phase bridge is 15.7A and for three-phase bridge the r.m.s. current rating for the diodes is 11.58A. Hence the r.m.s. diode rating must be 20 A, and type BYX 25-600 diodes were selected to match this rating. The peak voltage rating of the diode used must be greater than the peak voltage it experiences in the course of operation. The peak off-state voltage of the diode used is 600 V. However, transients momentarily raise the voltage in excess of the rating and this voltage must be prevented from appearing across the off-state diode. Each diode is protected by an R-C suppressor; a capacitor of 0.22 μF (100V, d.c.) across the diode means that any high "dv/dt" appearing at the diode terminal will set up an appropriate current "C dv/dt" in the capacitor. A 50 Ω resistor in series with the capacitor will limit the magnitude of the current in the capacitor.

The large electrolytic capacitor is included for smoothing. When the power transistor is non-conducting, the capacitor voltage is the instantaneous bridge output voltage. On chopper switch-on the capacitor tries to discharge into the small resistence R_{ex}. This produces a high "di/dt" and a large opposing e.m.f. "L di/dt" across the 90 mH reactor. Hence, the current through the chopping circuit is regulated to a steady value. The value of capacitance must be very large to ensure that $1/C \int i\,dt > L\,di/dt$.

4.10.2. The Power Transistor

The chopper control circuit using a high power Darlington transistor is built as shown in Fig. 4.49. The Darlington transistor is in effect a combination of two transistors with a common collector. The emitter of the first transistor is connected to the base of the second transistor. This combination gives a very high gain. The Darlington transistor is a single package combination which tends to act rather like a slow transistor, because the first transistor cannot turn off the second

transistor quickly. However, this problem is improved in the package unit by including resistor from base to emitter of the second transistor.

The reference voltage in Fig. 4.49. sets the mark-space ratio of the transistor. A definition of mark-space ratio is

$$\gamma = \frac{\text{(ON TIME)}}{\text{(ON TIME)} + \text{(OFF TIME)}} \tag{4.102}$$

where

$$\text{(ON TIME)} + \text{(OFF TIME)} = \text{PERIOD} \tag{4.103}$$

and the period of the triggering cycle is fixed but the ON time interval can be varied, which in turn varies the mark-space ratio.

To turn on the transistor a base current of 1.3 A minimum is needed. The transistor acts as a short circuit as long as the base current is supplied. The transistor used has a maximum collector to emitter current of 30 A with maximum collector-to-emitter voltage of 200V, and the base current required for switch-on is 1.3A. The drive circuit supplies 2.2A base current which is sufficient to turn the transistor on. The transistor package is also a very fast switch (3 μs for turn-on, 5 μs for turn-off, compared with 15-20 μs for thyristors) and turn-off problems are practically non existent. Commutation circuitry, which is costly and bulky is not required. If the base current is removed, the transistor turns off. When it conducts, the forward voltage drop is in the order of 0.3V as compared to 2V for thyristors. Therefore, the power dissiption in a power transistor is lower than that of a thyristor of similar power rating.

The peak value of the voltage to be chopped in the phase converter is the peak voltage of the controlled phase. However due to the smoothing capacitor and the high chopping frequency the chopped voltage is not perfectly chopped. This, in turn, decreases the harmonic effect.

Varying the mark-space ratio varies the ON and OFF times of the voltage. This in turn effectively varies the r.m.s. value of the line current. The currents defined in Fig. 4.52. can be expressed in terms of the mark-space ratio γ as follows:

$$\frac{I_{TRrms}}{I_{LD}} = \sqrt{\gamma} \tag{4.104}$$

$$\frac{I_{Drms}}{I_{LD}} = \sqrt{1-\gamma} \tag{4.105}$$

A chopping frequency of 400 Hz was chosen as a rate significantly greater than the supply frequency of 50 Hz. The device was originally selected for slip voltage chopping in the rotor circuit of a wound rotor machine, hence the limit of the voltage is 200V. A Darlington power transistor with a larger voltage rating is needed for effective phase control. The phase control experiments were carried out at reduced voltage to allow for them.

If the power generated in switching is considered:

$$P = \left[\frac{1}{2} V_{ce} i_c\right] \left[\frac{\text{turn on time + turn off time}}{\text{chopping period}}\right] \tag{4.106}$$

where V_{ce} is the collector to emitter voltage of the power transistor, i_c is the load current. For V_{ce} = 85 V, i_c = 12 A and turn on and turn off times of the transistor are 3 μs and 5 μs respectively; the power generated in the transistor will be 1.632 W at the chopping frequency of 400 Hz and a d.c. load current of 12 A.

An appropriate heat sink was selected, having about a quarter of the size required by a thyristor of comparable rating.

4.10.3. The Flywheel Diode, Series Inductor and External Resistance

The inductor shown in Figs. 4.49. and 4.50. has a value of 98 mH and during the conducting interval of the chopper the energy "½ Li^2" will be stored, where i indicates the rectified load current. When the transistor switch is off, the stored energy will be dissipated through R_{ex} and the flywheel diode. Hence, the load current is transferred away from the Darlington transistor during the on time, the inductor presents a large impedance of high-frequency harmonics; reducing the fluctuation of the load current.

4.10.4. The Driver Circuits

The components of the firing circuit of the transistor is shown in Figs. 4.51., 4.52. and 4.53. Synchronised current triggering pulses from the logic circuit need to be amplified by a factor of 100 to turn the power transistor on. Also, the collector to emitter voltage of the transistor is at a higher potential than the control circuit, which should not be directly connected to the power circuit. The pulse transformers shown in Fig. 4.51. enable both to increase the triggering signals to the sufficient level to turn on the transistor and also to isolate the control circuit from the power circuit.

Four modulated output pulses from the logic circuit (Fig. 4.52.) are supplied to the FETs of the driver circuit as shown in Fig. 4.51. The FETs are ideal switches for digital application and have a very high input impedance. However, they are very liable to be damaged by high voltages; for this reason a zener diode must be connected across the FET as voltage clamp.

The triggering pulses supplied to the FETs at 800 Hz are fed into the pulse transformer primary. These steep-fronted pulses are amplified in voltage by the pulse transformer and in current by the Darlington transistor. The sum of two amplified triggering pulses of 1.1 A at 800 Hz gives the final triggering pulses of 2.2 A at 400 Hz for the base drive of the power transistor, as shown in Fig. 4.56.

4.10.5. Pulse Width Modulation for the Generation of Driver Pulses

The chopper firing circuit is schematically shown in Fig. 4.54. The mark-space ratio is set by varying the negative reference voltage (i.e. control voltage). The comparator acts as a pulse-width modulator, selecting the points of intersection of the sawtooth voltage and the reference voltage. The sawtooth wave is generated by the synchronous wave generator 566 (Fig. 4.53.) fed into the

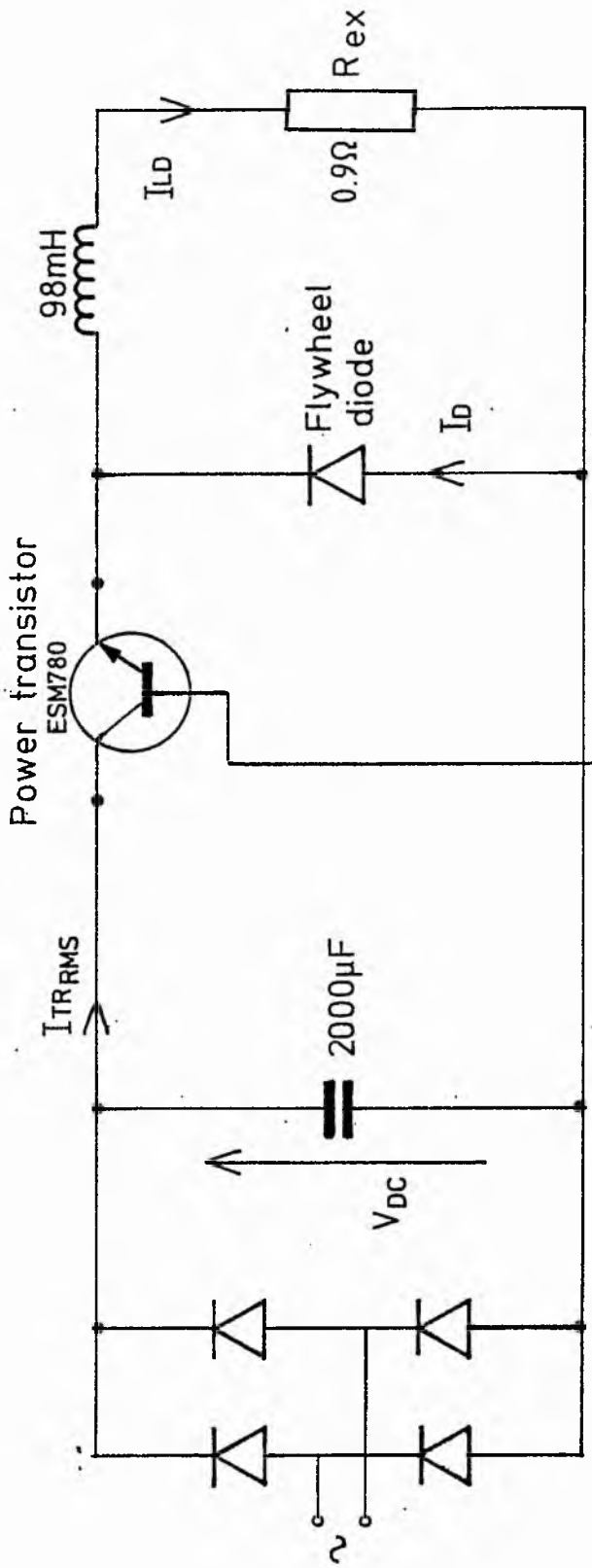

Fig.4.50 D.C. equivalent circuit of the chopper.

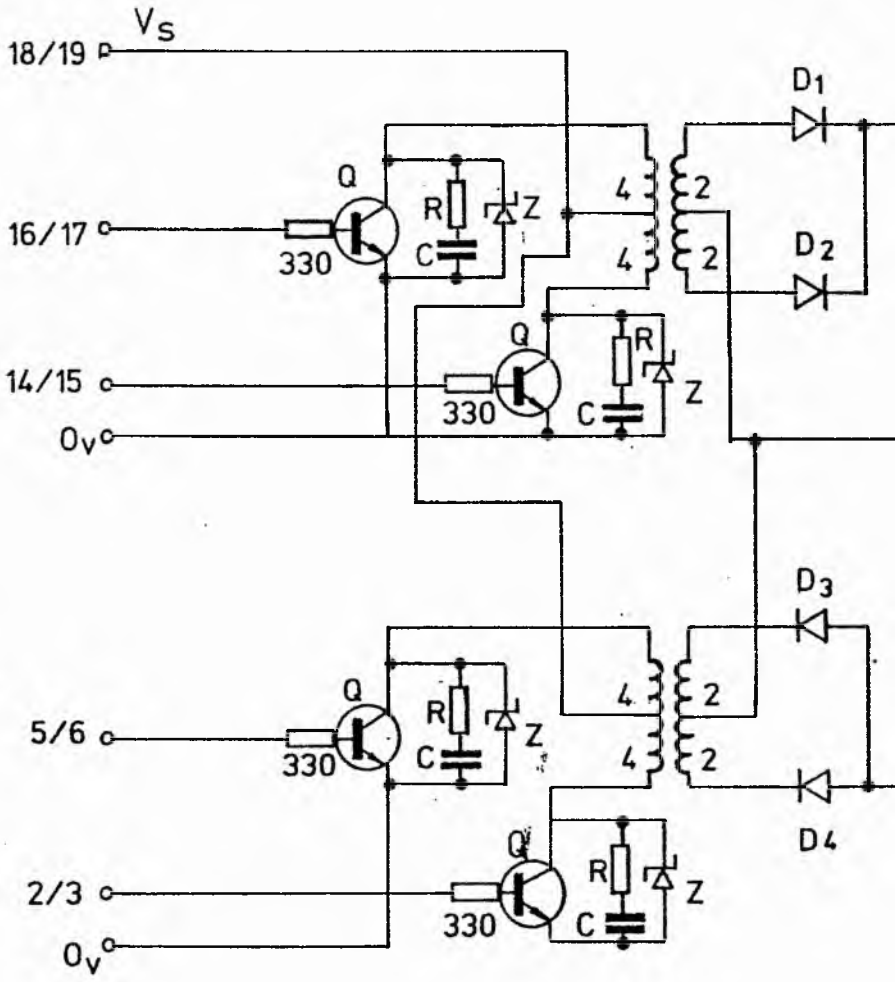

Fig.4.51 Chopper driver circuit.

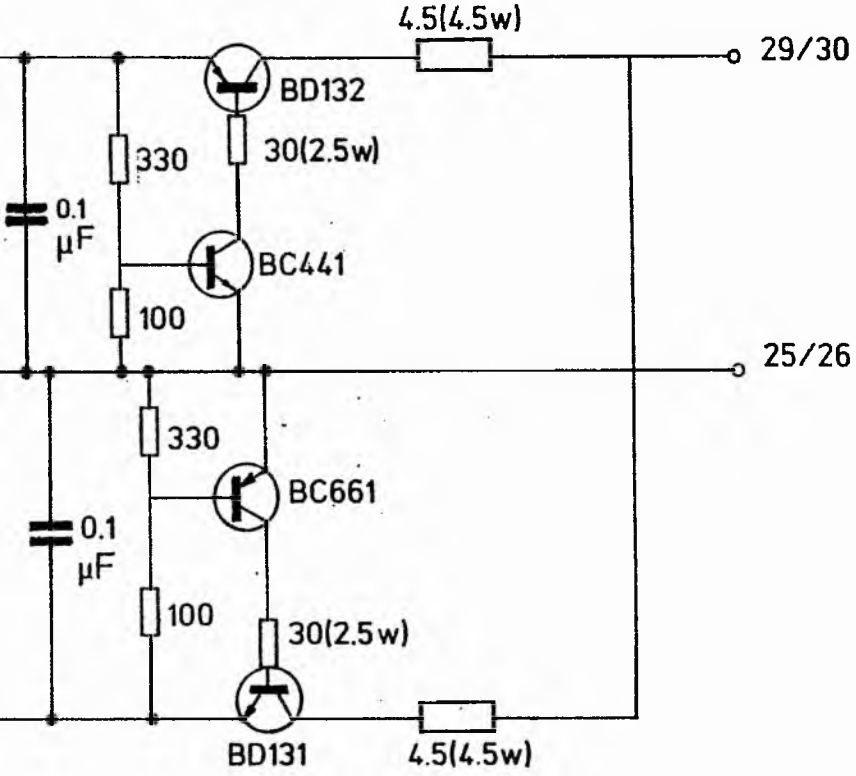

Q VN66
R 22 ohms
C 0.01µF
Z BY88

D_1 D_2 D_3 D_4 Schotley RS262-466

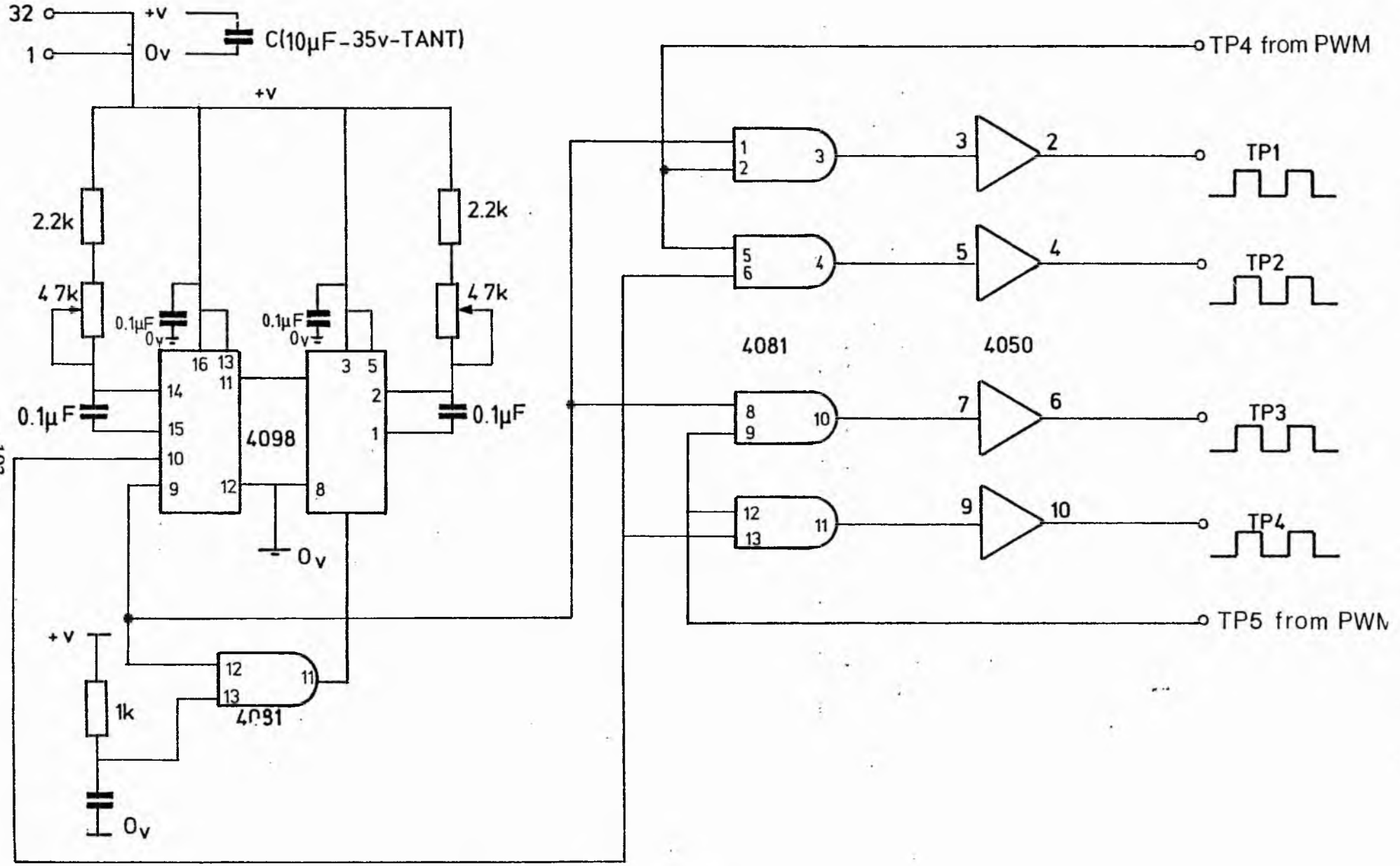

Fig.4.52 Logic circuit

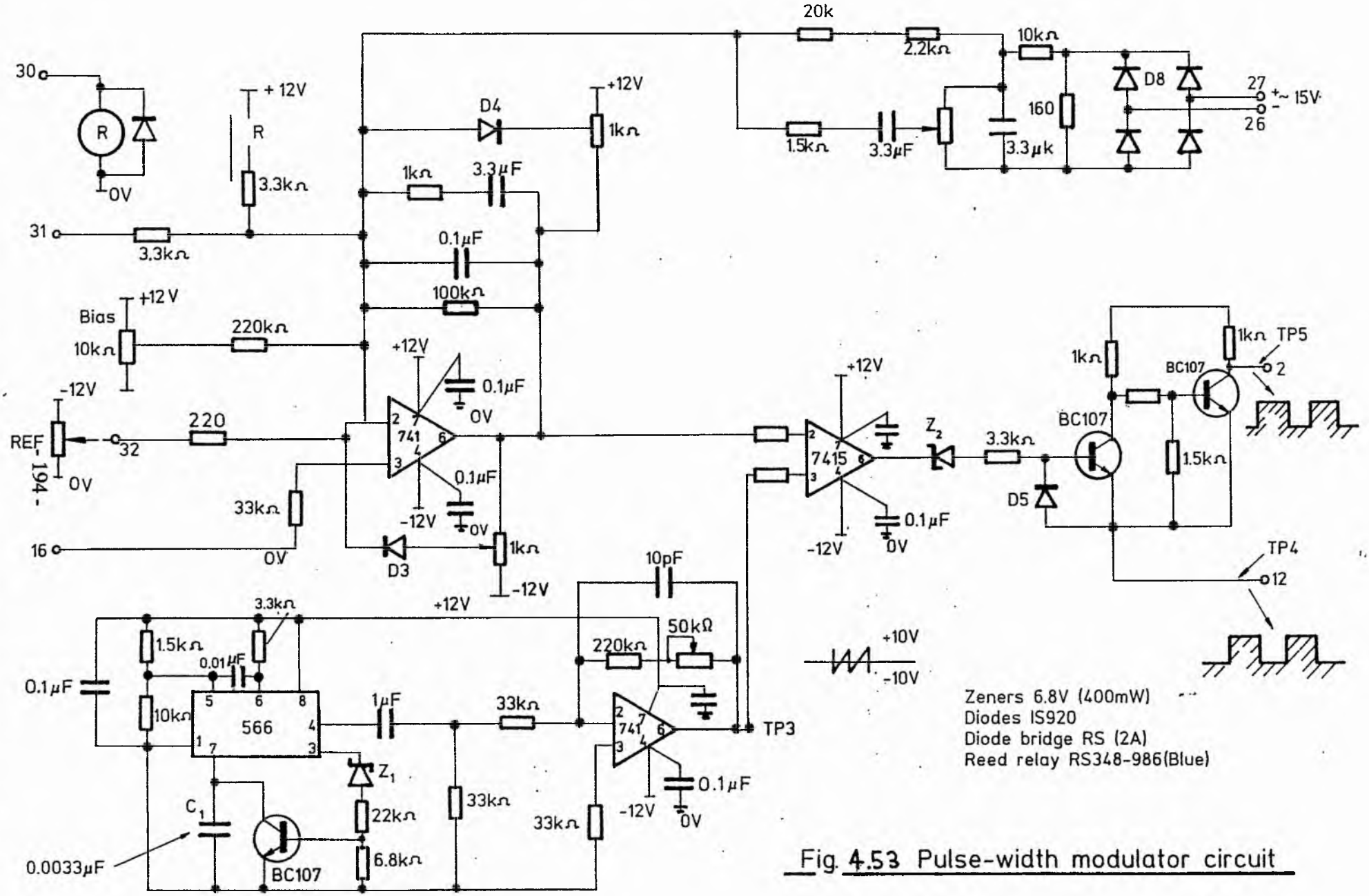

Fig. 4.53 Pulse-width modulator circuit

comparator, which is in effect an operational amplifier.

Figure 4.55. shows the positive ramp generator. The transistor driven by the pin 3 output rapidly discharges at the end of the charging period so that charging can resume instantaneously. The pnp transistor likewise rapidly charges the timing capacitor C_1 at the end of the discharge period. The circuit resets so quickly that the thermal stability is excellent. The period is fixed at 800 Hz where $f_o = \frac{1}{2}\tau$ is the free-running frequency of the 566 chip in normal operation. Thus,

$$\tau = \frac{1}{2f_o} = \frac{R_{T\varepsilon}C_1 V^+}{5(V^+ - V_C)} \qquad (4.107)$$

where V_c is the bias voltage at pin 5 (Fig. 4.58.) and $R_{T\varepsilon}$ is the total resistance between pin 6 and V^+.

If the sawtooth voltage, V_{ramp}, is greater than the reference voltage, V_r, the comparator output will be V_o as shown in Fig. 4.56. If $V_{ramp} < V_r$, then the output voltage will be zero. Hence as V_r increases, it linearly decreases the width of the output pulse. Similar modulation can be carried out on the negative voltages. The generated pulse train has an average value which is proportional to the modulating (i.e. reference) voltage.

The PWM is in effect a square-wave generator with an independent control of duty cycle. These pulses are fed into the logic circuit. The monostable multivibrator 4098 (i.e. clock) generates periodic signals at fixed frequency of 800 kHz as shown in Fig. 4.52. The one-shot pulses from the PWM and the clock pulses are fed into AND gates. When the clock is HIGH, the pulse trains will be gated. The clock pulse period is higher than the modulated pulses generated in the PWM circuit. This double input synchronising in the logic circuit ensures a train of triggering pulses at all times. When the clock is LOW, no pulses will be gated.

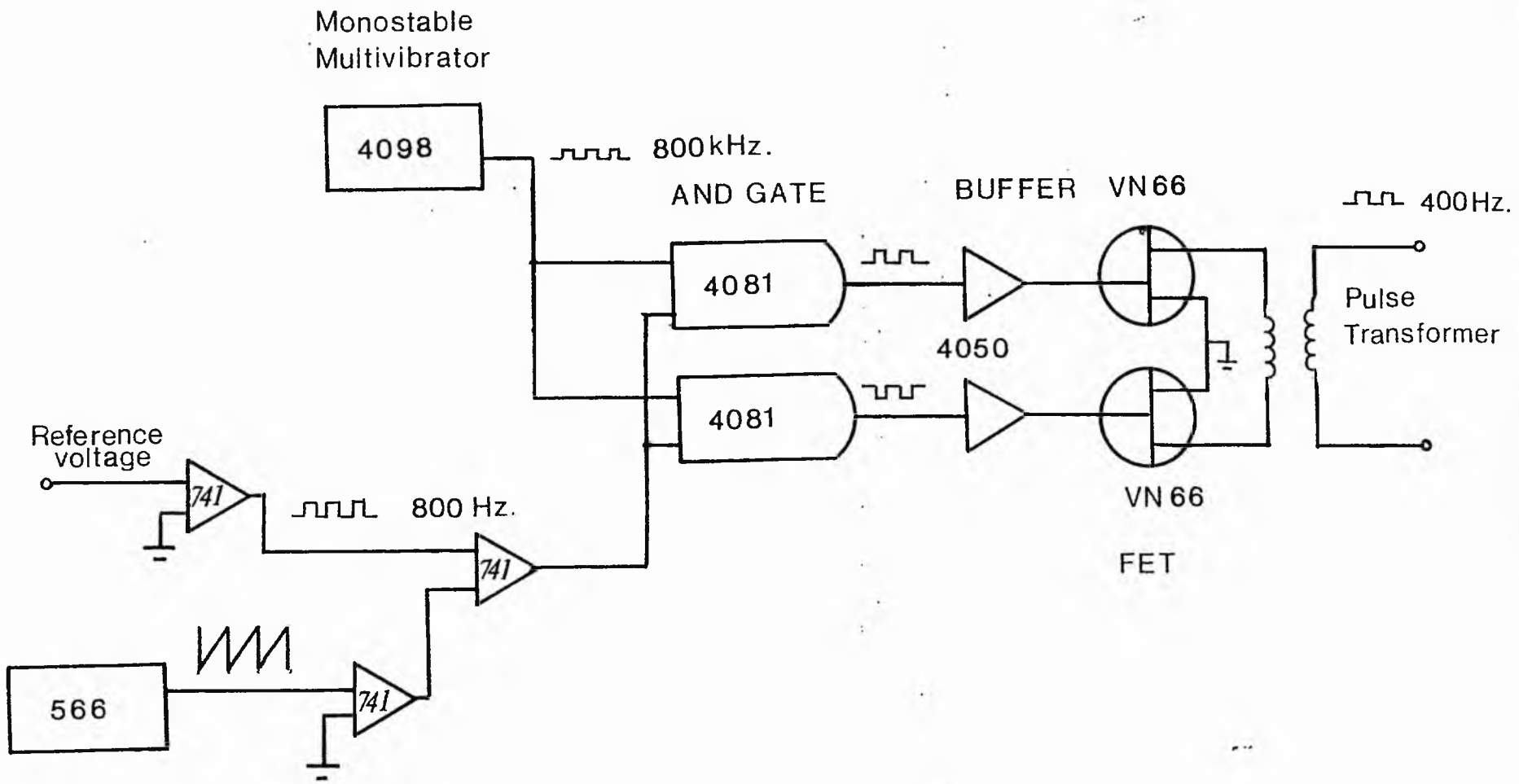

Fig. 4.54 Schematic of Chopper firing circuit

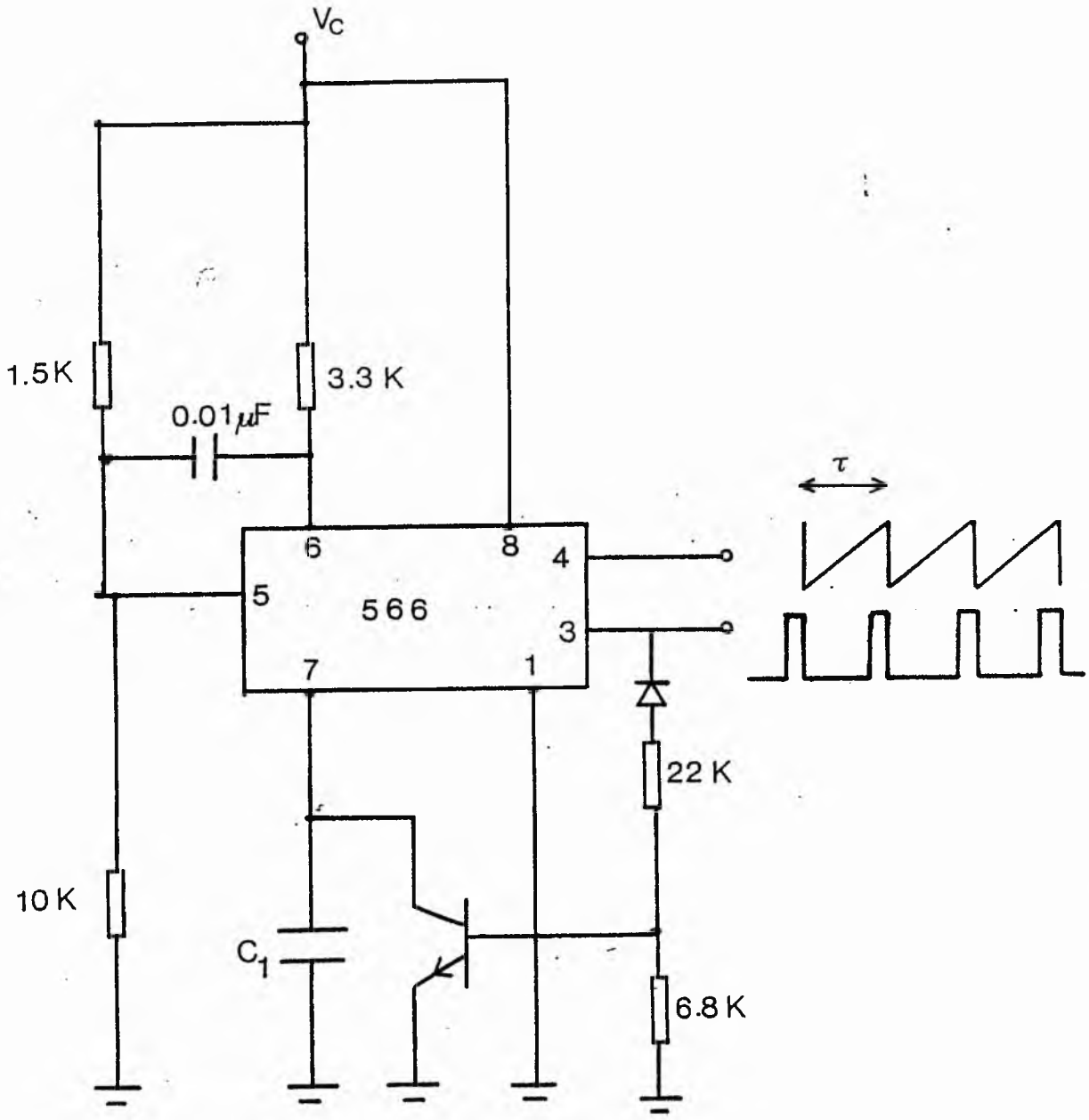

Fig 4.55 Ramp generator

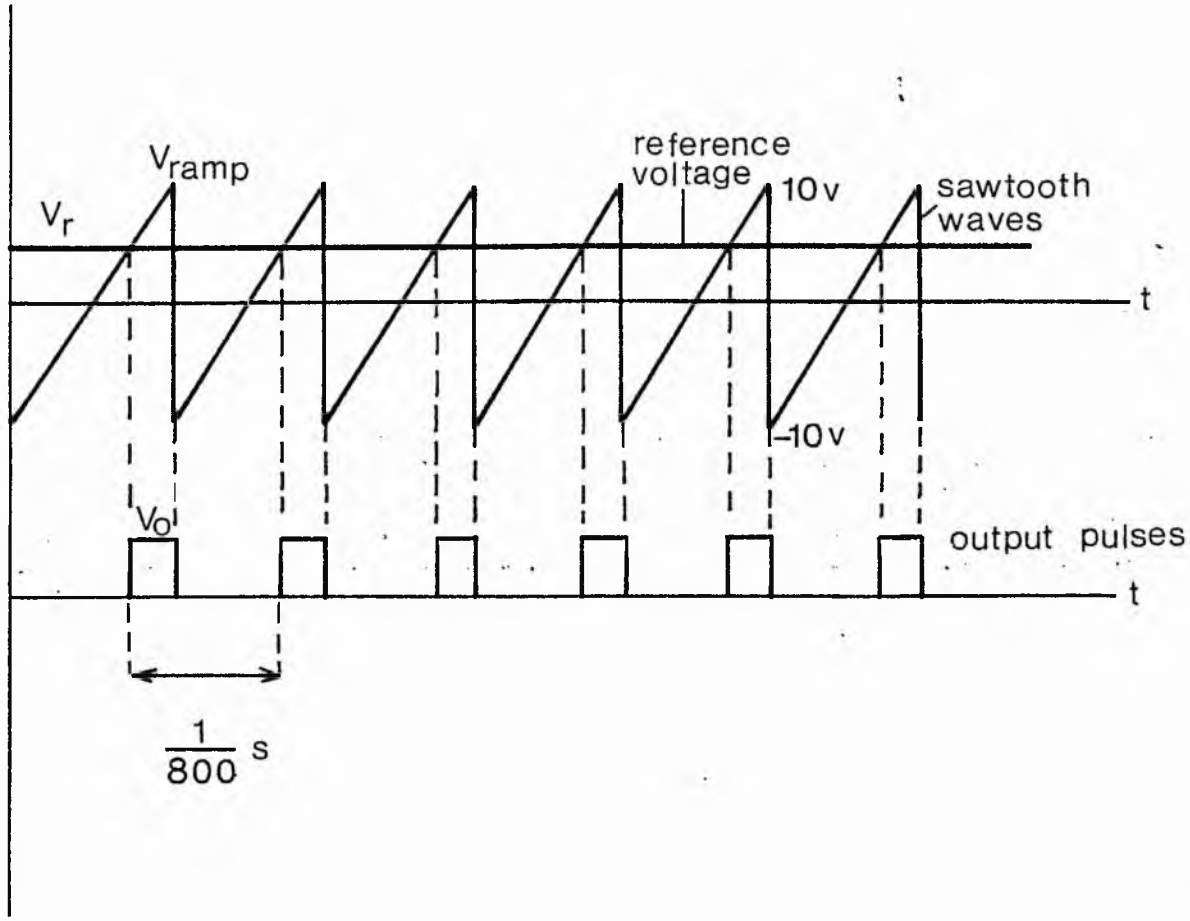

Fig.4.56 Modulated pulses in PWM circuit

4.11. Conclusion and Future Requirements for Closed-Loop Feedback

In sections 4.8. and 4.10. an open loop control system producing controlled chopping of an a.c. source has been described. The a.c. current is controlled by a d.c. reference voltage which controls the mark-space ratio of a d.c. chopper. Similarly a further reference voltage achieves a similar control in a back-to-back thyristor system.

Earlier sections show the required variation of reference voltage in each case, so that balanced three-phase motor operation can be achieved. A closed-loop system to provide these reference voltages automatically as a function of slip is required.

Fig. 4.57. shows a schematic of such a system. Slip can be detected by an optical system incorporating a slotted disc on the shaft of the motor. Suppose the disc had n_1 slots equally spaced over 360° then at a motor speed of n rev/s the disc with generate nn_1 pulses/s. If the disc could be driven at synchronous speed, the pulses generated per second would be n_1 f/p. This pulse train can be generated by a counter synchronised to the supply frequency. Then a pulse train proportional to slip can be generated as

$$\left(\frac{n_1 f}{p} - n n_1\right) = n_1 \left(\frac{f}{p} - n\right) \text{ pulses/s}$$

The digital requirements to produce the two reference voltages are stored in two separate EPROM memories. Each memory is activated by the pulse train proportional to slip. Digital to analog conversion gives the required analogue reference voltage.

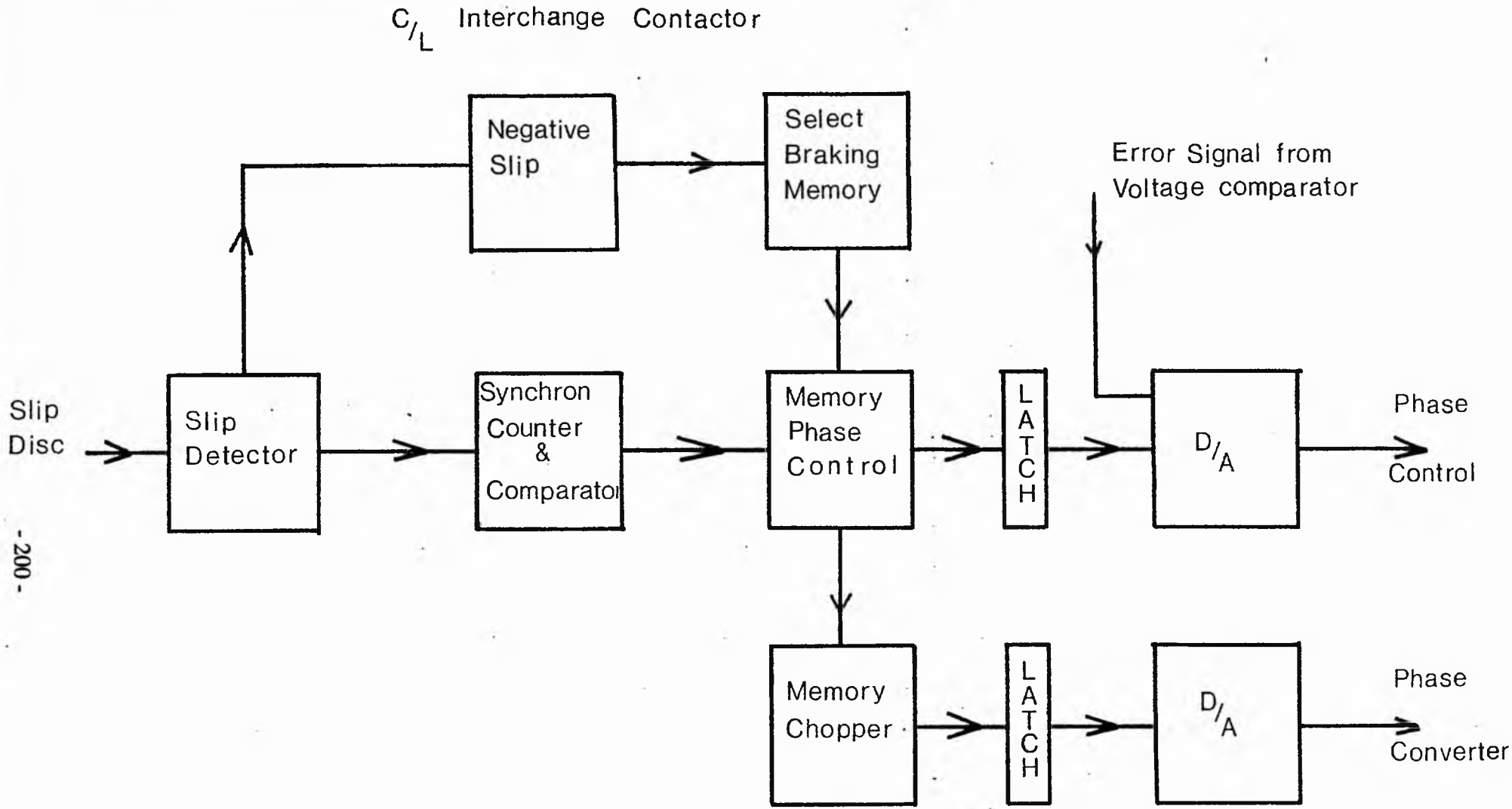

Fig. 4.57 Feedback control for the phase converter

A complete control system requires two extra facilities:

1) A braking loop to detect a negative-slip (regenerative) condition. If super-synchronous, negative-slip operation occurs, the C and L requirements of the phase-balancer are interchanged. This must be achieved by a changeover contactor initiated by the slip-detector.

2) Figs. 4.35. and 4.39. show that resonant imbalance of phase voltages occurs at small slip. Ideally a phase voltage comparator should feed the r.m.s. phase voltage differences as error signals to the D/A converter during the phase controller, then the analogue reference voltage can be adjusted to compensate and give a better phase voltage balance. This error comparator can enable the system to balance automatically when the motor paramaters are not known in detail. The order of power and required line voltage will always be necessary for system design.

4.12. Gate Turn-Off Thyristor (G.T.O.)

Further improvement is possible by replacing the high power Darlington transistor by the G.T.O. thyristor. Although the G.T.O. is not a new device, it is only recently with advances in ion implantation, neutron display, fine-line photolithography and process control, that its transfer from the laboratory to large-scale production has been made possible.

Referring back to section 4.9.2., where it was found that the Darlington transistor tends to respond slowly because the first transistor cannot turn off the second transistor quickly and that to turn on the transistor, a high base current of 1.3 A minimum is needed, whereas with the G.T.O., a faster switching off capability is possible together with a much lower turn-on-current by virtue of its construction. A typical example is the BTW58 G.T.O. which requires only about 100 mA. to switch on 5 A, while fast switch off ($< 0.5\mu S$) is achieved by applying a negative gate voltage of $> 5V$.

The use of smoothing capacitance can also be avoided when the G.T.O. is

used in the chopper circuit in direct a.c. switching. The four layer structure of the G.T.O. gives it several advantages over three layer devices, such as the transistor and Darlingtons. The most obvious of these is that a four layer device has an inherently higher standoff voltage. A second advantage is that for a four layer device, the latching action is provided by a built in gain. A more detailed look at the operation of a G.T.O. and typical G.T.O. is given in Appendix E.

CHAPTER 5

SYSTEM PERFORMANCE

Phase conversion systems from the single-capacitor system to the full electronic transient phase-balancing converter have been investigated. A study of the contrasting system performances reveals the following:-

Type of Converter Operating	% of Normal starting torque	% of Peak torque available	Negative sequence voltage at full speed full-load	Efficiency at full-load %
SINGLE CAPACITOR (Page 3)	100	55	30	55
SWITCHED CAPACITOR (2 values) (Page 10)	100	70	20	70
SWITCHED CAPACITOR (4 values) (Page 21)	100	75	15	75
SWITCHED INDUCTANCE AND CAPACITANCE (Page 34)	100	80	0	85
TRANSIENT PHASE CONVERSION (Page 96)	100	100	0	85

TABLE 5.1.

From Table 5.1. it can be seen that the single capacitor converter system (the most basic) is the least efficient, with efficiency at full load being 55%. The negative sequence voltage at full speed/full load is 30V and only 55% of the peak torque is available.

However, a switched capacitor converter with two values of capacitance gives a 15% increase in system efficiency, the efficiency at full-load being 70%, with a negative sequence voltage at full speed/full load reduced to 20V and peak torque available increased to 70%. A switched capacitor converter system with four values gives a 5% increase in efficiency and available peak torque and the negative sequence voltage reduced to 15V.

From references [3,5,6] it was deduced that increasing the number of capacitor values, will not produce a significant increase in efficiency or decrease in negative sequence. However, if an inductance is added, then a more appreciable increase in efficiency and decrease in negative sequence is obtained.

As can be seen from the performance results of a switched inductance/ capacitor converter, the efficiency at full load rises to 85%, with 80% of normal starting torque available and negative voltage at full load eliminated.

Ultimately, we arrive at the Transient phase converter, which gives a system efficiency at full load of 85% with 100% of normal torque available and no imbalance. The 15% losses are incurred in the motor. This result is mainly due to its ability to react quickly to a particular condition and to maintain phase balance by virtue of its design, which has been described in Chapter 4.

CHAPTER 6

CONCLUSION

Transient phase conversion gives excellent performance for a single motor drive, but it is difficult to provide stability for a motor running, when another one is started, whereas switched phase converters use the 'FERRARIS ARNO" effect to stabilise the running motor when another is started.

Transient phase conversion is ideal for air conditioning, refrigeration, etc., where continuous operation is required. Maximum efficiency with minimum imbalance is achieved.

Electrically switched 2-capacitor systems are ideal for frequent starting drives with limited full-speed operation in the duty cycle. A 5 to 10% reduction in full-load efficiency is not significant in this case [6].

Where the motor changes speed by switched pole-changing, the electronically switched capacitor system is the only system able to cope with the transient currents.

The electronically switched capacitor system is the ideal converter for multiple-motor load. Each machine running adds to the converter's effectiveness.

The addition of inductance enchances the switched converter system to increase the efficiency at full-load, and in some cases, to improve starting torque [3].

On a cost basis, the full-transient phase converter electronics and power costs £500 for a 15 kW drive compared with the £200 cost for the switched converter of comparable rating. Capacitor and inductor costs do not vary between systems. Hence, the full-transient converter becomes more attractive at higher power levels where maximum efficiency is important.

Programmable logic controlled (PLC) multiple capacitor switching can enhance performance and has advantages in a frequent start, multi-machine system.

6.1. Further Work

Improvements in fabrication of solid state devices has led to more reliable and cheaper devices of much better characteristics than before. This in turn has led to improvements in existing control methodology, e.g. inverter, PLC etc. Again as a result of improvements in technology, a new method devised at the Nottingham Polytechnic, called "Application Specific Integrated Circuits" (ASIC) for controlling power circuits. It is felt that this methodology, apart from making improvements and saving time in development (due to software simulation) is the way forward to implementing reliable automative power control systems [14]. (A copy of a paper describing the methodology can be seen in Appendix D.) If we consider the traditional design method, as shown in Fig. 6.1., in which the engineer begins with the idea then normally proceeds to the circuit design stage on paper. The designer would then continue through the prototype stage using any of the traditional construction methods. This prototype design would be tested and verified against specification. At this point if any conceptual fault is found then it would have to be rectified to the design stage and the process repeated. The design cycle can be reduced considerably by removing three parts of the design cycle before the design is verified. This technique is known as the simulation method, and allows a product to be produced for the market in a much shorter time than using traditional methods. The simulation method, shown in Fig. 6.2. allows the development of the design using the computer aided design (CAD) system whereby verification is carried out by simulating the circuit design using software models. At this point any design faults should be identified and rectified without going through the costly path of prototype construction for verification. The simulation method allows the design to be about 98% certain of working correctly first time. Ref. 14 shows this technique applied to a cycloconverter and can easily be adapted for the purpose of this project. Further development of present work indicates that the full system modelling is feasible and will include the simulation of electrical machines.

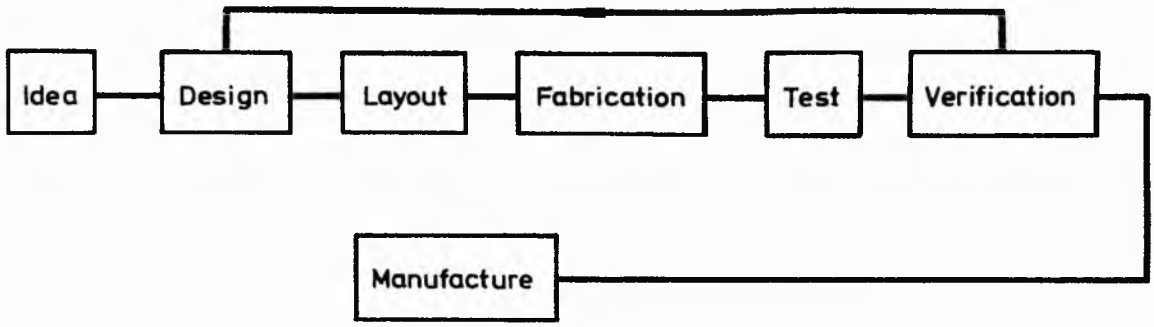

Fig. 6.1 Traditional Method

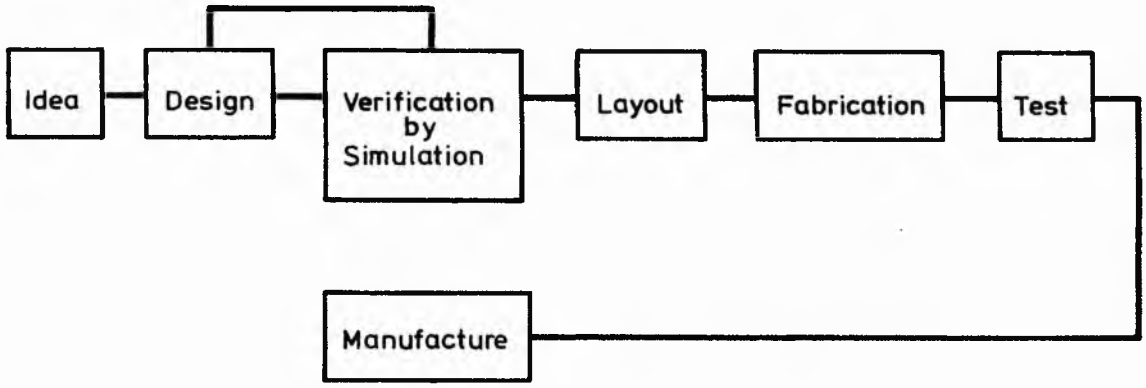

Fig. 6.2 Simulation Method

APPENDIX A

INDUCTION MOTOR EQUIVALENT CIRCUIT

A.1. Basic Theory Leading To Equivalent Circuit and Simplified Equivalent Circuit

Rotor Circuits

It has been shown in Appendix A that the induced rotor frequency per phase is sEbr. Since this voltage acts in the short-circuited rotor winding, it will set up currents that will only be limited by the rotor impedance. This impedance is made up of two components: (1) the rotor resistance Rs, and (2) the leakage reactance sXr, where Xr is rotor reactance at standstill. Since the reactance is a function of frequency, the leakage reactance is proportional to the slip. As a result, the rotor current becomes.

$$I_2 = \frac{sEbr}{\sqrt{Rr^2 + (sXr)^2}} \qquad \text{(eqn. A.1)}$$

If both numerator and denominator of equation A.1. are divided by the slip s, we obtain

$$I_2 = \frac{Ebr}{\sqrt{\left(\frac{Rr}{s}\right)^2 + (Xr)^2}} \qquad \text{(eqn. A.2)}$$

Although this implies a simple algebraic operation, its ramifications are significant. As equation A.2. indicates, the current I_2 can now be produced by a voltage Ebr of line frequency where as the current determined by equation A.2. is

$$R2/s = R + R2(1-s)/s$$

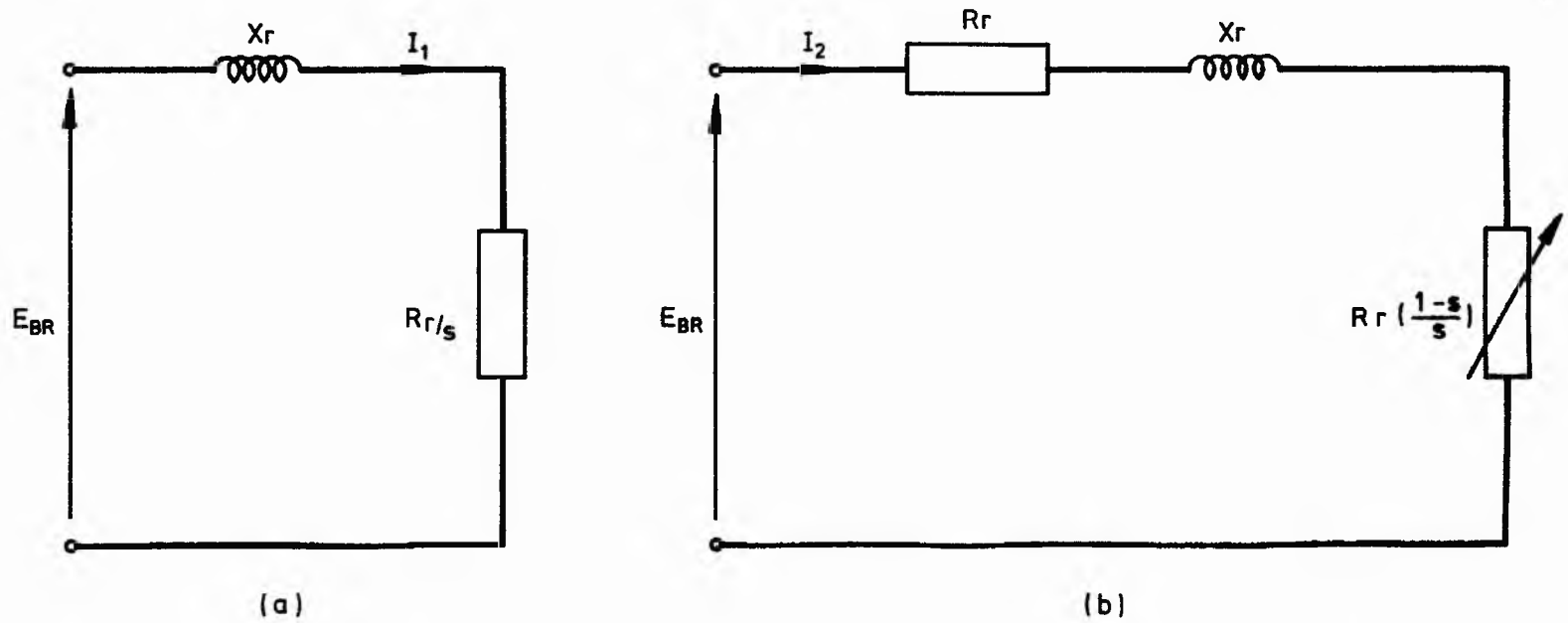

Fig. A.1 Rotor circuit diagram on a per phase basis. Resistive element representing rotor copper loss and rotor power developed: (a) combined; (b) separated

of slip frequency. In other words, the division by s has changed the point of reference from the rotor to the stator circuit. Translating equation A.2. into an equivalent circuit diagram it becomes that shown in Figure A.1.(a).

Since it is convenient to deal with the actual rotor resistance Rr/Rr, the term Rr/s is split into two components, namely

$$\frac{Rr}{s} = \frac{Rr}{s} + Rr - Rr = Rr + Rr\left(\frac{1}{s} - 1\right)$$

$$= Rr + Rr\frac{(1 - s)}{s} \qquad \text{(eqn. A.3)}$$

and the corresponding circuit diagram is that of Figure A.1.(b). If equation A.3. is now multiplied through 1_2^2 we obtain an equation representing power terms

$$I_2^2\frac{Rr}{s} = I_2^2 Rr + I_2^2 Rr\frac{(1 - s)}{s} \qquad \text{(eqn. A.4)}$$

The left-hand side of the equation represents the total power input to the rotor circuit, which is made up of two components:

(1) the power dissipated as copper loss in the rotor circuit I_2^2Rr, and

(2) the electric power that is converted into mechanical power, $I_2^2Rr\,(1 - s)/s$.

Thus on a per phase basis,

Rotor Power Input (RPI)

= Rotor Copper Loss (RCL) + Rotor Power Developed (RPD)

Where:

$$RPI = I_2^2\frac{Rr}{s} \qquad \text{(eqn. A.5)}$$

$$RCL = I_2^2 Rr = sRPI \qquad \text{(eqn. A.6)}$$

$$RPD = I_2^2 Rr\frac{(1 - s)}{s} = RPI\,(1 - s) \qquad \text{(eqn. A.7)}$$

It is interesting to note that the mechanical output power is represented in the electrical circuit by a resistance having a value Rr (1-s) / s. In general, the power developed by a motor is the product of its torque and the angular velocity of the rotor. Therefore,

$$P_d = \omega_r T$$

It follows, then, that the developed torque by the motor is

$$T_d = \frac{RPD}{\omega_r} \quad Nm$$

where $\omega_r = 2\pi\, n_r/60$ rad/seconds and n_r = rotor speed in revolutions per minute at which the power is developed. Later it will be seen that to obtain the output torque, the losses must be accounted for.

A.2. Complete Circuit Diagram

So far, the rotor circuit has been developed and it was shown that the power transformed across the air gap represents the rotor copper losses and the mechanical power developed by the motor. To complete the equivalent circuit diagram, the stator circuit must be included. The circuit may be drawn as shown in Figure A.2.

To develop this circuit further, the rotor quantities need to be expressed as referred to the stator. For this purpose, the transformation ratio must be known.

The voltage transformation ratio in the induction motor must include the effect of the stator and rotor winding distributions. It can be shown that, for a cage-type rotor, the rotor resistance per phase, Rr' referred to the stator, is

$$Rr' = a^2 Rr \qquad \text{where } a^2 \equiv \frac{m_1}{m_2}\frac{kw_1\, N_1}{kw_2\, N_2} \qquad \text{(eqn. A.8)}$$

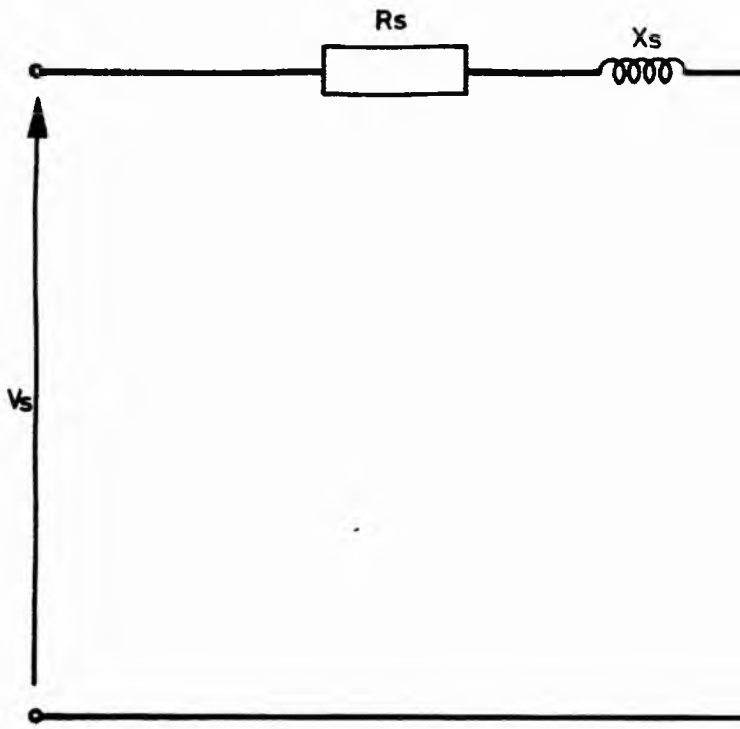
Rs
Xs
Vs

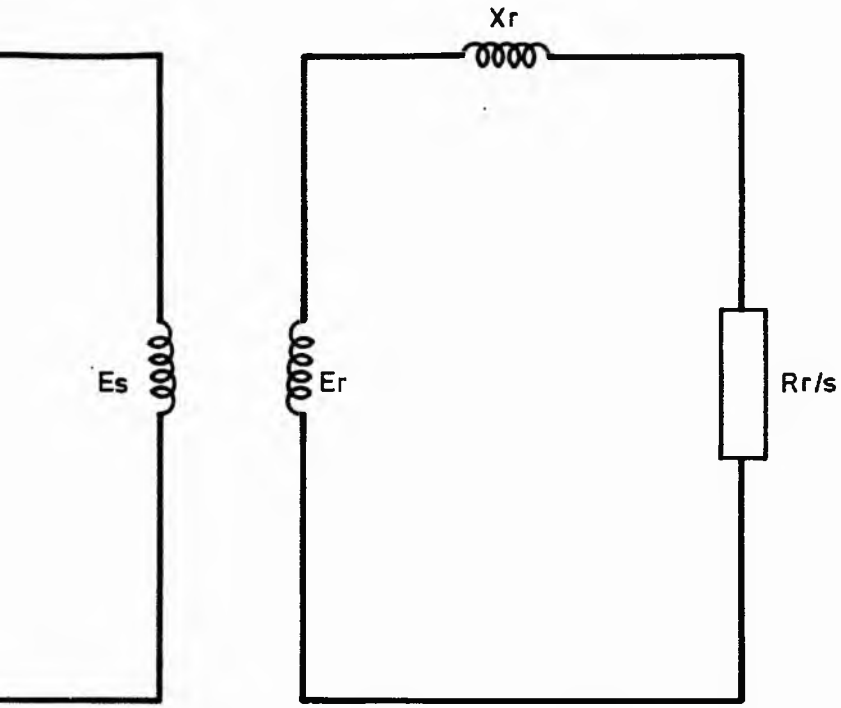

Fig. A·2

Here,

kw_1 ≡ winding factor of the stator having N_1 series-connected turns per phase

kw_2 ≡ winding factor of the rotor having $N_2 = p/4$ series-connected turns per phase, for a cage rotor, where p is the number of poles

m_1 ≡ number of phases on the stator

M_2 ≡ number of bars per poles pair

Rr ≡ resistances of one bar

Similarly, $Xr' = a^2Xr$

where Xr' is the rotor leakage, reactance per phase, referred to the stator.

The rotor quantities are now referred to the stator to obtain from Figure A.2. the exact equivalent circuit (per phase) shown in Figure A.3.(a). For reasons as been explained earlier, Rr'/s is split as

$$\frac{Rr'}{s} = Rr' + Rr' \frac{(1 - s)}{s}$$

to obtain the circuit shown in Figure A.3.(b). Here, Rr' is simply the per phase standstill rotor resistance referred to the stator and Rr'(1-s)/s is a per phase dynamic resistance that depends on the rotor speed and corresponds to the load on the motor. Notice that all the parameters shown in Figure A.3. are standstill values.

To simplify the circuit, it is assumed that

$|Rm + j\,Xm| >> |Rs + j\,Xr|$

thus current Im << Is

Hence, the parallel 'no-load' impedance branch can be moved toward the supply terminals. The simplified equivalent circuit of the induction motor is approximated by the one shown in Figure A.4.

A.3. Error in any Simplified Equivalent Circuit

From the equivalent circuit diagram it can now be appreciated why induction motors at light load operate under such poor power factors. At light loads (small slip values), the resistor representing the mechanical power Rr' (1-s) / s is large. This means that I'_2 is relatively small compared to the magnetizing current Im. Therefore, the circuit behaves largely inductive since Xm is the dominating element in the equivalent circuit. Therefore, the circuit behaves almost purely inductively and the power factor is small. With increased loading, the resistance Rr'(1-s)/s decreases quickly since the slip s increases.

Therefore, it rapidly becomes the dominating element in its branch, with a corresponding large improvement in the overall circuit power factor with increasing loads.

The load current in Figure A.4. in stator terms is:

$$I'_2 = \frac{V_S}{\left(Rs + \frac{Rr'}{s}\right) + j(Xs + Xr')} \qquad \text{(eqn. A.9)}$$

which enables calculation of RPI, RCL, and RPD according to equations A.5 to A.7.

The magnetizing current Im is

$Im = V_S/jXm$

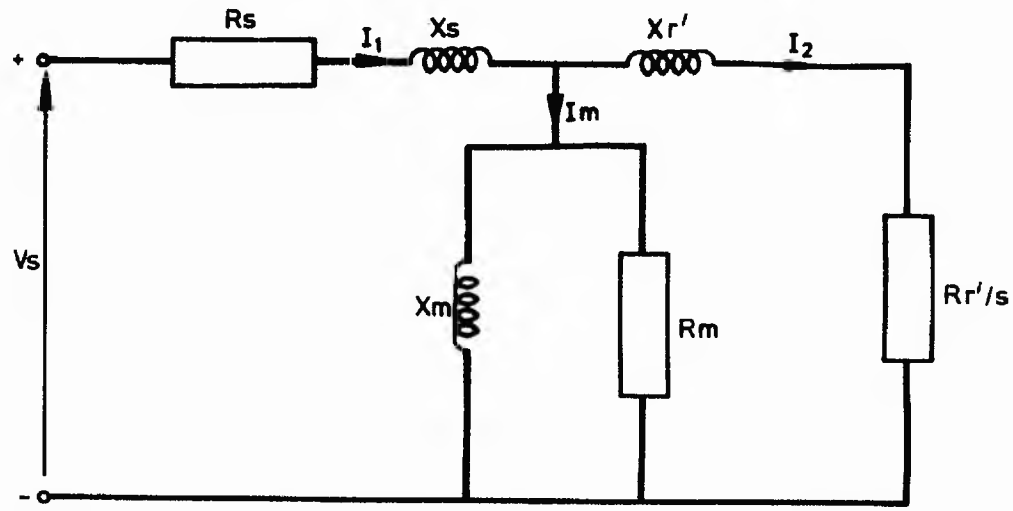

(a)

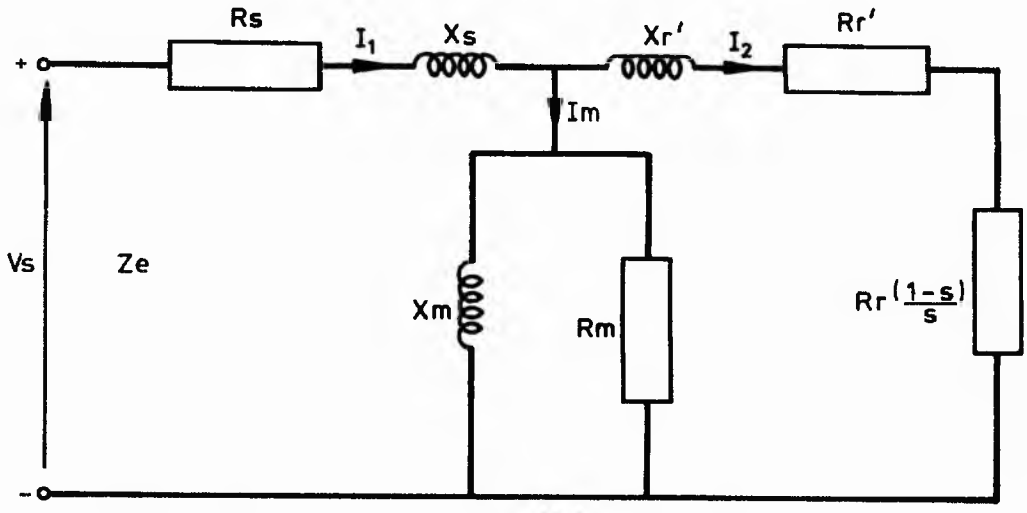

(b)

Fig. A·3

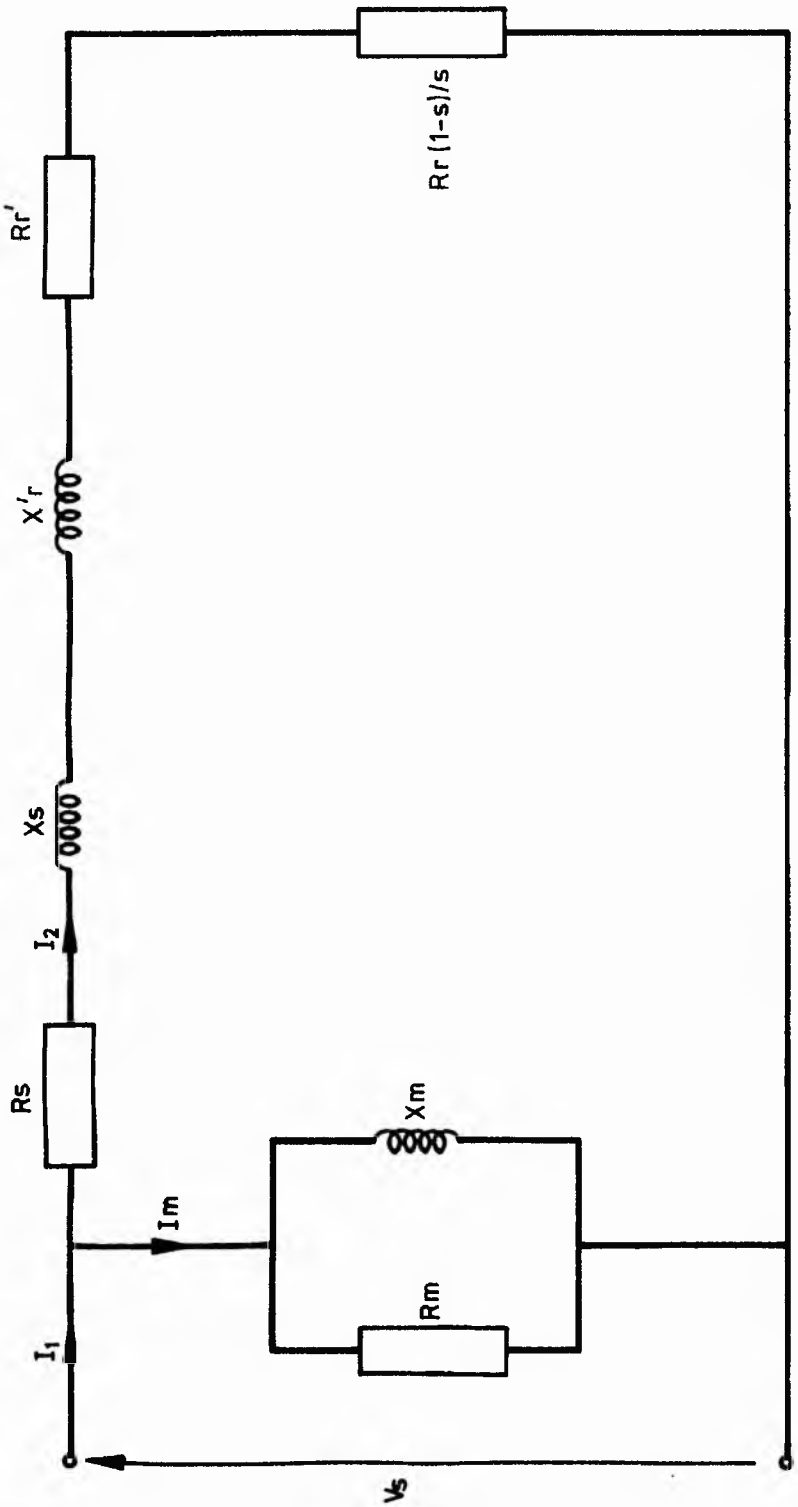

Fig. A-4 Equivalent circuit diagram for the induction motor on a per phase basis referred to the stator

and therefore the motor line current

$$\bar{I}_1 = \bar{I}m + \bar{I}'_2 \qquad \text{(eqn. A.11)}$$

where the current must be added vectorially.

Since the magnetizing branch is moved to the input terminals, the stator quantities appear as part of the rotor circuit. This would result in negligible error if V = E in Figure A.5.

In practical work, this simplification in the normal operating range of the motor leads to insignificant errors and is therefore adopted as explained. However, for efficiency calculations, the copper stator loss will be calculated as follows:

$$P_{cu\ stator} = 3\ Is^2Rs \qquad \text{(eqn. A.12)}$$

since the stator winding also carries the magnetization current, which, as was mentioned, is significant in terms of rated current. Furthermore, the output or shaft torque is

$$T = \frac{RPD - \text{mechanical losses}}{\omega_r}$$

where the mechanical losses include friction, windage, and core losses. The mechanical loss is obtained from a no-load test.

A.4. Determining Circuit Model Impedances

The equivalent circuit of an induction motor is a very useful tool for determining the motor's response to changes in load. However, if a model is to be used for a real machine, it is necessary to determine what the element values are that go into the model. How can Rs, Rr, Xs and Xr be determined for a real motor?

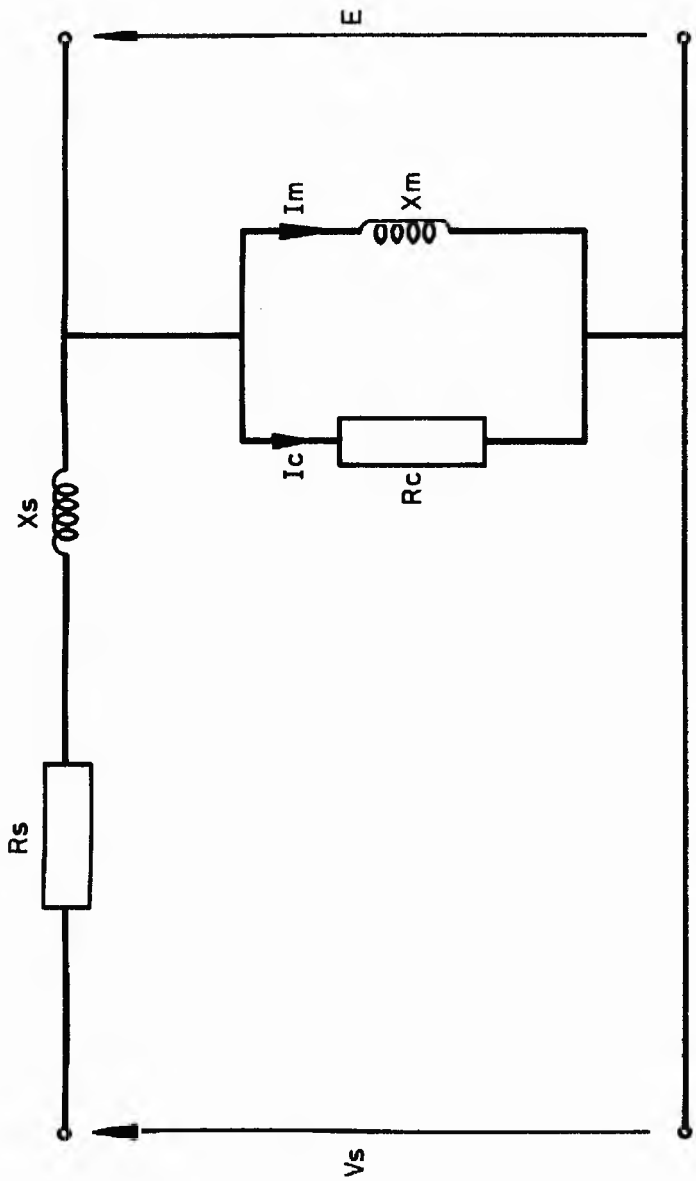

Fig. A·5 Stator equivalent circuit diagram of induction motor per phase

These pieces of information may be found by performing a series of tests on the induction motor as described by S. Chapman [15]. The tests must be performed under precisely controlled conditions, since the resistances vary with temperature and the rotor resistance also varies with rotor frequency.

A.4.1. The No-Load Test

The no-load test of an induction motor measures the rotational losses of the motor and also provides information about its magnetizing current. The test circuit for this test is shown in Figure A.6.(a). Wattmeters, a voltmeter, and three ammeters are connected to an induction motor, which is allowed to spin freely. The only load on the motor is the friction and windage losses, so all of power converted, Pconv, in this motor is consumed by mechanical losses, and the slip of the motor is very small (possibly as small as 0.001 or less). The equivalent circuit of this motor is shown in Figure A.6.(b). With its very small slip, the resistance corresponding to its power converted, Rr(1-s)/s, is very much larger than the resistance corresponding to the rotor copper losses Rr, and much larger than the rotor reactance Xr. In this case, the equivalent circuit reduces approximately to Figure A.6.(c). There, the output resistor is in parallel with the magnetizing reactance Xm. The current needed to establish a magnetic field is quite large in an induction motor, because of the high reluctance of its airgap, so the reactance Xm will be much smaller that the resistances in parallel with it, and the overall input power factor will be very small. With the large lagging current, most of the voltage drop will be across the inductive components in the circuit. The equivalent input impedance is thus approximately

$$Z_{eq} = \frac{V_S}{I_1, n_1} \approx Xs + Xm$$

and if Xs can be found in some other fashion, the magnetizing impedance, Xm, will be known for the motor.

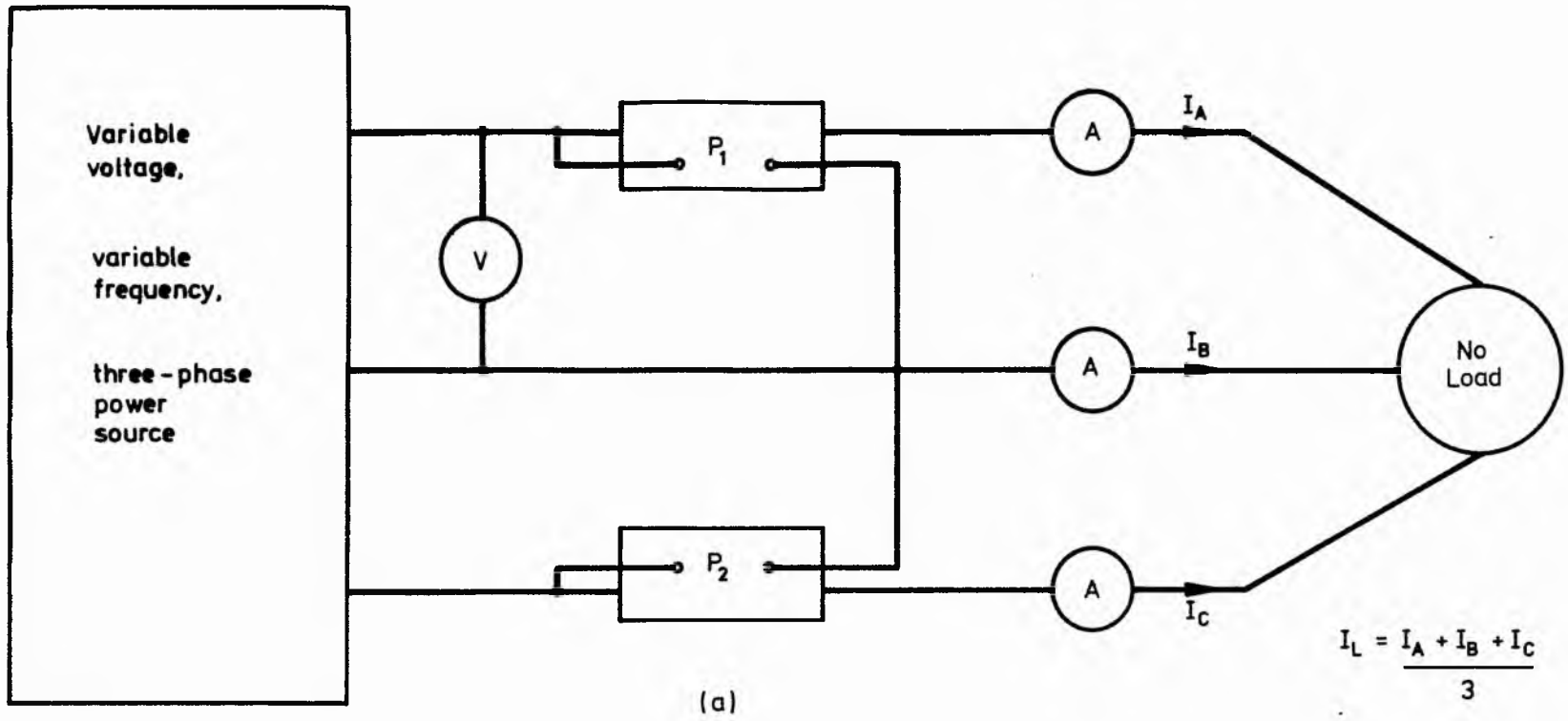

Fig. A·6 The no-load test of an induction motor test circuit

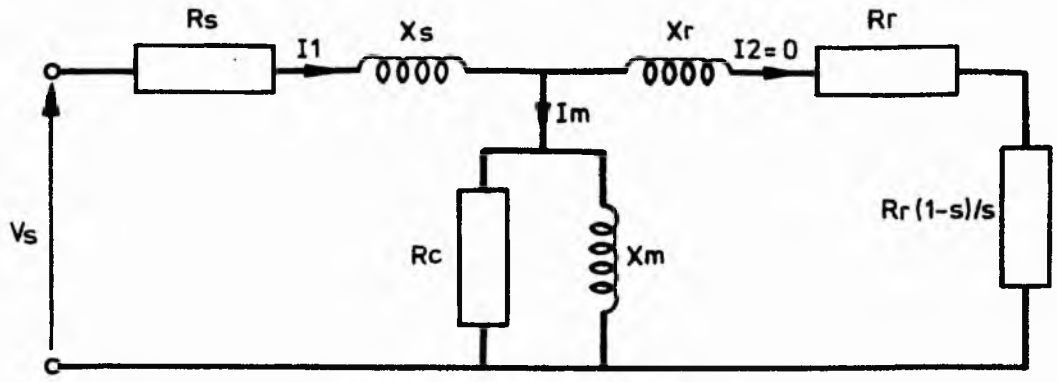

Initial equivalent circuit

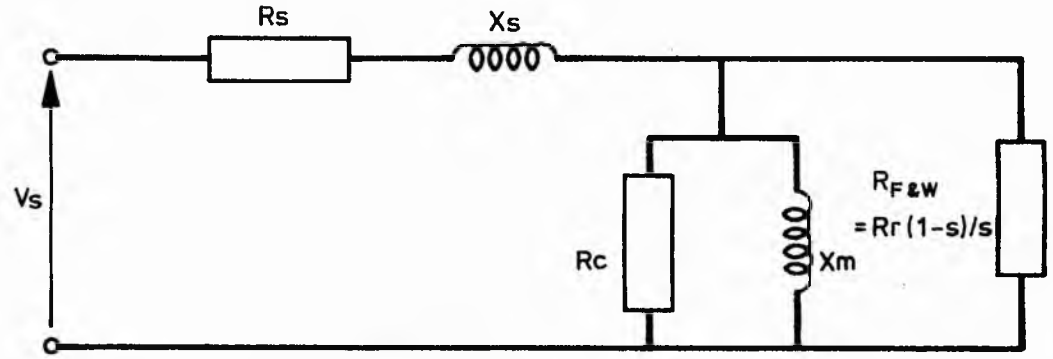

Since $Rr(1-s)/s \gg Rr$ and $Rr(1-s)/s \gg Xr$ then the above circuit reduces to this circuit

Fig. A.6b

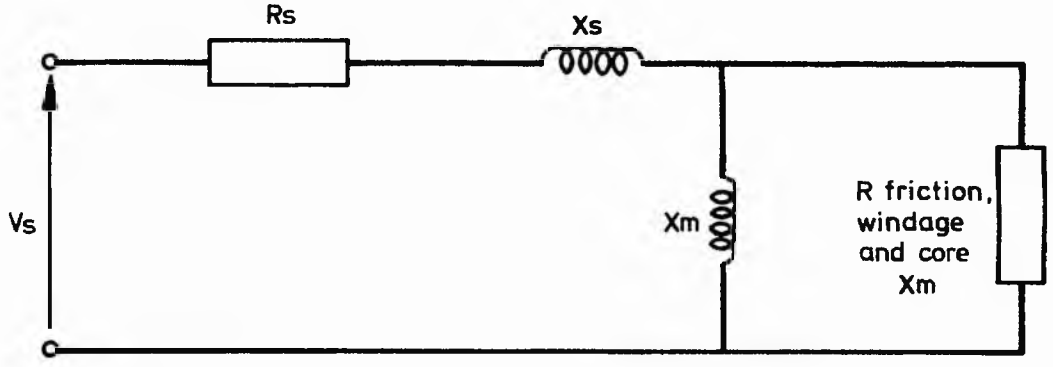

Combining $R_{F\&W}$ and R_C yields this circuit

Fig. A.6c

A.4.2. The dc Test for Stator Resistance

The rotor resistance Rs plays an extremely critical role in the operation of an induction motor. Among other things, Rr determines the shape of the torque-speed curve, determining the speed at which the pullout torque occurs. There is a standard test called the locked-rotor test which can be used to determine the total motor circuit resistance.

However, this test only finds the total resistance resistance. in order to find the rotor resistance Rr accurately, it is necessary to Rs, to that it can be subtracted from the total.

There is a test for Rs independent of Rr, Xs and Xr. This test is called the dc test. Basically, a dc voltage is applied to the stator windings of an induction motor. Because the current is dc, there is no induced voltage in the rotor circuit, and no resulting rotor current flow. Also, the reactance of the motor is zero at direct current. Therefore, the only quantity limiting current flow in the motor is the stator resistance and that resistance can be determined.

The basic circuit for the dc test is shown in Figure A.7. The current in the circuit flows through two of the windings, so the total resistance in the current patch is 2Rs.

$$\text{Therefore, } 2Rs = \frac{V_{dc}}{I_{dc}}$$

$$\text{or} \qquad Rs = \frac{V_{dc}}{2\, I_{dc}}$$

With this value of Rs, the stator copper losses at no-load may be determined, and the rotational losses may be found as the difference between the input power at no-load and the stator copper losses.

The value of Rs calculated in this fashion is not completely accurate, since it neglects the skin effect that occurs when an ac voltage is applied to the windings.

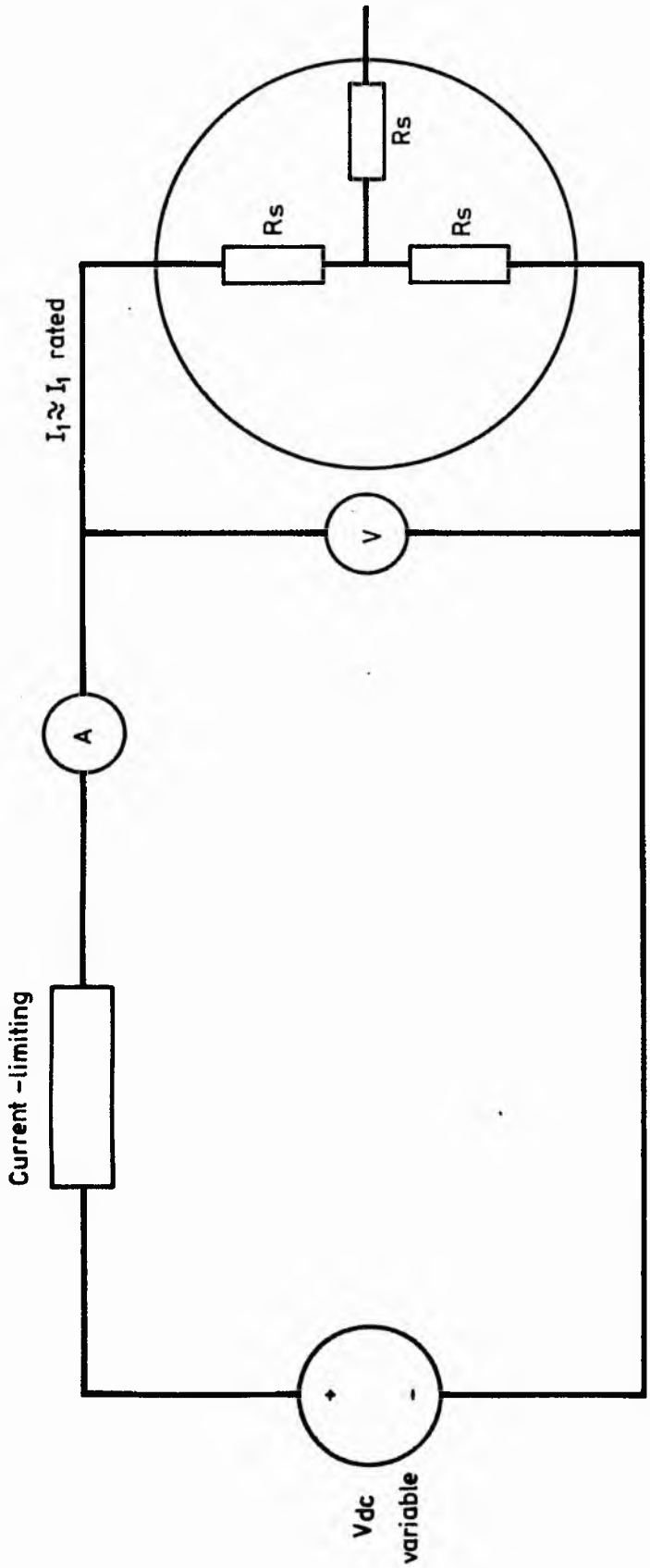

Fig. A.7 Test circuit for a dc resistance test

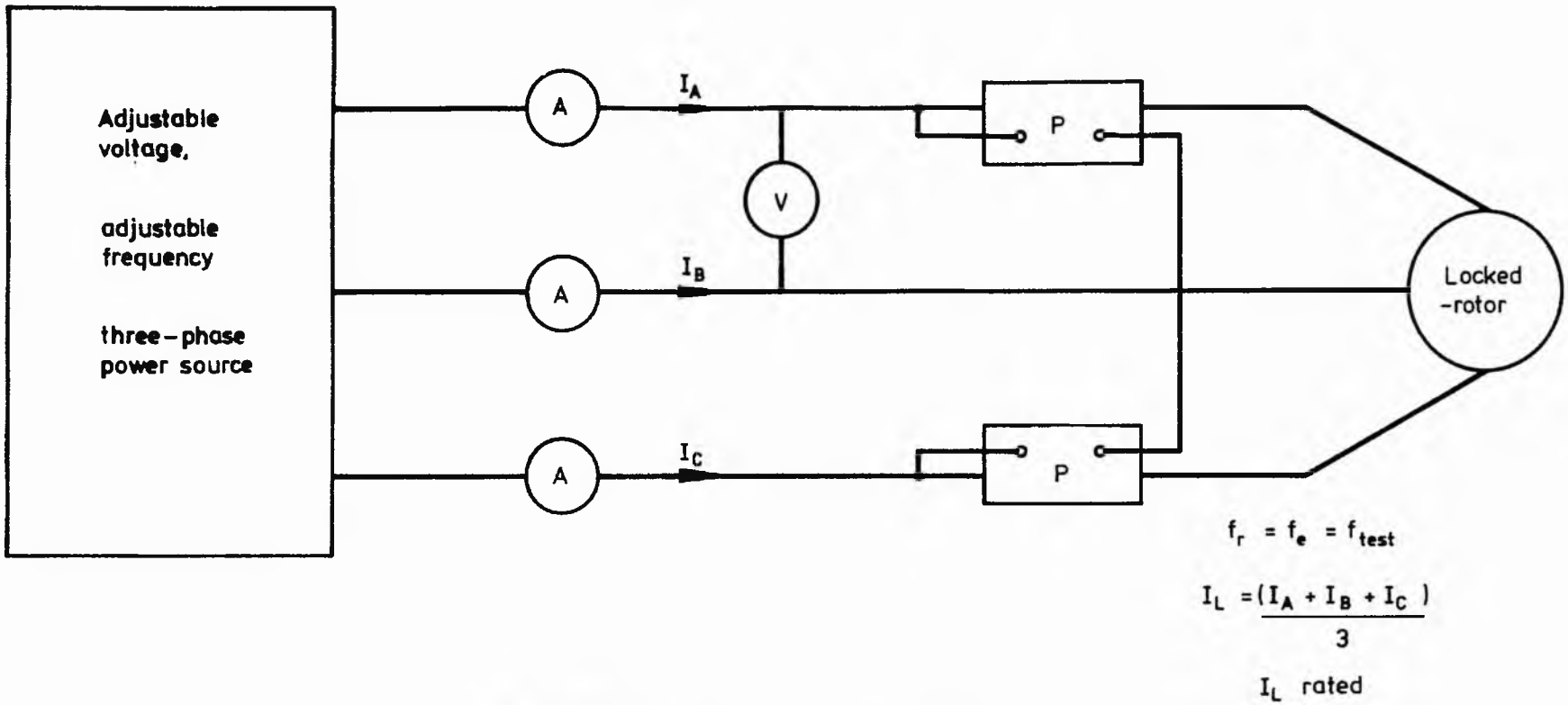

Fig. A·8a The locked-rotor test for an induction motor test circuit

A.4.3. The Locked-Rotor Test

The third test that can be performed on an induction motor to deterime its circuit parameters is called the locked-rotor test, or sometimes the blocked-rotor test.

Figure A.8.(a) shows the connections for the locked-rotor test. As the name implies, the test is performed with the rotor blocked such that the rotor is prevented from turning. Since it cannot turn, $n_r = 0$ and the slip, $s = 1.\theta$ or 100%. This corresponds to the condition at startup and the currents are expected to be five to six times their rated value. It is for this reason that the applied stator voltage is reduced to such a voltage permitting rated stator current to flow. Furthermore, at this greatly reduced input voltage of about 10 to 205 of rated value the air-gap flux is relatively small, implying that Xm is much larger than normal. Therefore, the circuit under these conditions looks like a series combination of Xs, Rs, Xr and Rr, with the magnetizing reactance neglected. The circuit with R'r/s = R'r reduces to that of Figure A.8.(b).

After a test voltage and frequency have been set up, the current flow in the motor is quickly adjusted to about the rated value, and input power, voltage, and current are measure before the rotor can heat up too much. The input power to the motor can be described by the equation:

$$P_{in} = \sqrt{3}\, V_T I_L \cos\theta$$

so the locked-rotor power can be found as:

$$PF = \cos\theta = \frac{P_{in}}{\sqrt{3}\, V_T I_L}$$

and the impedance angle θ is just equal to $\cos^{-1}$ PF.

The magnitude of the total impedance in the motor circuit at this time is:

$$Z_{LR} = \frac{V_1}{I_1} = \frac{V_T}{\sqrt{3}\, I_L}$$

and the angle of the total impedance is θ. Therefore,

$$Z_{LR} = R_{LR} + j\, X'_{LR}$$
$$= |Z_{LR}| \cos\theta + j\, |Z_{LR}| \sin\theta$$

The locked-rotor resistance PLR is equal to

$R_{LR} = Rs + Rr$

while the locked-rotor reactance X'_{LR} is equal to

$X'_{LR} = X's + X'r$

where X's and X'r are the stator and rotor reactances at the test frequency, respectively.

The rotor resistance Rr can now be found as

$Rr = R_{LR} - Rs$

where Rs was determined in the dc test, the total rotor reactance referred to the stator can also be found. Since the reactance is directly proportional to the frequency, the total equivalent reactance at the normal operation frequency can be found as

$$X_{LR} = \frac{f_{rated}}{f_{test}} X'_{LR} = Xs + Xr$$

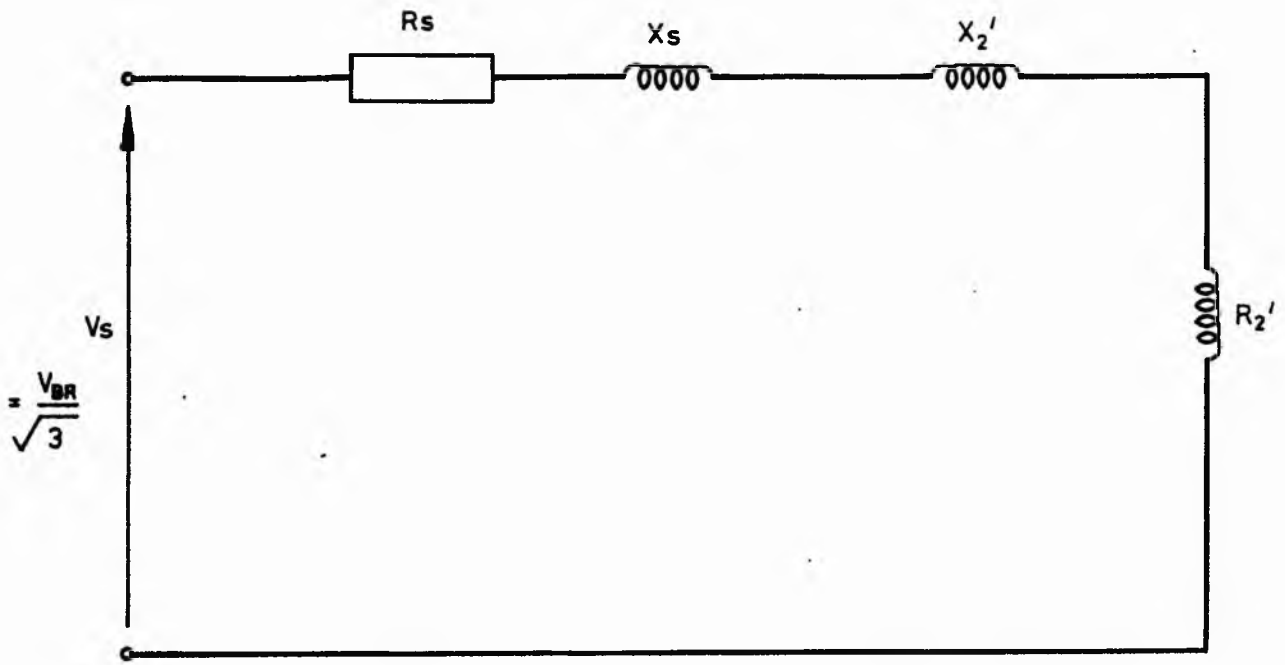

Fig. A-8b The locked-rotor test of an induction motor equivalent circuit

A.4.4. Example of Induction Motor Parameter Determination

The following test data were taken on a 7.5 hp four-pole 208 V 60 Hz star-connected induction motor having a rated current of 28 A.

dc test:

$V_{DC} = 13.6$ V $\qquad I_{DC} = 28.0$ A

no-load test:

$V_T = 208$ V $\qquad f = 60$ Hz

$I_A = 8.12$ A $\qquad P_{in} = 420$ W

$I_B = 8.20$A $\qquad I_C = 8.28$ A

locked-rotor test:

$V_T = 25$ V $\qquad f_{test} = 15$ Hz

$I_A = 28.1$ A $\qquad P_{in} = 920$ W

$I_B = 28.0$ A $\qquad I_C = 27.6$ A

Sketch the per-phase for this motor.

Solution:

From the dc test, $= \dfrac{V_{dc}}{I_{dc}} = \dfrac{13.6\text{ V}}{2(28.0\text{ A})} = 0.243$

From the no-load test, $I_{L,av} = \dfrac{(8.12 + 8.20 + 8.18)}{3}$ A

$= 8.17$ A

$V_1, n_1 = \dfrac{208\text{ V}}{\sqrt{3}} = 120$ V

Therefore, $|Z_{n1}| = \dfrac{120\text{ V}}{8.17\text{ A}} = 14.7 = Xs + Xm$

When Xs is known, Xm can be found. The stator copper losses are

$$P_{SCL} = 3\ I_1^2 Rs = 3\ (8.17\ A)\ (0.243) = 48.7\ W$$

Therefore, the no-load rotational losses are

$$P_{ROT} = P_{in,\ n_1} - P_{SCL,\ n_1}$$
$$= 420\ W - 48.7\ W = 371.3\ W$$

From the locked-rotor test,

$$I_L = \frac{(28.1 + 28.0 + 27.6)}{3}\ A = 27.9A$$

The locked rotor impedance is

$$|Z_{LR}| = \frac{V_1}{I_A} = \frac{V_T}{\sqrt{I_L}} = \frac{25\ V}{\sqrt{3}\ (27.9\ A)} = 0.517$$

and the impedance angle θ is

$$\theta = \cos^{-1} \frac{(P_{in})}{\sqrt{3}\ V_T\ I_L}$$

$$= \cos^{-1} \frac{(920\ W)}{\sqrt{3}\ (25\ V)\ (27.9\ A)}$$

$$= \cos^{-1} 0.762 = 40.4°$$

Therefore, $R_{LR} = 0.517 \cos 40.4° = 0.394 = R1 + R2$. Since Rs = 0.243, Rr must be 0.151 . The reactance at 15 Hz is

$$X'_{LR} = 0.517 \sin 40.4° = 0.335$$

The equivalent reactance at 60 Hz is

$$X_{LR} = \frac{(60\ Hz)}{15\ Hz}\ (0.335) = 1.34$$

This reactance is assumed to be divided equally between the rotor and the stator, so Xs = Xr = 0.67 and Xm = 14.03 . The final per-phase equivalent circuit is shown in Figure A.9.

Rs
= 0·243

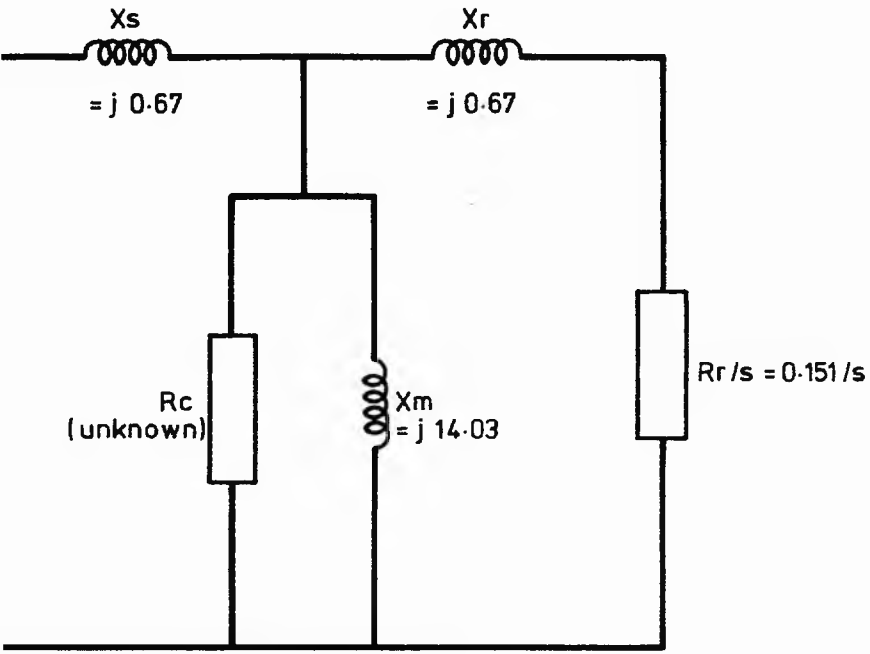

Fig. A·9 Motor per phase circuit

APPENDIX B

COMPUTER PROGRAM

A program to determine the value of system capacitance, phase converter capacitance and inductance has been written in BASIC computer language. The program has been developed into a user friendly package, operatable on the MS-DOS system.

This package runs on the A: drive of the MS-DOS system, by simply typing in "CAPCALC". Once the program is loaded, requests for data results of the NO-LOAD best, LOCKED ROTOR test and D.C. test for stator resistance are made.

The program then calculates the value of all the equivalent circuit parameters, together with power factor and efficiency.

It then draws an equivalent circuit and gives the user options to view data and graphs of system capacitance, phase converter capacitance and inductance against slip in the range 0.001 to 1. An extra facility is provided to expand the graph in the small slip ranges.

In each case, once it has plotted the graph, the program goes back to the main menu, which displays the other options. By means of an example, listing of what the user sees on the VDU screen are given, after this section.

Also, the main computer programme listing, together with the floppy disc is given.

C A P C A L C

Written by M.Latif

Department of Electrical and Electronic Engineering

Nottingham Polytechnic 1990

PRESS RETURN TO CONTINUE

Are the Motor conections STAR or DELTA (S/D) s

Enter the No Load Test Data as indicated:-

Vl	Stator Volts	415
Il	Stator Amps	1.25
P1 Two Meter Method	Watts	-400
P2 Two Meter Method	Watts	-120
Speed	Rev/min	2990
Torque	Nm	1
Resistance r1	Ohms	2.5

Is this the correct Data (Y/N)

Enter the locked rotor Test Data as indicated:-

Vb Locked Rotor	Volts	73
Ib Locked Rotor	Amps	3.85
P1b Two Meter Method	Watts	-240
P2b Two Meter Method	Watts	-9.5
Frequency of the supply	Hertz	50
No of Poles		2

Is this the correct Data (Y/N)

Slip s	=	0.33 %
X1	=	3.76
X2	=	5.64
Xm	=	152.56
Rm	=	108.43
r2	=	3.11
Stator current I1	=	0.82 amps
output power	=	177.26 watts
Efficiency	=	34.09 %
Power factor	=	0.73

Press the SPACE BAR to continue

Equivalent circuit for one phase

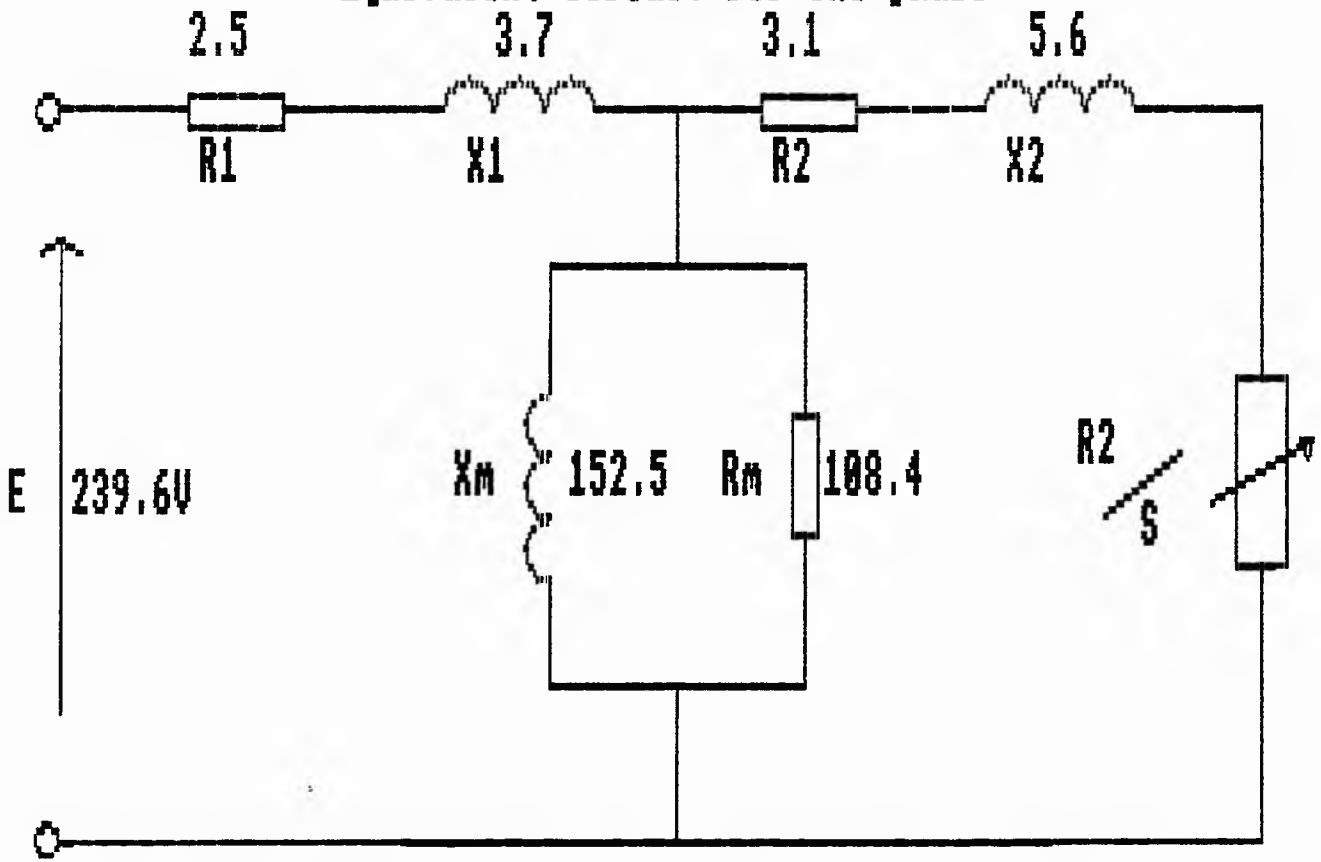

Press the SPACE BAR to Continue

M A I N M E N U

Select operation Required
Expand graph for a Slip of 0.1.....1
Converter Cap.....2
Converter Ind.....3
Re-run this program (with SAME input Data)...4
Re-run Capcalc (with NEW Data).....5
EXIT and return to DOS.....6

Operation Required (1 to 6)

SLIP	CAPACITANCE UF
0.0005	59.1820
0.0010	60.4567
0.0015	61.7478
0.0020	63.0548
0.0025	64.3774
0.0030	65.7152
0.0035	67.0678
0.0040	68.4349
0.0045	69.8160
0.0050	71.2108
0.0055	72.6189
0.0060	74.0398
0.0065	75.4733
0.0070	76.9189
0.0075	78.3762
0.0080	79.8448
0.0085	81.3244
0.0090	82.8144
0.0095	84.3146

Press the SPACE BAR to continue

SLIP	CAPACITANCE UF
0.0100	85.8245
0.0150	101.3715
0.0200	117.4644
0.0250	133.7454
0.0300	149.9025
0.0350	165.6785
0.0400	180.8731
0.0450	195.3413
0.0500	208.9868
0.0550	221.7551
0.0600	233.6252
0.0650	244.6020
0.0700	254.7098
0.0750	263.9858
0.0800	272.4758
0.0850	280.2309
0.0900	287.3037
0.0950	293.7474

Press the SPACE BAR to continue

SLIP	CAPACITANCE UF
0.1000	299.6137
0.1500	335.8675
0.2000	350.3998
0.2500	356.4870
0.3000	359.0253
0.3500	359.9585
0.4000	360.1281
0.4500	359.9257
0.5000	359.5444
0.5500	359.0831
0.6000	358.5939
0.6500	358.1043
0.7000	357.6289
0.7500	357.1749
0.8000	356.7453
0.8500	356.3412
0.9000	355.9621
0.9500	355.6069
1.0000	355.2744

Press the SPACE BAR to continue

SLIP
0
0,1
0,2
0,3
0,4
0,5
0,6
0,7
0,8
0,9
1
0
40
80
120
160
200
240
280
320
360
400

SLIP	CAPACITANCE UF
0.0025	64.3774
0.0050	71.2108
0.0075	78.3762
0.0100	85.8245
0.0125	93.5060
0.0150	101.3715
0.0175	109.3730
0.0200	117.4644
0.0225	125.6021
0.0250	133.7454
0.0275	141.8569
0.0300	149.9025
0.0325	157.8520
0.0350	165.6785
0.0375	173.3588
0.0400	180.8731
0.0425	188.2051
0.0450	195.3413
0.0475	202.2712

Press the SPACE BAR to continue

SLIP	CAPACITANCE UF
0.0500	208.9868
0.0525	215.4826
0.0550	221.7551
0.0575	227.8026
0.0600	233.6252
0.0625	239.2241
0.0650	244.6020
0.0675	249.7625
0.0700	254.7098
0.0725	259.4490
0.0750	263.9858
0.0775	268.3259
0.0800	272.4758
0.0825	276.4420
0.0850	280.2309
0.0875	283.8492
0.0900	287.3037
0.0925	290.6009
0.0950	293.7474
0.0975	296.7496
0.1000	299.6137

Press the SPACE BAR to continue

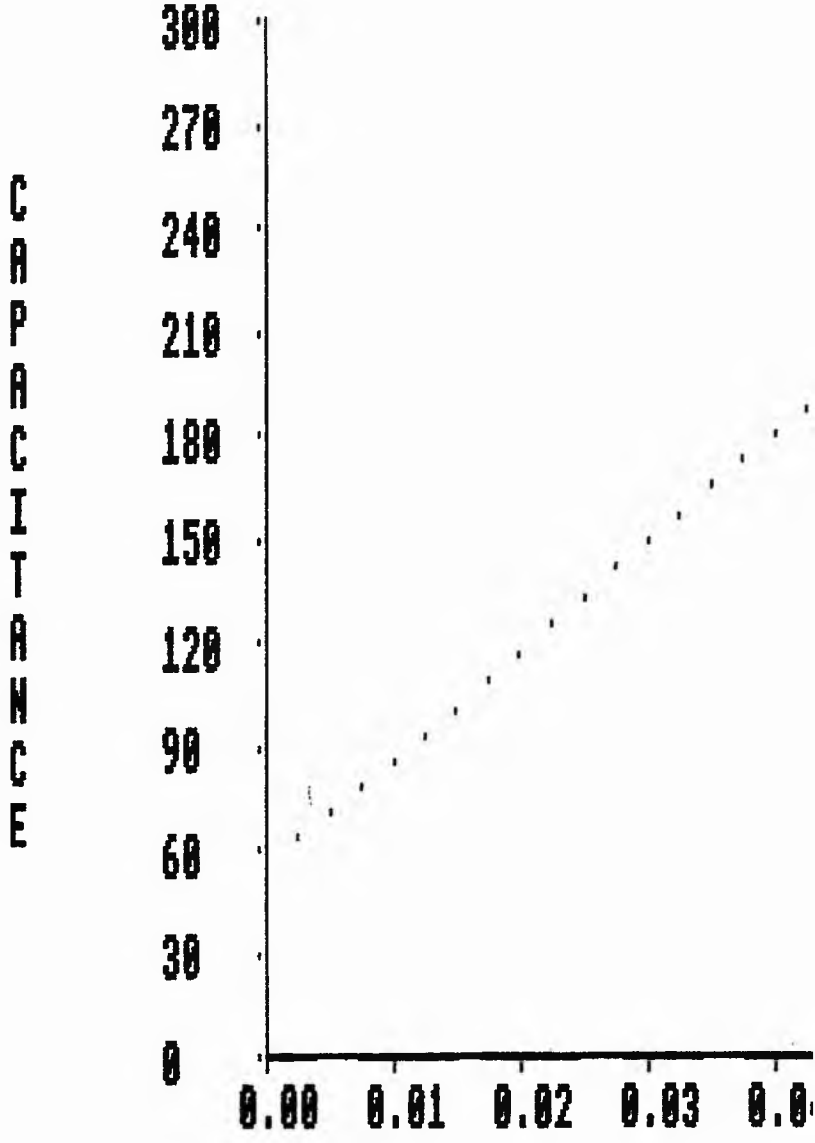
CAPACITANCE
300
270
240
210
180
150
120
90
60
30
0
0.00
0.01
0.02
0.03

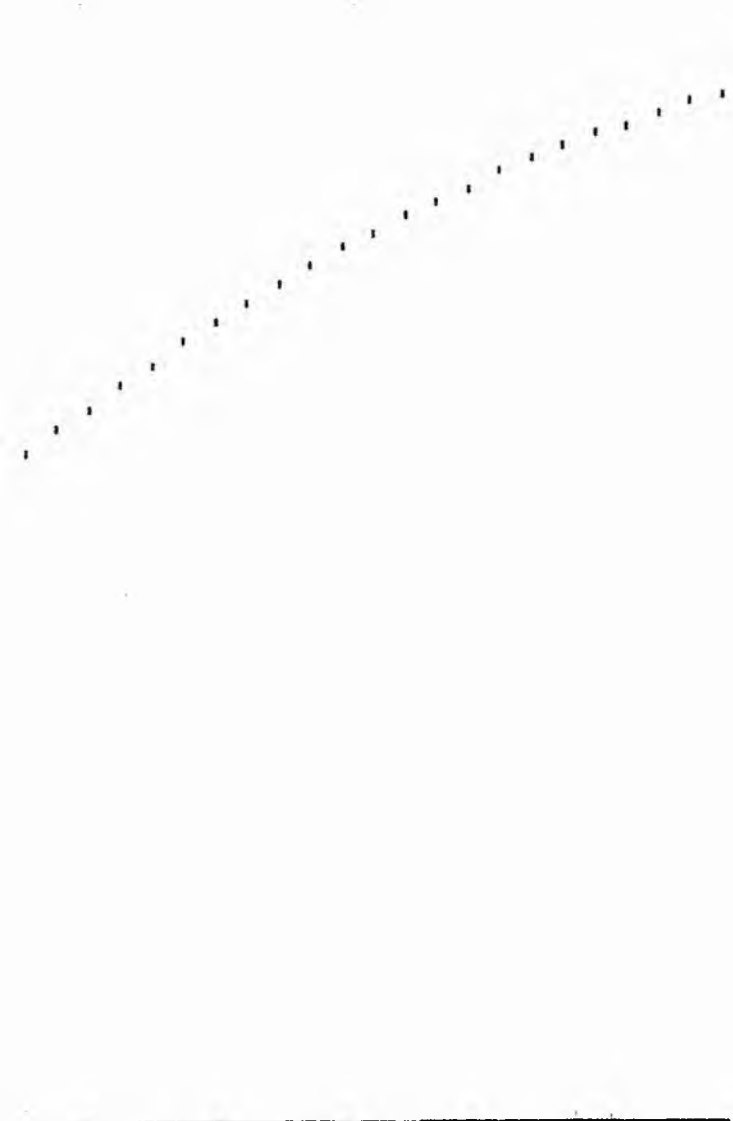
4 0.05 0.06 0.07 0.08 0.09 0.10
S L I P

CONVERTER

INDUCTANCE

Press the SPACE BAR to continue

SLIP	CONVERTER INDUCTANCE (Henries)
0.0005	11.4489
0.0010	5.7318
0.0015	3.8261
0.0020	2.8733
0.0025	2.3016
0.0030	1.9205
0.0035	1.6483
0.0040	1.4441
0.0045	1.2854
0.0050	1.1583
0.0055	1.0544
0.0060	0.9678
0.0065	0.8946
0.0070	0.8318
0.0075	0.7774
0.0080	0.7298
0.0085	0.6878
0.0090	0.6504
0.0095	0.6170

Press the SPACE BAR to continue

SLIP	CONVERTER INDUCTANCE (Henries)
0.0100	0.5870
0.0150	0.3968
0.0200	0.3018
0.0250	0.2450
0.0300	0.2073
0.0350	0.1804
0.0400	0.1604
0.0450	0.1449
0.0500	0.1326
0.0550	0.1226
0.0600	0.1143
0.0650	0.1073
0.0700	0.1015
0.0750	0.0964
0.0800	0.0921
0.0850	0.0883
0.0900	0.0849
0.0950	0.0820

Press the SPACE BAR to continue

SLIP	CONVERTER INDUCTANCE (Henries)
0.1000	0.0794
0.1500	0.0648
0.2000	0.0603
0.2500	0.0602
0.3000	0.0627
0.3500	0.0672
0.4000	0.0735
0.4500	0.0816
0.5000	0.0917
0.5500	0.1043
0.6000	0.1200
0.6500	0.1399
0.7000	0.1655
0.7500	0.1996
0.8000	0.2469
0.8500	0.3168
0.9000	0.4300
0.9500	0.6439
1.0000	1.1994

Press the SPACE BAR to continue

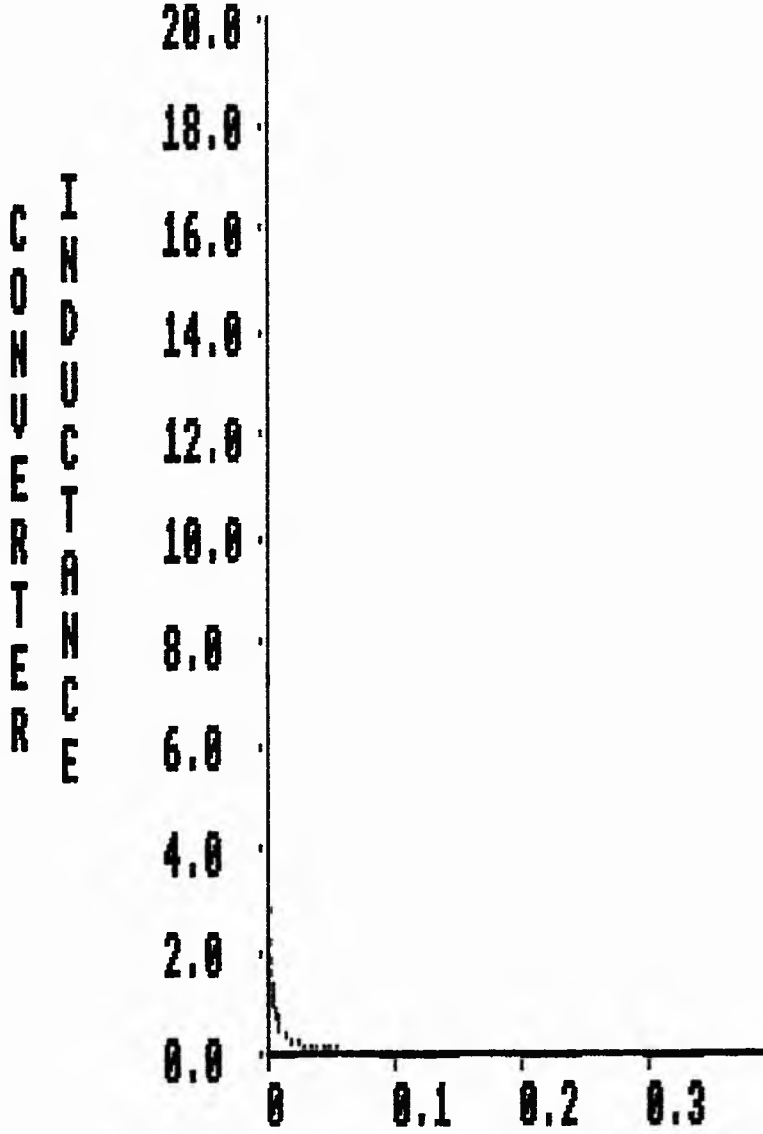
CONVERTER INDUCTANCE
20.0
18.0
16.0
14.0
12.0
10.0
8.0
6.0
4.0
2.0
0.0
0
0.1
0.2
0.3

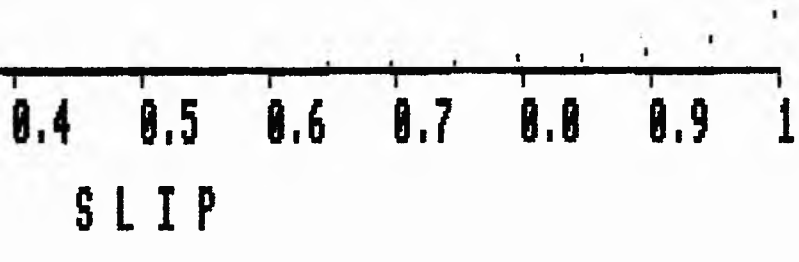
0.4
0.5
0.6
0.7
0.8
0.9
1
SLIP

SLIP	CONVERTER INDUCTANCE (HENRIES)
0.0025	2.3016
0.0050	1.1583
0.0075	0.7774
0.0100	0.5870
0.0125	0.4728
0.0150	0.3968
0.0175	0.3425
0.0200	0.3018
0.0225	0.2703
0.0250	0.2450
0.0275	0.2244
0.0300	0.2073
0.0325	0.1928
0.0350	0.1804
0.0375	0.1697
0.0400	0.1604
0.0425	0.1522
0.0450	0.1449
0.0475	0.1384

Press the SPACE BAR to continue

SLIP	CONVERTER INDUCTANCE(HENRIES)
0.0500	0.1326
0.0525	0.1273
0.0550	0.1226
0.0575	0.1182
0.0600	0.1143
0.0625	0.1107
0.0650	0.1073
0.0675	0.1043
0.0700	0.1015
0.0725	0.0988
0.0750	0.0964
0.0775	0.0942
0.0800	0.0921
0.0825	0.0901
0.0850	0.0883
0.0875	0.0865
0.0900	0.0849
0.0925	0.0834
0.0950	0.0820
0.0975	0.0807
0.1000	0.0794

Press the SPACE BAR to continue

HORIZONTAL DISPLACEMENT
0.0 0.3 0.6 0.9 1.2 1.5 1.8 2.1 2.4 2.7 3.0
SLIP
0.00 0.01 0.02 0.03 0.04 0.05 0.06 0.07 0.08 0.09 0.10

C O N V C A P M E N U

Select operation Required

Expand graph for a slip of 0.1.....1
Converter Ind.....2
Re-run Convcap (with SAME input Data).....3
Capcalc (with NEW Data).....4
Return to Main Menu.....5
EXIT and return to DOS.....6

Operation Required (1 TO 6)

CONVERTER

CAPACITANCE

Press the SPACE BAR to continue

SLIP	CONVERTER CAPACITANCE UF
0.0005	0.8865
0.0010	1.7739
0.0015	2.6620
0.0020	3.5510
0.0025	4.4407
0.0030	5.3312
0.0035	6.2224
0.0040	7.1143
0.0045	8.0070
0.0050	8.9004
0.0055	9.7944
0.0060	10.6891
0.0065	11.5845
0.0070	12.4805
0.0075	13.3772
0.0080	14.2744
0.0085	15.1723
0.0090	16.0707
0.0095	16.9697

Press the SPACE BAR to continue

SLIP	CONVERTER CAPACITANCE UF
0.0100	17.8692
0.0150	26.8921
0.0200	35.9547
0.0250	45.0432
0.0300	54.1443
0.0350	63.2451
0.0400	72.3332
0.0450	81.3968
0.0500	90.4248
0.0550	99.4065
0.0600	108.3319
0.0650	117.1916
0.0700	125.9767
0.0750	134.6791
0.0800	143.2912
0.0850	151.8062
0.0900	160.2175
0.0950	168.5195

Press the SPACE BAR to continue

SLIP	CONVERTER CAPACITANCE UF
0.1000	176.7069
0.1500	251.4934
0.2000	312.4596
0.2500	360.3432
0.3000	397.1618
0.3500	425.1590
0.4000	446.3397
0.4500	462.3333
0.5000	474.4044
0.5500	483.5113
0.6000	490.3732
0.6500	495.5278
0.7000	499.3779
0.7500	502.2262
0.8000	504.3014
0.8500	505.7775
0.9000	506.7872
0.9500	507.4330
1.0000	507.7940

Press the SPACE BAR to continue

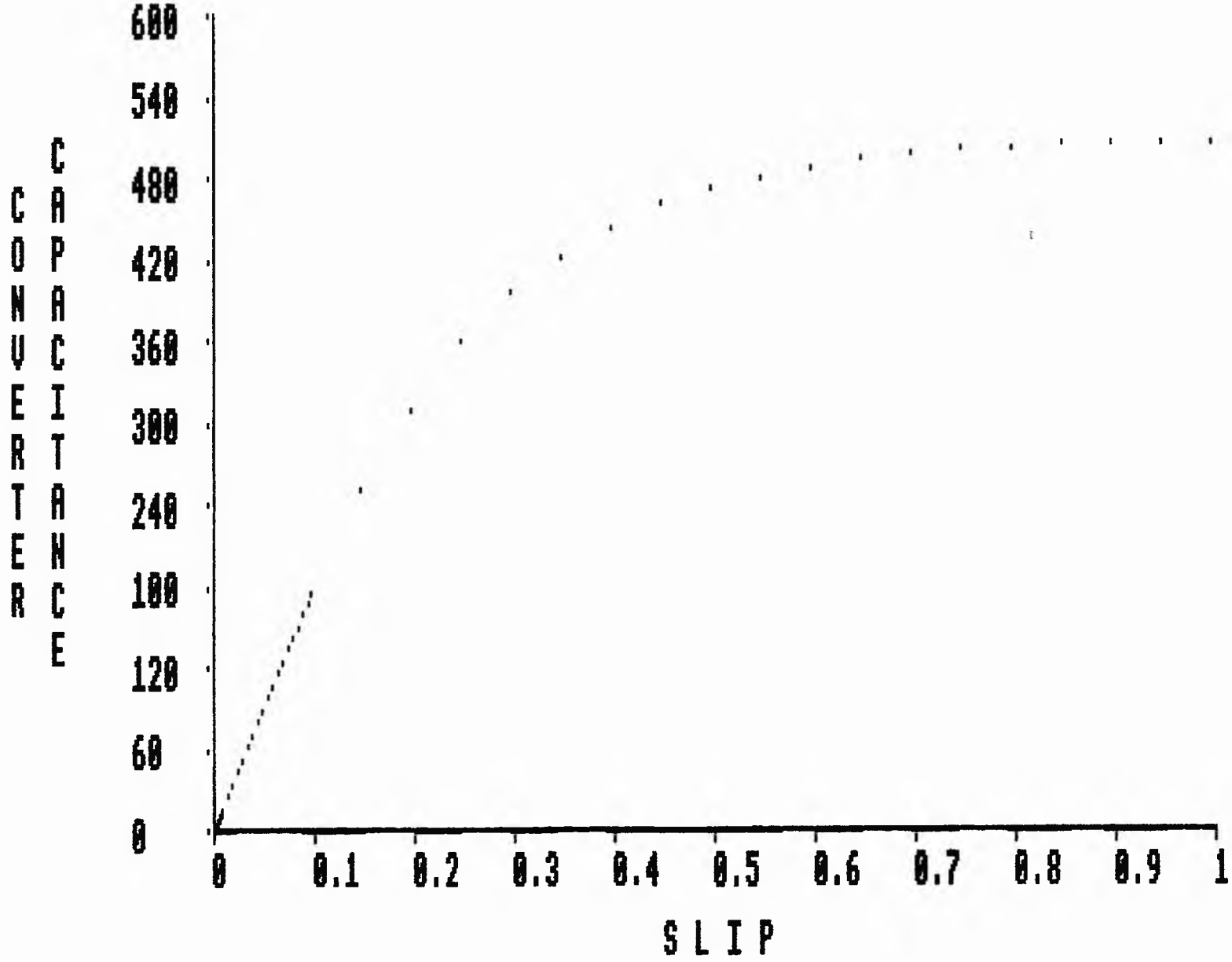
CONVERTER CAPACITANCE
600
540
480
420
360
300
240
180
120
60
0
0
0.1
0.2
0.3
0.4
0.5
0.6
0.7
0.8
0.9
1
SLIP

SLIP	CONVERTER CAPACITANCE UF
0.0025	4.4407
0.0050	8.9004
0.0075	13.3772
0.0100	17.8692
0.0125	22.3748
0.0150	26.8921
0.0175	31.4193
0.0200	35.9547
0.0225	40.4965
0.0250	45.0432
0.0275	49.5930
0.0300	54.1443
0.0325	58.6955
0.0350	63.2451
0.0375	67.7914
0.0400	72.3332
0.0425	76.8688
0.0450	81.3968
0.0475	85.9160

Press the SPACE BAR to continue

SLIP	CONVERTER CAPACITANCE UF
0.0500	90.4248
0.0525	94.9221
0.0550	99.4065
0.0575	103.8769
0.0600	108.3319
0.0625	112.7705
0.0650	117.1916
0.0675	121.5940
0.0700	125.9767
0.0725	130.3387
0.0750	134.6791
0.0775	138.9969
0.0800	143.2912
0.0825	147.5613
0.0850	151.8062
0.0875	156.0252
0.0900	160.2175
0.0925	164.3825
0.0950	168.5195
0.0975	172.6278
0.1000	176.7069

Press the SPACE BAR to continue

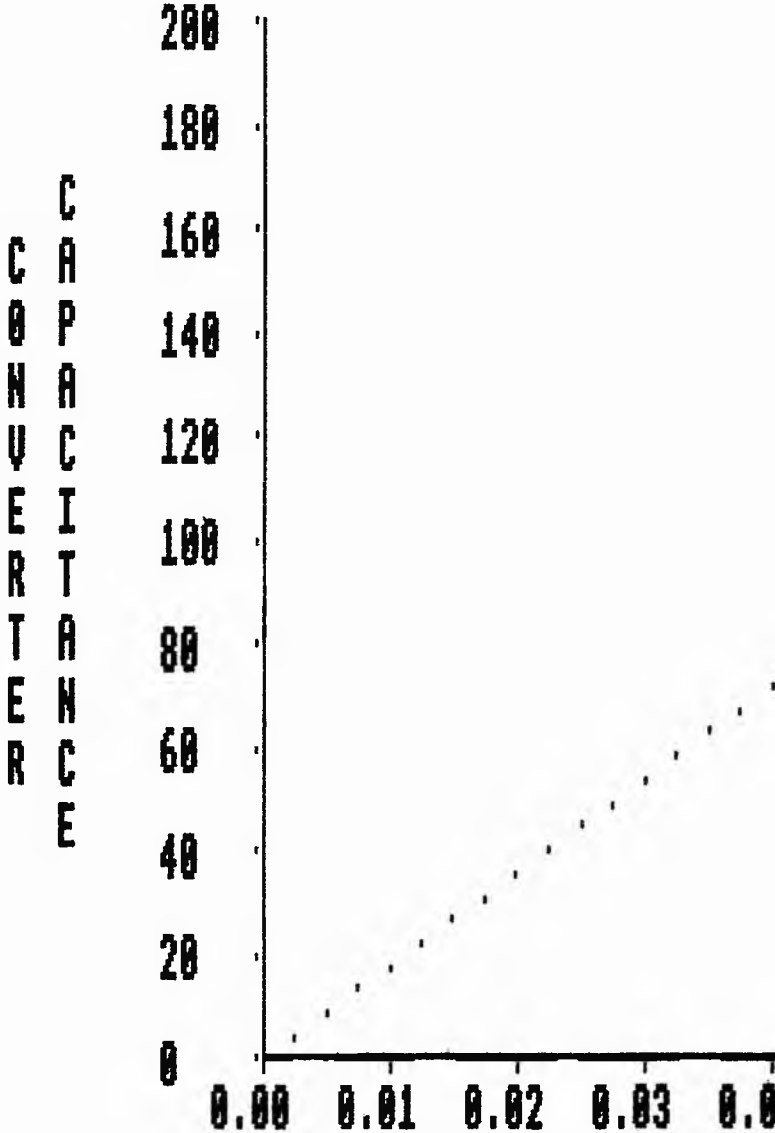
CONVERTER CAPACITANCE
200
180
160
140
120
100
80
60
40
20
0
0.00
0.01
0.02
0.03

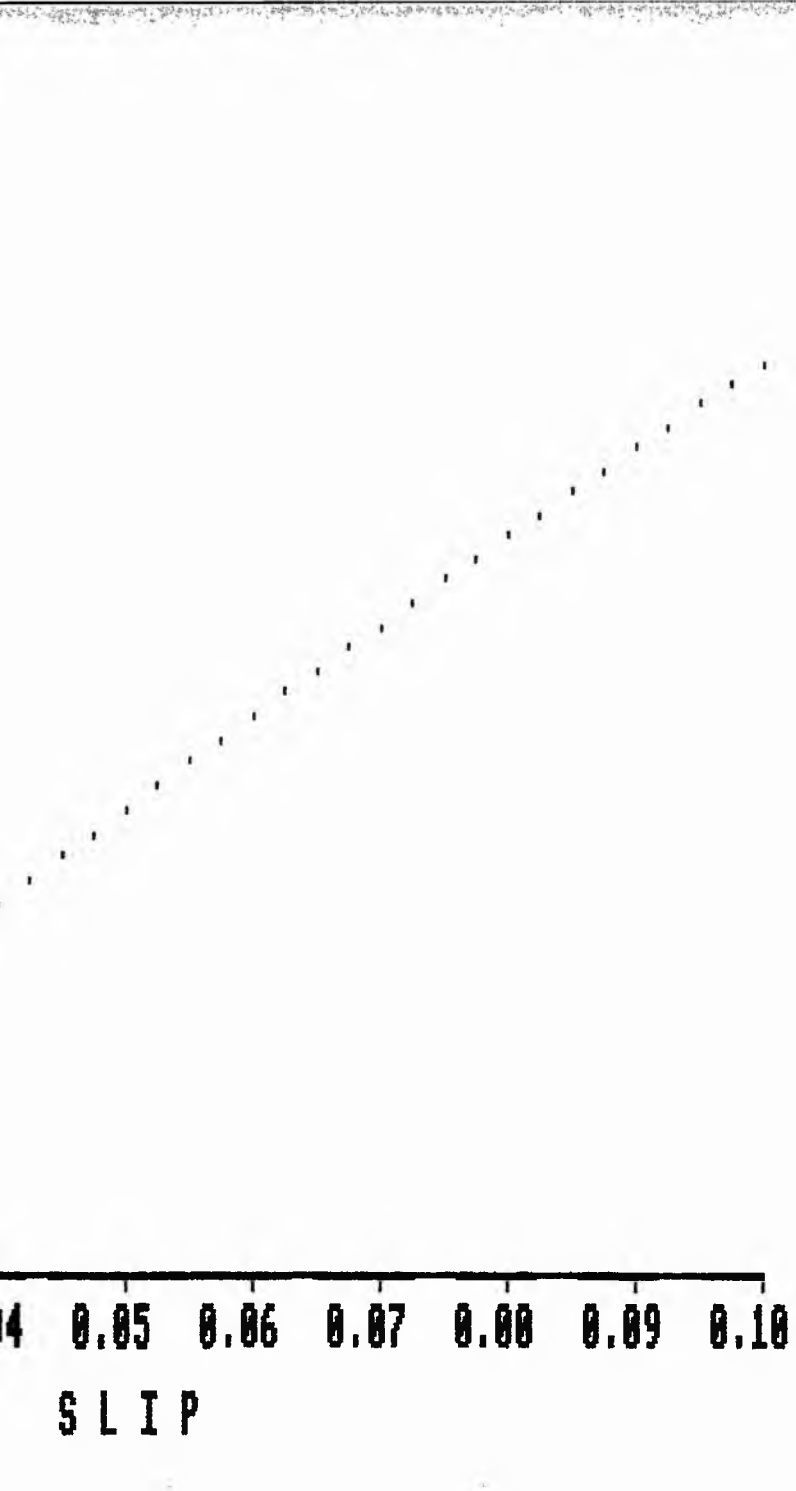
4 0.05 0.06 0.07 0.08 0.09 0.10
S L I P

```
   10 Pt=0
   20 DIM DAT(14),CAP(100),S1(100),Y(100),CC(100),IND(100),CAPZ(100),CCZ(100),IN
DZ(100)
   30 MODE1
   40 COLOUR 6:PRINTTAB(14,3);"C A P C A L C"
   50 PRINTTAB(9,6);"Written by M.Latif
   60 PRINTTAB(0,12);"Department of Electrical and Electronic"
   70 PRINTTAB(14,14)"Engineering"
   80 PRINTTAB(6,18);"Nottingham Polytechnic 1990"
   90 PRINT:INPUTTAB(8,24)"PRESS RETURN TO CONTINUE"CO
  100
  110 PROCinput
  120 PROCcalc
  130 PROCstatus
  140 PROCcct
  150 PROCtable1
  160 PROCtable2
  170 PROCtable3
  180 PROCaxes
  190 PROCgraph
  200 PROCmenu
  210 END
  220
  230 DEFPROCinput
  240 MODE 3
  250 Pt=0
  260 COLOUR 6:PRINTTAB(15,0)"Are the Motor conections STAR or DELTA (S/D) ";:CO
LOUR 11:INPUT;A$
  270 IF A$="D" OR A$="d" STAR=0 ELSE STAR=1
  280 COLOUR 6:PRINTTAB(15,2)"Enter the No Load Test Data as indicated:-"
  290 COLOUR 6:PRINTTAB(15,4)"V1                    Stator Volts          ";:CO
LOUR 11:INPUT;V11
  300 COLOUR 6:PRINTTAB(15,6)"I1                    Stator  Amps          ";:CO
LOUR 11:INPUT;I11
  310 COLOUR 6:PRINTTAB(15,8)"P1 Two Meter Method          Watts          ";:CO
LOUR 11:INPUT;P1
  320 COLOUR 6:PRINTTAB(15,10)"P2 Two Meter Method          Watts          ";:C
OLOUR 11:INPUT;P2
  330 COLOUR 6:PRINTTAB(15,12)"Speed                      Rev/min          ";:C
```

```
  330 COLOUR 6:PRINTTAB(15,12)"Speed                          Rev/min          ";:C
OLOUR 11:INPUT;N
  340 COLOUR 6:PRINTTAB(15,14)"Torque                             Nm           ";:C
OLOUR 11:INPUT;T
  350 COLOUR 6:PRINTTAB(15,16)"Resistance   r1                  Ohms           ";:C
OLOUR 11:INPUT;r1
  360 COLOUR 6:PRINTTAB(15,20);"Is this the correct Data (Y/N) "
  370 REPEAT:A$=GET$:UNTIL A$="Y" OR A$="y" OR A$="N" OR A$="n"
  380 IF A$="N" OR A$="n" THEN CLS:GOTO260
  390 CLS
  400 COLOUR 6:PRINTTAB(15,2)"Enter the locked rotor Test Data as indicated:-"
  410 COLOUR 6:PRINTTAB(15,4)"Vb Locked Rotor                  Volts          ";:CO
LOUR 11:INPUT;Vb1
  420 COLOUR 6:PRINTTAB(15,6)"Ib Locked Rotor                   Amps          ";:CO
LOUR 11:INPUT;Ib1
  430 COLOUR 6:PRINTTAB(15,8)"P1b Two Meter Method             Watts          ";:CO
LOUR 11:INPUT;P1b
  440 COLOUR 6:PRINTTAB(15,10)"P2b Two Meter Method            Watts          ";:C
OLOUR 11:INPUT;P2b
  450 COLOUR 6:PRINTTAB(15,12)"Frequency of the supply         Hertz          ";:C
OLOUR 11:INPUT;f
  460 COLOUR 6:PRINTTAB(15,14)"No of Poles                                    ";:C
OLOUR 11:INPUT;p
  470 COLOUR 6:PRINTTAB(15,20);"Is this the correct Data (Y/N) "
  480 REPEAT:A$=GET$:UNTIL A$="Y" OR A$="y" OR A$="N" OR A$="n"
  490 IF A$="N" OR A$="n" THEN GOTO 390
  500 ENDPROC
  510
  520 DEFPROCcalc
  530 DAT(1)=V11:DAT(2)=I11:DAT(3)=P1:DAT(4)=P2:DAT(5)=N:DAT(6)=T:DAT(7)=r1
  540 DAT(8)=Vb1:DAT(9)=Ib1:DAT(10)=P1b:DAT(11)=P2b:DAT(12)=f:DAT(13)=p:DAT(14)=
STAR
  550 @%=&20206
  560 IF STAR=0 THEN PROCdelta ELSE PROCstar
  570 CLS
```

```
 580 LET ns=(f*2)/p
 590 LET s=(ns-(N/60))/ns
 600 a0=(INT((s*10000)+.5))/10000
 610 ENDPROC
 620
 630 DEFPROCstatus
 640 CLS
 650 COLOUR 6:PRINTTAB(20,2)"Slip s
%"
 660 LET z1=V1/I1
 670 LET R1=ABS(P1+P2)/(3*I1*I1)
 680 LET X1=(SQR((z1*z1)-(R1*R1)))
 690 LET zb=Vb/Ib
 700 LET Rb=ABS(P1b+P2b)/(3*Ib*Ib)
 710 LET Xb=(SQR((zb*zb)-(Rb*Rb)))
 720 LET X1=0.4*Xb
 730 LET a1=(INT((X1*1000)+.5))/1000
 740 COLOUR 6:PRINTTAB(20,4)"X1
 750 LET X2=0.6*Xb
 760 LET a2=(INT((X2*1000)+.5))/1000
 770 COLOUR 6:PRINTTAB(20,6)"X2
 780 LET Xm=X1-X1
 790 LET a3=(INT((Xm*1000)+.5))/1000
 800 COLOUR 6:PRINTTAB(20,8)"Xm
 810 LET Rm=R1-(r1)
 820 LET a4=(INT((Rm*1000)+.5))/1000
 830 COLOUR 6:PRINTTAB(20,10)"Rm
 840 LET r2=Rb-r1
 850 LET a5=(INT((r2*1000)+.5))/1000
 860 COLOUR 6:PRINTTAB(20,12)"r2
 870 LET Rs=r2/s
 880 LET Y2=SQR((X2*X2)+(Rs*Rs))
 890 LET AN1=ATN(X2/r2)
 900 LET Q2=SQR((Xm*Xm)+(Rm*Rm))
 910 LET AN2=ATN(Xm/Rm)
 920 LET W2=Y2*Q2
 930 LET AN3=AN1+AN2
 940 LET Y3 =Rs+Rm
 950 LET I2=Y2+Ym
```

```
=    ";:COLOUR 11:PRINT;a0*100;"

=    ";:COLOUR 11:PRINT;a1

=    ";:COLOUR 11:PRINT;a2

=    ";:COLOUR 11:PRINT;a3

 =    ";:COLOUR 11:PRINT;a4

 =    ";:COLOUR 11:PRINT;a5
```

```
 960 LET W3=SQR((Y3*Y3)+(J2*J2))
 970 LET AN4=ATN(J2/Y3)
 980 LET Qab=W2/W3
 990 LET AN5=AN3-AN4
1000 LET Rab=Qab*COS(AN4)
1010 LET Xab=Qab*SIN(AN4)
1020 LET Rt= r1+Rab
1030 LET Xt=X1+Xab
1040 LET zt=SQR((Rt*Rt)+(Xt*Xt))
1050 LET I1=(V1/1.732)/zt
1060 LET a6=(INT((I1*1000)+0.5))/1000
1070 COLOUR 6:PRINTTAB(20,14)"Stator current I1   =
s"
1080 LET T1=T*(5/12)
1090 LET Hp=(T1*2*3.147*N)/33000
1100 LET OP=Hp*746
1110 LET a7=(INT((OP*1000)+0.5))/1000
1120 COLOUR 6:PRINTTAB(20,16)"output power        =
tts"
1130 LET Ef=(OP/ABS(P1+P2))*100
1140 LET a8=(INT((Ef*1000)+0.5))/1000
1150 COLOUR 6:PRINTTAB(20,18)"Efficiency          =

1160 LET Pf=1/(SQR(1+(3*((P2-P1)/(P1+P2))^2)))
1170 LET a9=(INT((Pf*1000)+0.5))/1000
1180 COLOUR 6:PRINTTAB(20,20)"Power factor        =
1190 PRINT
1200 PROCspace
1210 ENDPROC
1220
1230 DEFPROCcct
1240 LET X3=Xm*(Rm*Rm)/((Rm*Rm)+(Xm*Xm))
1250 LET R3=Rm*(Xm*Xm)/((Rm*Rm)+(Xm*Xm))
1260 @%=10
1270 MODE0
1280 *LOAD SCREEN B8000000
1290 VDU5
1300 MOVE 30,468:PRINT(INT(V1*10))/10;"V"
1310 MOVE 420,482:PRINT(INT(Xm*10))/10
1320 MOVE 620,482:PRINT(INT(Rm*10))/10
```

```
=    ";:COLOUR 11:PRINT;a6" amp

=    ";:COLOUR 11:PRINT;a7;" wa

=    ";:COLOUR 11:PRINT;a8;" %"

=    ";:COLOUR 11:PRINT;a9
```

```
1330 MOVE 90,760:PRINT(INT(r1*10))/10
1340 MOVE 330,760:PRINT(INT(X1*10))/10
1350 MOVE 540,760:PRINT(INT(r2*10))/10
1360 MOVE 750,760:PRINT(INT(X2*10))/10
1370 VDU4
1380 A=GET
1390 ENDPROC
1400
1410 DEFPROCtable1
1420 MODE3
1430 CLS
1440 LET X4=X3+X2
1450 COLOUR 6:PRINTTAB(20,0);"SLIP";TAB(17);"CAPACITANCE   UF"
1460 PRINT
1470 @%=&00020407
1480 LET X%=0
1490 FOR S1=0.0005 TO 0.0100 STEP 0.0005
1500 LET X%=X%+1
1510 LET R2=r2/S1
1520 LET R4=R3+R2
1530 LET X5=(R2*R4*X3+R3*R4*X2+X2*X3*X4-R2*R3*X4)/((R4*R4)+(X4*X4))
1540 LET CAP(X%)=1000000.0/((X5+X1)*2*f*3.141)
1550 COLOUR 6:PRINTTAB(19);S1;TAB(41);:COLOUR 11:PRINT;CAP(X%)
1560 NEXT S1
1570 PROCspace
1580 ENDPROC
1590
1600 DEFPROCtable2
1610 COLOUR 6:PRINTTAB(20,0);"SLIP";TAB(17);"CAPACITANCE   UF"
1620 PRINT
1630 FOR S1=0.010 TO 0.10 STEP 0.005
1640 LET X%=X%+1
1650 LET R2=r2/S1
1660 LET R4=R3+R2
1670 LET X5=(R2*R4*X3+R3*R4*X2+X2*X3*X4-R2*R3*X4)/((R4*R4)+(X4*X4))
1680 LET CAP(X%)=1000000.0/((X5+X1)*2*f*3.141)
1690 COLOUR 6:PRINTTAB(19);S1;TAB(41);:COLOUR 11:PRINT;CAP(X%)
1700 NEXTS1
1710 PROCspace
1720 ENDPROC
```

```
1730
1740 DEFPROCtable3
1750 COLOUR 6:PRINTTAB(20,0);"SLIP";TAB(17);"CAPACITANCE   UF"
1760 PRINT
1770 FOR S1=0.10 TO 1.05 STEP 0.05
1780 LET X%=X%+1
1790 LET R2=r2/S1
1800 LET R4=R3+R2
1810 LET X5=(R2*R4*X3+R3*R4*X2+X2*X3*X4-R2*R3*X4)/((R4*R4)+(X4*X4))
1820 LET CAP(X%)=1000000.0/((X5+X1)*2*f*3.141)
1830 COLOUR 6:PRINTTAB(19);S1;TAB(41);:COLOUR 11:PRINT;CAP(X%)
1840 NEXTS1
1850 @%=10
1860 PROCspace
1870 ENDPROC
1880
1890 DEFPROCspace
1900 COLOUR 6:PRINTTAB(20,24);"Press the SPACE BAR to continue";
1910 REPEAT:A$=GET$:UNTIL A$=" "
1920 PRINT
1930 CLS
1940 ENDPROC
1950
1960 DEFPROCstar
1970 LET Vl=Vl1/SQR(3)
1980 LET Vb=Vb1/SQR(3)
1990 LET Il=Il1
2000 LET Ib=Ib1
2010 ENDPROC
2020
2030 DEFPROCdelta
2040 LET Il=Il1/SQR(3)
2050 LET Ib=Ib1/SQR(3)
2060 LET Vl=Vl1
2070 LET Vb=Vb1
2080 ENDPROC
2090
```

```
2100 DEFPROCaxes
2110 MODE 0
2120 VDU5
2130 J=0
2140 PROCmaxmin
2150 PROCnewy
2160 MOVE 200,100:DRAW 1200,100:MOVE 200,100:DRAW 200,760
2170 FOR X%=200 TO 1200 STEP 100:MOVE X%,100:DRAW X%,95:NEXT
2180 FOR Y%=100 TO 760 STEP 66:MOVE 195,Y%:DRAW 195,Y%:NEXT
2190 RESTORE 2210
2200 FORC=660 TO 240 STEP -40:READ A$:MOVE 0,C:PRINT;A$:NEXTC
2210 DATA C,A,P,A,C,I,T,A,N,C,E,
2220 MOVE 650,25:PRINT"S L I P"
2230 @%=10
2240 FORX%=200 TO 1200 STEP 100:MOVE X%,80:PRINT;(X%-200)/1000:NEXT
2250 @%=&00020005
2260 FOR Y%=100 TO 760 STEP 66:MOVE 120,Y%+10:PRINT;YN*J:J=J+0.1:NEXT
2270 @%=10
2280 ENDPROC
2290
2300 DEFPROCgraph
2310 @%=&00020405
2320 VDU5
2330 MOVE 0,0
2340 X%=-1
2350 FOR S1=0.000 TO 0.0096 STEP 0.0005
2360 LET X%=X%+1
2370 LET X=S1*1000+200
2380 LET Y=(660*CAP(X%)/YN)+100
2390 PLOT 69,X,Y
2400 NEXTS1
2410 @%=&00020304
2420 X=10
2430 FOR S1=0.0096 TO 0.096 STEP 0.005
2440 X%=X%+1
2450 LET X=S1*1000+200
2460 LET Y=(660*CAP(X%)/YN)+100
2470 PLOT 69,X,Y
2480 NEXTS1
```

```
2490 FOR S1=0.096 TO 1.01 STEP 0.05
2500 X%=X%+1
2510 LET X=S1*1000+200
2520 LET Y=(660*CAP(X%)/YN)+100
2530 PLOT 69,X,Y
2540 NEXTS1
2550 VDU29,0;0;
2560 A=GET
2570 ENDPROC
2580
2590 DEFPROCzoom
2600 PROCzoomt
2610 CLS
2620 PROCzmaxmin
2630 MODE0
2640 VDU5
2650 J=0
2660 PROCnewz
2670 MOVE 200,100:DRAW 1200,100:MOVE 200,100:DRAW 200,760
2680 FOR X%=200 TO 1200 STEP 100:MOVE X%,100:DRAW X%,95:NEXT
2690 FOR Y%=100 TO 760 STEP 66:MOVE 195,Y%:DRAW 195,Y%:NEXT
2700 RESTORE 2720
2710 FORC=660 TO 240 STEP -40:READ A$:MOVE 0,C:PRINT;A$:NEXT
2720 DATA C,A,P,A,C,I,T,A,N,C,E,
2730 MOVE 650,25:PRINT"S L I P"
2740 @%=&00020203
2750 FOR X%=200 TO 1200 STEP 100:MOVE X%-20,80:PRINT;(X%-200)/10000:NEXT
2760 @%=&00020005
2770 FOR Y%=100 TO 760 STEP 66:MOVE 120,Y%+10:PRINT;ZN*J:J=J+0.1:NEXT
2780 @%=&00020405
2790 MOVE 0,0
2800 X%=-1
2810 FOR S1=0.0000 TO 0.10001 STEP 0.0025
2820 LET X%=X%+1
2830 LET X=S1*10000+200
2840 LET Y=(660*CAPZ(X%))/(ZN)+100
2850 PLOT 69,X,Y
2860 NEXT S1
2870 VDU29,0;0;
2880 A=GET
```

```
 2880 A=GET
 2890 ENDPROC
 2900
 2910 DEFPROCmenu
 2920 MODE 3
 2930 O%=0
 2940 COLOUR 6:PRINTTAB(32,2)"M A I N  M E N U"
 2950 PRINTTAB(17,5)"Select operation Required"
 2960 PRINTTAB(17,6)"Expand graph for a Slip of 0.1.............1"
 2970 PRINTTAB(17,7)"Converter Cap..............................2"
 2980 PRINTTAB(17,8)"Converter Ind..............................3"
 2990 PRINTTAB(17,9)"Re-run this program (with SAME input Data)...4"
 3000 PRINTTAB(17,10)"Re-run Capcalc (with NEW Data).............5"
 3010 PRINTTAB(17,11)"EXIT and return to DOS.....................6"
 3020 PRINTTAB(17,15)"Operation Required (1 to 6)   ";:COLOUR 11:INPUT;O%:IF O%<
1 OR O%>6 GOTO 3090
 3030 IF O%=1 PROCzoom:GOTO 2920
 3040 IF O%=2 PROCsave:PROCconvcap:PROCaxescc:PROCgraphcc:PROCmenucc:ENDPROC
 3050 IF O%=3 PROCsave:PROCconvind:PROCaxesci:PROCgraphci:PROCmenuci:ENDPROC
 3060 IF O%=4 PROCinfo:PROCagain:PROCcalc:PROCstatus:PROCcct:PROCtable1:PROCtabl
e2:PROCtable3:PROCaxes:PROCgraph:GOTO 2920
 3070 IF O%=5 PROCrestart
 3080 IF O%=6 CLS:END
 3090 VDU7:COLOUR 9:PRINTTAB(17,19)"INPUT ERROR:- RE ENTER SELECTION";
 3100 COLOUR 6:PRINTTAB(17,15)STRING$(52," "):GOTO 3020
 3110 ENDPROC
 3120
 3130 DEFPROCsave
 3140 DAT(1)=V1:DAT(2)=I1:DAT(3)=P1:DAT(4)=P2:DAT(5)=N:DAT(6)=r1
 3150 DAT(7)=Vb:DAT(8)=Ib:DAT(9)=P1b:DAT(10)=P2b:DAT(11)=f:DAT(12)=p:DAT(13)=Pt
 3160 DAT(14)=STAR
 3170 X=OPENOUT "DAT"
 3180 FOR I=1 TO 14
 3190 PRINT£X,DAT(I)
 3200 NEXTI
 3210 CLOSE£X
 3220 ENDPROC
 3230
```

```
 3240 DEFPROCinfo
 3250 X=OPENOUT "DATC"
 3260 FOR I=1 TO 14
 3270 PRINT£X,DAT(I)
 3280 NEXTI
 3290 DAT(1)=V11:DAT(2)=I11:DAT(3)=P1:DAT(4)=P2:DAT(5)=N:DAT(6)=T:DAT(7)=r1
 3300 DAT(8)=Vb1:DAT(9)=Ib1:DAT(10)=P1b:DAT(11)=P2b:DAT(12)=f:DAT(13)=p:DAT(14)=
STAR
 3310 CLOSE£X
 3320 ENDPROC
 3330
 3340 DEFPROCagain
 3350 X=OPENIN "DATC"
 3360 FOR I=1 TO 14
 3370 INPUT£X,DAT(I)
 3380 NEXT I
 3390 CLOSE£X
 3400 ENDPROC
 3410
 3420 DEFPROCmaxmin
 3430 YMAX=0
 3440 FOR I%=1 TO 57 STEP 1
 3450 IF CAP(I%) > YMAX THEN YMAX=CAP(I%)
 3460 NEXT I%
 3470 YMIN=YMAX
 3480 FOR I%=1 TO 57 STEP 1
 3490 IF CAP(I%) < YMIN THEN YMIN=CAP(I%)
 3500 NEXT I%
 3510 ENDPROC
 3520
 3530 DEFPROCnewy
 3540 IF YMAX < 10 THEN GOTO 3570
 3550 IF YMAX < 100 THEN GOTO 3580
 3560 IF YMAX > 100 THEN GOTO 3590
 3570 YN=((YMAX DIV 1)+1):ENDPROC
 3580 YN=((YMAX DIV 10)+1)*10:ENDPROC
 3590 YN=((YMAX DIV 100)+1)*100:ENDPROC
 3600 ENDPROC
 3610
 3620 DEFPROCzoomt
```

```
3630 MODE 3
3640 IF STAR=0 THEN PROCdelta ELSE PROCstar
3650 LET ns = (f*2)/p
3660 LET s = (ns-(N/60))/ns
3670 a0=(INT((s*10000)+0.5))/10000
3680 CLS
3690 YMAX=0
3700 LET X4 = X3+X2
3710 COLOUR 6:PRINTTAB(20,0);"SLIP";TAB(17);"CAPACITANCE   UF"
3720 PRINT
3730 @%=&00020407
3740 LET X% = 0
3750 FOR S1 = 0.0025 TO 0.0500 STEP 0.0025
3760 LET X% = X%+1
3770 LET R2 = r2/S1
3780 LET R4 = R3+R2
3790 LET X5 = (R2*R4*X3+R3*R4*X2+X2*X3*X4-R2*R3*X4)/((R4*R4)+(X4*X4))
3800 LET CAPZ(X%) = 1000000.0/((X5+X1)*2*f*3.141)
3810 COLOUR 6:PRINTTAB(19);S1;TAB(41);:COLOUR 11:PRINT;CAPZ(X%)
3820 NEXT S1
3830 PROCspace
3840 COLOUR 6:PRINTTAB(20,0);"SLIP";TAB(17);"CAPACITANCE   UF"
3850 PRINT
3860 FOR S1 = 0.0500 TO 0.10001 STEP 0.0025
3870 LET X% = X%+1
3880 LET R2 = r2/S1
3890 LET R4 = R3+R2
3900 LET X5 = (R2*R4*X3+R3*R4*X2+X2*X3*X4-R2*R3*X4)/((R4*R4)+(X4*X4))
3910 LET CAPZ(X%) = 1000000.0/((X5+X1)*2*f*3.141)
3920 COLOUR 6:PRINTTAB(19);S1;TAB(41);:COLOUR 11:PRINT;CAPZ(X%)
3930 NEXT S1
3940 PROCspace
3950 ENDPROC
3960
3970 DEFPROCzmaxmin
3980 YMAX = 0
3990 FOR I% = 1 TO 41 STEP 1
4000 IF CAPZ(I%) > YMAX THEN YMAX = CAPZ(I%)
4010 NEXT I%
```

```
4010 NEXT I%
4020 YMIN = YMAX
4030 FOR I% = 1 TO 41 STEP 1
4040 IF CAPZ(I%) < YMIN THEN YMIN = CAPZ(I%)
4050 NEXT I%
4060 ENDPROC
4070
4080 DEFPROCnewz
4090 IF YMAX < 10 THEN GOTO 4120
4100 IF YMAX < 100 THEN GOTO 4130
4110 IF YMAX > 100 THEN GOTO 4140
4120 ZN = ((YMAX DIV 1)+1):ENDPROC
4130 ZN = ((YMAX DIV 10)+1)*10:ENDPROC
4140 ZN = ((YMAX DIV 100)+1)*100:ENDPROC
4150 ENDPROC
4160
4170 DEFPROCconvcap
4180 @%=&00020407
4190 PROCccap
4200 MODE 3
4210 CLS
4220 LET zb=Vb/Ib
4230 LET Rb=ABS(P1b+P2b)/(3*Ib*Ib)
4240 LET Xb=(SQR((zb*zb)-(Rb*Rb)))
4250 LET r2=Rb-r1
4260 COLOUR 6:PRINTTAB(19,2)"CONVERTER"
4270 COLOUR 6:PRINTTAB(30,4)"CAPACITANCE"
4280 PROCspace
4290 COLOUR 6:PRINTTAB(40,0)" CONVERTER"
4300 COLOUR 6:PRINTTAB(20,1);"SLIP";TAB(17);"CAPACITANCE   UF"
4310 PRINT
4320 LET X%=0
4330 FOR S1=0.0005 TO 0.0100 STEP 0.0005
4340 LET R2=r2/S1
4350 LET real=(r1+R2)
4360 LET X%=X%+1
4370 PROCconvertercap
4380 COLOUR 6:PRINTTAB(19);S1;TAB(41);:COLOUR 11:PRINT;CC(X%)
4390 NEXT S1
```

```
4390 NEXT S1
4400 PROCspace
4410 COLOUR 6:PRINTTAB(40,0)" CONVERTER"
4420 COLOUR 6:PRINTTAB(20,1);"SLIP";TAB(17);"CAPACITANCE   UF"
4430 PRINT
4440 FOR S1=0.010 TO 0.10 STEP 0.005
4450 LET R2=r2/S1
4460 LET real=(r1+R2)
4470 LET X%=X%+1
4480 PROCconvertercap
4490 COLOUR 6:PRINTTAB(19);S1;TAB(41);:COLOUR 11:PRINT;CC(X%)
4500 NEXTS1
4510 PROCspace
4520 COLOUR 6:PRINTTAB(40,0)" CONVERTER"
4530 COLOUR 6:PRINTTAB(20,1);"SLIP";TAB(17);"CAPACITANCE   UF"
4540 PRINT
4550 FOR S1=0.10 TO 1.05 STEP 0.05
4560 LET R2=r2/S1
4570 LET real=(r1+R2)
4580 LET X%=X%+1
4590 PROCconvertercap
4600 COLOUR 6:PRINTTAB(19);S1;TAB(41);:COLOUR 11:PRINT;CC(X%)
4610 NEXTS1
4620 PROCspace
4630 @%=10
4640 ENDPROC
4650
4660 DEFPROCccap
4670 X=OPENIN "DAT"
4680 FORI=1 TO 14
4690 INPUT£X,DAT(I)
4700 NEXTI
4710 V1=DAT(1):I1=DAT(2):P1=DAT(3):P2=DAT(4):N=DAT(5):r1=DAT(6)
4720 Vb=DAT(7):Ib=DAT(8):P1b=DAT(9):P2b=DAT(10):f=DAT(11):p=DAT(12):Pt=DAT(13)
4730 STAR=DAT(14)
4740 CLOSE£X
4750 ENDPROC
4760
4770 DEFPROCconvertercap
```

```
4770 DEFPROCconvertercap
4780 LET CC(X%)=((1.732*real+Xb)/(real^2+Xb^2))*1E6/(100*PI)
4790 ENDPROC
4800
4810 DEFPROCaxescc
4820 MODE 0
4830 VDU5
4840 J=0
4850 PROCmaxmincc
4860 PROCnewycc
4870 MOVE 200,100:DRAW 1200,100:MOVE 200,100:DRAW 200,760
4880 FOR X%=200 TO 1200 STEP 100:MOVE X%,100:DRAW X%,95:NEXT
4890 FOR Y%=100 TO 760 STEP 66:MOVE 195,Y%:DRAW 195,Y%:NEXT
4900 RESTORE 4920
4910 FORC=660 TO 240 STEP -40:READ A$:MOVE 40,C:PRINT;A$:NEXT
4920 DATA C,A,P,A,C,I,T,A,N,C,E,
4930 RESTORE 4950
4940 FORC=620 TO 300 STEP -40:READ A$:MOVE 0,C:PRINT;A$:NEXT
4950 DATA C,O,N,V,E,R,T,E,R, ,
4960 MOVE 650,25:PRINT"S L I P"
4970 @%=10
4980 FOR X%=200 TO 1200 STEP 100:MOVE X%,80:PRINT;(X%-200)/1000:NEXT
4990 @%=&00020005
5000 FOR Y%=100 TO 760 STEP 66:MOVE 120,Y%+10:PRINT;CN*J:J=J+0.1:NEXT
5010 @%=10
5020 ENDPROC
5030
5040 DEFPROCgraphcc
5050 @%=&00020405
5060 VDU5
5070 MOVE 0,0
5080 X%=-1
5090 FOR S1=0.000 TO 0.0096 STEP 0.0005
5100 LET X%=X%+1
5110 LET X=S1*1000+200
5120 LET Y=(660*CC(X%)/CN)+100
5130 PLOT 69,X,Y
5140 NEXTS1
5150 @%=&00020304
5160 X=10
```

```
 5170 FOR S1=0.0096 TO 0.096 STEP 0.005
 5180 X%=X%+1
 5190 LET X=S1*1000+200
 5200 LET Y=(660*CC(X%)/CN)+100
 5210 PLOT 69,X,Y
 5220 NEXTS1
 5230 FOR S1=0.096 TO 1.01 STEP 0.05
 5240 X%=X%+1
 5250 LET X=S1*1000+200
 5260 LET Y=(660*CC(X%)/CN)+100
 5270 PLOT 69,X,Y
 5280 NEXTS1
 5290 VDU29,0;0;
 5300 A=GET
 5310 ENDPROC
 5320
 5330 DEFPROCmenucc
 5340 MODE3
 5350 COLOUR 6:PRINTTAB(28,2)"C O N V C A P  M E N U"
 5360 PRINTTAB(17,4)"Select operation Required"
 5370 PRINTTAB(17,6)"Expand graph for a slip of 0.1.............1"
 5380 PRINTTAB(17,7)"Converter Ind..............................2"
 5390 PRINTTAB(17,8)"Re-run Convcap (with SAME input Data).......3"
 5400 PRINTTAB(17,9)"Capcalc (with NEW Data).....................4"
 5410 PRINTTAB(17,10)"Return to Main Menu.........................5"
 5420 PRINTTAB(17,11)"EXIT and return to DOS.....................6"
 5430 PRINTTAB(17,15)"Operation Required  (1 TO 6)     ";:COLOUR 11:INPUT;O%:IF
O%<1 OR O%>6 GOTO 5500
 5440 IF O%=1 PROCzoomcc:GOTO 5330
 5450 IF O%=2 PROCconvind:PROCaxesci:PROCgraphci:PROCmenuci:ENDPROC
 5460 IF O%=3 PROCsave:PROCconvcap:PROCaxescc:PROCgraphcc:PROCmenucc:ENDPROC
 5470 IF O%=4 PROCrestart
 5480 IF O%=5 PROCmenu
 5490 IF O%=6 CLS:MODE 3:END
 5500 VDU7:COLOUR 9:PRINTTAB(17,21)"INPUT ERROR:- RE ENTER SELECTION"
 5510 COLOUR 6:PRINTTAB(17,15)STRING$(52," "):GOTO 5430
 5520 ENDPROC
 5530
 5540 DEFPROCmaxmincc
```

```
5550 YMAX=0
5560 FOR I%=1 TO 57 STEP 1
5570 IF CC(I%) > YMAX THEN YMAX=CC(I%)
5580 NEXT I%
5590 YMIN=YMAX
5600 FOR I%=1 TO 57 STEP 1
5610 IF CC(I%) < YMIN THEN YMIN=CC(I%)
5620 NEXT I%
5630 ENDPROC
5640
5650 DEFPROCnewycc
5660 IF YMAX < 10 THEN GOTO 5690
5670 IF YMAX < 100 THEN GOTO 5700
5680 IF YMAX > 100 THEN GOTO 5710
5690 CN=((YMAX DIV 1)+1:ENDPROC
5700 CN=((YMAX DIV 10)+1)*10:ENDPROC
5710 CN=((YMAX DIV 100)+1)*100:ENDPROC
5720 ENDPROC
5730
5740 DEFPROCzoomcc
5750 PROCzoomtcc
5760 CLS
5770 MODE0
5780 VDU5
5790 J=0
5800 PROCzmaxmincc
5810 PROCnewzcc
5820 MOVE 200,100:DRAW 1200,100:MOVE 200,100:DRAW 200,760
5830 FOR X%=200 TO 1200 STEP 100:MOVE X%,100:DRAW X%,95:NEXT
5840 FOR Y%=100 TO 760 STEP 66:MOVE 195,Y%:DRAW 195,Y%:NEXT
5850 RESTORE 5870
5860 FORC=660 TO 240 STEP -40:READ A$:MOVE 40,C:PRINT;A$:NEXT
5870 DATA C,A,P,A,C,I,T,A,N,C,E,
5880 RESTORE 5900
5890 FORC=620 TO 300 STEP -40:READ A$:MOVE 0,C:PRINT;A$:NEXT
5900 DATA C,O,N,V,E,R,T,E,R, ,
5910 MOVE 650,25:PRINT"S L I P"
5920 @%=&00020204
5930 FOR X%=200 TO 1200 STEP 100:MOVE X%-40,80:PRINT;(X%-200)/10000:NEXT
5940 @%=&00020005
```

```
5940 @%=&00020005
5950 FOR Y%=100 TO 760 STEP 66:MOVE 120,Y%+10:PRINT;CZ*J:J=J+0.1:NEXT
5960 @%=&00020405
5970 MOVE 0,0
5980 X%=-1
5990 FOR S1=0.000 TO 0.10001 STEP 0.0025
6000 LET X%=X%+1
6010 LET X=S1*10000+200
6020 LET Y=(660*CCZ(X%))/(CZ)+100
6030 PLOT 69,X,Y
6040 NEXT S1
6050 VDU29,0;0;
6060 A=GET
6070 ENDPROC
6080
6090 DEFPROCzoomtcc
6100 MODE 3
6110 @%=&00020407
6120 PROCccap
6130 YMAX=0
6140 CLS
6150 COLOUR 6:PRINTTAB(40,0)" CONVERTER"
6160 COLOUR 6:PRINTTAB(20,1);"SLIP";TAB(17);"CAPACITANCE   UF"
6170 PRINT
6180 LET X% = 0
6190 FOR S1 = 0.0025 TO 0.0500 STEP 0.0025
6200 LET R2 = r2/S1
6210 LET real = (r1+R2)
6220 LET X% = X%+1
6230 LET CCZ(X%)=((1.732*real+Xb)/(real^2+Xb^2))*1E6/(100*PI)
6240 COLOUR 6:PRINTTAB(19);S1;TAB(41);:COLOUR 11:PRINT;CCZ(X%)
6250 NEXT S1
6260 PROCspace
6270 COLOUR 6:PRINTTAB(40,0)" CONVERTER"
6280 COLOUR 6:PRINTTAB(20,1);"SLIP";TAB(17);"CAPACITANCE   UF"
6290 PRINT
6300 FOR S1 = 0.0500 TO 0.10001 STEP 0.0025
6310 LET R2 = r2/S1
6320 LET real = (r1+R2)
```

```
6330 LET X% = X%+1
6340 LET CCZ(X%)=((1.732*real+Xb)/(real^2+Xb^2))*1E6/(100*PI)
6350 COLOUR 6:PRINTTAB(19);S1;TAB(41);:COLOUR 11:PRINT;CCZ(X%)
6360 NEXT S1
6370 PROCspace
6380 ENDPROC
6390
6400 DEFPROCzmaxmincc
6410 YMAX = 0
6420 FOR I% = 1 TO 41 STEP 1
6430 IF CCZ(I%) > YMAX THEN YMAX = CCZ(I%)
6440 NEXT I%
6450 YMIN = YMAX
6460 FOR I% = 1 TO 41 STEP 1
6470 IF CCZ(I%) < YMIN THEN YMIN = CCZ(I%)
6480 NEXT I%
6490 ENDPROC
6500
6510 DEFPROCnewzcc
6520 IF YMAX < 10 THEN GOTO 6550
6530 IF YMAX < 100 THEN GOTO 6560
6540 IF YMAX > 100 THEN GOTO 6570
6550 CZ = ((YMAX DIV 1)+1):ENDPROC
6560 CZ = ((YMAX DIV 10)+1)*10:ENDPROC
6570 CZ = ((YMAX DIV 100)+1)*100:ENDPROC
6580 ENDPROC
6590
6600 DEFPROCconvind
6610 MODE3
6620 @%=&00020407
6630 PROCcind
6640 CLS
6650 LET zb=Vb/Ib
6660 LET Rb=ABS(P1b+P2b)/(3*Ib*Ib)
6670 LET Xb=(SQR((zb*zb)-(Rb*Rb)))
6680 LET r2=Rb-r1
6690 COLOUR 6:PRINTTAB(16,6)"CONVERTER"
6700 PRINTTAB(24,8)"INDUCTANCE"
6710 PROCspace
6720 COLOUR 6:PRINTTAB(42,0)"CONVERTER"
```

```
6730 COLOUR 6:PRINTTAB(20,1);"SLIP";TAB(17);"INDUCTANCE (Henries)"
6740 PRINT
6750 LET X%=0
6760 FOR S1=0.0005 TO 0.0100 STEP 0.0005
6770 LET R2=r2/S1
6780 LET real=(r1+R2)
6790 LET X%=X%+1
6800 PROCconverterind
6810 COLOUR 6:PRINTTAB(19);S1;TAB(43);:COLOUR 11:PRINT;IND(X%)
6820 NEXTS1
6830 PROCspace
6840 COLOUR 6:PRINTTAB(42,0)"CONVERTER"
6850 COLOUR 6:PRINTTAB(20,1);"SLIP";TAB(17);"INDUCTANCE (Henries)"
6860 PRINT
6870 FOR S1=0.010 TO 0.10 STEP 0.005
6880 LET R2=r2/S1
6890 LET real=(r1+R2)
6900 LET X%=X%+1
6910 PROCconverterind
6920 COLOUR 6:PRINTTAB(19);S1;TAB(43);:COLOUR 11:PRINT;IND(X%)
6930 NEXTS1
6940 PROCspace
6950 COLOUR 6:PRINTTAB(42,0)"CONVERTER"
6960 COLOUR 6:PRINTTAB(20,1);"SLIP";TAB(17);"INDUCTANCE (Henries)"
6970 PRINT
6980 FOR S1=0.10 TO 1.05 STEP 0.05
6990 LET R2=r2/S1
7000 LET real=(r1+R2)
7010 LET X%=X%+1
7020 PROCconverterind
7030 COLOUR 6:PRINTTAB(19);S1;TAB(43);:COLOUR 11:PRINT;IND(X%)
7040 NEXTS1
7050 PROCspace
7060 @%=10
7070 ENDPROC
7080
7090 DEFPROCcind
7100 LET X=OPENIN "DAT"
7110 FOR I=1 TO 14
7120 INPUT £X,DAT(I)
```

```
 7130 NEXT I
 7140 VL=DAT(1):IL=DAT(2):P1=DAT(3):P2=DAT(4):N=DAT(5):r1=DAT(6):Vb=DAT(7):Ib=DA
T(8):P1b=DAT(9):P2b=DAT(10):f=DAT(11):p=DAT(12):Pt=DAT(13)
 7150 STAR=DAT(14)
 7160 CLOSE£X
 7170 ENDPROC
 7180
 7190 DEFPROCconverterind
 7200 LET IND(X%)=(-(real^2+Xb^2))/((-1.732*real+Xb)*100*PI)
 7210 ENDPROC
 7220
 7230 DEFPROCaxesci
 7240 MODE 0
 7250 VDU5
 7260 J=0
 7270 PROCmaxminci
 7280 PROCnewyci
 7290 MOVE 200,100:DRAW 1200,100:MOVE 200,100:DRAW 200,760
 7300 FOR X%=200 TO 1200 STEP 100:MOVE X%,100:DRAW X%,95:NEXT
 7310 FOR Y%=100 TO 760 STEP 66:MOVE 195,Y%:DRAW 195,Y%:NEXT
 7320 RESTORE 7340
 7330 FOR I=660 TO 240 STEP -40:READ A$:MOVE 40,I:PRINT;A$:NEXTI
 7340 DATA I,N,D,U,C,T,A,N,C,E, ,
 7350 RESTORE 7370
 7360 FOR I=640 TO 300 STEP -40:READ A$:MOVE 0,I:PRINT;A$:NEXT
 7370 DATA C,O,N,V,E,R,T,E,R, ,
 7380 MOVE 650,25:PRINT"S L I P"
 7390 @%=10
 7400 FOR X%=200 TO 1200 STEP 100:MOVE X%,80:PRINT;(X%-200)/1000:NEXT
 7410 @%=&00020105
 7420 FOR Y%=100 TO 760 STEP 66:MOVE 120,Y%+10:PRINT;IN*J:J=J+0.1:NEXT
 7430 @%=10
 7440 ENDPROC
 7450
 7460 DEFPROCgraphci
 7470 @%=&00020d05
 7480 VDU 5
 7490 MOVE 0,0
 7500 X%=-1
 7510 FOR S1=0.000 TO 0.0096 STEP 0.0005
```

```
 7510 FOR S1=0.000 TO 0.0096 STEP 0.0005
 7520 LET X%=X%+1
 7530 LET X=S1*1000+200
 7540 LET Y=(660*IND(X%)/IN)+100
 7550 PLOT 69,X,Y
 7560 NEXTS1
 7570 @%=&00020304
 7580 X=10
 7590 FOR S1=0.0096 TO 0.096 STEP 0.005
 7600 X%=X%+1
 7610 LET X=S1*1000+200
 7620 LET Y=(660*IND(X%)/IN)+100
 7630 PLOT 69,X,Y
 7640 NEXTS1
 7650 FOR S1=0.096 TO 1.01 STEP 0.05
 7660 X%=X%+1
 7670 LET X=S1*1000+200
 7680 LET Y=(660*IND(X%)/IN)+100
 7690 PLOT 69,X,Y
 7700 NEXTS1
 7710 VDU29,0;0;
 7720 A=GET
 7730 ENDPROC
 7740
 7750 DEFPROCmenuci
 7760 MODE 3
 7770 COLOUR 6:PRINTTAB(28,2)"C O N V I N D  M E N U"
 7780 PRINTTAB(17,4)"Selelct operation Required"
 7790 PRINTTAB(17,6)"Expand graph for a slip of 0.1.............1"
 7800 PRINTTAB(17,7)"Converter Cap..............................2"
 7810 PRINTTAB(17,8)"Re-run Convind (with SAME input Data).......3"
 7820 PRINTTAB(17,9)"Capcalc (with NEW Data).....................4"
 7830 PRINTTAB(17,10)"Return to Main Menu........................5"
 7840 PRINTTAB(17,11)"EXIT and return to DOS.....................6"
 7850 PRINTTAB(17,15)"Operation Required  (1 TO 6)     ";:COLOUR 11:INPUT;O%:IF
O%<1 OR O%>6 GOTO 7920
 7860 IF O%=1 PROCzoomci:GOTO 7750
 7870 IF O%=2 PROCsave:PROCconvcap:PROCaxescc:PROCgraphcc:PROCmenucc:ENDPROC
 7880 IF O%=3 PROCinfo:PROCagain:PROCconvind:PROCaxesci:PROCgraphci:PROCmenuci:E
NDPROC
```

```
NDPROC
 7890 IF O%=4 PROCrestart
 7900 IF O%=5 PROCmenu
 7910 IF O%=6 CLS:MODE 3:END
 7920 VDU7:COLOUR 9:PRINTTAB(17,21)"INPUT ERROR:- RE ENTER SELECTION"
 7930 COLOUR 6:PRINTTAB(17,15)STRING$(52," "):GOTO 7850
 7940 ENDPROC
 7950
 7960 DEFPROCmaxminci
 7970 YMAX=0
 7980 FOR I%=1 TO 57 STEP 1
 7990 IF IND(I%) > YMAX THEN YMAX=IND(I%)
 8000 NEXT I%
 8010 YMIN=YMAX
 8020 FOR I%=1 TO 57 STEP 1
 8030 IF IND(I%) < YMIN THEN YMIN=IND(I%)
 8040 NEXT I%
 8050 ENDPROC
 8060
 8070 DEFPROCnewyci
 8080 IF YMAX < 10 THEN GOTO 8110
 8090 IF YMAX < 100 THEN GOTO 8120
 8100 IF YMAX > 100 THEN GOTO 8130
 8110 IN=((YMAX DIV 1)+1):ENDPROC
 8120 IN=((YMAX DIV 10)+1)*10:ENDPROC
 8130 IN=((YMAX DIV 100)+1)*100:ENDPROC
 8140 ENDPROC
 8150
 8160 DEFPROCzoomci
 8170 PROCzoomtci
 8180 MODE0
 8190 VDU5
 8200 J=0
 8210 PROCzmaxminci
 8220 PROCnewzci
 8230 MOVE 200,100:DRAW 1200,100:MOVE 200,100:DRAW 200,760
 8240 FOR X%=200 TO 1200 STEP 100:MOVE X%,100:DRAW X%,95:NEXT
 8250 FOR Y%=100 TO 760 STEP 66:MOVE 195,Y%:DRAW 195,Y%:NEXT
 8260 RESTORE 8280
 8270 FORI=660 TO 240 STEP -40:READ A$:MOVE 40,I:PRINT;A$:NEXT
```

```
8270 FORI=660 TO 240 STEP -40:READ A$:MOVE 40,I:PRINT;A$:NEXT
8280 DATA I,N,D,U,C,T,A,N,C,E,
8290 RESTORE 8310
8300 FORI=640 TO 300 STEP -40:READ A$:MOVE 0,I:PRINT;A$:NEXT
8310 DATA C,O,N,V,E,R,T,E,R, ,
8320 MOVE 650,25:PRINT"S L I P"
8330 @%=&00020204
8340 FOR X%=200 TO 1200 STEP 100:MOVE X%-40,80:PRINT;(X%-200)/10000:NEXT
8350 @%=&00020105
8360 FOR Y%=100 TO 760 STEP 66:MOVE 120,Y%+10:PRINT;IZ*J:J=J+0.1:NEXT
8370 @%=&00020405
8380 MOVE 0,0
8390 X%=-1
8400 FOR S1=0.0000 TO 0.10001 STEP 0.0025
8410 LET X%=X%+1
8420 LET X=S1*10000+200
8430 LET Y=(660*INDZ(X%))/(IZ)+100
8440 PLOT 69,X,Y
8450 NEXT S1
8460 VDU29,0;0;
8470 A=GET
8480 ENDPROC
8490
8500 DEFPROCzoomtci
8510 MODE 3
8520 @%=&20206
8530 PROCcind
8540 YMAX = 0
8550 CLS
8560 COLOUR6:PRINTTAB(40,0)"CONVERTER"
8570 COLOUR 6:PRINTTAB(20,1);"SLIP";TAB(17);"INDUCTANCE (HENRIES)"
8580 PRINT
8590 @%=&00020407
8600 LET X% = 0
8610 FOR S1 = 0.0025 TO 0.0500 STEP 0.0025
8620 LET R2 = r2/S1
8630 LET real = (r1+R2)
8640 LET X% = X%+1
8650 LET INDZ(X%)=(-(real^2+Xb^2))/((-1.732*real+Xb)*100*PI)
8660 COLOUR 6:PRINTTAB(19);S1;TAB(43);:COLOUR 11:PRINT;INDZ(X%)
```

```
8660 COLOUR 6:PRINTTAB(19);S1;TAB(43);:COLOUR 11:PRINT;INDZ(X%)
8670 NEXT S1
8680 PROCspace
8690 COLOUR 6:PRINTTAB(40,0)"CONVERTER"
8700 COLOUR 6:PRINTTAB(20,1);"SLIP";TAB(17);"INDUCTANCE(HENRIES)"
8710 PRINT
8720 FOR S1 = 0.0500 TO 0.10001 STEP 0.0025
8730 LET R2 = r2/S1
8740 LET real = (r1+R2)
8750 LET X% = X%+1
8760 LET INDZ(X%)=(-(real^2+Xb^2))/((-1.732*real+Xb)*100*PI)
8770 COLOUR 6:PRINTTAB(19);S1;TAB(43);:COLOUR 11:PRINT;INDZ(X%)
8780 NEXT S1
8790 PROCspace
8800 ENDPROC
8810
8820 DEFPROCzmaxminci
8830 YMAX = 0
8840 FOR I% = 1 TO 41 STEP 1
8850 IF INDZ(I%) > YMAX THEN YMAX = INDZ(I%)
8860 NEXT I%
8870 YMIN = YMAX
8880 FOR I% = 1 TO 41 STEP 1
8890 IF INDZ(I%) < YMIN THEN YMIN = INDZ(I%)
8900 NEXT I%
```

```
 8820 DEFPROCzmaxminci
 8830 YMAX = 0
 8840 FOR I% = 1 TO 41 STEP 1
 8850 IF INDZ(I%) > YMAX THEN YMAX = INDZ(I%)
 8860 NEXT I%
 8870 YMIN = YMAX
 8880 FOR I% = 1 TO 41 STEP 1
 8890 IF INDZ(I%) < YMIN THEN YMIN = INDZ(I%)
 8900 NEXT I%
 8910 ENDPROC
 8920
 8930 DEFPROCnewzci
 8940 IF YMAX < 10 THEN GOTO 8970
 8950 IF YMAX < 100 THEN GOTO 8980
 8960 IF YMAX > 100 THEN GOTO 8990
 8970 IZ = ((YMAX DIV 1)+1):ENDPROC
 8980 IZ = ((YMAX DIV 10)+1)*10:ENDPROC
 8990 IZ = ((YMAX DIV 100)+1)*100:ENDPROC
 9000 ENDPROC
 9010
 9020 DEFPROCrestart
 9030 Pt=0
 9040 PROCinput:PROCcalc:PROCstatus:PROCcct:PROCtable1:PROCtable2:PROCtable3:PRO
Cmaxmin:PROCaxes:PROCgraph:PROCmenu
 9050 ENDPROC
```

APPENDIX C

PICTURES OF THE TRANSIENT PHASE CONVERTER IN THE LABORATORY

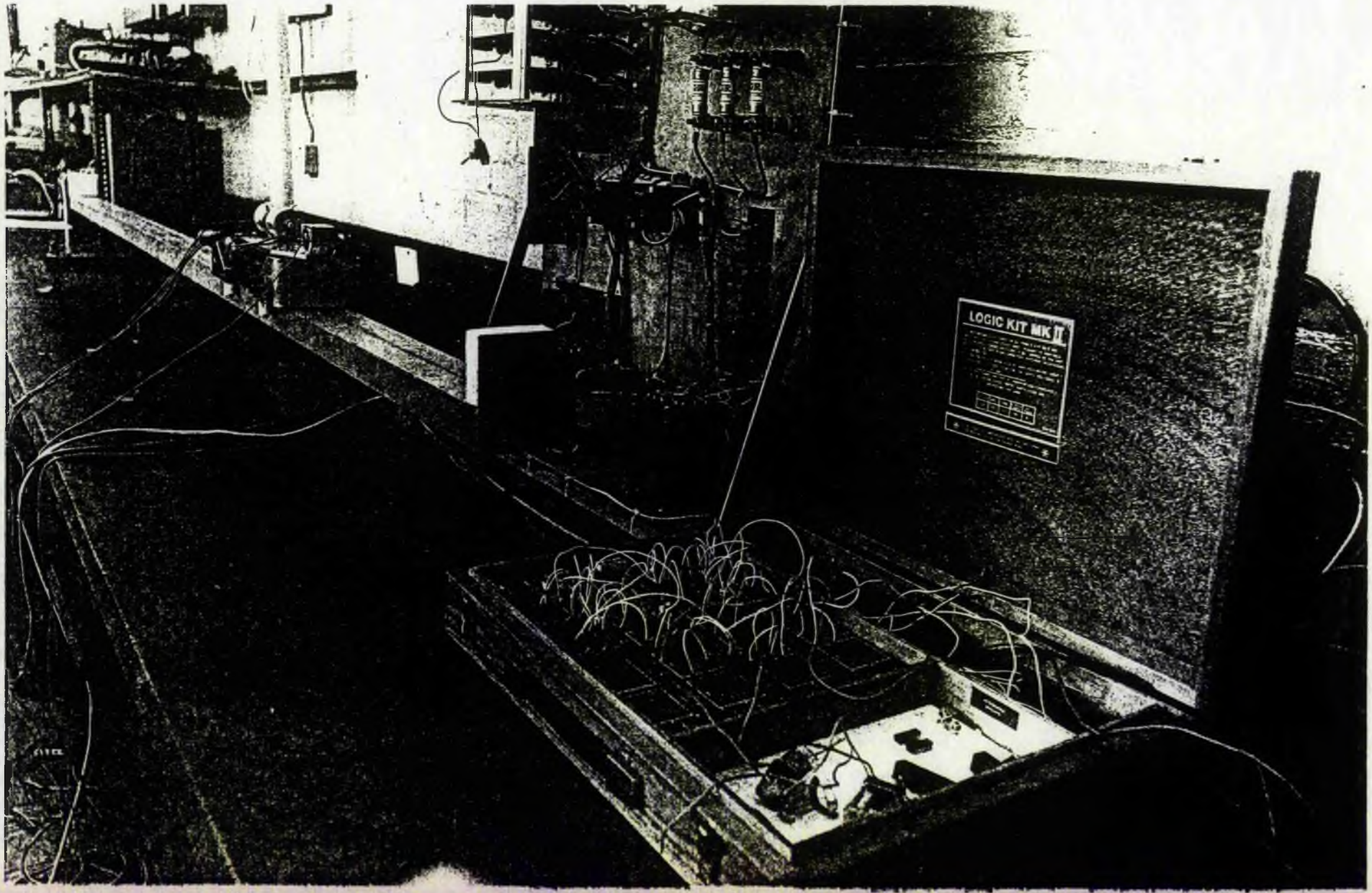
LOGIC KIT MK II

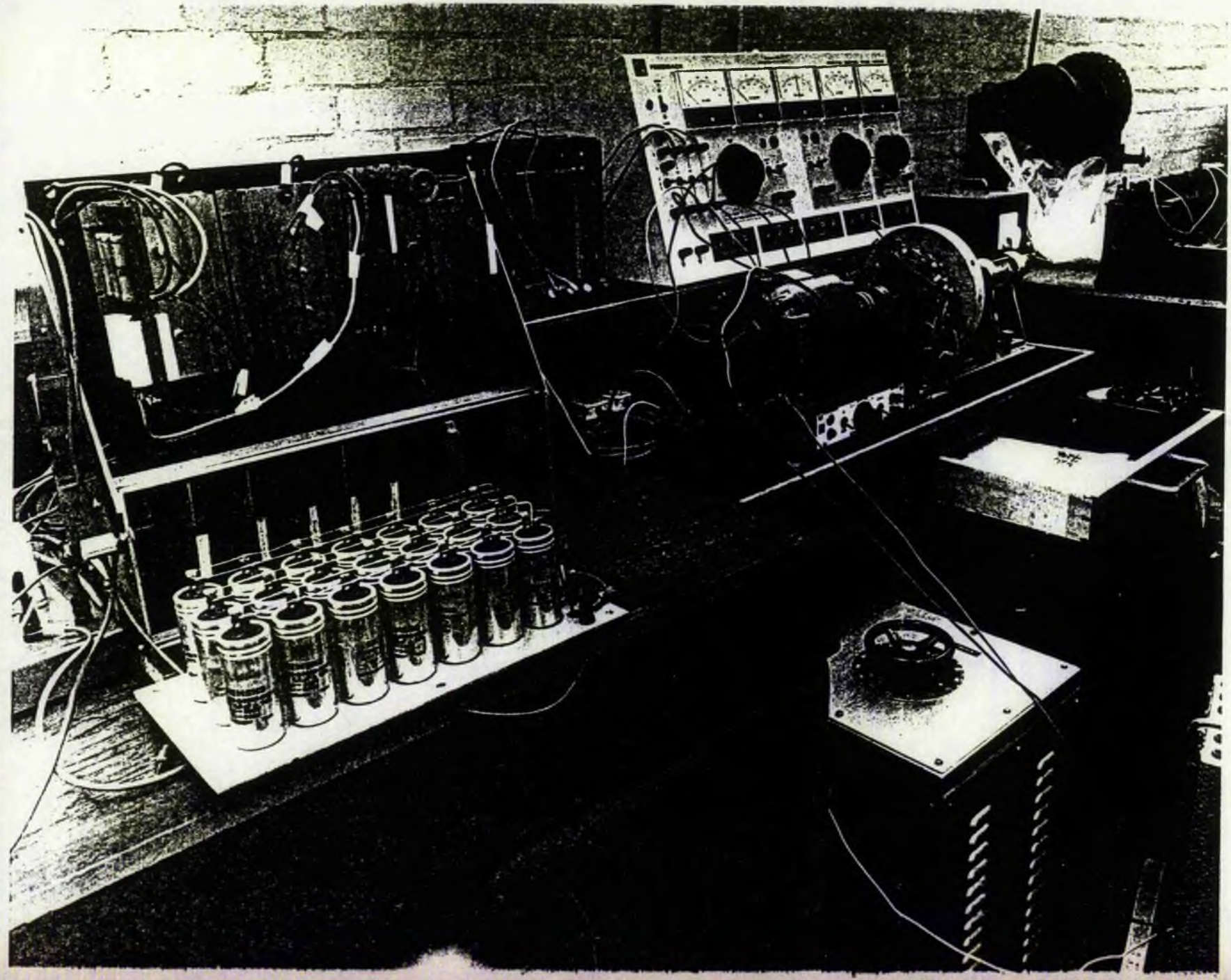

APPENDIX D

SOME EXAMPLES OF THE PHASE CONVERTERS ON THE MARKET

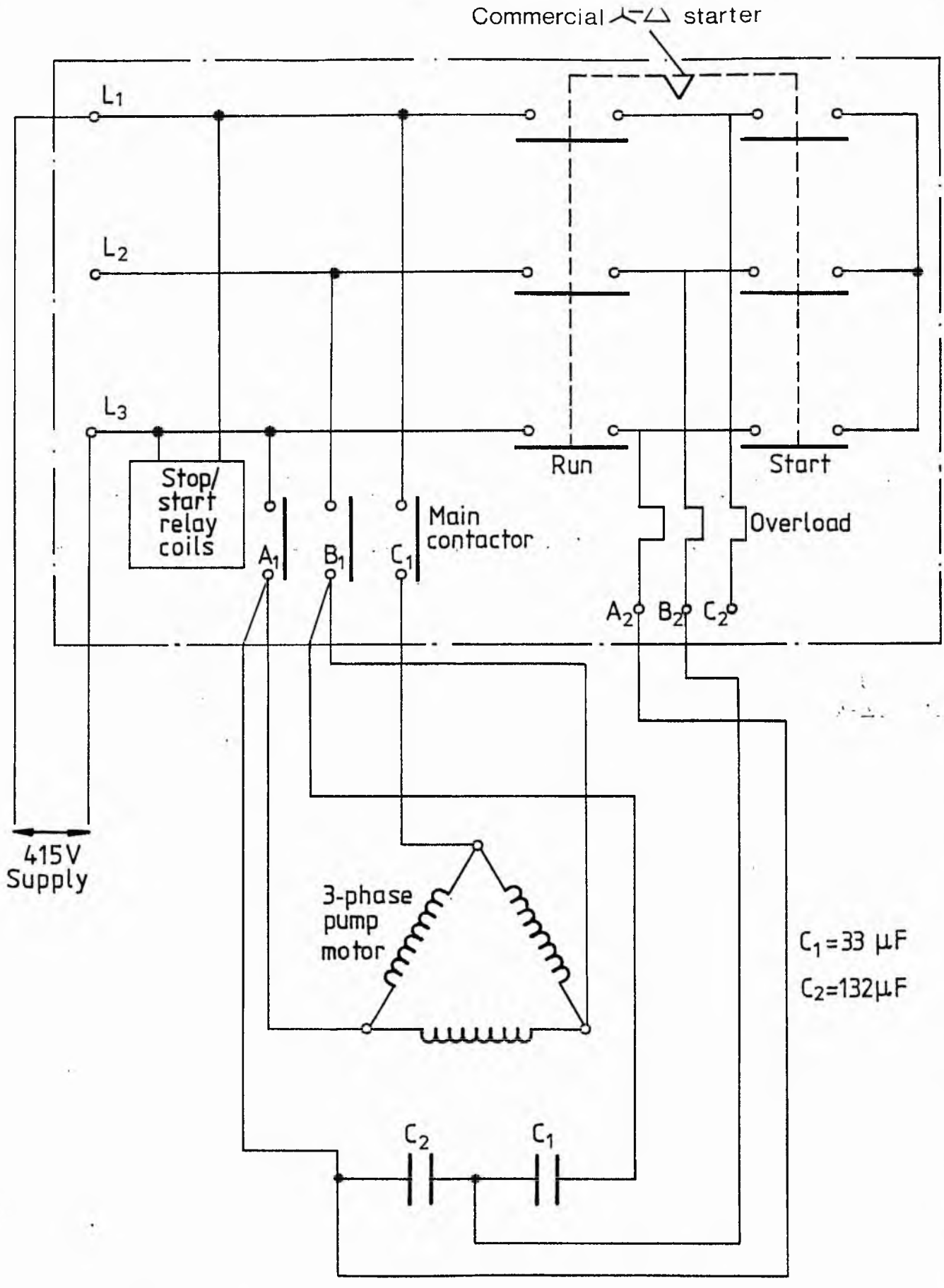

Fig. 1 1/3 Phase converter for Northumberland Water Board

AUTOMATIC STATIC SINGLE TO THREE PHASE CONVERSION SYSTEMS

Electronically-controlled system for **separately** driving two three phase motors (single or two speed machines) from a single phase supply (picture).

MANUFACTURED IN THE UNITED KINGDOM AND UNDER LICENCE AT POINTS AROUND THE WORLD

SELECTED USES

- **Pumps**
- **Compressors**
- **Sheep Shearing Equipment**
- **Refrigeration Plant**
- **Variable Speed Drives**
- **Machine Tools**
- **Food Processors**
- **Hoists**
- **Welders**

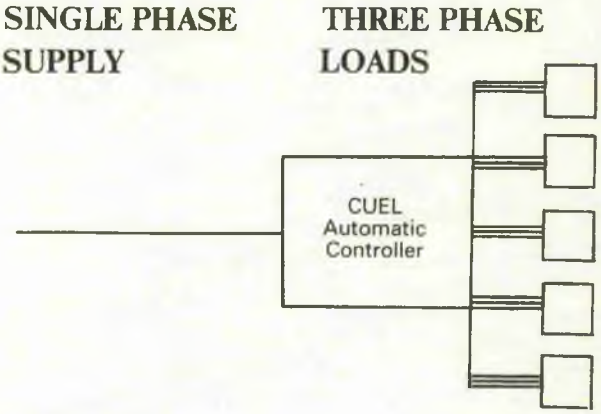

Power Control Engineering from:—

CUEL LTD.
12 Tulip Tree Avenue
Kenilworth
England CV8 2BU

Tel. 0926-54293 Telex 311248

Local agent and/or manufacturer:—

TECHNICAL DATA*

SYSTEM EFFICIENCY	Over 90%.
WAVE FORM	Pure sine. No harmonic distortion.
TORQUE	Starting torque almost 100% of mains three phase supply.
CONTINUOUS WORKING LIFE (excluding contactors)	Projected 20 years (380v) before major overhaul. Very frequently started installations (or 440/575v) may require high-voltage components (small extra cost).
STARTING (variable speed on request)	Handles direct-on-line currents without problem. Self-compensating against load variation.
OPERATING TEMPERATURE	Up to 60°C ambient.

*Empirical data from tests carried out by University of Leicester Department of Engineering.

STANDARD MODELS

Single Phase Inputs 100–120, 220–250, 480v (or as specified) 40, 50, 60HZ

Three Phase Outputs 200–230, 270, 380, 415, 440, 575v (or as specified)

SINGLE OUTPUT
1.0kW
2.5kW
5.0kW
7.5kW
10.0kw

TWO OUTPUTS
2.5kW (1.5 + 1.0)
5.0kW (3.0 + 2.0)
7.5kW (5.0 + 2.5)
12.0kW (8.0 + 4.0)

THREE OUTPUTS
3.0kW (1.5 + 1.0 + 0.5)
6.0kW (3.0 + 2.0 + 1.0)
9.0kW (4.0 + 3.0 + 2.0)
12.0kW (6.0 + 4.0 + 2.0)
15.0kW (8.0 + 5.0 + 2.0)

FOUR OUTPUTS
7.0kW (2.5 + 2.0 + 1.5 + 1.0)
10.0kW (4.0 + 3.0 + 2.0 + 1.0)
14.0kW (5.0 + 4.0 + 3.0 + 2.0)
16.0kW (7.0 + 4.0 + 3.0 + 2.0)
21.0kW (9.0 + 6.0 + 4.0 + 2.0)

Extra outputs may subsequently be added. One single unit can be constructed to supply a theoretically unlimited number of motors up to a maximum of 30kW.

Enclosures are either polyester or steel, to IP55. IP65 on request.
Basic system size is 600 x 400 x 220mm.

CUEL LIMITED has close university associations. CUEL specialises in products of applied technologies (which must be unique in some way to be eligible for the programme) and the licensing of those technologies. The latest "Technology Bulletin" is available on request.

GLENTRONIC **GLENPHASE**

SINGLE TO THREE PHASE POWER IN ONE EASY STEP

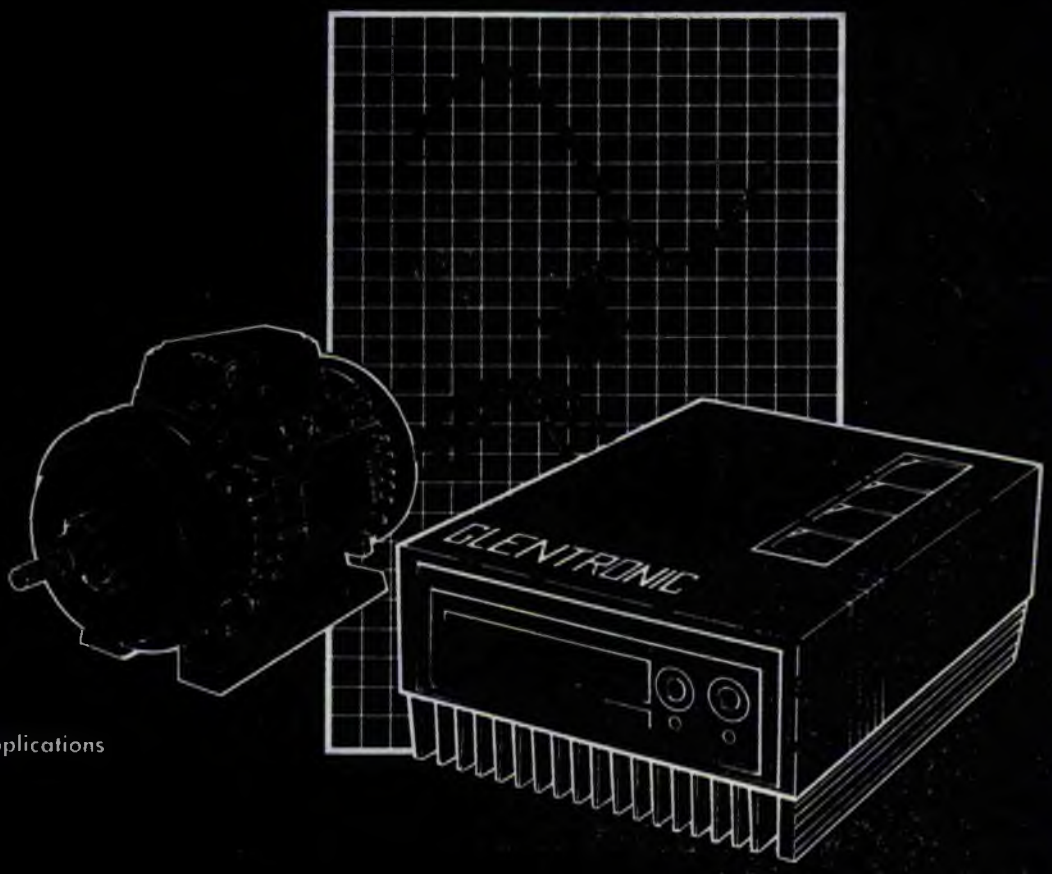

APPLICATIONS

Heating and Ventilation
Mechanical Handling
Pumping Applications
Agriculture
Bulk Materials Transfer
Cleaning Equipment
Frequency Conversion Applications

GLENPHASE

SINGLE TO THREE PHASE POWER IN ONE EASY STEP

By means of the latest G.T.O. solid state technology, the Glenphase range of single to three phase advanced conversion units provides the ability to:

- Generate three phase output from a single phase input with a high degree of accuracy resulting in reduced power line installation costs – plus the ability to use existing single phase supplies.
- Use soft start and soft stop facilities reducing start-up current surge to a maximum of 1.15 x FLC, giving power saving, reduction of electrical or mechanical stress on motors and therefore reducing maintenance costs.
- Maintain constant torque from the motor throughout its speed range, thus eliminating transformers and starters of all kinds and further reduces maintenance costs.
- Control acceleration and deceleration, both of which are user-adjustable to provide optimization of individual system characteristics.

OPTIONS

Glenphase provides further control and monitoring options for example: variable speed control, motor reversing, analogue and digital inputs and interfacing to PLC's and Bussed Control Systems. Also the provision of signal indicators in addition to frequency conversion.

Glenphase applications include: Pumps, blowers, fans, mixers, agitators, conveyer systems, grain/silo dryers, packing machines, centrifuges etc.

PROTECTIVE FEATURES

Current Limit:
Limits current delivered by the unit to prevent damage to the drive. This feature is user-adjustable.

Over-current Trip:
Protects the unit from damage under fault conditions. This level is factory set at 4 times the maximum current capability of the unit.

Frequency deviation: better than 1%
Phase displacement: better than 0.5%
Voltage displacement: better than 1%

	MAX MOTOR OUTPUT	MAX CURRENT	SUPPLY VOLTAGE	OUTPUT FREQUENCY	OUTPUT VOLTAGE
GLENPHASE 40	3 Kw	6 A	208/240 V 50/60Hz	(50/60Hz)	380/415 V 3ø
GLENPHASE 75	5.5 Kw	12 A			
GLENPHASE 150	11 Kw	22 A			
GLENPHASE 250	18.5 Kw	35 A			

These models are also available with variable speed control.

DISTRIBUTED BY:-
LANE INTERNATIONAL LTD
LYGON COURT,
HEREWARD RISE,
HALESOWEN,
WEST MIDLANDS. B62 8AN ENGLAND
TEL: 021 550 6368 TELEX: 338679

Gleutronic Ltd
Young Square
Bracefield Industrial Park
Livingstone EH54 9BX
Tel. 0506 414333
Telex 728191

CAP ZORO™

ENERGY-CONSERVING SINGLE TO THREE PHASE MOTOR CONTROL PANELS

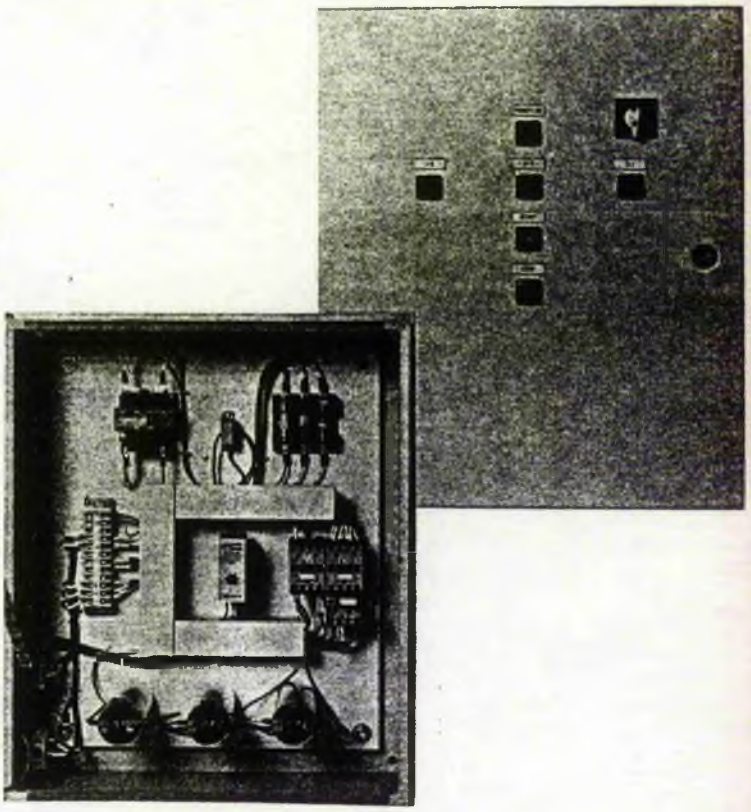

RUNS STANDARD THREE-PHASE MOTORS FROM A SINGLE-PHASE SOURCE.

CLOSE TO 100% OF REGULAR THREE-PHASE SERVICE STARTING TORQUE.

QUICK ENERGY-SAVING PAYBACK COMPARED TO SINGLE-PHASE MOTORS OR ROTARY PHASE CONVERTERS.

NO DOWN-RATING NEEDED.

SYSTEM AVAILABLE FOR MULTIPLE MOTOR INSTALLATIONS.

ACROSS-THE-LINE STARTING, OR AS REQUESTED.

COMPLETE MOTOR CONTROL AND POWER PANEL IN ONE ENCLOSURE.

LOWER STARTING CURRENT THAN ROTARY PHASE CONVERTERS OR SINGLE-PHASE MOTORS.

CAP ZORO™

144 SOUTH PARK BOULEVARD
GLEN ELLYN, ILLINOIS 60137
(312) 858-8200

ıe CAPTORQ system runs standard three-phase induction motors off a single-phase supply. The system has limits on neither maximum horsepower r on the number of motors which may be connected.

ıe product is designed, engineered, manufactured and supported in the U.S.A., and installed around the world.

here a customer already has a 'phase converter', the CAPTORQ system may be substituted. It can pay for itself in 12 months on **KW energy savings** way of much **higher efficiency.**

ıstallation is simple. Connect the single-phase supply to the panel disconnect switch. Connect the motor to the starter. No extra components are eded to make the system work.

ıe system is also available without a starter where the customer has one - or it is supplied with the motors.

RINCIPLE OF OPERATION

ıe CAPTORQ system uses variable capacitance to provide torque to start a three-phase standard induction motor on a single-phase supply.

ıe system applies a second, smaller amount of capacitance to maintain running torque, and ensure balanced operation.

ıe system is probably unique in two ways:

Research has produced a method of balancing the requirements of a motor(s) when starting with its running condition.

Research also produced a type of capacitor which allows a three-phase induction motor to be started across-the-line as if on a utility three-phase service, and develop close to 100% of three-phase starting torque.

ıpacitors are switched in and out according to the motor power requirements, and are not connected directly across the motor. Starting torque capacitance switched out once the motor attains running speed.

ıe capacitors were specially developed to withstand the stress of repeated across-the-line a.c. motor starting. Electrolytic, power factor, commutation metalized paper capacitors, for example, can be dangerous and/or cause nuisance failures.

LTERNATE PHASE CONVERTERS

ıe CAPTORQ system gets more motor HP out of available single-phase current than other designs, and is probably the only "converter" on the arket which is suitable for two-speed motors.

requires no manual starting or phase balancing.

:her "phase converters" of both the static and rotary variety tend to suffer from poor starting torque (unless grossly oversized), high starting current, w efficiency and unsuitability for repeated across-the-line starting (owing to capacitor limitations).

ıus, most other "converters" tend to be of limited use where single-phase current from the utility is restricted.

MOTOR HP	STARTING CURRENT ON SINGLE-PHASE SUPPLY			AVERAGE ANNUAL SAVING WITH CAPTORQ
	CAPTORQ	SINGLE-PHASE MOTOR	ROTARY CONVERTER	
1½	29 A	59 A	50 A	$456
2	40 A	79 A	62 A	$604
3	57 A	125 A	87 A	$851
5	85 A	165 A	140 A	$1,418
7½	120 A	230 A	195 A	$2,127
10	164 A	285 A	260 A	$2,835
15	245 A	460 A	390 A	$4,253
20	325 A	570 A	520 A	$5,671

OTES:

Starting current values are not guaranteed. Values are averages from utility and laboratory tests, and motor manufacturers.

Energy savings are not guaranteed. Values are based on efficiency figures from utility and laboratory tests, compared to a rotery phase converter or single-phase motor performimg equivalent work. $0.10 per KWH. (single-phase rate).

Many rotary systems also consume energy even when motors are switched off. The working life of single-phase motors and rotary phase converters is generally significantly shorter. Saving may be greater if motor ever run at less than full load.

Rotary systems are the oldest and most common type of "phase converter" in the U.S.

CAPTORQ is available through 150 HP.

TANDARD DATA - ALL HORSEPOWERS

ONTROL VOLTAGE - 220-240VAC. (120V on application)

PERATING RANGE: -40 F - +120 F

IOTOR CONTROL CAPACITORS: Film with non-pcb impregnant.

/ORKING LIFE: 94% of systems run unimpaired after seven years of normal duty. Contacts may need earlier replacement.

NDUCED HARMONIC DISTORTION ON VOLTAGE: Under 0.1%

COMPONENTS - Standard factory-selected brands. Customer preferences can be accommodated, but price may change. The brand supplied may be substituted with an equivalent without losing performance.

Spare capacitors and control modules must be obtained from the factory.

TORQUE: OVER 80% of three-phase across-the-line value.

STARTS PER HOUR: Maximum 60.

CAPTORQ™

FULL-TORQUE REDUCED-CURRENT MOTOR STARTER PANELS

- STANDARD FULL-VOLTAGE ACROSS-THE-LINE STARTER
- FULL TORQUE AND POWER TO MOTOR
- REDUCES STARTING CURRENT TO 35 TO 65% OF NORMAL ACROSS -THE-LINE INRUSH CURRENT
- POWER FACTOR CORRECTION AT NO CHARGE (POSSIBLE POWER BILL SAVINGS)
- SUITABLE FOR MULTIPLE MOTORS
- MAY BE RETRO-FITED
- IDEAL FOR HIGH-INERTIA MOTORS
- STANDARD SYSTEMS 30 THROUGH 800 HP
- COUNTERACTS LINE VOLTAGE DROP

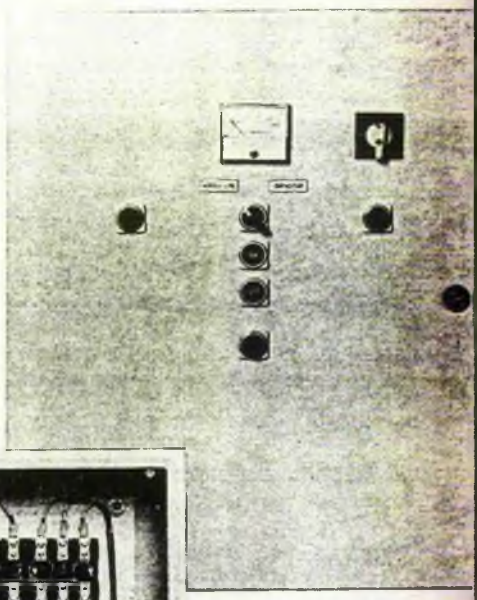

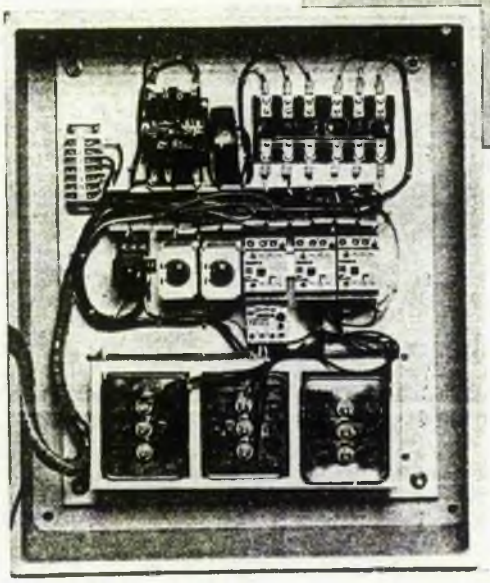

CAPTORQ™

144 SOUTH PARK BOULEVARD
GLEN ELLYN, ILLINOIS 60137
(312) 858-8200

The CAPTORQ across-the-line reduced-**current** capacitive starting system starts standard induction motors across-the-line with a standard starter, but a much lower current.

The CAPTORQ system was designed to accommodate applications which conventional reduced-current starting methods (reduced-**voltage**) cannot meet. The main reason is torque.

PRINCIPLE OF OPERATION

The CAPTORQ system reduces starting and running current by switching specialized capacitors into the motor circuit. Unlike reduced voltage starting, which achieves a reduction in starting current at the expense of torque and motor horsepower - and is not suitable for motors with much inertia - the CAPTORQ system reduces starting current without loss of torque and horsepower.

The principle of the CAPTORQ system was introduced by major U.S. corporations in the 1970's. Although some corporations still build such systems, they decided not to pursue the technology on a wide commercial basis owing to the cost of production. The CAPTORQ system makes good use of a breakthrough in capacitor technology from the early 1980's, which makes capacitive starting highly cost-effective in comparison to reduced-voltage starting.

TORQUE

The motor(s) receives full across-the-line torque. In a situation where a motor would otherwise cause the line voltage to drop, the capacitance can actually raise the line voltage.

With across-the-line and CAPTORQ capacitive starting, motor acceleration is based upon the motor load. Unlike autotransformer starting, where there are two shock points during the motor acceleration cycle, with CAPTORQ starting there is only one.

APPLICATIONS

CAPTORQ capacitive starting is ideal for high-inertia loads, especially where frequently started, or with rapid-changing duty cycles, such as a load applied after start.

The no-cost power factor correction feature may also save on power bills, and allow more motors to be operated on the same service.

In addition to almost any positive displacement load, good examples are: (loaded) conveyors, crushers, compressors, deep hole pumps, mills, fans, food mixers, and hoists.

BEFORE CAPTORQ

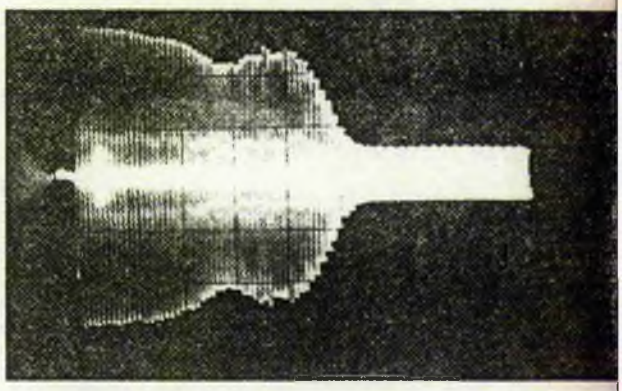

AFTER CAPTORQ

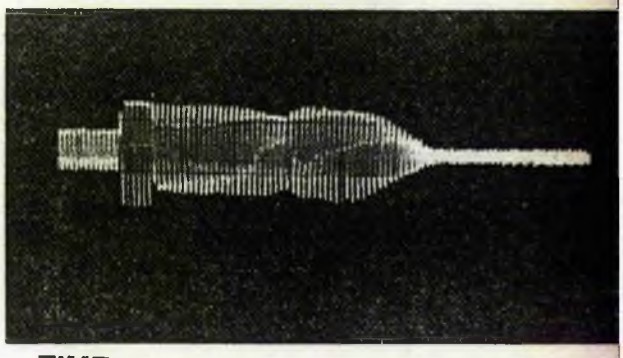

	TYPICAL REDUCED-VOLTAGE (80% of Full Voltage) STARTING	CAPTORQ FULL-VOLTAGE CAPACITIVE STARTING
TORQUE (1)	64%	At least 100% (5)
% OF ACROSS-THE-LINE CURRENT	68%	See Tables
MAXIMUM STARTS/HOUR	15 (2)	60 (4)
SURGE CURRENT REDUCTION (3)	Generally none	Automatic (6)
ENERGY-SAVING PAY-BACK	Generally none	Standard (7)
SUITABLE FOR JOGGING	No	Yes (8)

NOTES (SEE NUMBERS IN PARENTHESES)

1. Percentage of full-voltage across-the-line torque.
2. Above 200HP, typically 3.
3. After motor has reached full speed.
4. Re-starting before motor completely stops may significantly shorten working life.
5. CAPTORQ capacitive starting partly or completely corrects line voltage drop.
6. Load fluctuation surge currents automatically reduced. Current control capacitors switched into circuit. Factory pre-set at 1.5 times full-load current (approximately). User-variable on request.
7. Refer to utility and CAPTORQ for advice for energy savings other than power factor correction.
8. Select magnetic starter two sizes greater than motor HP. Select 300HP starter for 200HP motor, for example.

CONTROL CIRCUIT: 120V or 240V (120V supplied unless specified).
OPERATING RANGE: -40 F - +120 F.
MOTOR CURRENT-CONTROL CAPACITORS: Custom-made film-type. Non-pcb impregnant. Fitted with UL-recognized switch to avoid rupture and provide visible indication of failure.
CAPACITOR LIFE: 94% still functional after seven years operation at motor voltage.
COMPONENTS: All items switching or breaking motor or capacitor current are UL-listed. Factory-selected brands. Customer brand preference may be accommodated. Prices may change.
SPARE PARTS: Standard magnetic components. Factory brand may be substituted by other equivalent without impairing performance. Capacitors and control modules only from factory.
CONTACT LIFE: Average 1.5 million operations (from manufacturer's catalog).
CAPACITORS CONNECTION: Not directly across motor termanals. All capacitors disconnected when motor stopped.

THE BASIC PANEL INCLUDES:

- Indoor Enclosure.
- Power Factor Correction to 93-99%.
- Capacitor Switching Contactors.
- Current Reduction.
- Pushbuttons.
- Surge Suppression.
- Pilot Light.
- Control Module.
- Current Metering.

The appropriate magnetic starter and non-fusible / fused disconnect switch / circuit breaker must be separately selected.

POWER CONVERTER

3-PHASE POWER from Single-Phase Lines by RONK

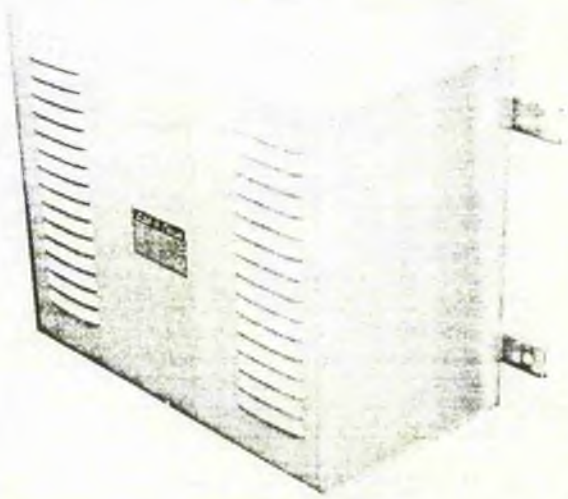

Add-A-Phase is a rugged, high efficiency power converter that is capable of producing balanced three-phase power for one or two motor systems of up to 150 H.P. **from single-phase lines** or from an auxiliary single-phase generator.

This Ronk static phase conversion unit has been used successfully by utilities, co-ops, industry, farm equipment manufacturers, rural communities and pumping station manufacturers throughout the nation since 1952, providing long and dependable power service in all types of environments.

It is guaranteed to develop full load rating of the motor, plus normal overload, and it automatically limits inrush current when the motor is starting, a critical factor on many rural lines.

The Add-A-Phase can be balanced at a fixed load to provide current balance matching three-phase systems. This means maximum motor life, a prime concern when using a large, expensive motor.

The standard Add-A-Phase line offers customers off-the-shelf units to match a wide range of applications. For special applications, Ronk offers the Duo Add-A-Phase with which you can operate two 3-phase motors from single-phase lines. A pad mounted Add-A-Phase is supplied for ratings over 30 HP. Also available are step-up and step-down Add-A-Phases which eliminate the need for external transformers.

SYSTEM ANALYZER DIV
RONK ELECTRICAL INDUSTRIES, INC.
106 East State Street • Nokomis, Ill. 62075
217/563-8333

ADD·A·PHASE

for FARM and INDUSTRY

lanced 3-Phase Power from Single-Phase Lines for Wide Variety of Applications:

op Drying	Oil Pumping
igation	Oil Refining
itch Drying	Oil Field Water Flooding
o Unloading	Booster Pumps
ay Drying	Machine Shop Equipment
ain Augers	Air Conditioning

. . .and many others

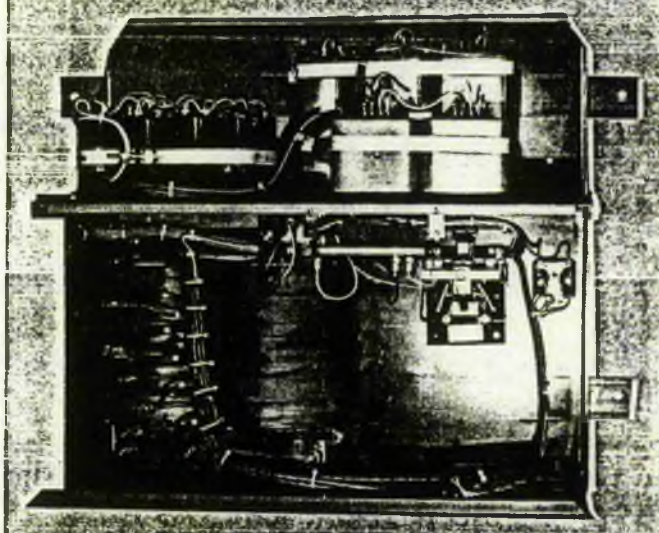

RONK has been Converting Single-Phase to Three-Phase Power Since 1952

"S" MODEL ADD-A-PHASE
-Standard Motors-Normal Torque Requirements

SINGLE-PHASE AMPERAGE VALUES FOR ADD-A-PHASE MODELS			
	2S/3S		4S
HP	RUNNING CURRENT	STARTING CURRENT	
1	5	APPROXIMATELY 300% OF FULL LOAD RUNNING CURRENT AMPS	ALL VALUES ½ OF THOSE GIVEN FOR CORRESPONDING H.P. IN 2S/3S COLUMN
1½	7		
2	9		
3	13		
5	20		
7½	30		
10	40		
15	60		
20	75		
25	95		
30	110		
40	140		
50	170		
60	200		
75	260		
100	340		

Ronk Electrical Industries pioneered single to three-phase power conversion with the introduction of Add-A-Phase in 1952. It was the first practical phase converter on the market. This unit is still the most widely used, most dependable static phase converter in use.

Three-Time Winner of Coveted Silver Switch Award

The Silver Switch Award is presented by Farm Electrification Council annually. Ronk Electrical Industries is the first company in the manufacturers category to receive three of these highly prized awards. The first of which was in 1966 for the development of the ADD-A-PHASE to 75 H.P.

For multiple-motor applications and widely varying loads, Ronk offers a complete line of rotary converters from the economical Roto-Con® / Mark II to the patented ROTOVERTER®. Write for complete information.

vailable From

SYSTEM ANALYZER DIV.
RONK ELECTRICAL INDUSTRIES, INC.
106 East State Street • Nokomis, Illinois 62075
217/563-8333

Printed in U.S.A.

available as OEM module

AUTOMATIC DYNAMIC CURRENT AND ENERGY REGULATION SYSTEMS

Full-Torque Soft Starters Save Energy Too

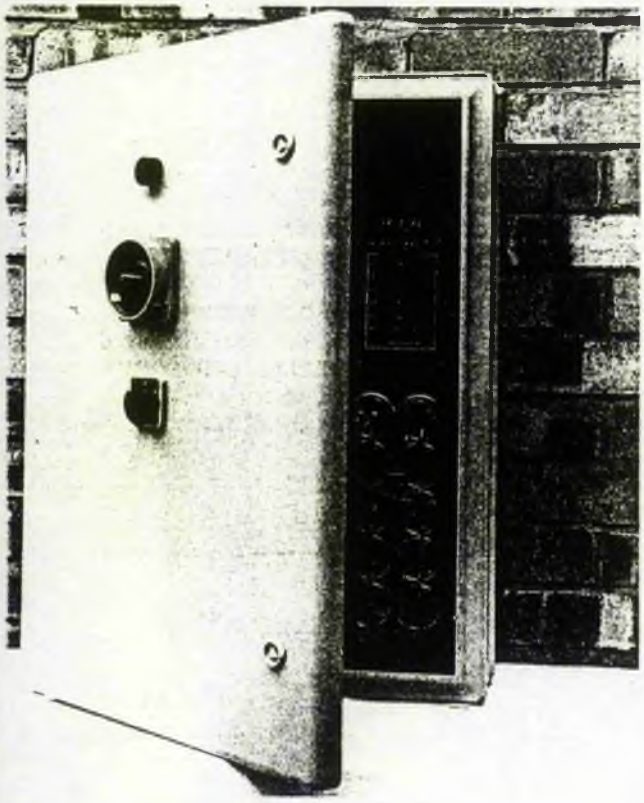

Developed by university experts in motor and energy control, the CUEL Dynamic Regulator is an advanced performance dimension, giving adjustable "SOFT STARTING" (current reduction) and power factor compensation (ENERGY SAVING) from the same box.

It is easily retro-fitted to mains or generating set networks.

Thus, "soft starting" has a pay-back period.

Reduced current starting and running are achieved by cutting the machine energy demand, maximising **useful** power consumption.

Unregulated industrial and agricultural machines can create overcurrents, especially on starting. This may overburden the supply (or generating set) network through voltage drops, consuming power unnecessarily. Frequent starting and/or light running aggravates the problem.

SELECTED APPLICATIONS (System A or System B)

Motor Loads
Agricultural or Industrial Machines
Generating Sets

→

- Pumps
- Air-Conditioning
- Refrigeration Plant
- Machine Tools
- Process Plant
- Hoists/Cranes
- Variable Speed Drives
- Welders
- *— Induction Heaters
- CUEL Static Phase Converters (combinable)

→

Small Users

Any network benefitting from reduced current or lower energy consumption

Factories

---

wer Control Engineering from:—

JEL LTD.
Tulip Tree Avenue
nilworth
gland CV8 2BU

lephone — 0926-54293 Telex 311248

*40% efficiency enhancement on running also.

SYSTEM A

ıe soft-starting time loop permits direct-on-line starting (manual or automatic) and is user-variable according to achine power. It is viable even for loads down to 2.5kW.

ɔmpared to many soft starters (no energy-saving bonus) price and running costs are low. Torque (starting speed) not lost. More machines may be started/run simultaneously for the same mains or generating set site rating, ıproving productivity and reducing maintenance.

ECTRONIC OPTIMISATION

ıe Static Transient Electronic Capacitance Optimiser reacts to changed load conditions, applying special high-rrent continuous start capacitors. Motor performance and life (less motor winding stress) are enhanced, with ınimal system power loss.

ır the electricity supplier, Dynamic Regulators improve voltage stability, especially on long (rural) transmission es.

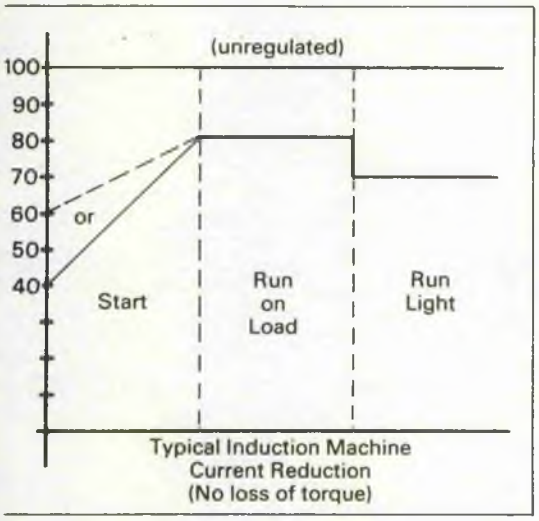

SYSTEM B

The Dynamic Regulator is a highly-effective power factor compensation system, compensating the **start** condition too (when energy demand is highest) – unlike many other system

System B is custom-engineered: pre-programmable with automatic energy factor calculation and boost control for multiple outputs of various power ratings, achieving near-unity power factor. Re-setting is automatic in the event of load reduction. (System A is standard for small numbers of loads).

CUEL LIMITED has close university associations. CUEL specialises in products of applied Electrical and Electronic Engineering Technologies (which must be unique in some way to be eligible for the programme) and the licensing of those technologies.

SENTIAL TECHNICAL DATA

ɔMBER OF (a.c.) MACHINES CONNECTABLE	**System A** – small number, (similar power rating) **System B** – Any
ANDARD POWER RATINGS **ıriable according to precise needs)**	**System A** – 1 to 500kW (1.34 to 670HP) **System B** – 50kW (67 HP) upwards.
\VE FORM	Sine wave. No harmonic distortion on basic unit.
\CHINE VOLTAGES (1 or 3 phase)	200–250, 380–415, 440–460, 575v at 40/50/60Hz
ARTING/RUNNING CURRENT REDUCTION	Up to 60%. More loads may be started simultaneously than on unregulated networks.
TAINABLE POWER FACTOR	Nominal 1.0 (100%) under all load conditions. Standard version based on typical induction machine with 0.8 (80%) power factor run, 0.6 (60%) start, 0.7 (70%) light run. Variable to accommodate less efficient loads.
WER CONSUMPTION	Below 1% – compare with other soft start devices.
ARTING	Direct-on-line no problem, including 2 speed.
RQUE	At least 100% of that on mains unregulated supply. Downward voltage regulation when starting heavy loads avoided.
NFIGURATION	Simple to install stand-alone control box.

GLENTRONIC

GLENPHASE

SINGLE TO THREE PHASE POWER IN ONE EASY STEP

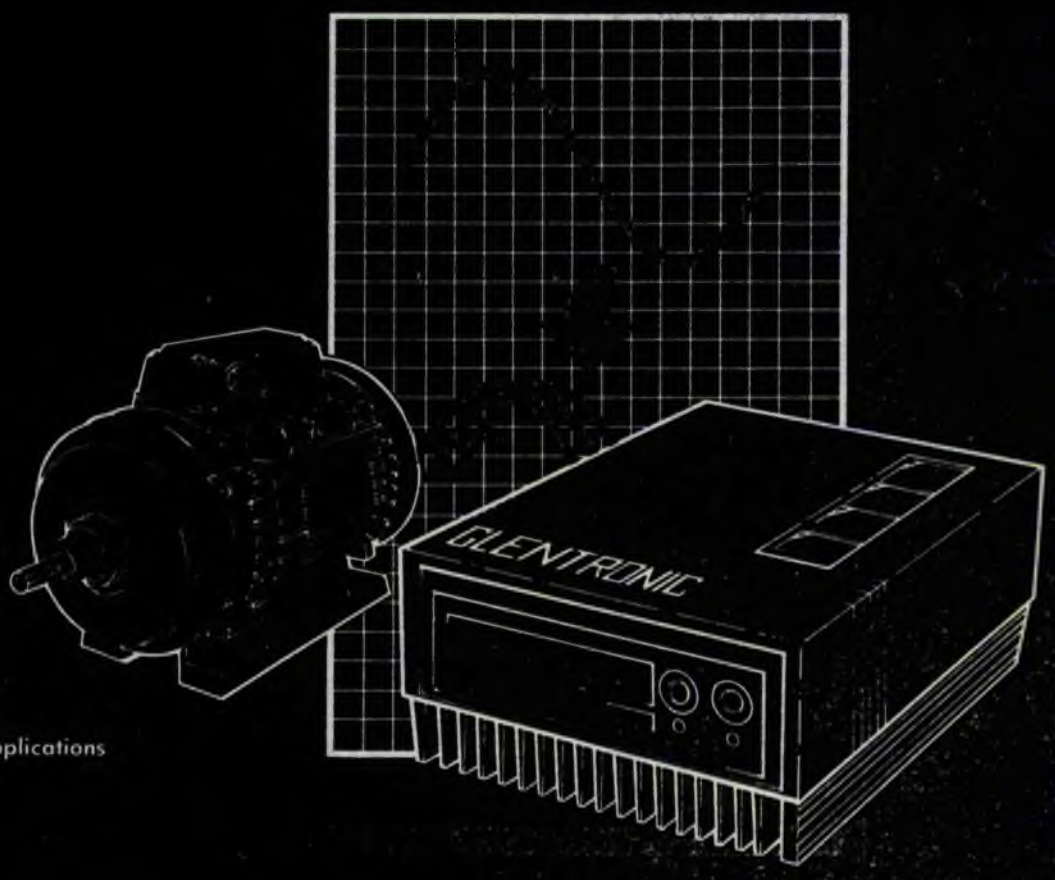

APPLICATIONS

Heating and Ventilation
Mechanical Handling
Pumping Applications
Agriculture
Bulk Materials Transfer
Cleaning Equipment
Frequency Conversion Applications

GLENPHASE

SINGLE TO THREE PHASE POWER IN ONE EASY STEP

By means of the latest G.T.O. solid state technology, the Glenphase range of single to three phase advanced conversion units provides the ability to:

- Generate three phase output from a single phase input with a high degree of accuracy resulting in reduced power line installation costs – plus the ability to use existing single phase supplies.
- Use soft start and soft stop facilities reducing start-up current surge to a maximum of 1.15 x FLC, giving power saving, reduction of electrical or mechanical stress on motors and therefore reducing maintenance costs.
- Maintain constant torque from the motor throughout its speed range, thus eliminating transformers and starters of all kinds and further reduces maintenance costs.
- Control acceleration and deceleration, both of which are user-adjustable to provide optimization of individual system characteristics.

OPTIONS

Glenphase provides further control and monitoring options for example: variable speed control, motor reversing, analogue and digital inputs and interfacing to PLC's and Bussed Control Systems. Also the provision of signal indicators in addition to frequency conversion.

Glenphase applications include: Pumps, blowers, fans, mixers, agitators,conveyer systems, grain/silo dryers, packing machines, centrifuges etc.

PROTECTIVE FEATURES

Current Limit:
Limits current delivered by the unit to prevent damage to the drive. This feature is user-adjustable.

Over-current Trip:
Protects the unit from damage under fault conditions. This level is factory set at 4 times the maximum current capability of the unit.

Frequency deviation: better than 1%
Phase displacement: better than 0.5%
Voltage displacement: better than 1%

	MAX MOTOR OUTPUT	MAX CURRENT	SUPPLY VOLTAGE	OUTPUT FREQUENCY	OUTPUT VOLTAGE
GLENPHASE 40	3 Kw	6 A	208/240 V 50/60Hz	(50/60Hz)	380/415 V 3ø
GLENPHASE 75	5.5 Kw	12 A			
GLENPHASE 150	11 Kw	22 A			
GLENPHASE 250	18.5 Kw	35 A			

These models are also available with variable speed control.

DISTRIBUTED BY:-
LANE INTERNATIONAL LTD
LYGON COURT,
HEREWARD RISE,
HALESOWEN,
WEST MIDLANDS. B62 8AN ENGLAND
TEL: 021 550 6368 TELEX: 338679

Glentronic Ltd
Young Square
Bracefield Industrial Park
Livingstone EH54 9BX
Tel. 0506 414333
Telex 728191

AUTOMATIC STATIC SINGLE TO THREE PHASE CONVERSION SYSTEMS

Electronically-controlled system for **separately** driving two three phase motors (single or two speed machines) from a single phase supply (picture).

MANUFACTURED IN THE UNITED KINGDOM AND UNDER LICENCE AT POINTS AROUND THE WORLD

SELECTED USES

- **Pumps**
- **Compressors**
- **Sheep Shearing Equipment**
- **Refrigeration Plant**
- **Variable Speed Drives**
- **Machine Tools**
- **Food Processors**
- **Hoists**
- **Welders**

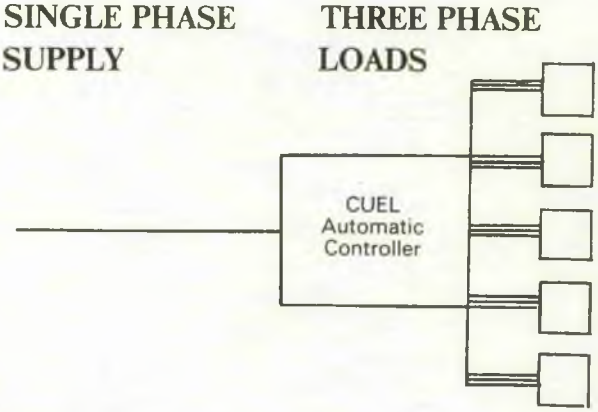

Power Control Engineering from:–

CUEL LTD.
12 Tulip Tree Avenue
Kenilworth
England CV8 2BU

Tel. 0926-54293 Telex 311248

Local agent and/or manufacturer:–

E.D.A. Techniques Used to Develop a Cycloconverter Drive System.

Mr E.B. Patterson, Dr D. Morley.

Nottingham Polytechnic, Nottingham, UK.

ABSTRACT

This paper illustrates the advantages arising from the use of Electronic Design Automation tools in the development of digital control circuits for cycloconverter induction motor drives. Time critical circuits close to the waveform generation in power electronic applications may be closely simulated, giving an accurate representation of the performance of the expected hardware without recourse to physical prototyping. However, more sophisticated and flexible solutions for the control strategy may also be developed using simulated hardware models, thus allowing an extremely high confidence in the final product before committing to experimental hardware. The 'right first time' ethos which is predominant in the integrated circuit environment may now be expanded to encompass power engineering digital control systems design. The process is illustrated by practical design examples implemented by the authors.

INTRODUCTION

Electronic Design Automation (EDA) techniques have been used by electronics engineers for the production of semi-custom and custom integrated circuits with great success for years. The present authors have developed this technique of using EDA software tools to design and implement digital signal processing circuit in Application Specific Integrated Circuits (ASIC) for controlling power circuits [1,2].

Low-level, high speed hardware to implement the control functions in power electronic systems are an ideal candidate for the application of EDA tools [3]. The Computer Aided Design (CAD) software supplied by Mentor Graphics running on Apollo workstations, enables the design and evaluation of these complex digital circuits within the workstation environment without the requirement for physical hardware at this stage. A knowledge of available technologies and EDA techniques for design, simulation, layout, PCB production and verification is required for the successful development of the specialised microelectronics hardware.

The cycloconverter is a typical example of a power control system which benefits from the application of these techniques, being a relative complex digital circuit susceptible to accumulative delays. The alternative prototype method involves the application of three phase voltages to verify circuit operation with possible destructive consequences on the power electronic output devices.

DESIGN METHODOLOGY

The design of electrical systems has always had many different design methods, most of which are similar to the one shown in **figure 1**. With the advent of EDA software a new design methodology has been developed to take advantage of simulation techniques for the design of electronic/electrical systems.

A comparison of the traditional methods of design with the EDA method illustrates the advantages of circuit and board level simulation in the production of a practical system.

The traditional design method is illustrated in **figure 1**, in which the engineer begins with the idea then normally proceeds to the circuit design stage on paper. The designer would then continue through to the prototype stage using any of the traditional construction methods. This prototype design would be tested and verified against its specification. At this point if any conceptual fault is found then it would have to be rectified by a return to the design stage and the process repeated.

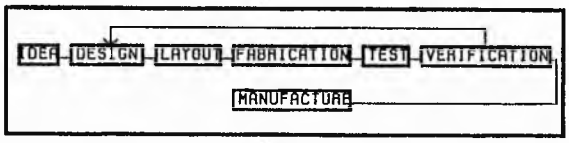

Figure 1 Traditional Method

The design cycle can be reduced considerably by removing three parts of the design cycle before the design is verified. This technique is known as the simulation method, and allows a product to be produced for the market in a much shorter time than using traditional methods. The simulation method, illustrated in **figure 2** below, allows the development of the design using the CAD system whereby verification is carried out by simulating the circuit design using software models. At this point any design faults should be identified and rectified without going through the costly path of prototype construction for verification. The simulation method allows the design to be about 98% certain of working correctly first time.

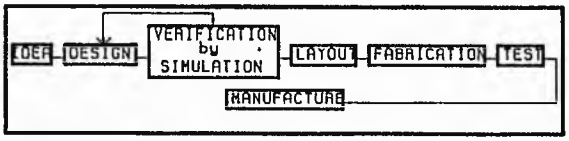

Figure 2 Simulation Method

Board Level Simulation

The previously simulated ASICs or custom Integrated circuits may be combined with standard components to produce a sub, or main, system which may also be verified by simulation prior to the production of the PCB artwork. The board can be simulated on the CAE system using QUICKSIM and smart part models produced by Mentor Graphics and Logic Automation (microprocessors). This method allows complete systems to be verified before the cost of producing and testing a PCB is incurred. The PCB layout tools also check the layout process with respect to the original circuit diagram generated with the software which reduces the problems inherent in hand layout or netlist input systems.

Design Team Approach

The variety of software that is integrated into the CAE environment allows multi-disciplinary teams to work in their own environment whilst maintaining a common pool of information which is used to simulate the whole system. Thus improving the efficiency of the design process by integrating the expertise of the specialists into this enabling environment.

Practical Examples

The EDA methodology will be illustrated with examples of two gate arrays developed for power electronic control of a cycloconverter induction motor drive. Two digital ASICs were developed to replace the Microprocessor/ASIC cycloconverter induction motor drive developed in the department. The block diagram of the original system is illustrated in **figure** 3.

DESIGN PROCEDURE FOR DEVELOPING THE TDAC SYSTEM

The Microprocessor/ASIC [1], design solution produced in the Department was examined to determine which parts of the design could be implemented in a 3 micron CMOS digital gate array supplied by MCE.

Design Partitioning

The block diagram in **figure** 4 shows the partitioning of the control system, this was used to determine which parts of the cycloconverter's control system could be implemented in 3 micron CMOS gate arrays supplied by MCE. The following method was used to produce the ASICs for the cycloconverter:
Seven individual functions within the circuit were identified: The power and analogue circuits; consisting of the thyristor stack, zero crossing detector, frequency multiplier cannot be implemented in the gate array. The look-up tables; containing the Sine and Arc Cos data, were efficiently implemented in EPROM. However the data manipulation and the generation of the delayed trigger signals were ideal candidates for scrutiny. A strategy was developed which enabled the Three Phase Reference Waveform Generator (TPRWG) and Counter/Comparator/Pulse Amplifier (CCPA) ASICs to be redesigned to perform all the operations of the microprocessor. The sections shown on **figure** 3 which are implemented in the 3 micron CMOS gate arrays supplied by MCE are :-

- **The Three Phase Reference Waveform Generator (TPRWG) with zero crossing emulation.**
- **The 18 off Counter/Comparator/Pulse Amplifier (CCPA) with data transfer synchronization.**

In developing the new TPRWG from the microprocessor version 79 pins were required, this included the outputs of the zero crossing emulator used in testing the operation of the ASICs. These circuits were implemented in the 3 micron CMOS gate array because of the high pin count. The internal control logic was modified to give a steer output to synchronize the data transfer between the TPRWG and the CCPA. The CCPA circuit was redesigned to remove the decode circuit for the microprocessor and implement the steer synchronization for data transfer. The design was developed so that one design of the CCPA ASIC could be used for both the positive and negative thyristor stacks.
This method allows three ASIC gate arrays to replace the control logic and microprocessor of the full cycloconverter drive system.

ASIC Design and Development

The three phase reference waveform generator and counter/comparator/pulse amplifier were produced using Mentor Graphics EDA design tools NETED and SYMED in conjunction with MCE's 3 micron libraries.

The second level schematic diagram for the TPRWG is shown in **figure** 5. Each of the five modules; multiplier, latchout, divide by 512 counter, divide by 3 and steering logic were produced as modules. The technique of top down hierarchical design was used to produce the overall solution. After each module was designed it was simulated using QUICKSIM to evaluate it for correct operation. The whole ASIC design was then integrated into one sheet and simulated as a circuit using QUICKSIM.

The design of the CCPA circuit for the ASIC was produced in a similar manner to the design of the TPRWG. **Figure** 6 shows the top-level schematic diagram of the design, it consists of three identical modules with steering logic. The design of each module is illustrated in **figure** 7, which consist of the following five parts; three 8 bit data registers, 8 bit comparator, 8 bit counter, pulse control logic and the fire pulse generation circuit. All of the modules were produced using NETED and SYMED and simulated by QUICKSIM.

After the design and simulation of each individual gate array the ASICs were integrated into the complete Total Digital ASIC Controller (TDAC) which is shown in **figure** 9. This consists of the TPRWG connected to the SIN and ARC COS look-up EPROMs programmed with the control data and the interconnection to the two CCPA ASICs. This allows a system level simulation to be carried out which verifies the operation of the control strategy for cycloconverter. The results of the circuit simulation are shown in **figure** 11, this confirms the operation of the of the control strategy by producing 32 firing pulses with the negative pulses sequence delayed by 180° which is the main requirement for the cycloconverter's operation.

The power electronics used to control the mains supply to the induction motor (**figure** 10) may now be designed using the ACCUSIM library parts which allow the analogue simulation and verification of these power components. Further, the EDA environment enables the integration of the digital control system and the power electronics so that the whole of the control system may be developed without producing a physical prototype. Once satisfactory simulation has been achieved the EDA system allows the direct production of the PCB artworks for the prototype system. The boards may then be produced in parallel with the gate array fabrication.

Models of the induction motor are now being developed which will also integrate into the EDA environment. This will allow the simulation of the complete control system including the digital, analogue circuits and machine.

The information resulting from the digital simulation may be used by the analogue simulator ACCUSIM enabling the investigation of the thyristor and machine response. Thus a greater confidence in the operation of the proposed design may be achieved.

CONCLUSIONS

The experience of using these EDA tools has convinced the authors that the design and verification of complex digital signal processing control systems for power electronic control applications can be executed more efficiently than previously and with a higher level of confidence. Timing requirements in this environment are forcing the development of more complex circuits which must be implemented on dedicated integrated circuits, the breadboarding of such implementations is impractical and unrepresentative of the production device. The accurate simulation of the physical circuit within the EDA environment is essential to maintain the quality of product and decrease the development time.

Future developments of present work indicate that the full system modelling is feasible and will include the simulation of the elctrical machine. This will extend the bounds of 'right first time' to encompass areas which have traditionally been closed to this technology and dependent upon 'manufacture in hope' technique.

REFERENCES

1. E.B. Patterson **ASIC Design For Cycloconverter Drives.**
   P.G. Holmes 24th Power Engineering Conference,
   Belfast 19 – 21 September 1989.
2. E.B. Patterson **ASIC Control Strategies for Cycloconverter**
   D. Morley **Drives.**
   P.G. Holmes 6th Conf. on Power Electronics & Motion Control
   L. Haydock Budapest, Hungary, October 1 – 3 1990.
3. W.Leonhard **High Performance Digital Motion Control With AC–Servo Drives.**
   6th Conf. on Power Electronics & Motion Control
   Budapest, Hungary, October 1 – 3 1990.

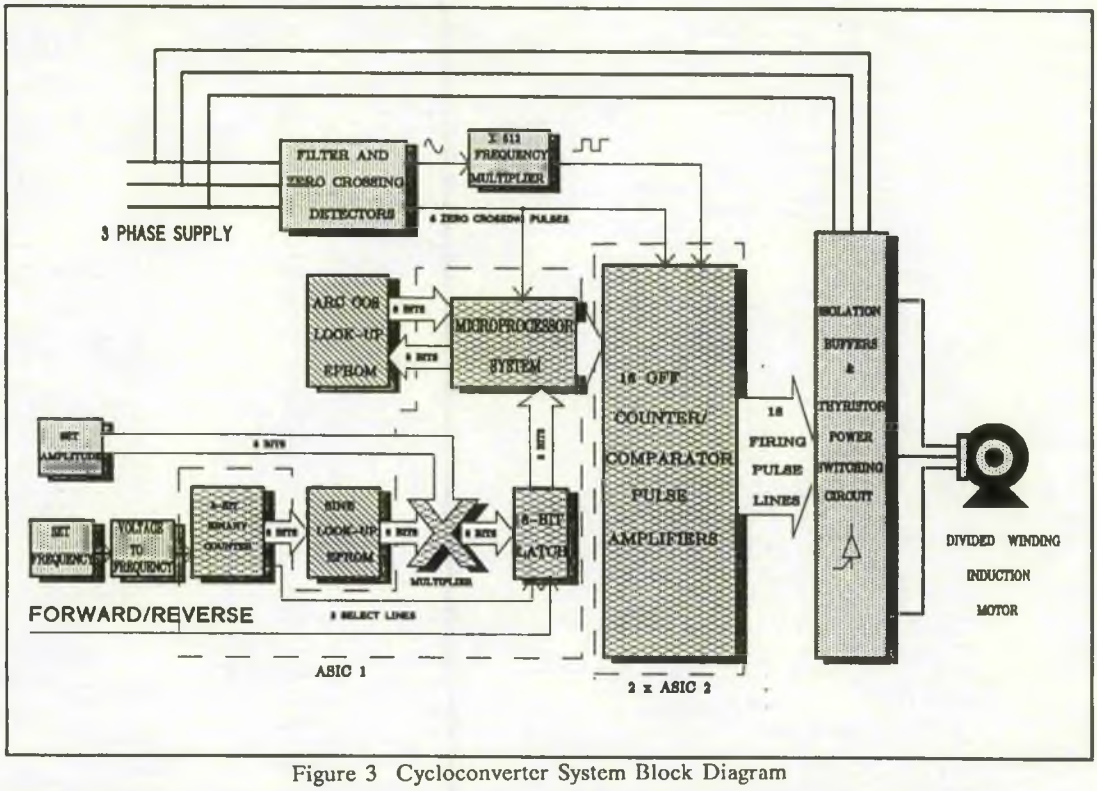

Figure 3 Cycloconverter System Block Diagram

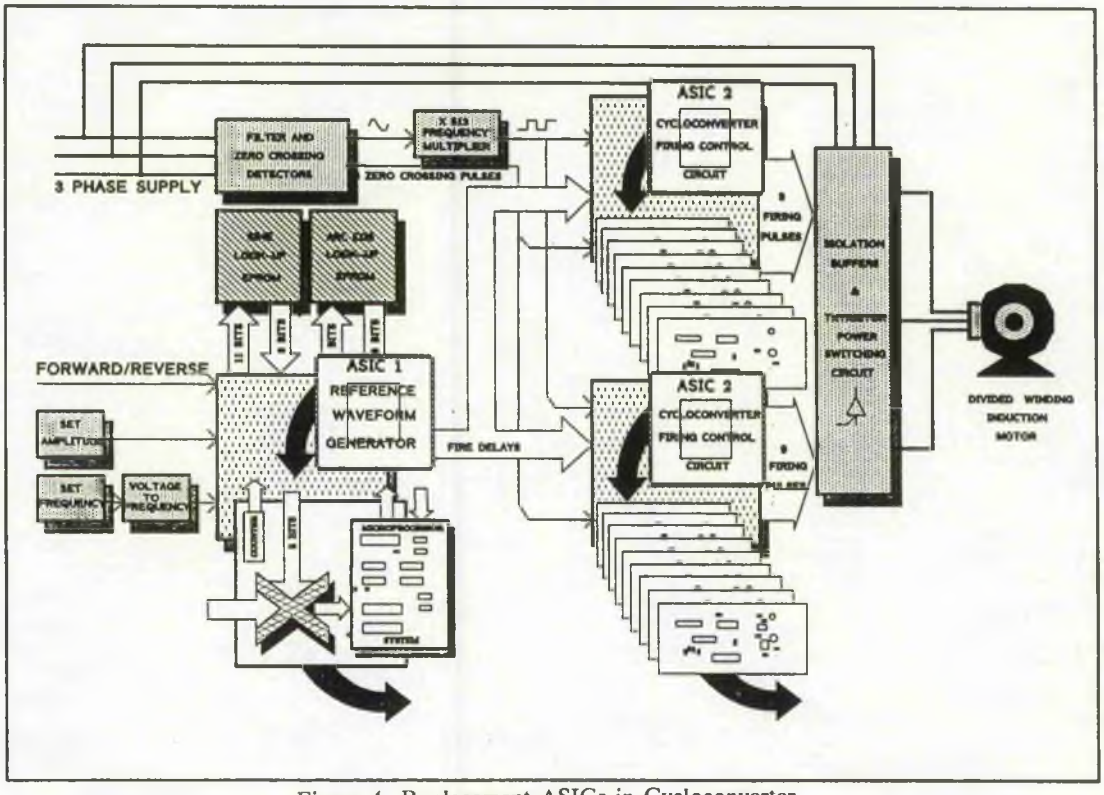

Figure 4 Replacement ASICs in Cycloconverter

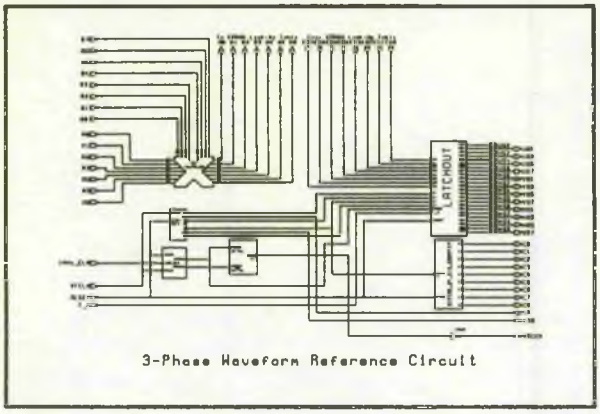

Figure 5 Three Phase Reference Waveform Generator

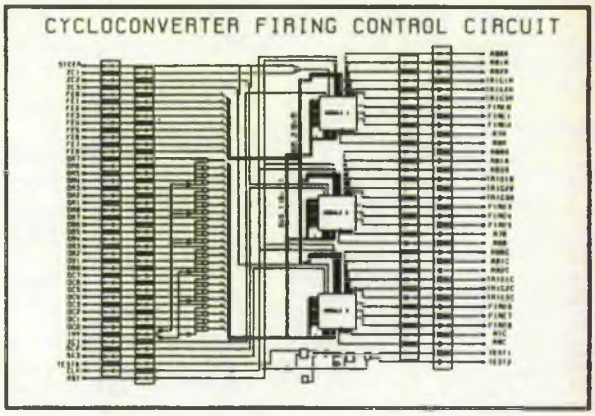

Figure 6 Counter/Comparator/Pulse Amplifier

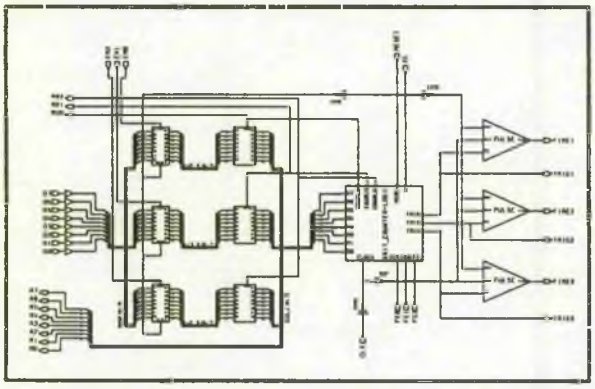

Figure 7 Counter/Comparator/Pulse Amplifier Module

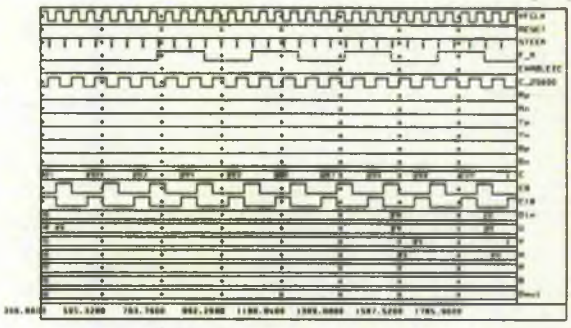

Figure 8 Simulation Waveforms

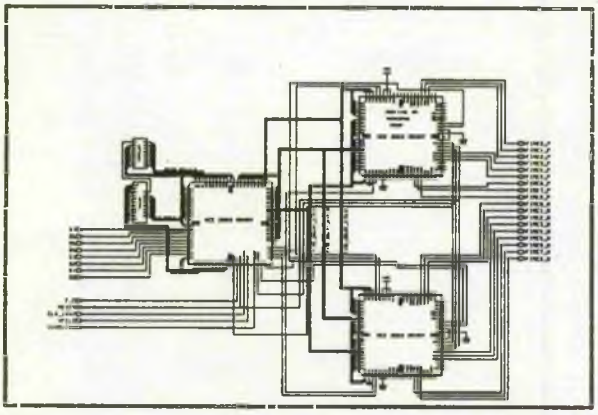

Figure 9 Total Digital ASIC Controller (TDAC)

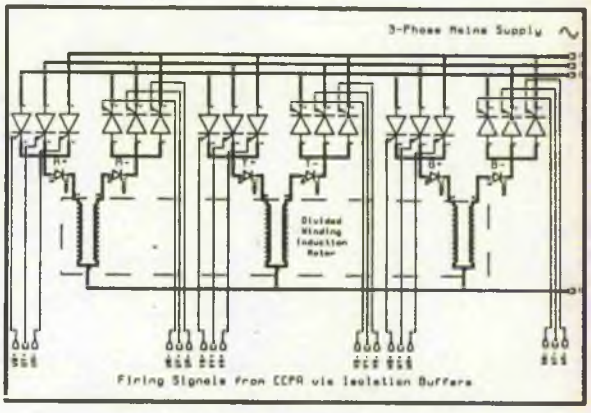

Figure 10 Thyristor Drive Circuit

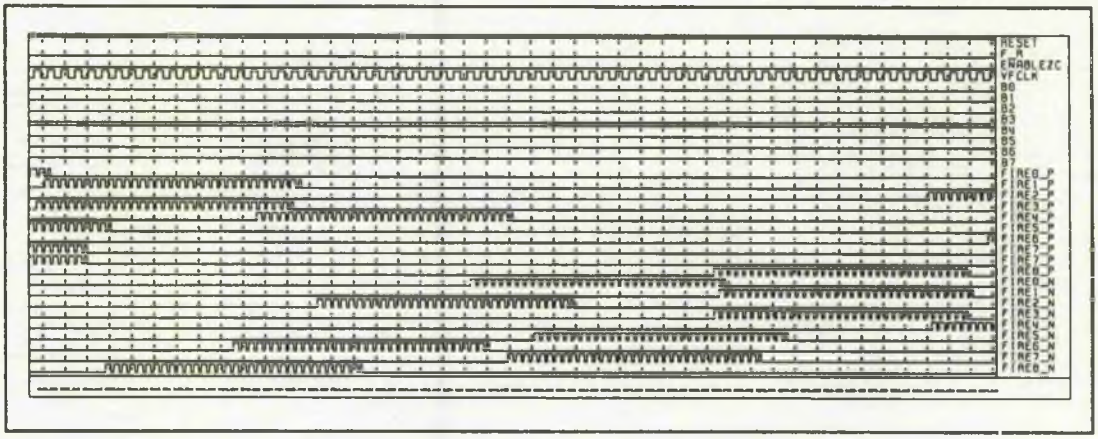

Figure 11 The TDACs Simulation Waveforms

APPENDIX E

G.T.O.

E.1. Introduction

The development of power electronic switching techniques has received a strong impetus from the introduction of the gate turn-off Thyristor (GTO). It is now currently realised that the GTO is one of the most versatile switching devices yet developed.

The GTO is a three junction bistable semiconductor switch for controlling the flow of unidirectional current. Like a conventional thyristor, it can block a high-level forward voltage whilst turned off, and pass a peak forward current far in excess of its average current rating whilst turned on. Like a bipolar transistor however, it can be switched on and off at high speed by controlling a low-level current flowing into or out of its gate. The GTO therefore combines the most desirable characteristics of the thyristor with those of the transistor, and offers outstanding static and dynamic dv/dt performance.

Although the GTO is not a new device, it is only recently wit advances in ion implantation, neutron doping, fine-line photlithography, and process control, that its transfer from the laboratory to large-scale production has been made possible. Excellent yields are now being achieved and the manufacturer of GTOs with characteristics suitable for wide range of applications is now feasible. The BTW58 for example has a blocking voltage of up to 1500V, a surge current rating of 50A, dv/dt capabilities of 100kV/μS static and 1 kV/μS dynamic, and very fast switching times of less than 0.5 μS.

E.2. Operation

Like the thyristor, the operation of a GTO can be considered in terms of a simplified two transistor model shown in Fig. E.1.

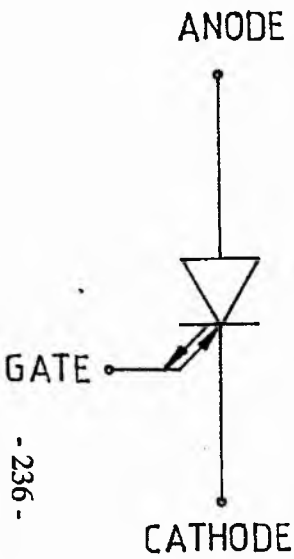

(a)

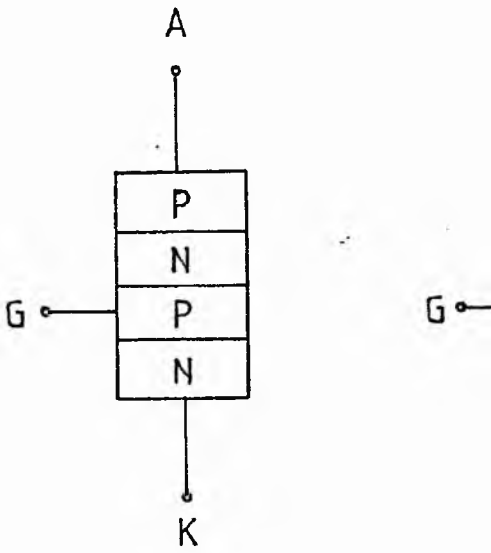

(b)

Fig **E.1** (a) GTO symbol
(b)&(c) Equivalent block diagram of GTO
(d) Two transistor model of GTO

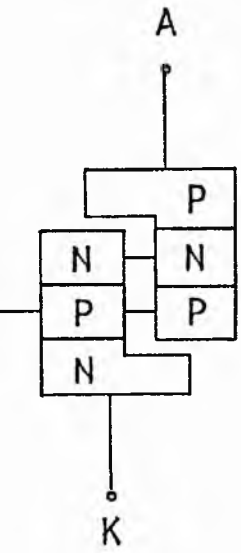

(c)

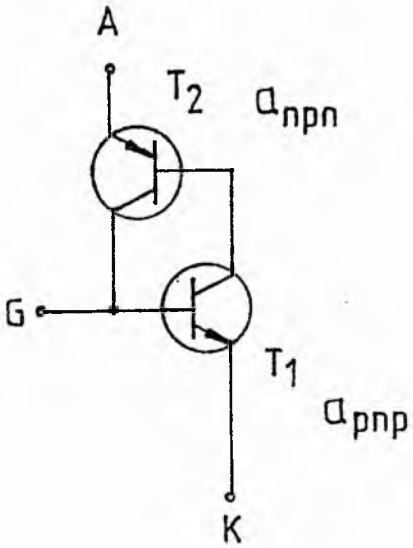

(d)

When positive gate drive is applied to the base of T_1, the transistor turns off, and since the collector of this transistor is connected to the base of T_2, it is driven low and also turns on. The collector current of T_2 then flows into the base of T_1 setting up regenerative conditions. If the main current I_A is sufficient for the sum of the transistor gains to exceed unity (anpn + apnp > 1), the device will latch on.

Unlike the thyristor, the GTO is designed so that negative gate drive can be used to turn off the device. This is achieved by making anpn of T_2 relatively large and apnp of T_1 small. In practice, apnp is maximised by careful control of the diffusion profiles, and apnp is minimised by making the base wide, by controlling the carrier lifetime and by controlled shorting of the emitter. The gate and cathode regions are interdigitated providing low gate resistance and high current turn off capability. This also ensures good silicon utilization. Such control is only possible by those processes mentioned earlier.

The four layer structure of the GTO gives it several advantages over three layer switches such as transistors and darlingtons. The most obvious of these is that a four layer device has an inherently higher standoff voltage. A second advantage is that for a four layer device, the latching action is provided by a built in gain. This means that the higher the current, the more the GTO saturates, unlike the transistor which comes out of the saturation at higher currents. Thus a smaller chip can be used. The GTO also has a higher overload capability than a transistor and can be protected by a fuse.

In BTW58, gold doping is used to obtain a lower storage time and a faster, cleaner turn off (less than 0.5 μS) compared with high voltage bipolar devices or thyristors. The permissible rate of rise of reapplied off state voltage, 1000V/μS, is also far superior to present day bipolar switches.

In any switch, a low drive current requirement is advantageous. However, in a GTO a low gate drive (approximately 10mA) would necessitate a high internal gain which in turn would make the device difficult to turn off. A compromise is therefore necessary between gate drive and turn off performance.

The BTW58 requires only about 100mA to switch on 5A, while fast switch of (<0.5μS) is achieved by applying a negative gate voltage of ≥ 5V.

E.3. Comparison of Solid State Switches

The GTO thyristor is primarily useful in power switching applications. It is always difficult to know where a new device fits in relation to the existing semiconductors and related methods, so an attempt is made here to give a simplified view of relative merits and demerits.

E.3.1. Comparison With Thyristors (SCRs)

The GTO thyristor is now replacing the forced commutated SCR in many applications. The arguments for using GTOs, rather than forced commutated SCRs, are overwhelming.

Elimination of components required for forced commutation resulting in reduction cost, weight and volume.

Reduction in acoustic and electromagnetic noise due to the elimination of the commutation circuits.

Faster turn off, permitting the use of higher switching frequencies and smaller fault-current limiting reactors.

Improved efficiency.

These benefits are achieved at the cost of a more complicated gate drive circuit. However, the size and cost of the gate drivers required by the GTO are small compared with the size ad cost of the forced commutation components required by an SCR.

E.3.2. Comparison with Bipolar Transistors

For applications in the lower current and lower voltage ranges, the GTO has a revival in the bipolar transistor. However, the GTO possesses significant advantages over the bipolar transistor.

High blocking voltage capability. This permits the use of wider safety margins on voltage ratings.

High ratio of peak controllable current to average current. This is particularly advantageous in systems such as pulse width modulated inverters, where the ratio of peak to average current is high. Furthermore, a GTO can safely turn off a greater current under fault conditions than can a bipolar transistor with the same average current rating.

High ratio of peak surge current to average current (typically 10:1 for the GTO). The regenerative switching action of the GTO drives it deeper into saturation under surge conditions, while the bipolar transistor tends to come out of saturation.

High on state gain.

The principal advantage of the bipolar transistor over the thyristor has been the capability of the bipolar to be turned off by control of the base current. The development of the GTOs with good turn off performance has eliminated this advantage.

Table E.1 compares the GTO thyristor with the thyristor,the reverse conducting or asymmetric form, the power bipolar transistor and the mosfet. The table compares the turn-on and turn-off capabilities. It must be noted that the comparison refers to the drive circuit complexity, not to the device switching speed or dissipation. Figure E.2. indicates areas of operation and application in terms of

voltage and frequency for the various switching devices listed in Table E.1.

Figure E.3. attempts to show the predicted power ratings of the devices tabulated in Table E.1. to the year 1990.

E.4. Application of GTOs

The high forward blocking voltage, ease of drive, an fast switching capability of the GTO make it eminently suitable for use in a vast range of applications. These include:-

E.4.1. Industrial Appliances

Power supplies	- General
AC Inverters	- AC motor control
	Induction heating
	Ultrasonic cleaning
Lighting	- Starters; ballast
Automobiles	- Ignition

E.4.2. Domestic Appliances

Motor Control	- White goods
	Small appliances
Power Control	- Microwave cookers
Ignition Systems	- Gas

E.4.3. Television

Power Supplies

EHT Regulation

Line Deflection

Device	On-state dissipation	Ease of turn-on	Ease of turn-off	Switching frequency	Overcurrent capability	Chip area
GTO	Moderate	Moderate (regenerative)	Good	Good	Good (10 to 15×)	Small
Thyristor (conventional)	Low	Good (regenerative)	Very poor (external commutating devices required)	Very poor	Very good (20×)	Small
ASCR	Low	Good (regenerative)		Moderate	Very good (20×)	Small
Darlington with speed-up	Moderate	Moderate (non-regenerative)	Moderate	Good	Poor	Moderate
Bipolar transistor	Low	Poor (non-regenerative)	Moderate	Good	Poor	Moderate
VMOS	High	Very good but capacitive (non-regenerative)	Very good	Very good	Moderate	Large

Table E.1 Comparison of power switches

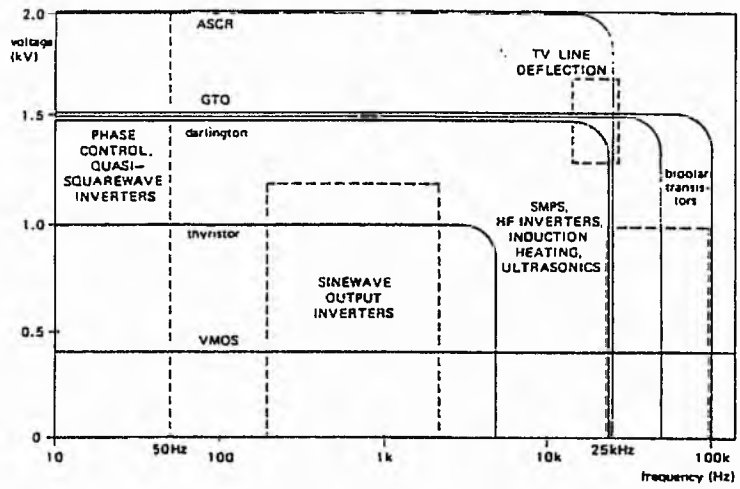

Fig E.2 Performance of power switches

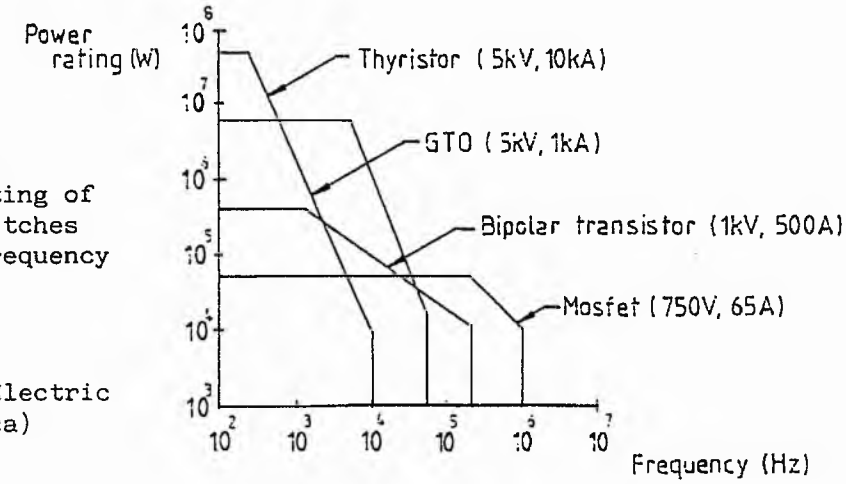

Fig E.3

Power rating of power switches versus frequency

(Source: General Electric of America)

REFERENCES

1. HABERMANN, R.: "Single-phase operation of a 3-phase motor with a simple static phase converter". TRANS. Amer. Inst. Electr. Engrs. 1954. 73, pp.833-837.

2. BROWN, J.E. and JHA, C.S.: 'The Starting of a 3-Phase induction motor connected to a single-phase supply system', Proc. IEE. 1959. IDGA. pp.183-190.

3. HOLMES, P.G.: 'Single to 3-phase transient phast conversion in induction motor drives'. Proc Iee. 1985. 132, pt. B N=5. pp.289-296.

4. MURTHY, S.S., BERG, G.J., BHIM SINGH, JHA, C.S. and SINGH, B.P.: 'Transient analysis of a three phase induction motor with single phase supply' IEEE Trans. 1983, PAS - 102, pp.28-37.

5. TINDALL, C.E. and MONTEITH, W.: 'Balanced operation of 3-phase induction motors connected to single phase supplies'. Proc. IEE, 1976, 123 (6), pp.517-522.

6. MOHAMADEIN, A.L., AL-OHALY, A. and AL-BAHRANI, A.: 'On the choice of phase-balancer capacitance for induction motors led from single-phase supply'. IEEE Trans. 1987.

7. BROWN, J.E. and BUTLER, O.I.: 'A general method of analysis of 3-phase inducting motors with assymetrical primary connections', Proc. IEE. 1953. 100A, PE II, Paper 1421U, pp. 25-34.

8. BROWN, J.E. and RUSSELL, R.L.: 'Symmetrical component analysis applied to phase converters of the Ferraris-Arus type'. Ibid, 1958, 105A, pp. 538-544.

9. HOLMES, P.G. and OZPOLAT, M.: 'Static Phase conversion for the operation of 3-phase induction motors in pumping systems'. IEE Conference, Power Electronics and variable speed drives, March 1984.

10. HOLMES, P.G. and OZPOLAT, M.: "Static phase conversion for the operation of 3-phase induction motors in pumping systems' PROC. 18th UPEC. Surrey University, 1983.

11. KAUFMAN, M. and WILSON, A. 'Electronics Technology', McGraw-Hill (Schaum) 1982.

12. MAZDA, F.: 'Thyristor Control' (Newnes, 1973).

13. DANIEL, A.R.L. 'The Performance of Electrical Machine'. McGraw Hill, 1968.

14. PATTERSON, E.B. and MORLEY, D. 'EDA Techniques used to Develop a Cycloconverter Drive System', Nottingham Polytechnic, Oct. 1990.

15. CHAPMAN, S.J. 'Electric Machinery Fundamentals', International Student Edition.